UNIVERSIDAD DE GRANADA

FACULTAD DE CIENCIAS

Departamento de Física Aplicada

Miguel Wulff Pérez

Tesis Doctoral

Editor: Editorial de la Universidad de Granada
Autor: Miguel Wulff Pérez
D.L.: GR 2882-2012
ISBN: 978-84-9028-199-4

Editor: Editorial de la Universidad de Granada
Autor: Abdul Jabar H. Jabur
D.L.: En trámite
ISBN: En trámite

Preparation and characterization of nanoemulsions for the controlled delivery of hydrophobic compounds.

por

Miguel Wulff Pérez

Directores del trabajo:

Antonio Martín Rodríguez
Catedrático de Física Aplicada

María José Gálvez Ruiz
Catedrática de Física Aplicada

Juan de Vicente Álvarez de Manzaneda
Prof. Titular de Física Aplicada

Trabajo presentado para aspirar al grado de DOCTOR
por la Universidad de Granada

Miguel Wulff Pérez, Granada, Abril 2012

Agradecimientos

En primer lugar quiero agradecer esta tesis a mi familia: a mi madre, que me lo ha dado todo (y un poco más), a mi padre, que siempre ha estado para apoyarme, y a mi hermano, que me ha cuidado y me ha ayudado a crecer.

Esta tesis no habría sido posible sin el apoyo y la dedicación de mis directores de tesis, Antonio Martín Rodríguez, María José Gálvez Ruiz y Juan de Vicente, que me han enseñado y me han sabido guiar a lo largo de estos años, siendo más maestros que profesores.

También ha sido fundamental el apoyo de todo (y digo todo) el Grupo de Física de Fluidos y Biocoloides, desde los catedráticos hasta los becarios, demostrando que los sistemas cooperativos también pueden ser extraordinariamente fructíferos. Debo destacar a Miguel, a Amelia, a César y a Efrén, que empezaron casi conmigo y con los que he andado buena parte del camino.

He de agradecer a la Junta de Andalucía el apoyo financiero recibido bajo el proyecto P07-FQM-03099 así como al proyecto MAT2010-20370 del Ministerio de Educación, Cultura y Deporte.

Y por supuesto, gracias Mireia. Sin ti no es que esta Tesis no hubiera sido posible, es que no lo serían tampoco mi vida, ni la salida del Sol por las mañanas, ni la vida en la Tierra, ni la danza de las esferas celestes.

Index

Index

Chapter 1. Introduction

From ancient times, to find the most suitable way for drug administration has been a challenging issue. For example, plants and minerals were pulverized and drunk together with either milk or wine by the ancient Egyptians, as described in Ebers papyrus (circa 1500 BC). Even before, Sumerians widely used creams and lotions combining plants, oils and water for medicinal and cosmetic purposes. A Sumerian tale, recorded on a clay tablet more than four thousand years ago, describes how two friendly gods reveal to a prince the "secrets of Heaven and Earth": first, "They showed him how to observe oil on water - a secret of Anu, Enlil and Ea", and after that "They taught him how to make calculations with numbers" (Yechiel & Coste, 2005)This early text, specifically linking medicine and mathematics, could be considered as the first step towards the present-day science behind the study of drug delivery systems.

An ideal drug delivery system should transport the drug to the targeted organ or receptor in the required dose, preserving it intact after crossing the different physiological barriers. Developing the appropriate drug delivery system solves plenty of the complications related with drug delivery, since it will help to minimize drug degradation and loss, to prevent harmful side-effects and to increase both drug bioavailability and the fraction of the drug accumulated in the required zone (Kaparissides, Alexandridou, Kotti, & Chaitidou, 2006).

This problem becomes even more complicated when the drug to be administered has low solubility in water. Highly potent, but poorly water-soluble drug candidates are

common outcomes of contemporary drug discovery programs (Porter, Trevaskis, & Charman, 2007), reaching percentages as high as 80-90% of the total of the possible candidates depending on the therapeutic area (Williams, Watts, & Miller, 2012). However, frequently these promising drugs are dismissed in the first stages of the selection because of the difficulties related with their administration. As a way of example, their very low solubility hinders dissolution and therefore limits drug concentration at the target site, often to an extent that the therapeutic effect is not achieved. This could be overcome by increasing the dose; however, this dose escalation would cause local toxicity, increased risk of side effects or even drug precipitation.

In order to by-pass these difficulties, great attention has been paid to lipid-based drug delivery systems, i.e., systems that present lipids in their composition, mainly triglycerides and/or phospholipids. Lipids are known to enhance the bioavailability and solubility of hydrophobic drugs when they are administered together (Porter, Pouton, Cuine, & Charman, 2008), and present the great advantage of being highly biocompatible and biodegradable, as one of the main components of the human body. Lipids are natural compounds present both in plants and animals as oils/fats (triglycerides) and in all cell membranes (phospholipids).

Among the proposed lipid-based delivery systems are micelles (Narang, Delmarre, & Gao, 2007), microemulsions (Spernath & Aserin, 2006), liposomes (Immordino, Dosio, & Cattel, 2006), solid lipid nanoparticles (Bunjes, 2010), self-emulsifying drug delivery systems (Porter et al., 2008), nanostructured lipid carriers (Mäder, 2006) and nanoemulsions. Each system has specific physicochemical properties that confer particular functionalities. These properties need, however, to be carefully considered and characterized to provide a rational basis for their development into effective carrier systems for a given delivery task (Bunjes, 2010). It appears then as a (beautiful) paradox that the "divine gift" of knowing "how to observe oil and water" could be the key to solve important health problems affecting people in 21st century.

1.1 Nanoemulsions: concept and advantages as drug delivery system

1.1.1 Concept of nanoemulsion and main properties

An emulsion can be defined as a heterogeneous mixture of at least two immiscible liquids, i.e., a dispersion of one liquid (dispersed phase) as droplets into another one (continuous phase). Depending on the nature of the dispersed and the continuous phase, different types of emulsions can be distinguished. For example, a dispersion of oil in water is referred to as an oil-in-water (O/W) emulsion, whereas the opposite case will be referred to as a water-in-oil (W/O) emulsion (Buszello & Muller, 2000). If the dispersed phase represents an emulsion itself the systems formed are called multiple emulsions (O/W/O, W/O/W, and so forth).

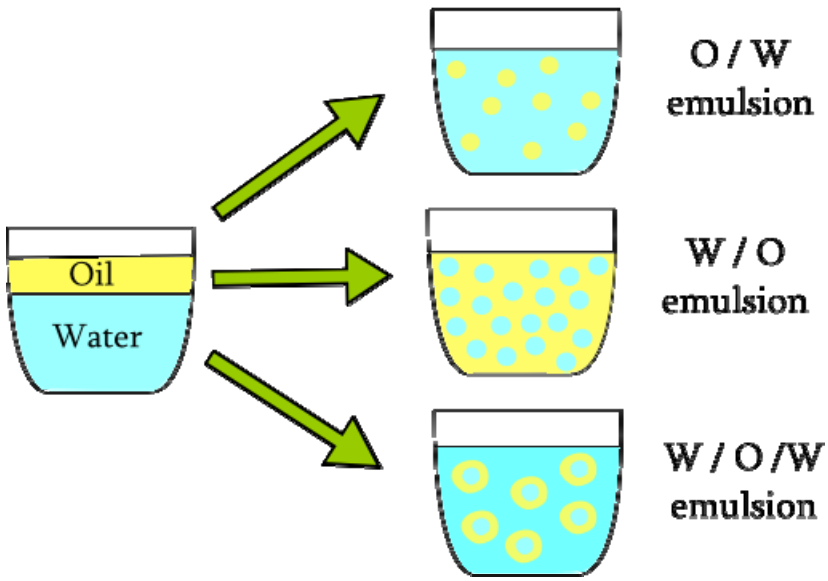

Figure 1. Different types of emulsions according to the nature of the dispersed and continuous phases.

1. Introduction

Emulsions are not a thermodynamically stable system. They do not form spontaneously when their components are mixed, and they tend to separate into the original phases. However, the presence of a surfactant between the different phases confers them enough kinetic stability to be used in their many applications. The manner in which surfactants stabilize emulsions will be explained more in depth in Section 1.2. Likewise, the way in which surfactants influence the properties of nanoemulsions will be a recurrent theme throughout this dissertation.

Nanoemulsions are emulsions with a droplet size in the nanometer scale, and typically with a diameter under 500 nm (Fast & Mecozzi, 2009; Forgiarini, Esquena, González, & Solans, 2001; Gutiérrez et al., 2008; Izquierdo et al., 2001; Solè et al., 2006). Some authors consider 200 nm or even 100 nm as the upper limit (Mason, Wilking, Meleson, Chang, & Graves, 2007), as they establish a correlation with the word "nanotechnology" as defined by the US government's National Nanotechnology Initiative, i.e., "the understanding and control of matter at dimensions of roughly 1–100 nm". Even within that definition, there is no unanimity about if the size should refer to the radius or the diameter (Mason et al., 2006). Though this usage might match current language trends, it establishes an arbitrary size boundary because emulsion properties do not instantly change upon crossing the 100 nm threshold (Fast & Mecozzi, 2009), as will be seen throughout the explanation of the main properties of nanoemulsions.

Nanoemulsions can be also found in the literature as ultrafine emulsions (Nakajima, 1997), submicron emulsions (Benita, 1998), colloidal emulsions (Maksimochkin, Pasechnik, Slavinec, Svetec, & Kralj, 2007), lipidic core nanocapsules (Saulnier & Benoit, 2006), nanosized emulsions (Tamilvanan, 2009) or miniemulsions (Du, Wang, Dong, Yuan, & Hu, 2010), although this last denomination is more frequently used when the nanoemulsion serves as a base for a polymerization. Also the term "parenteral emulsion" or "intravenous emulsion" refers implicitly to a nanoemulsion, as emulsions to be administered intravenously must have droplet sizes within a similar range to that of nanoemulsions (Buszello & Muller, 2000).

Although having similar names, nanoemulsions should not be confused with microemulsions. "Microemulsion" is an unfortunate term that refers to a

thermodynamically stable, spontaneous-forming system. From a physical point of view, a microemulsion is therefore not an emulsion, since emulsions are defined as dispersions, and "dispersion" implies non-equilibrium, in the same way as "solution" implies the opposite. The prefix "micro-" is also misleading, since microemulsions actually have much smaller sizes than a micron (Fast & Mecozzi, 2009), usually well under 200 nm. However, due to the historical precedence the term "microemulsion" is still used.

The distinction between conventional emulsions and nanoemulsions is not arbitrary. Due to the small droplet size of nanoemulsions, new interesting properties arise, especially those related with the use of nanoemulsions as drug delivery systems. Some of these properties are:

- Great stability against creaming/sedimentation: due to the different densities between oil and water phases, in conventional emulsions the droplets tend to float (creaming) or to sink (sedimentation). In nanoemulsions, however, the small droplet size causes a large reduction in the gravity force, and the Brownian motion becomes then sufficient for overcoming gravity (Izquierdo et al., 2001).

- Large surface area: for a given volume of dispersed phase, the smaller the droplet size, the larger the total surface area. In many cases, a high amount of surface area is related with a high absorption of a drug. For example, if the topical administration is considered, the large surface area of the nanoemulsion allows rapid penetration of actives (Tadros, Izquierdo, Esquena, & Solans, 2004).

- Possibility of intravenous administration: it has been documented that for intravenous applications the droplets should not be larger than the diameter of the capillaries (about 5 μrn) to avoid blockage (Lucks, Müller, & Klütsch, 2000). Conventional emulsions possessing a droplet size around 4-6 μm or higher are known to increase the incidence of emboli and can cause changes in blood pressure (Floyd, 1999). Actually, the United States Pharmacopeia has established recently that the mean droplet size must be <500 nm for injectable emulsions (Driscoll, Ling, & Bistrian, 2009), thus pertaining to the nanoemulsion range.

1.1.2 Nanoemulsions as drug delivery systems

The basis for the actual and future use of nanoemulsions as drug delivery systems comes from the emulsions developed for total parenteral nutrition. These emulsions were first developed with the aim of helping patients to overcome a critical nutrition state (patients in intensive care or in convalescence) by providing them with triglycerides by parenteral route (Lucks et al., 2000). These emulsions contained highly purified triglyceride oils, and egg phospholipids as surfactant. With an average particle diameter around 300 nm, these systems fall in the nanometer range, which makes them the first therapeutic nanoemulsion. Probably, the thinking behind the parenteral emulsions idea was to mimic the composition and structure of chylomicrons, the physiological carriers of triglycerides and other lipid components in the bloodstream (Bunjes, 2010). Such emulsions were first introduced to the market in Europe in the early 1960s and have developed into an indispensable, widely accepted component of parenteral nutrition, with marketed products such as Intralipid (Pharmacia & John), Abbolipid/Liposyn (Abbot), Lipofundin/Medianut (B. Braun), Lipovenos (Fresenius Kabi), Intralipos (Green Gross) or Trivè 1000 (Baxter SA) (Tamilvanan, 2004). The biocompatibility of emulsions for parenteral nutrition, together with the subsequent FDA approval, has led them to act as a template for future nanoemulsion development. Hence, the initial examples of nanoemulsions for drug delivery were all conceptually similar to nutritional emulsions, and consisted basically on adding a drug to a preformed parenteral emulsion like those mentioned above. For example, the administration of amphotericine B in its commercial form (Fungizone) was compared with the administration of amphotericine B together with Intralipid, and it was demonstrated that the latest form was able to reduce both in vivo and in vitro toxicity (Marti-Mestres & Nielloud, 2002).

In recent years, development has continued into more innovative emulsion formulations, e.g. varying the emulsified oil and/or the surfactants. The combination of the advantages of traditional parenteral emulsions (mainly biocompatibility and biodegradability) with the new functionalities has led to the first marketed drug delivery systems based on nanoemulsions, listed in Table 1. Some of the main advantages of nanoemulsions in the field of drug delivery systems for hydrophobic drugs are:

- Inexpensive and easy-to-scale production: in comparison with other systems, nanoemulsions can be (and in fact are) relatively cost-effective. Vegetable oils, the main component of nanoemulsions, are not expensive, event those highly purified. In addition, the technology for large-scale production is already proven and available (S. Tamilvanan, 2004) (e.g. high-pressure homogenizers), as will be explained in depth in the experimental section "Preparation of nanoemulsions".

Product	Drug	Administration	Producer
Diazepam-Lipuro	Diazepam	Intravenous	B. Braun Melsungen
Diprivan	Propofol	Intravenous	AstraZeneca
Limethason	Dexamethasone palmitate	IV / intraarticular	Green Cross
Vitalipid	Lipohilic vitamins	Intravenous	Fresenius Kabi
Stesolid	Diazepam	Intravenous	Dumex
Lipo-NSAID	Flurbiprofen axetil	Intravenous	Kaken Pharma.
Restasis	Cyclosporin A	Ocular topical use	Allergan
Gengraf	Cyclosporin A	Oral	Abbott
Etomidat-Lipuro	Etomidate	Intravenous	B. Braun Melsungen
Cleviprex	Clevidipine Butyrate	Intravenous	Medicines Co.

Table 1. Emulsions as drug delivery systems already in the market, obtained from Marti-Mestres & Nielloud, 2002; Fast & Mecozzi, 2009; Tamilvanan, 2009; Bunjes, 2010; Hippalgaonkar, Majumdar, & Kansara, 2010.

- Low amount of surfactant required: nanoemulsions can be prepared using reasonable surfactant concentrations (e.g. under 2% for an O/W emulsion with a volume fraction of 0.25), whereas systems as microemulsions require a high surfactant concentration, usually in the region of 20% and higher (Tadros, 1994). This will have an impact on the production cost, as well as in the toxicity of the system.

- Independence of dilution: the stability of some thermodynamically stable systems is compromised when they are diluted. Self-microemulsifying drug delivery systems can suffer significant phase changes and loss of solvent capacity (Porter et al., 2008), whereas micellar systems turn unstable under a certain concentration, the critical micelle concentration, which leaves to drug precipitation. Dilution is an inherent consequence of some routes of administration, e.g. oral and intravenous routes, and therefore the resistance against its effects is not a trivial issue.

- Reduction of the irritation/pain at the site of injection: some drugs (e.g. amphotericin B or propofol) can cause local irritation and painful inflammation at the direct site of injection when they are administered intravenously as aqueous solutions. Some co-solvents traditionally used for the administration of hydrophobic drugs, such as ethanol, can lead to the same results. Nanoemulsions eliminate the need for co-solvents and prevent the local effect of the drug (Fast & Mecozzi, 2009). The pain is also reduced in comparison with other systems like microemulsions (Doenicke, Roizen, Rau, Kellermann, & Babl, 1996), probably due to the reduction of free drug on the aqueous phase (Sim et al., 2009).

- Simplicity of the system: with respect to other lipid carrier systems, especially those comprising lipids that are solid at room temperature, nanoemulsions usually present a less complex physicochemical behavior (Bunjes, 2010). As a way of example, solid lipid nanoparticles can suffer gel formation on solidification and upon storage, unexpected dynamics of polymorphic transitions, extensive annealing of nanocrystals over significant periods of time or drug expulsion from the carrier particles on crystallization and upon storage (Mäder, 2006).

-Possibility of passive targeting: in many solid tumors, the vasculature becomes hyperpermeable (see Figure 2). This is known as the enhanced permeability and retention

(EPR) effect. Pore sizes in such tumors vary from 100 to 780 nm. By comparison, normal tissues generally have continuous and non-fenestrated vascular endothelia (Kozlowska et al., 2009). As a result, the droplets of a nanoemulsion (and the drugs transported in them) will accumulate preferentially around those tumors, since they are able to penetrate within these abnormal capillaries.

In addition to this, the use of less traditional surfactants to formulate nanoemulsions has opened a new field of possibilities. Two of the most significant are:

- Long circulation: as will be explained in detail in Section 1.5, traditional nanoemulsions were rapidly cleared from circulation, which could lead to poor bioavailability and hinders a sustainable release of the drug. These circulating times are notably increased by using different surfactants, such as those derived from polyoxyethylene (Lucks et al., 2000).

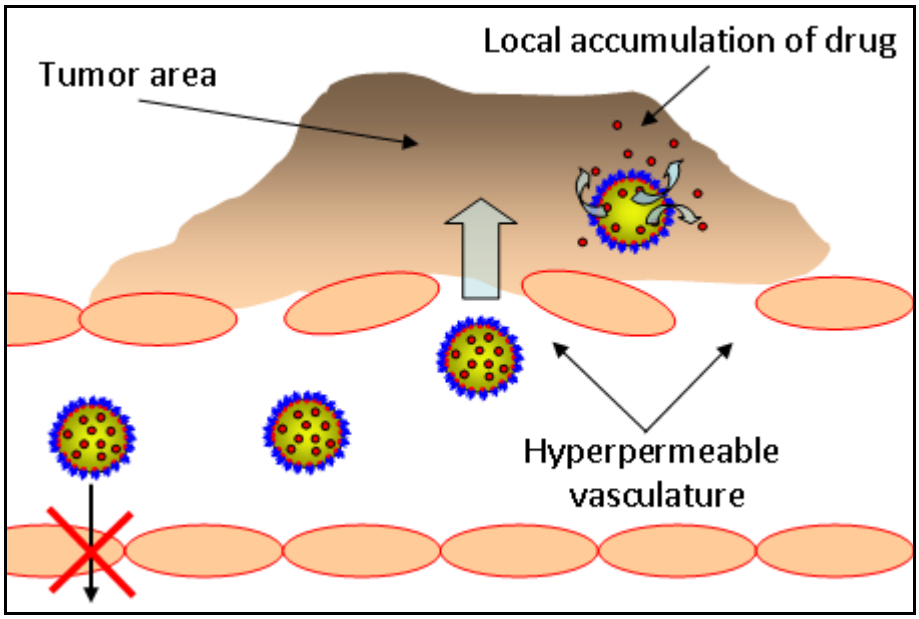

Figure 2. Schematic representation of passive targeting: the nanoemulsion droplets can only penetrate through the leaky vasculature of the tumor tissue, producing there a local accumulation of drug.

- Active targeting: it is also possible to increase the affinity of the droplets for a given cell type or tissue by linking a signal molecule, either directly onto the droplet surface or to the surfactant. For example, some tumors overexpress a certain type of protein, called tumor antigen. By linking the corresponding antibody to the droplets, the local concentration of drug close to the tumor will be enhanced, even facilitating the drug intracellular entry by endocitosis (Tamilvanan, 2009).

For all the above mentioned advantages, nanoemulsions appear as a highly promising drug delivery system for hydrophobic compounds, and therefore we will try throughout this dissertation to carry on an in-depth study of their formation, properties, degradation and so forth.

1.2 Nanoemulsions and surfactants

As seen in the previous section, a surfactant is needed to prepare and stabilize nanoemulsions. Surfactants are molecules which have a chemical structure that makes it particularly favorable for them to link and reside at interfaces; hence they are termed "surface-active agents" or simply "surfactants", a contracted form of the previous term. Depending on their properties and/or the application field, they are often termed as "emulsifiers", "detergents" or "tensioactives" (Goodwin, 2009). Surfactants have a characteristic molecular structure consisting of (at least) one structural group that has very low affinity for polar solvents like water, known as a hydrophobic (or lipophilic) group, together with a group that has strong attraction for polar solvents, called the hydrophilic group. This structure with both a water insoluble component and a water soluble component is called amphiphilic or amphipathic. In emulsions, this amphiphilic structure is the main cause of the positioning of the surfactant at the interface between oil and water, with the subsequent decrease in the interfacial tension. The proportion between hydrophilic and lipophilic groups is called hydrophilic/lipophilic balance (HLB) and it determines the functionality of the surfactant at a given interface and hence the final nature of the emulsion. A surfactant with a high HLB value will have a hydrophilic part that predominates over the hydrophobic one and will form O/W emulsions, whereas in a surfactant with a low HLB the hydrophobic group predominates over the hydrophilic one, producing W/O emulsions (Rosen, 2004).

However, the stabilizing effect of surfactants over nanoemulsions is not only due to the decrease in interfacial tension. The presence of a surfactant at the interface provides the droplets with new properties that prevent the merging of the droplets and the subsequent phase separation. The most common stabilizing effect is that of repulsion, where some force do not allow the droplets to come in close contact.

Traditionally, nanoemulsions have been prepared using phospholipids, which are a characteristic example of ionic surfactants (see Figure 3). This mechanism of stabilization is based on electrostatic repulsion: the polar heads of the surfactant provides the droplets with a net charge, and the droplets, stabilized for the same surfactant and therefore having

charges of the same sign, repel each other. If this charge is quantified as zeta-potential, it is generally assumed that droplets with a zeta potential more positive than (approximately) +30 mV or more negative than -30 mV will be stable (Freitas & Müller, 1998).

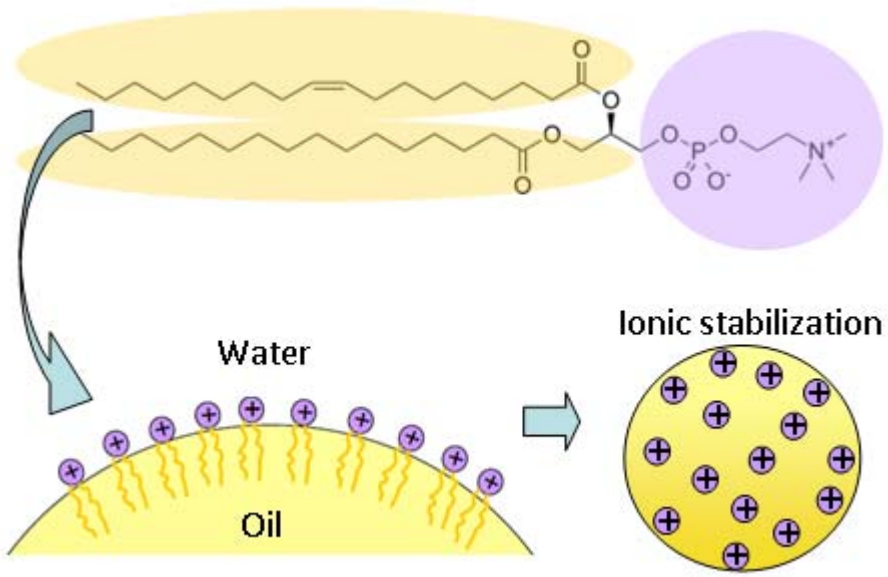

Figure 3. Typical structure, disposition at the interface and mechanism of stabilization of phospholipids.

However, the stability of nanoemulsions stabilized with ionic surfactants is compromised if the ionic strength is considerable, i.e., in the presence of high concentrations of ions. This is a common situation in some administration routes, mainly the oral and intravenous ones. With increasing electrolyte concentration, the accumulation of counterions near the interface causes the droplet charges to be screened, thus reducing the zeta potential. Consequently, the repulsion is decreased, and so it is the stability of the nanoemulsion (Lucks et al., 2000). In order to solve these problems, the use of non-ionic surfactants has attracted special attention. These are called steric surfactants, since the droplets are stabilized by means of steric repulsion (see Figure 4). Steric surfactants possess bulky groups protruding into the dispersion media, which create a brush-like barrier

around the droplets. When two droplets approach each other, the free movement of these groups is hindered by interpenetration of the adsorbed layers, resulting in entropic repulsion. As in the example given in Figure 4, the hydrophilic bulky group is frequently polyoxyethylene (POE), which can be also found in the literature as poly(ethylene oxide) (PEO), polyethylene glycol (PEG) or even the old-fashioned term macrogol (the first two terms are more often used by chemists, whereas the last two terms are more common in the pharmaceutical field). These groups are strongly hydrated, which makes them more voluminous and hinders even more the compression of the adsorbed layers (Mollet, Grubenmann, & Payne, 2008).

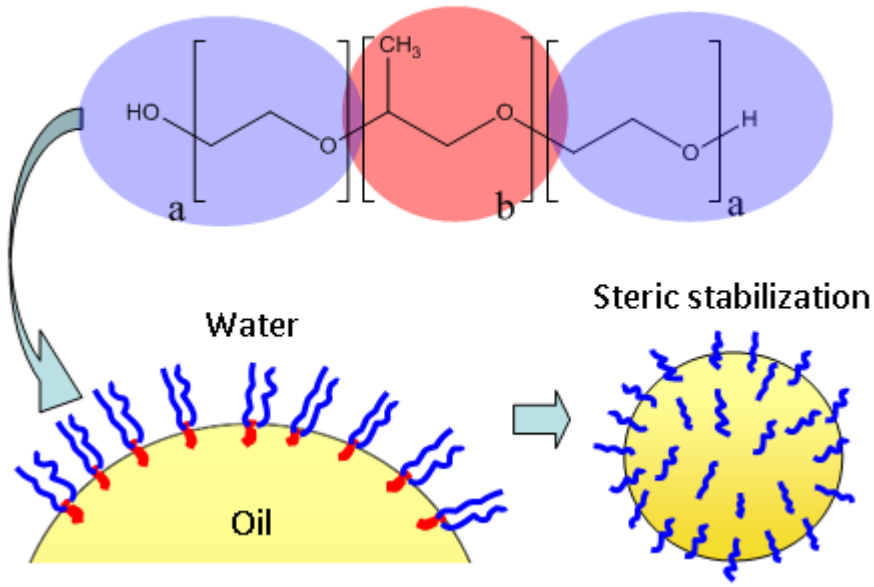

Figure 4. Typical structure, disposition at the interface and mechanism of stabilization of Pluronics.

Among steric surfactants, the tri-block copolymers known as Pluronics are one especially interesting example. De Gennes already predicted their possibilities in 1987, defining their structure as "extremely useful", although also ponting out that "the formation process of the adsorbed layer is delicate and poorly understood" (de Gennes, 1987). Fortunately, the knowledge about the adsorbed layers of Pluronics is being expanded nowadays. Pluronic, which can also be found in the literature as poloxamer,

1. Introduction

Lutrol or Synperonic, is a polymer with an ABA structure composed of polyoxyethylene-polyoxypropylene-polyoxyethylene (POE-POP-POE, see Figure 4). In O/W emulsions, the hydrophobic central group links strongly to the oil, while the two lateral chains are hydrophilic and protrude into the water forming the brush-like barrier around the droplet (Svitova & Radke, 2004).

As Pluronics can be produced with the desired number of subunits and with the proportion between hydrophilic and hydrophobic blocks at will, it is possible to prepare "tailor-made" surfactants with the required properties (Kabanov, Batrakova, & Alakhov, 2002), e.g., a Pluronic with short hydrophilic tails and a long hydrophobic block will be predominantly hydrophobic, and therefore it will stabilize W/O emulsions, whereas a Pluronic with longer hydrophilic tails and a shorter hydrophobic block will produce O/W emulsions.

As in the last example, the possibility of influencing the final properties of the emulsions by modifying the structure of the surfactant should not be dismissed. Indeed, it can be expected that this influence becomes even higher in nanoemulsions, as in this system the area is larger relative to the total volume, and therefore a more substantial fraction of the system is present at interfaces. Hence, the study of the properties that these surfactants confer to the interface and to the final properties of nanoemulsions appears as a necessary step towards the "extreme usefulness" foreseen by de Gennes.

1.3 Nanoemulsions and colloidal stability

1.3.1 Nanoemulsion stability

The stability of nanoemulsions is a key issue for most of their applications. This capability to remain unchanged becomes of the utmost importance when nanoemulsions are to be used as drug delivery systems, since a change on their properties could render them useless or even harmful, e.g., a considerable increase in droplet size would prevent a nanoemulsion for being administered intravenously. Therefore, the mechanisms of nanoemulsion destabilization have to be known and understood thoroughly in order to avoid them. These mechanisms are quite similar to those of conventional emulsions, although some particularities should be highlighted. The main mechanisms of nanoemulsion destabilization, depicted in Figure 5, are:

- Coalescence: as previously explained, nanoemulsions are not a thermodynamically stable system. If two droplets are allowed to come in close contact, they will merge to form a bigger droplet, since this brings a reduction of the total interfacial area, and hence a reduction of the total free energy of the system. This new droplet could merge with another one and so forth, leading to the final phase separation. It is an irreversible process and it changes several properties of the emulsions such as droplet size, droplet number, total surface area or monodispersity. For these reasons, it is one of the worst destabilizing effects that affect nanoemulsions. Fortunately, with the appropriate preparation method, type and amount of surfactant, it can be avoided for long periods of time, even for years (Lucks et al., 2000; Mason et al., 2007).

- Creaming: due to the different densities, the dispersed phase floats to the top of the continuous phase, according to the Stokes equation. In emulsions, this means that the oil droplets accumulate at the top (in fact, the word "creaming" comes from the top layer of compressed oil droplets observable in raw milk, forming a "cream"). However, in nanoemulsions this destabilization is reduced enough due to the small droplet size, which

allows Brownian motion to overcome gravity forces, as the diffusion rate becomes faster than the creaming rate (Izquierdo et al., 2004).

- Sedimentation: is the opposite of the last mechanism, i.e., in this case the dispersed phase possesses a higher density than the continuous phase, and therefore it sinks to the bottom. This is less common in emulsions related with drug delivery, since the used oils are usually less dense than water. In addition, this destabilization would be prevented in nanoemulsions due to the small size of the droplets, in an analogous way as destabilization by creaming.

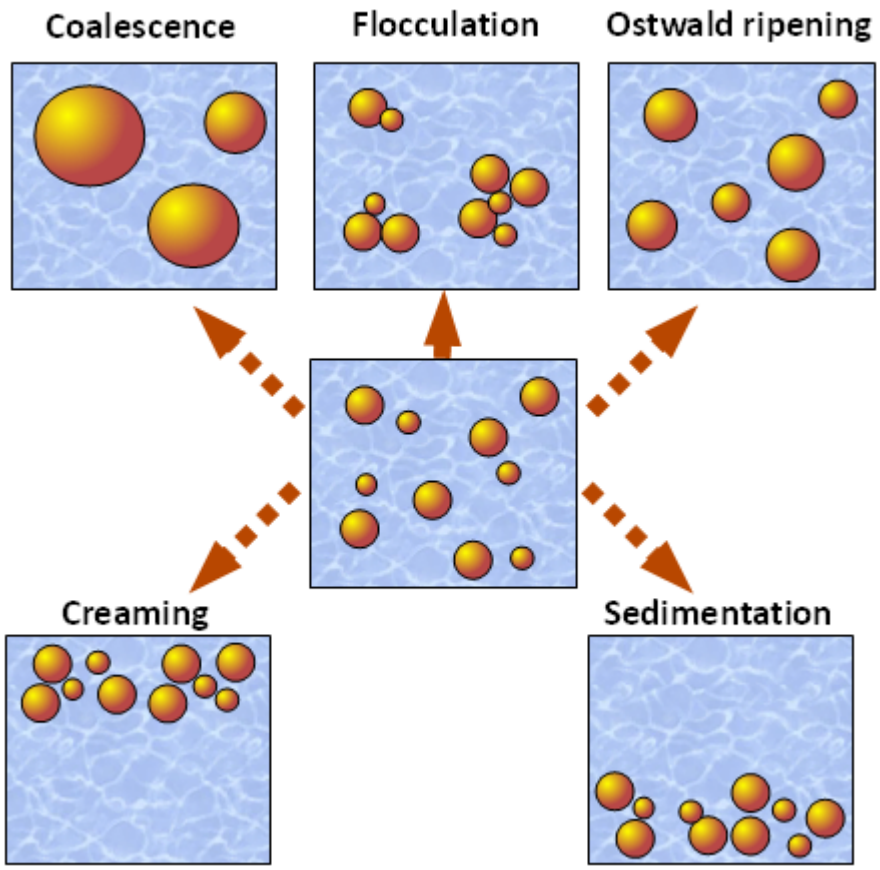

Figure 5. Schematic representation of the main destabilization mechanisms of emulsions

- Flocculation: is the aggregation of droplets without merging, i.e., the droplets retain their individual integrity (in contrast to emulsions destabilized by coalescence). It is a reversible process, and it can be prevented if the proper type and amount of surfactant is used.

- Ostwald ripening: is the process whereby the higher Laplace pressure inside small drops drives the transfer of dispersed oil from small to large drops through the dispersion medium. As a result, larger droplets grow at the expense of the smaller ones. It requires a high solubility of the disperse phase in the continuous phase, and therefore is only appreciable in emulsions of low molecular weight oils, e.g., alkanes such as decane in water. It is stated that an emulsion is stable to Ostwald ripening when at least 50% of the oil phase is an insoluble triglyceride (Wooster, Golding, & Sanguansri, 2008), such as the long chain triglycerides that conform vegetable oils, i.e., the biocompatible oils widely used in pharmaceutical emulsions. In addition, Ostwald ripening is greatly reduced if the droplets are monodisperse, i.e., if they posses a narrow size distribution, a characteristic frequently inherent to pharmaceutical nanoemulsions (Floyd, 1999). The use of a large block copolymer such as Pluronic as surfactant has been also reported to reduce Ostwald ripening, due to its strong absorption at the oil/water interface (Tadros, 1994).

Of course, these mechanisms can also combine and influence each other, e.g., creaming can lead to coalescence since the droplets are forced to come in close contact; flocculation can lead to creaming, as the aggregates of droplets are large enough to be more influenced by gravity than by their own Brownian motion, and so forth.

1.3.2 Nanoemulsions as colloids: theoretical background

Due to their nature (dispersion of one phase into another) and their small droplet size (well under a micron), nanoemulsions can be classified as colloids. As a result, a good approach to study and understand their stability is to use the theoretical background usually applied to colloidal systems. When dealing with the theory behind colloidal stability,

it is almost mandatory to start from the DLVO theory. This theory was a landmark in colloid chemistry history as the first successful attempt to explain the dependence of colloidal dispersions' stability on the ionic strength of the electrolyte, and it was named after the people who proposed it independently both in Russia (Derjaguin and Landeau) and Netherlands (Vervew and Overbeek) (Salager, 2000). . It is also worth to mention here that "colloidal stability" in this context means that the particles do not aggregate, in opposition against what we could call "mechanical stability", that refers to the floating or sedimentation of the particles (despite the fact that both types of stability are strongly related in nanoemulsions, as explained in the previous section).

The DLVO theory describes the interaction between two colloidal particles as a balance between repulsive and attractive potential energies of interaction of these particles. Hence, the total potential energy of interaction, i.e., the pair potential (V_T), is calculated as the sum of two components: an attractive one (V_A) and a repulsive one (V_R):

$$V_T = V_A + V_R \tag{1.1}$$

V_A is due to London-van der Waals (dispersion) energy and decays according to a power law with the distance of separation, whereas V_R is due to the overlap between the diffuse electrical double layers surrounding the particles, which are similarly charged, and decays almost exponentially. The non-simplified expression for the attractive potential is given by

$$V_A = -\frac{A}{6}\cdot\left[\frac{2a^2}{H(4a+H)} + \frac{2a^2}{(2a+H)^2} + \ln\frac{H(4a+H)}{(2a+H)^2}\right] \tag{1.2}$$

where A is the Hamacker constant for particles interacting with the medium (water), a is the radius of the particle and H is the distance between the surface of the particles (Hidalgo-Álvarez et al., 1996).For moderate surface potentials, the repulsive electrostatic interaction (V_R) without considering ion size can be described by the expression

$$V_R = 2\pi\varepsilon_R\varepsilon_0\left(\frac{4k_BT}{z_ie}\gamma\right)^2 e^{-\kappa H} \tag{1.3}$$

where ε_0 is the permittivity of the vacuum, ε_R is the dielectric constant of the electrolyte solution, e is the elementary charge, k_B is the Boltzmann constant, T is the absolute temperature, κ is the Debye parameter referred to as the reciprocal double-layer thickness, and γ is defined as

$$\gamma = \tanh\left(\frac{z_i e \psi_d}{4 k_B T}\right) \tag{1.4}$$

being Ψ_d the diffuse potential (Ortega-Vinuesa, Martín-Rodríguez, & Hidalgo-Álvarez, 1996). The total or partial energies of interaction are usually plotted against the interparticle distance, obtaining curves like those plotted in Figure 6. In the first case, the attractive force is prevailing at every interparticle distance and thus the two approaching interfaces will get into contact sooner or later. The minimum of the curve, called *primary minimum*, corresponds to the notion of contact and occurs at an essentially zero distance. In this scenario, the particles will aggregate and, if they are fluid (e.g. nanoemulsions), coalescence will take place. In the second case, nevertheless, a prevailing repulsive interaction is observed. This barrier is called *primary maximum*. If the value of this repulsive potential is high enough, no particle would possess the sufficient kinetic energy to surpass it, and the repulsion would end up dominating, with a resulting colloidal stability. It is generally assumed that this repulsive barrier should be at least higher than 15 k_BT to effectively avoid aggregation/coalescence (De Vleeschauwer & Van der Meeren, 1999). In the third case, there is a second region where the attractive force predominates over the repulsive one. This is called the *secondary minimum*, and is considerably less deep than the first one, as the long-range attractive forces are weak forces at this distance. Hence, a small amount of kinetic energy, like mechanical mixing, can offset it to redisperse the particles. This kind of aggregation is frequently called *flocculation*, and corresponds to the phenomenon described before in the section regarding nanoemulsion stability (as a reversible aggregation of droplets that are not close enough to suffer coalescence). This phenomenon often occurs when the repulsive forces of the second case are weakened, e.g., by adding electrolytes. In this case, the potential well should be below -15 k_BT for the particles to experience flocculation and above -100 k_BT to be redispersed with moderate shearing forces (Goodwin, 2009).

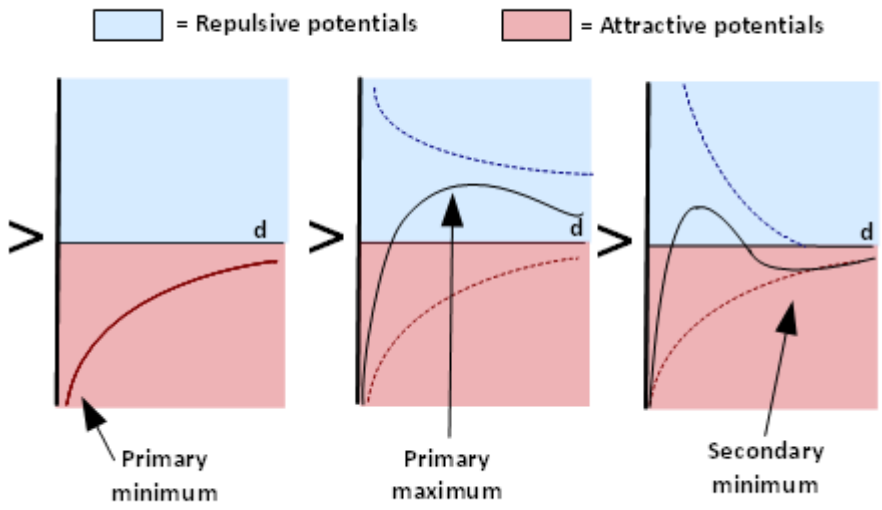

Figure 6. Examples of potential curves obtained from plotting interaction potentials versus interparticle distance: solid lines, total potential; dotted lines, partial potentials.

DLVO theory allowed to explain and to predict a series of phenomena related with the electrostatic stabilization of colloidal systems. However, it started to fail when it was applied to slightly different systems, especially when non-ionic surfactants were used. The effect of long polymeric surfactants led to additions and modifications of the original DLVO theory, turning it into what is known today as "extended DLVO"(Hidalgo-Álvarez et al., 1996). As a way of example, it was necessary to introduce the effect of the steric repulsion, since the original DLVO recognized only electrostatic repulsion. This steric repulsion, caused by the long polymeric surfactants, is the combination of two effects: on the one hand, an enthalpic contribution that has been also referred to as osmotic repulsion (Tadros, 1986), V_{OSM}, because it is related with the spontaneous flow of solvent into the interparticle zone, which pushes the particles apart in the region where adsorbed surfactant layers overlap. Therefore, this effect takes place when the particles approach each other to slightly less than twice the thickness of the adsorbed surfactant layer, and its contribution can be expressed as

$$V_{OSM} = \frac{4\pi a}{\upsilon_1}(\phi_2)^2\left(\frac{1}{2}-\chi\right)\left(\delta-\frac{H}{2}\right) \tag{1.5}$$

where υ_1 is the molecular volume of the solvent, ϕ_2 is the effective volume fraction of segments in the adsorbed layer, χ is the Flory–Huggins solvency parameter, characteristic of the polymer for a given solvent, and δ is the thickness of the adsorbed polymer layer. On the other hand, if the particles are closer than a distance equal to δ, a new repulsive effect takes place when some of the polymer molecules are forced to undergo elastic compression. Thermodynamically, this compression corresponds to a net loss in configurational entropy, as the polymer chains lose degrees of freedom due to restriction of their motion. This effect is expressed as

$$V_{EL} = \left(\frac{2\pi a}{Mw_2}\phi_2\delta_2\rho_2\right)\left[\frac{H}{\delta}\ln\left(\frac{H}{\delta}\left(\frac{3}{2}-\frac{H}{2\delta}\right)^2\right)-6\ln\left(\frac{3}{2}-\frac{H}{2\delta}\right)+3\left(1+\frac{H}{\delta}\right)\right] \tag{1.6}$$

being ρ_2 and Mw_2 the density and the molecular weight of the polymer forming the hydrophilic tail, respectively (Einarson & Berg, 1993). At this distance, i.e., when $H<\delta$, the osmotic contribution is also slightly modified, and the expression given by Eq. 1.5 turns into

$$V_{OSM} = \frac{4\pi a}{\upsilon_1}(\phi_2)^2\left(\frac{1}{2}-\chi\right)\left(\delta-\frac{H}{2}\right)\delta^2\left(\frac{H}{2}-\frac{1}{4}-\ln\left(\frac{H}{2}\right)\right) \tag{1.7}$$

As in the original DLVO, the total interaction energy is assumed to be the sum of all the attractive and repulsive potentials. E.g., in this last case, the pair potential will be given by

$$V_T = V_A + V_R + V_{OSM} + V_{EL} \tag{1.8}$$

The study of the stabilizing effects of polymeric surfactants has introduced modifications also in the equations describing the attractive potentials. E.g., the adsorption onto a dispersed particle of a layer that is chemically more similar to the solvent than to the particle itself causes a decrease in the effective Hamaker constant (Rosen, 2004). This influence on the Hamaker constant was thoroughly studied by Vincent (Vincent, 1973),

taking into account the non-homogenous character of adsorbed polymer layers as well. As a result, the Hamaker constant to be used in the calculation of the attractive potential for these systems would be given by

$$A = \left(\Phi A_P^{1/2} + (1-\Phi) A_M^{1/2}\right)^2 \tag{1.9}$$

where Ap is the Hamaker constant of the adsorbed polymer, A_M the constant of the medium and Φ the volume fraction of the polymer at a separation H, given by

$$\Phi = \frac{2\delta\Phi_0}{H} \tag{1.10}$$

where Φ_0 is the volume fraction of the polymer on the surface of the particle.

Finally, a last effect related with polymeric surfactants should be highlighted in this introduction. Vincent et al. (Vincent, Luckham, & Waite, 1980) studied the theory behind the flocculation caused by the addition of a non-adsorbing polymer to a sterically stabilized colloidal dispersion. Later, it was demonstrated that this destabilization could be caused also by an excess of surfactant, especially when this surfactant is able to form micelles (Ma, 1987). The mechanism for this counter-intuitive destabilization driven by an excess of surfactant is called depletion-flocculation, and is depicted in Figure 7. After interface saturation by the adsorbed surfactant, the micelles do not adsorb on the surfactant coated surface of the droplets. Thus, when two droplets approach in a solution of non-adsorbing micelles, the latter are expelled from the gap, generating a local region with almost pure solvent. The osmotic pressure in the liquid surrounding the particle pair exceeds that between the drops and consequently forces the droplets to aggregate (Tuinier, Rieger, & de Kruif, 2003).

The theorical study of this phenomenon started with the works of Asakura and Oosawa describing the attraction experienced by two plates immersed in a solution of ideal non-adsorbing polymers. These studies were further expanded in the 1980s as mentioned previously, and in 1994 Walz et al. developed a theoretical model to study the interaction between two spherical particles due to the presence of spherical macromolecules (Walz &

Sharma, 1994), a model that was successfully adapted and applied recently to describe the experimental behavior of polystyrene nanoparticles under a wide range of ionic surfactant concentrations (Jódar-Reyes, Martín-Rodríguez, & Ortega-Vinuesa, 2006). This model is described by the equation

$$\frac{V_{dep}}{k_B T} = -\rho_\infty \pi \left(\frac{4}{3} r^3 + 2r^2 a - r^2 H - 2raH + \frac{aH^2}{2} + \frac{H^3}{12} \right) \qquad (1.11)$$

in the range $0 < H < 2r$, where r is the radius of the micelle and ρ_∞ is the number of micelles per unit volume in the system.

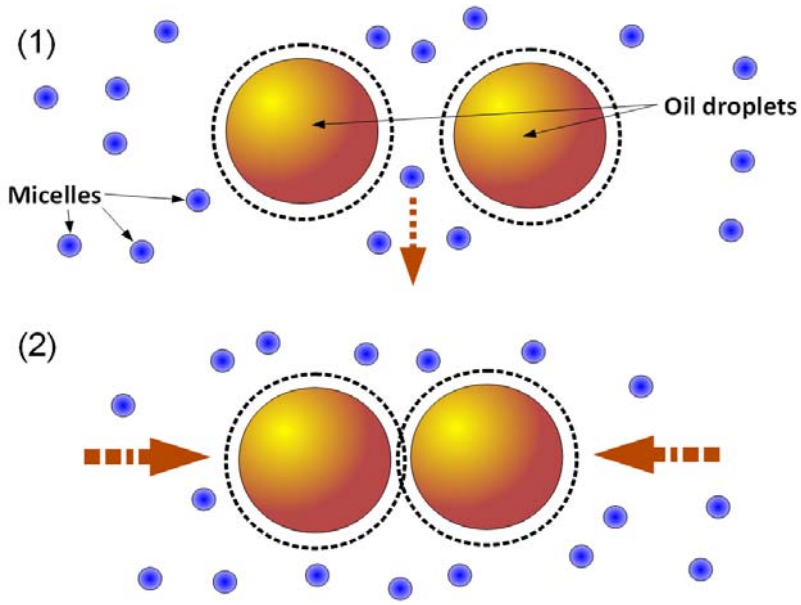

Figure 7. Schematic representation of the depletion mechanism: 1) the micelles are expelled from the gap; 2) The osmotic pressure surrounding the pair of droplets forces them to join.

As can be deducted from the equations showed in this section, an in-depth characterization of the system is necessary to provide realistic results that explain the mechanisms of stability and instability of nanoemulsions. This characterization includes parameters such as droplet size, micelle size or the concentration of surfactant present

when the destabilization process takes place. The experimental details referred to the obtaining of these parameters will be explained in Chapter 2.

1.4 Rheology of nanoemulsions

The first use of the word "Rheology" is credited to Eugene C. Bingham, inspired by the quotation mistakenly attributed to Heraclitus (actually coming from Simplicius) *panta rei*, meaning "everything flows" (Steffe, 1992). Rheology is now well established as the science of deformation and flow of matter, i.e., it studies the response of a material (deformation or strain) to a superimposed stress (force per unit area) as a function of time. Regarding emulsions and suspensions, the relationship between the force applied to the system and the type of flow observed is not a trivial issue, as it will depend on many factors. However, to study this relationship is of great interest due to many reasons:

- Correlation between the interparticle interactions and the rheological behavior. The manner in which the particles (or droplets) repel or attract each other influences the flow properties of a dispersion (van Vliet & Lyklema, 2005). As a result, it is possible to obtain information about the interparticle interactions by measuring the rheological properties of the system. Furthermore, understanding the relation between structure and rheology will allow the design of products with specific rheological properties.

- Impact of the rheological properties on the final stability of emulsions. The interfacial rheology is assumed to play an important role in destabilization mechanisms such as coalescence or Ostwald ripening (Georgieva, Schmitt, Leal-Calderon, & Langevin, 2009). In addition, this interfacial rheology is strongly related to the bulk-phase macroscale rheology of some emulsions, such as those with a high concentration of droplets. Furthermore, there is a correlation between rheological properties and the pair potential (Goodwin, Hughes, Partridge, & Zukoski, 1986), being this potential the same that was used to describe the stability of nanoemulsions in the previous section.

- Direct influence of the rheological properties on the stages involved in the preparation of emulsions in several industrial branches, as well as on the final applications. For example, in food manufacturing the rheological properties will determine filling/dosing behavior, shelf stability and sensorial properties (such as consistency, coarseness or roughness); in cosmetics and pharmaceutics, they could have an impact on the efficiency of drug delivery,

as well as on the effectiveness and the protection of a cream or lotion; in paint industry, they will influence quality parameters such as lightness, adhesion, spreadness or stability (Fischer & Windhab, 2011; Briceño, 2006; Carreau, Lavoie, & Yziquel, 1999).

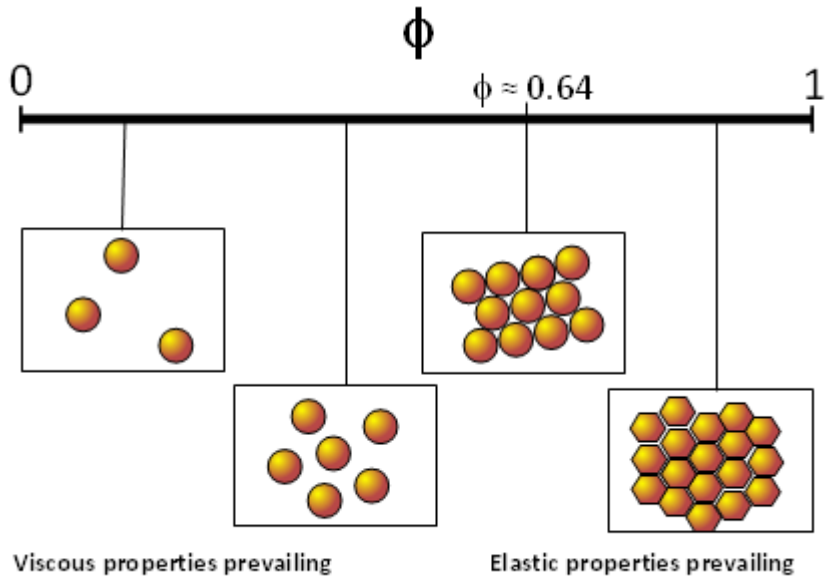

Figure 8. Schematic representation of droplet bidimensional structure and morphology for monodisperse emulsions as a function of the volume fraction of the dispersed phase, from a diluted system to a compressed one.

These interrelationships between the interfacial composition of dispersed systems, their stability and their rheological properties are better observed when the fraction volume of dispersed particles is high. As depicted in Figure 8, if the number of particles is increased, the interparticle distance decreases, i.e., the particles are forced to come into closer contact. If the particles are spherical, it can be deducted from geometry that the relationship between interparticle separation and volume fraction is given by the expression

$$H = d\left(\left(\frac{\phi_{MAX}}{\phi}\right)^{1/3} - 1\right) \tag{1.12}$$

where H is the interparticle separation, d is the diameter, ϕ is the volume fraction and ϕ_{MAX} is the maximum packing fraction, defined as the highest volume fraction of solid particles that can be achieved (Saiki, Prestidge, & Horn, 2007), e.g., the value of ϕ_{MAX} will be approximately 0.64 if we consider the particles to be random close-packed; for a face-centered cubic structure, $\phi_{MAX}\approx0.74$, and so forth. From equation 1.12, the main differences between the study of the rheology of suspensions, conventional emulsions and nanoemulsions can be inferred, as well as the increasing influence of the interfacial composition on this rheology. Unlike suspensions, the particles dispersed in emulsions and nanoemulsions are liquids, i.e., the droplets are highly deformable. This implies that they can be compressed and therefore they are able to achieve a volume fraction of almost 1 (Mason, 1999), as shown in Figure 8. For these systems, ϕ_{MAX} is more appropriately defined as the maximum volume of particles that the emulsion may contain without deformation of the particles (Briceño, 2006). As for the difference between conventional emulsions and nanoemulsions, if we consider a relatively concentrated system ($\phi=0.60$) with typical sizes for both types of emulsions (e.g., d=2μm and d=200nm), then the interparticle separation given by equation 1.12 would be H≈130-150 nm for conventional emulsions and H≈13-15 nm for nanoemulsions. This last distance is in (or very close to) the range of the interaction forces between droplets described in section 1.3.2, which means that the flow of the droplets after applying stress to the system will be greatly affected by these interactions. This presents a scenario where the relationship between interfacial composition and rheological properties is particularly magnified, remarking the differences between the study of the rheology of nanoemulsions and that of suspensions and conventional emulsions, in addition to the other special characteristics of nanoemulsions. In spite of this, although there is a considerable number of studies and extensive reviews concerning rheology of suspensions and emulsions (Barnes, 1994; Pal, 2011; Tropea, Yarin, & Foss, 2007), the literature devoted to nanoemulsion rheology is scarce. This lack of studies can be observed in the graphic represented in Figure 9. In addition to this, to the best of our knowledge there was no article relating specifically the influence of the surfactant on the final rheological properties of nanoemulsions. In our opinion, this sole fact justifies the studies presented in this work, both from a theoretical and a practical point of view.

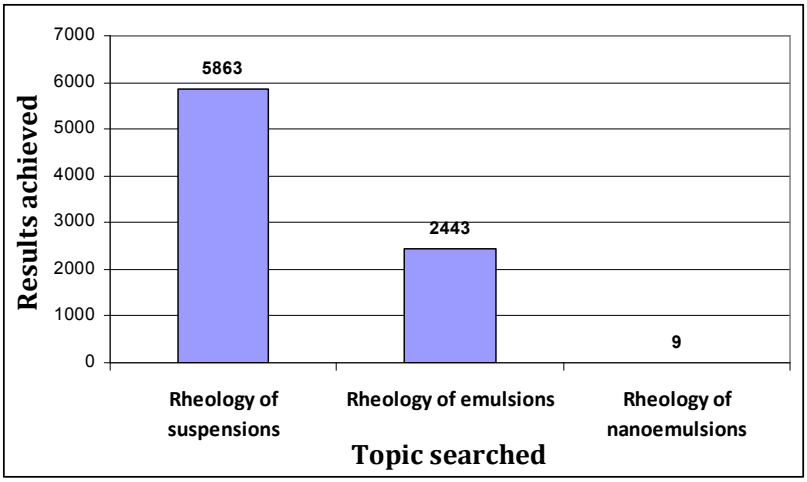

Figure 9. Results of searching in Web of Knowledge the topics "rheology of suspensions", "rheology of emulsions" and "rheology of nanoemulsions", March 2012.

1.4.1 Rheological properties of dispersed systems: basic concepts

When stress is imposed to a material, it is possible to observe two extremes of the spectrum of behavior: elastic solid (total storage of energy) or viscous liquid (total dissipation of energy). An ideal elastic material deforms instantaneously to a certain extent when a stress is applied, and regain its original shape after the stress has been removed. An ideal viscous material flows at a certain rate when a stress is applied and it retains the same shape after removal of the stress. The first behavior is described by Hooke´s law,

$$\tau = G \cdot \gamma \tag{1.13}$$

being τ the stress applied, γ the strain or deformation produced and G the elastic modulus, with a constant value. The opposite behavior is described by Newton´s law,

$$\tau = \mu \cdot \dot{\gamma} \tag{1.14}$$

where $\dot{\gamma}$ is the shear rate (the time derivative of the strain, i.e., the rate at which the material is deformed) and μ the viscosity of the material, a constant in this case (van Vliet & Lyklema, 2005). However, some materials exhibit both elastic and viscous characteristics, and therefore they are called "viscoelastics". Emulsions frequently present this kind of behaviour, which is influenced by several factors such as the nature of the emulsion (O/W) (W/O), the physical state (crystallized, liquid), the droplet concentration or the structure (agregated, non-aggregated) (Tropea et al., 2007). In these systems, the viscosity at a fixed temperature is not a constant anymore, and therefore new parameters are necessary to describe their rheological properties: the rheological material functions. These functions are always defined for a given standard flow, which may be extensional, elongational… In this introduction two of them will be described, since both were used to characterize the nanoemulsions.

- **Simple shear:** this flow is based on a system consisting on two parallel plates, the lower one being stationary and the upper plate moving linearly with a certain velocity, as represented in Figure 10. The material to be measured will be present between the two plates.

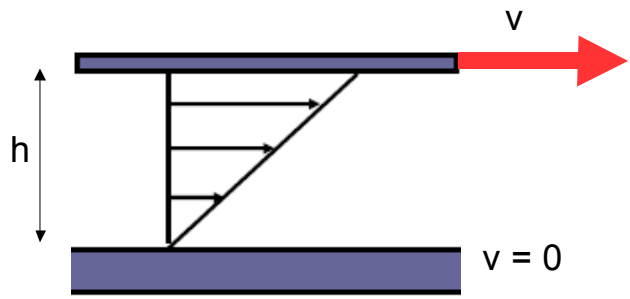

Figure 10. Schematic representation of the velocity profile of simple shear flow.

Simple shear experiments provide us with an important material function, the shear viscosity, defined as

$$\eta = \frac{\tau}{\dot{\gamma}} \tag{1.15}$$

Thus, in a typical experiment based on simple shear, a shear stress is applied while the shear rate is measured (or vice versa), obtaining the shear viscosity, which can be interpreted as the opposition to flow under shear. It is worth to highlight that in rheological literature this shear- and time-dependent viscosity is represented by the letter η, in opposition with the traditional, shear-independent Newtonian viscosity, represented by the letter μ. In this dissertation this notation will be respected.

Viscosity is usually represented in double log plots against shear rate, also known as *flow curves*, as depicted in Figure 11. Flow curves obtained from dilute emulsions are close to that of Newtonian fluids, with very little or no change in viscosity as the shear rate is modified (Mason, 1999). However, the flow curves obtained split up from the Newtonian behaviour as the volume fraction increases, i.e., viscosity becomes more dependent on shear rate. These emulsions frequently show a decreasing viscosity while shear rate increases. This is known as *shear-thinning* behavior and is typical from colloidal systems where the interactions between the particles create a microstructure: the increasing shear rate breaks down this colloidal structure and therefore the viscosity is reduced (Briceño, 2006). Hence, most of the information regarding droplet-droplet interactions is obtained from the low shear range. In this range, it is possible to find also another rheological property indicative of the formation of a three-dimensional structure under no-flow conditions: the presence of an *apparent yield stress*. This means that it is necessary to apply a minimum stress to induce the flow, remaining the system unchanged when lower stresses are applied. An apparent yield stress is inferred from the slope of -1 in the log-log representation and from the absence of a plateau at low shear rates (Pal, 1999) (see Figure 11). Its presence has been reported for dispersions of particles both electrostatically and sterically stabilized (Quemada & Berli, 2002). In general terms, the magnitude of this yield stress is known to increase with increasing particle volume fraction, decreasing particle size, and increasing magnitude of interparticle forces (Genovese, Lozano, & Rao, 2007).

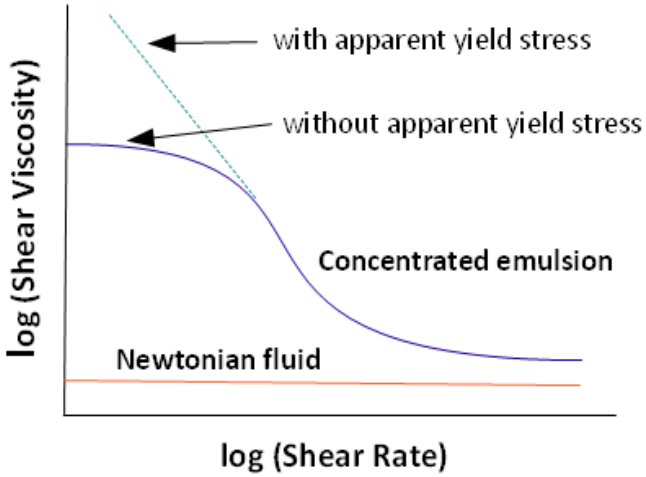

Figure 11. Typical flow curves obtained from simple shear experiments for a newtonian fluid and for a concentrated emulsion.

- Small Amplitude Oscillatory Shear (SAOS): this flow is based on a system where a small sinusoidal shear deformation with radian frequency ω is applied, oscillating around an equilibrium position. To illustrate this, consider again two parallel plates, the lower one fixed and the upper plate moving back and forth in a horizontal direction (see Figure 12).

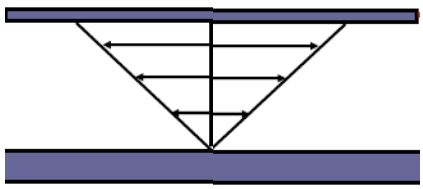

Figure 12. Representation of oscillatory shear.

From experiments based on SAOS it is possible to obtain information and quantify both the elastic and viscous properties of the emulsion. If an oscillatory stress is applied, the deformation produced in an elastic material will be in phase, whereas for a viscous material this deformation will be 90º out of phase, i.e., there will be a phase lag $\delta = 90º$. For a viscoelastic material, this lag will be between these two extremes, i.e., $0º<\delta<90º$, as depicted in Figure 13.

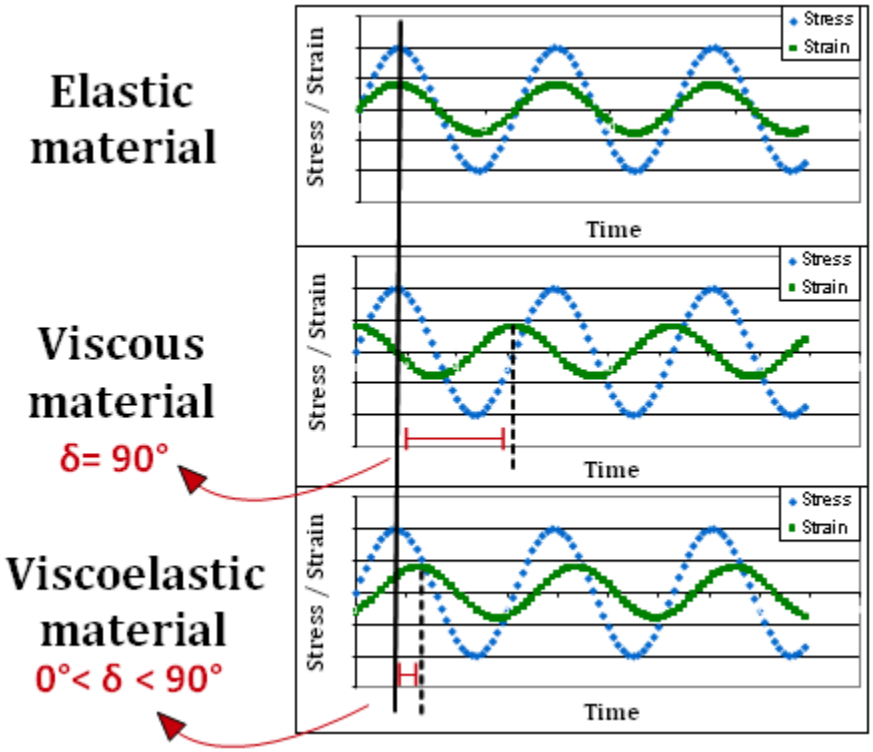

Figure 13. Relationship between stress and strain in oscillatory tests for an elastic, a viscous and a viscoelastic material.

Therefore, if a small sinusoidal strain input is applied,

$$\gamma = \gamma_0 \sin(\omega t) \tag{1.16}$$

then the stress may be expressed as

$$\tau = \tau_0 \sin(\omega t + \delta) \tag{1.17}$$

which expanding the sine of the sum gives rise to

$$\tau = \tau_0 \sin(\omega t)\cos\delta + \tau_0 \cos(\omega t)\sin\delta \tag{1.18}$$

and dividing by the amplitude of the strain, γ_0 ,

$$\frac{\tau}{\gamma_0} = \frac{\tau_0}{\gamma_0}\cos\delta \sin(\omega t) + \frac{\tau_0}{\gamma_0}\sin\delta \cos(\omega t) \tag{1.19}$$

which may be also written as

$$\frac{\tau}{\gamma_0} = G' \sin(\omega t) + G'' \cos(\omega t) \tag{1.20}$$

G´ is called the *shear storage modulus*, and is a measure of the amount of energy stored during a periodic application of stress. G´´ is the *shear loss modulus*, which is a measure of the energy dissipated during the periodic application of stress. The ratio between the second and the first is called the *loss tangent*, given by

$$\tan\delta = \frac{G''}{G'} \tag{1.21}$$

It is worth noting that these equations (and therefore the values of G´ and G´´) are only valid if the amplitude of the strain is small. G´ remains constant until a maximum value of strain amplitude is reached. This point marks the end of the *viscoelastic linear region*, i.e., the range of strain amplitudes where these equations are applicable. It is generally assumed that, over this range, measurements do not affect the microstructure of the sample, closely related to the interaction between droplets, and hence the measured shear modulus reflects both the interparticle energy and the structure (Quemada & Berli, 2002). The change from a liquid-like (G´´>G´) to a gel-like (G´>G´´) behavior is also linked to an increase of the interactions between particles (Tropea et al., 2007).

In addition to the interest in the study of nanoemulsion rheology per se, described at the beginning of this section, it is clear that there is a series of rheological properties strongly affected by fundamental characteristics of nanoemulsions. Therefore, a complete characterization of the nanoemulsion rheology should provide us with a clearer picture of our own system and the relationships between surfactants, droplets and interparticle forces.

1.5 Metabolic degradation of nanoemulsions

The ultimate goal of a drug delivery system is to deliver the drug at the right time in a safe and reproducible manner. However, the performance of a drug delivery system administered into the human body will depend on a complex array of physicochemical and biological factors (Moghimi & Hamad, 2009). Several factors such as ionic strength, pH, enzymes or immunological proteins will have a major impact on the drug release system, and they could be even used to control the drug release. In addition, these factors will differ depending on the organs or tissues involved in every route of administration. Therefore, a clear understanding of their influence is crucial for the rational development and optimization of a drug delivery system that suits our requirements.

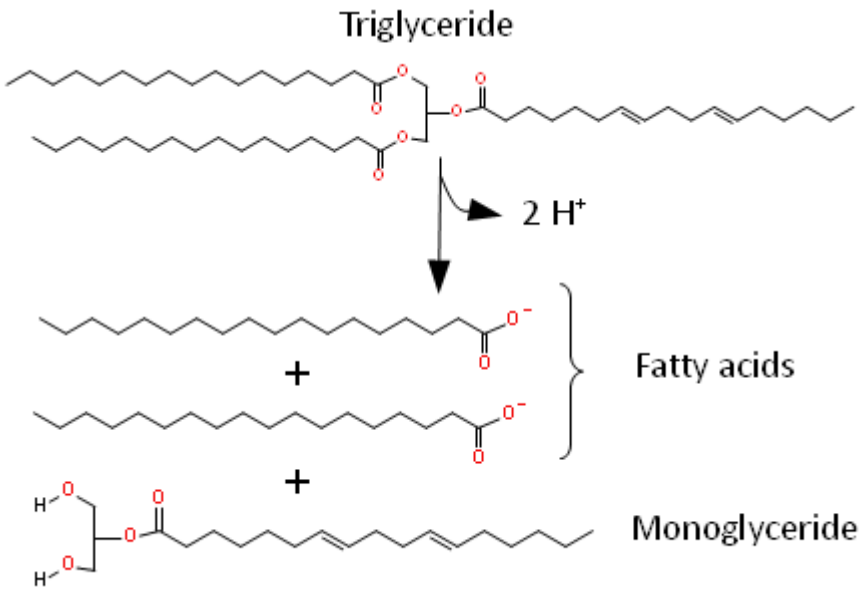

Figure 14. Reaction scheme of lipolysis, the enzymatic hydrolysis of triglycerides carried out by lipases.

In this dissertation, we will study the biodegradation of nanoemulsions to be administered by two different routes: oral and intravenous. As nanoemulsion droplets are composed of triglycerides, their biodegradation will be strongly related to the enzymatic hydrolysis of these triglycerides, i.e., the lipolysis, in which triglycerides are cleaved into diglycerides, monoglycerides and free fatty acids, as depicted in Figure 14. The main aspects concerning the lipolysis and the final fate of nanoemulsions when they are administered either orally or intravenously will be discussed in this section, as well as the implications for the rationale design of nanoemulsions as drug delivery systems.

1.5.1 Orally administered nanoemulsions

Oils and lipid-based systems are digested and absorbed within the gastrointestinal tract when administered via oral route. The first organ where the composition may affect strongly the emulsions is the stomach. As a way of example, due to the low pH, typically between 1-2 (Dressman, Amidon, Reppas, & Shah, 1998), the emulsion stability would be compromised if the emulsion is stabilized with labile surfactants, or if the electrostatic-stabilized droplets lose their net charge due to protonation. In addition, emulsions stabilized with proteins may also lose their stability, as the proteases of the stomach cleave easily the proteins when they are adsorbed at interfaces (Maldonado-Valderrama, Gunning, Wilde, & Morris, 2010). Regarding the processing of the triglycerides comprising the nanoemulsions, it may also begin in the stomach, as acid-stable lipases are present, mainly gastric lipase. This lipase hydrolyses the medium-chain triglycerides (predominantly those with 8- to 10-carbon chain lengths) better than it hydrolyses the long-chain triglycerides (Porter et al., 2008). The first ones are more common for preparing solid lipid nanoparticles, while the last ones are more frequently used in nanoemulsions. Gastric lipase is especially important for the absorption of lipids in newborns, but in healthy adult humans it only hydrolyzes 10–30% of ingested triglycerides (Singh, Ye, & Horne, 2009), and therefore plays an insignificant role in the overall lipid digestion in healthy human adults (Sarkar, Goh, Singh, & Singh, 2009).

1. Introduction

The majority of the lipid digestion occurs after the gastric stage, when the lipid droplets arrive to the duodenum (Wilde & Chu, 2011), the first part of the small intestine.

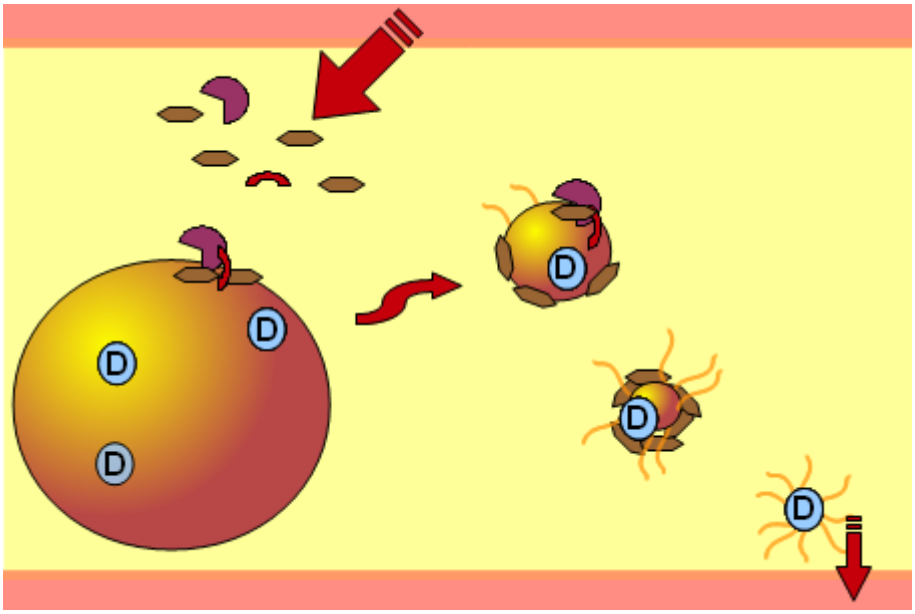

Figure 15. Scheme of the main processes involved in duodenal lipolysis.

These lipids are mixed there with secretions from the gallbladder, containing bile salts and phospholipids, and from the pancreas, containing pancreatic lipase and colipase (Di Maio & Carrier, 2011), as represented in Figure 15. Pancreatic lipase is the enzyme responsible for most of the digestion of the orally administered lipids, and cleaves the triglycerides at the sn-1 and sn-3 positions, producing 2-monoglyceride and free fatty acids (Hur, Decker, & McClements, 2009). Bile salts have two principal roles: on the one hand, they displace adsorbed molecules such as proteins and phospholipids from the oil-water interface (Torcello-Gómez et al., 2011), removing potential inhibitors of pancreatic lipase; on the other hand, they help to solubilize the products of lipolysis forming mixed micelles, cleaning the interface from monoglycerides and free fatty acids that also act as inhibitors for lipases (Porter et al., 2007). Pancreatic lipase needs the presence of a cofactor, named colipase, for the efficient lipolysis of lipids. Colipase helps the lipase to anchor to a bile salt-covered interface and activates the lipase through a conformational change (Lowe, 2002; Miled et al., 2001).

During enzymatic digestion, lipolysis products leave the droplet forming a series of colloidal structures, including multilamellar and unilamellar vesicles, micelles and mixed micelles, since they are notably more soluble than the former triglycerides. In this step, hydrophobic drugs leave the droplets within these species, which significantly increase the solubilization capacity of the small intestine for these drugs (Rübe, Klein, & Mäder, 2006).As highly hydrophobic drugs are frequently absorbed in these colloidal digestion phases, there is a direct link between lipid digestion and bioavailability (Kaukonen, Boyd, Charman, & Porter, 2004).

Most of the hydrophobic drugs and nutrients to be administered orally are absorbed by the enterocytes (Porter et al., 2007), which are epithelial cells present in the inner surface of the small intestine and colon. Thus, nanoemulsions for the delivery of one of these drugs should protect the drug against the harsh gastric conditions and remain intact themselves while passing the stomach, allowing the drug to arrive mostly unaffected to the duodenum. There, the nanoemulsion should be degraded to allow the partitioning of the drug between small, more water-soluble colloidal species. The control of this degradation will be then the main objective of the experiments regarding duodenal lipolysis. As previously explained, phospholipids are rapidly cleared from the interface by bile salts, preventing the control of the lipolysis if phospholipids are used as surfactants. For this reason, the release of drugs from traditional emulsions stabilized with these surfactants has been considered unpredictable (Buszello & Muller, 2000). The study of the impact of a different type of surfactant on the duodenal lipolysis should help us to design nanoemulsions with a controllable oral biodegradation.

1.5.2. Intravenously administered nanoemulsions

For a great number of bioactive compounds, the most direct route is the intravenous one, leading to high bioavailability because of the absence of an absorption process. In addition, if nanoemulsions are administered by other parenteral routes, e.g., intraperitoneally, subcutaneously, or intramuscularly, the majority of droplets enter the

lymphatic system and eventually the blood circulation where particles behave as if given intravenously (Buszello & Muller, 2000).

When lipid-based systems are administered intravenously, they can be recognized as foreign bodies, or they can enter the normal lipid metabolism pathway (Rossi & Leroux, 2007). In the first case, immune proteins present in plasma adsorb to the lipid-water interface, a process known as *opsonization*. Then, these proteins interact with receptors of the cells of the mononuclear phagocyte system (MPS), i.e., phagocytic cells such as monocites and macrophages that remove pathogens from blood to retain them in immune system organs (mainly liver, spleen or bone marrow) (Moghimi & Hamad, 2009). As MPS is also known as reticuloendothelial system (RES), this process is frequently found in the literature as *RES uptake*. In addition, the small changes in hydrophobicity of the oil/water interface may lead to significant changes in RES uptake, since hydrophobic particles are taken up by macrophages even without the necessity of opsonization (Buszello & Muller, 2000). For these reason, the use of steric surfactants such as polymers, more hydrophilic than phospholipids, reduces RES uptake of nanoemulsions considerably, by a combination of a decrease of the interfacial hydrophobicity of the droplet and steric hindrance, which prevents the adhesion of immune proteins (Illum, West, Washington, & Davis, 1989).

If nanoemulsions avoid this elimination mechanism, they will be recognized as chylomicrons and will be biodegraded via the lipid metabolism pathway. Chylomicrons are endogenous emulsions produced by the enterocytes of the small intestine after dietary lipids have been ingested. They are mainly composed of triglycerides and present a droplet size matching that of nanoemulsions. Chylomicrons belong to the family of the lipoproteins, which are responsible for the transport and delivery of lipids through the blood. The fate of lipoproteins will be determined by the presence of some proteins at their surface, known as apolipoproteins. One of these apolipoproteins is apolipoprotein-CII, which is obtained by chylomicrons from high-density lipoproteins. If chylomicrons possess apolipoprotein-CII at their surface, the triglycerides of chylomicrons are hydrolyzed into free fatty acids by a protein anchored to the endothelium, called lipoprotein lipase (LPL). The released fatty acids are transported into predominantly adipose and muscle tissue, frequently bound to the albumins of the blood (Rensen & van

Berkel, 1996).This lipolysis is an analogous process to that of duodenal lipolysis, with LPL, apolipoprotein-CII and albumin playing the role of pancreatic lipase, colipase and bile salts, respectively.

Nanoemulsions differ from chylomicrons in that they do not have apolipoproteins on their surface before entering the bloodstream, although they acquire these proteins soon after injection into the systemic circulation, being metabolized in a pathway comparable to that described for chylomicrons (Rossi & Leroux, 2007). Therefore, the biodegradation of nanoemulsions and the subsequent release of highly hydrophobic drugs will be directly related with the lipolysis rate also under intravenous conditions.

Although the recognition of lipid-based systems as foreign bodies has been extensively studied and reviewed (Harris, Martin, & Modi, 2001; Liu & Liu, 1995; Tamilvanan, 2009; Ueda, Kawaguchi, & Iwakawa, 2008), the literature concerning the lipolysis under intravenous conditions is scarce and covered only for a few groups (Kurihara et al., 1996; Rensen & van Berkel, 1996; Ton, Chang, Carpentier, & Deckelbaum, 2005; Yamamoto et al., 2003), and just one of them specifically devoted to drug delivery systems. The impact that this lipolysis could have on a lipid-based drug delivery system is also frequently ignored in studies involving in vitro testing, even for systems that have already proven to be stable against elimination by MPS. For these reasons, one objective of this dissertation will be then to study this lipolysis, and especially how the structure and properties of surfactants affect it, in order to use this knowledge to design nanoemulsions with the desired biodegradation rate.

Chapter 2. Experimental details

2.1 Surfactants

In this dissertation, special importance has been attached to the nature and characteristics of the surfactants used to prepare the nanoemulsions. The main reasons were to study how steric surfactants confer different properties to the nanoemulsions that they stabilize, in comparison with traditional ionic surfactants, and to determine the way in which the structure of these surfactants affects these properties. In order to do so, three main families of surfactants were used: phospholipids, Pluronics and Myrjs.

2.1.1 Phospholipids

Phospholipids are composed by two hydrophobic tails and a polar, hydrophilic head, as depicted in Section 1.2. The hydrophobic tails are two fatty acids, while the hydrophilic head is formed by a phosphate group linked to another polar group, which will define the type of phospholipid. In our experiments, a commercial mixture of phospholipids known as Epikuron 145 V has been used. Epikuron 145 V is a highly purified deoiled phosphatidylcholine-enriched fraction of soybean lecithin, which contains 61% phosphatidylcholine, 22% phosphatidylethanolamine and 16% phytoglycolipids and provides the droplets with a negative net charge (De Vleeschauwer & Van der Meeren, 1999). Epikuron 145 V has been successfully used to stabilize lipid nanocapsules with pharmaceutical purposes (Santander-Ortega, Lozano-López, Bastos-González, Peula-García, & Ortega-Vinuesa, 2010).

2.1.2 Pluronics

This family of polymeric surfactants is starting to be widely used in a variety of oral, parenteral, and topical pharmaceutical formulations and are generally regarded as nontoxic and nonirritant materials (Rowe, Sheskey, & Weller, 2006). Due to the possibility to combine blocks of different molecular weights, the properties of the resulting polymers vary in a wide range, as explained in Section 1.2. E.g., depending on the proportion between blocks, they will present a different physical state at room temperature, which is

designated by a capital letter: F for flakes, P for paste, L for liquid. When named as Pluronics, the numbers following the letter allow us to know size and proportion of the different blocks: the first digit (or the first two digits in a three-digit number) multiplied by 300, indicates the approximate molecular weight of the hydrophobic moiety; and the last digit multiplied by 10 gives the percentage of polyoxyethylene content (Pasquali, Chiappetta, & Bregni, 2005). For example, Pluronic F68 will present a solid, flake-like structure at room temperature, the molecular weight of POP will be around 6X300 = 1800 g/mol and each molecule will possess an 80% of POE. Throughout this dissertation, three different Pluronics were used, represented in Figure 16a.

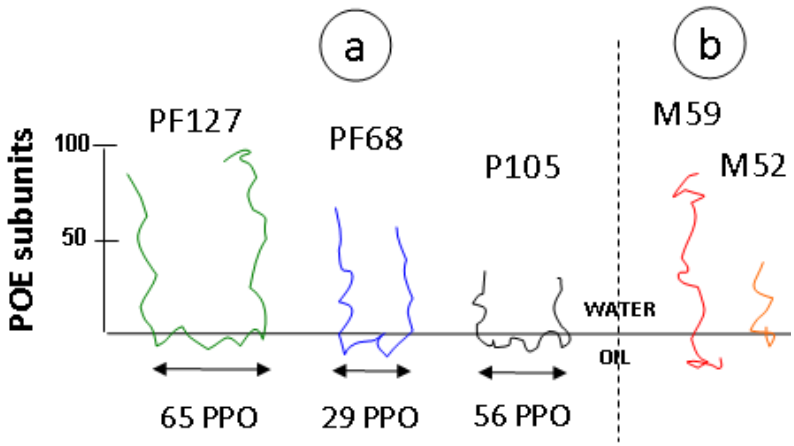

Figure 16. Schematic representation of the steric surfactants used. a) Pluronics, b) Myrjs.

-Pluronic F68: also known as poloxamer 188, its very low toxicity has led it to be accepted by the FDA for oral, topical, ophthalmic, periodontal, subcutaneous and intravenous administration, with relatively high doses of administration (10% oral, 0.60% intravenous (FDA, 2012)). Pluronic F68 possesses 75 subunits of POE in each tail, and 29 subunits of POP in the central block, and its molecular weight is 8400g/mol. Despite having a hydrophobic block notably smaller than the hydrophilic one, and therefore a high HLB of 29, Pluronic F68 adsorbs strongly, almost irreversibly to oil/water interfaces

(Torcello-Gómez et al., 2011). It has been also proven that the hydrophilic tails protect effectively against opsonizing proteins such as immunoglobulin G (Torcello-Gomez et al., 2011). For these reasons, it seemed reasonable to start the experiments with this polymer.

-Pluronic F127: also found in the literature as poloxamer 407. Pluronic F127 is the poloxamer with more applications accepted by the FDA after Pluronic F68, i.e., for oral, topical, ophthalmic and periodontal administration. Its molecular weight is 12600g/mol, and the approximate lengths of the two POE blocks are 100 subunits while the approximate length of the central POP block is 65 subunits. Therefore both their hydrophilic and hydrophobic moieties are longer than those of Pluronic F68, which means that the steric barrier around the droplets should be longer than for Pluronic F68, and the occupation of the interface should be higher.

-Pluronic P105: also referred as to poloxamer 335. Pluronic P105 possesses 37 subunits of POE in each tail, and 56 subunits of POP in the central block, and its molecular weight is 6500g/mol. Although not yet approved by the FDA, its structure will be useful to obtain a better understanding on how the structure of the surfactant influences the final properties of the nanoemulsions. E.g., Pluronic P105 has a shorter hydrophilic part and a longer hydrophobic part than Pluronic F68, and we can compare the effect of this on the rheological properties of a nanoemulsion.

2.1.3 Myrjs

Belonging to the family of PEG-fatty acids, these surfactants are composed by a polyoxyethylene tail linked to a stearic acid. They can be found also in the literature as PEG-XX-Stearate or as Polyoxyl (XX) stearate, bein XX the number of subunits of oxyethylene. In this dissertation, two different Myrjs were used in the experiments, Myrj 52 and Myrj 59, with a polyoxyethylene chain of 40 and 100 subunits, respectively. As the hydrophobic part is the same for both surfactants (stearic acid), these experiments will allow us to determine the influence of the length of the POE chain, which will be related to the length of the steric barrier around the droplet. Myrjs are frequently used in cosmetics and Myrj 52 is approved by both FDA and European Food Safety Authority as a food ingredient (number E431).

2.2 Oils

Oils from vegetable origin were used in the experiments such as olive, sesame, soybean and sunflower oil. Their properties are very similar, since they differ only in small variations in their fatty acids composition, as can be observed in Table 2.

Oil	Palmitic	Stearic	Oleic	Linoleic	α-linoleic	Unsat./Sat. ratio
Olive	13	3	71	10	1	4.6
Sesame	9	4	41	45	-	6.6
Soybean	11	4	24	54	7	5.7
Sunflower	7	5	19	68	1	7.3

Table 2. Oils, percentage of the main fatty acids composing the triglycerides and ratio between saturated and unsaturated fatty acids.

In all experiments, the oil was purified before preparing the emulsion in order to eliminate impurities, mainly free fatty acids, since the presence of these species may affect the interfacial properties of the emulsion. This purification was carried out by mixing the oil with particles of activated magnesium silicate (e.g., Florisil), in which polar molecules will adsorb. A typical purification protocol will consist in mixing 7g of Florisil with 50 mL of oil, the mix will be kept under mild agitation with a magnetic stirrer for 3 h and centrifuged at 15,000 g for 15 min in a bench centrifuge. The oil can be then filtered and stored away from light to avoid oxidation.

2.3 Preparation of nanoemulsions

As non-equilibrium systems, the formation of emulsions requires an input of energy. If one phase is dispersed into another immiscible phase, a considerable amount of interface between two phases is created. The free energy (ΔG) for this process is given by

2. Experimental details

$$\Delta G = \Delta A \cdot \gamma - T \cdot \Delta S \quad (2.1)$$

where ΔA is the increase in interfacial area when the bulk oil with area A_1 produces a number of droplets with area A_2, γ is the interfacial tension, T is the temperature and ΔS the entropy of dispersion. Since $A_2 >> A_1$, γ is positive (although slightly reduced by the use of surfactants) and ΔS very small, the energy required to expand the interface is large and positive (Forgiarini et al., 2001). For conventional emulsions, this energy can be provided easily by mechanical agitators. In the case of nanoemulsions, however, ΔA is notably higher, and therefore the energy to be supplied needs also to be increased. This energy can be supplied by either high shear/cavitation forces (high-energy methods) or by the chemical potential inherent within the components (low-energy methods). Low-energy emulsification methods involve transitional inversion induced by changing factors that affect the hydrophilic–lipophilic balance (HLB), e. g. temperature and/or electrolyte concentration, in order to transform an o/w emulsion into a w/o emulsion or vice versa (P. Izquierdo et al., 2001). However, they have some limitations that made their use in large-scale industrial production still inapplicable, such as their requiring of a large amount of surfactant, a thorough characterization and selection of surfactant–cosurfactant combination (e.g. by using phase diagrams), and careful control of the temperature (Jafari, He, & Bhandari, 2008).

In contrast, high-energy emulsification methods have some advantages that are applicable to large-scale processing. These advantages include the flexible control of droplet size distributions, the ability to produce fine emulsions from a wide variety of materials and the ease of the scaling-up process. One of these methods is ultrasound emulsification, in which the application of low frequency ultrasound causes acoustic cavitation, i.e., the formation and subsequent collapse of microbubbles by the pressure fluctuations of a simple sound wave. Each bubble collapse causes extreme levels of highly localized turbulence, which break droplets into smaller ones (Canselier, Delmas, Wilhelm, & Abismaïl, 2002).

Another method is high-pressure emulsification, by using the so-called high-pressure homogenizers. These homogenizers are widely used in industry to produce finely dispersed emulsions in a continuous way, and consist of a high pressure pump and a valve. The pump is used to compress a coarse emulsion (previously formed e.g. by mechanical

agitation) to the homogenizing pressure, forcing the product to pass through a specially designed valve with very a narrow gap, called the homogenizing valve (see Figure 17). In this valve, the fluid is subjected then to high pressures (typically 70-200 MPa), creating conditions of high turbulence and shear, that combined with compression, pressure drop and impacts produce an effective reduction of the droplet size (Jafari et al., 2008). One of the main advantages of high pressure homogenization is the ease of scaling-up, since a great variety of these homogenizers are already in the market, covering all the steps from the lab-scale emulsification to the industrial production carried out e.g. in the dairy industry to homogenize milk. However, some companies such as Hielscher or Industrial Sonomechanics are developing in-line homogenizers based on ultrasounds that could turn industrial ultrasonic homogenization into a cost-effective process.

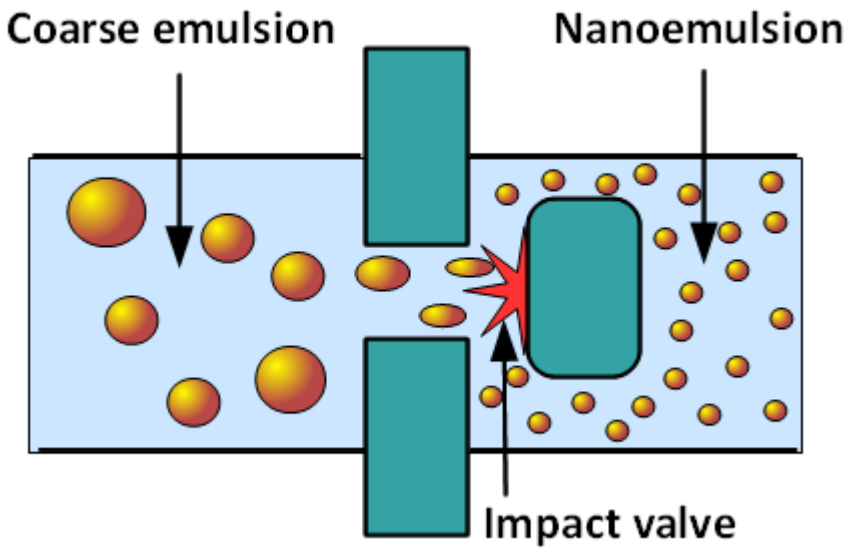

Figure 17. Schematic representation of the high-pressure homogenization process.

There are two major variables to take into account when dealing with high-pressure homogenizers. One is obviously the input pressure: higher pressures produce stronger turbulences and shear, and subsequently lower droplet sizes. The other one is number of passes or cycles, i.e., how many times the product is recirculated and homogenized again. It is stated that, for a given pressure and amount of surfactant, there is

a maximum number of efficient passes, and more passes do not lead to lower droplet sizes nor polydispersity (Meleson, Graves, & Mason, 2004). Therefore, to obtain nanoemulsions with the desired droplet size and monodispersity it is necessary to optimize the protocol of emulsification, and especially the input pressure, the number of passes and the amount of surfactant.

A typical protocol of emulsification could consist then in the pre-mixing of oil, water and surfactant to form a coarse emulsion (pre-emulsification) with a mechanical stirrer as Heidolph Diax 900 for 4 min at 13.000 rpm, followed by 11 passes through an Avestin-C3 high pressure homogenizer at 100 MPa.

2.4 Measurement of droplet size

By definition, the droplet size of nanoemulsions lies outside the limit observable by optical microscopy. Therefore, it is necessary to look for alternative methods, such as transmission/scanning electron microscopy or light scattering techniques. Conventional electron microscopy uses a high-energy electron beam that destroys soft matter systems such as nanoemulsions, and therefore they have to be used in combination with cryogenic techniques to analyze such labile systems. The other alternative techniques are based on the size determination due to the light scattered by the droplets in solution. One of these techniques is dynamic light scattering (DLS), also known as photon correlation spectroscopy (PCS) or quasi-elastic light scattering (QELS). In DLS, the speed at which the particles are diffusing due to Brownian motion is measured. This is done by measuring the rate at which the intensity of the scattered light fluctuates when detected using an optical arrangement, and after that a device called correlator treats this signal to obtain the autocorrelation function. This function compares photon counts from the same source at time t with those at time $t + \tau$, where τ is the delay or lag time, giving place to an exponential decay of the intensity of the scattered light. This decay will be related with the motion of the particles: large particles will present a slow motion and their signal will decay slowly, whereas smaller particles will move faster and therefore the decay will be reduced quickly (Finsy, 1994). The exponential decay can be fitted to a model function that will depend on the assumed distributions. Independently of the fit, the translational diffusion

coefficient *D* is be obtained, which can be employed to calculate the hydrodynamic diameter d_h by means of the Stokes-Einstein equation, given by

$$d_H = \frac{k_B T}{3\eta D} \tag{2.2}$$

where k_B is the Bolzmann constant, T the temperature and η the viscosity.

For monodisperse spheres (i.e. nanoemulsions), it is possible to fit a single exponential to the correlation function. This is called the cumulant method, and according to the ISO 13321:1996 produces an estimate of the mean droplet size, together with a width of the Gaussian-assumed particle size distribution called polydispersity index, defined in this case as $PDI=\sigma^2/d_h^2$, being σ the standard variation. As a rule of thumb, PDI values smaller than about 0.04 are considered monodisperse (Koppel, 1972).

In our experiments, the mean droplet size was measured at 25 ºC with an ALV-NIBS/HPPS (ALV-Laser Vertriebsgesellschaft GmbH, Langen, Germany). This set-up is specially designed to study very concentrated samples and minimizes multiple scattering by combining high performance particle sizer (HPPS) technology with a non-invasive backscattering (NIBS) method, where the measurement is taken at an angle of 173º. This technique detects only light scattered from the surface of the sample, which minimizes the optical path and consequently multiple scattering. The detected light was processed by a digital correlator (ALV 5000/E) that provides the correlation function as previously explained.

2.5 Evaluation of the stability of nanoemulsions

The stability of the nanoemulsions was evaluated using a Turbiscan MA 2000 (Formulaction, Toulouse, France), which allows the optical characterization of any type of dispersion in a faster and more sensitive way than just with the naked eye (Chauvierre, Labarre, Couvreur, & Vauthier, 2004). The nanoemulsion is placed in a flat-bottomed

cylindrical glass cell and scanned from the bottom to the top with a light source (near infrared, λ_{air}=850 nm) and 2 detector devices, in order to monitor light transmitted through the sample (180º from the incident light, transmission sensor), and light backscattered by the sample (45º from the incident radiation, backscattering detector) along the height of the cell. The Turbiscan

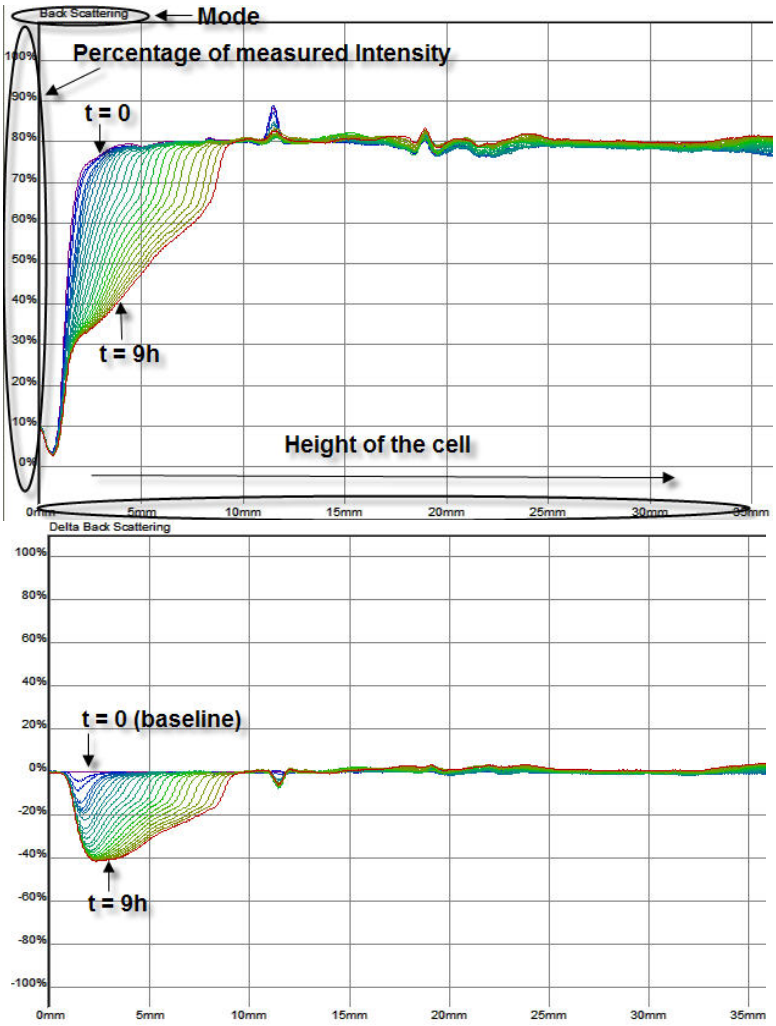

Figure 18. Typical curves obtained from the stability measurements: a) Intensity of backscattering (BS) against height of the cell; b) The same measurement, expressed in reference mode (ΔBS).

works in scanning mode: the optical reading head scans the length of the sample acquiring transmission and backscattering data every 40 μm. The corresponding curves provide the transmitted and backscattered light flux as a function of the sample height (in mm). Scans are repeated over time, each one providing a curve, and all curves are overlaid on one graph to show stability over time (see Figure 18a). We can also use the reference mode, which subtracts the first curve from the subsequent ones, in order to see the variations of profiles related to the initial state, that is, the loss or gain of backscattered intensity of each measure referred to the first one (obtained at zero time), as depicted in Figure 18b. Transmission is used to analyze clear to turbid dispersions and backscattering is used to analyze opaque dispersions, as in the case we are dealing with.

The most correct way to express the intensity of the light backscattered is to use the term *diffuse reflectance*. However, this intensity is expressed just as *Backscattering* (BS) in most of the literature concerning stability measurements with this kind of devices. For this reason, this intensity will be expressed as BS (or ΔBS in reference mode) throughout this dissertation, since it will facilitate the comparison with other bibliographic results.

The backscattered light intensity is related with the amount of droplets present in the dispersion: an increase of backscattered light in time measured in the bottom of the cell means an increase of particles in the bottom, i.e. sedimentation, whereas a decrease means a decreasing amount of particles, i.e. creaming (see Figure 18a). The same variation of backscattering in the whole cell height means a generalized change in the amount of particles, e.g. when coalescence is taking place (Mengual, Meunier, Cayre, Puech, & Snabre, 1999). Backscattering remains unchanged in almost the whole height of the cell when the number of particles and interfaces is not changing, i.e. if no coalescence, creaming or sedimentation occurs. Emulsions in which this behaviour was observed were considered stable.

A typical protocol for measuring stability would consist in measuring BS every 20 minutes, for 9 hours, which should be enough to observe destabilization phenomena due to the fact that Turbiscan detects them more than 20 times earlier than the naked eye for emulsions (Mengual, Meunier, Cayré, Puech, & Snabre, 1999). These measurements can be complemented with droplet size measurements at longer times.

2.6 Characterization of the micelles

In order to obtain experimental parameters needed to study the stability of some nanoemulsions, the size of the micelles formed by an excess of surfactant had to be measured, as well as the aggregation number. The hydrodynamic radius of micelles formed by Pluronic F68 molecules was determined using a 3D-DLS Spectrometer (LS Instruments) equipped with a 632.8 nm He–Ne laser. The basic principle of this spectrometer relies on the technique of cross-correlation, in a pretty similar way to that explained in Section 2.4. Here, two experiments are performed simultaneously under the compliance of a particular 3D geometry, having the same scattering volume and identical scattering vectors. The correlation of the measured scattering intensities of both experiments with each other results in a cross-correlation function where only single scattering events contribute to the signal, and thereby multiple scattered light is effectively suppressed (Urban & Schurtenberger, 1998). Four solutions of Pluronic F68 were measured, from 10 g/L to 30 g/L, and each solution was measured twice.

The aggregation number (N_{agg}) of a micelle is the average number of surfactant molecules that form this micelle. For micelles formed by Pluronic F68, the aggregation number was calculated as follows. The average molecular weight of the micelles ($MW_{MICELLE}$) was first determined by static light scattering, with the same device used to measure the micelle size. If the molecular weight of the surfactant molecule (MW) is known, N_{agg} can be calculated from the ratio between the former and the latter. The equation applied in this work to determine $MW_{MICELLE}$ was

$$\frac{K(C-CMC)}{R_{\theta}^{exc}} = \frac{1}{MW_{MICELLE}} + 2A_2(C-CMC) \qquad (2.3)$$

where R^{exc}_{θ} is the so-called excess Rayleigh ratio, i.e., the value resulting from the difference between the Rayleigh ratio of the sample and that of the solvent. The Rayleigh ratio of a given sample (R_{θ}) is calculated through that of toluene (R_{Tol}):

$$R_{\theta} = \frac{I_{\theta}}{I_{Tol}} \cdot R_{Tol} \tag{2.4}$$

where I_{θ} and I_{Tol} are the scattered intensity of the sample and the toluene, respectively (Jódar-Reyes et al., 2006). For a laser with λ = 632.8 nm, R_{Tol} = 1.34 · 10-3 m^{-1} at 25º C (Molina-Bolívar, Aguiar, & Ruiz, 2001). The scattering angle was set at 90º. In equation 2.3, C represents the surfactant concentration and A_2 is the second virial coefficient. K is an optical constant calculated from the following expression:

$$K = \frac{4\pi^2 n_0^2}{N_A \lambda_0^4} \left(\frac{dn}{dc} \right)^2 \tag{2.5}$$

where n_0 is the solvent refraction index (1.33262 ± 0.00003), λ_0 is the wavelength of the incident light, and (dn/dc) is the refractive index increment of the sample solution due to a change in the surfactant concentration. This increment was calculated at 25 ºC using an Abbé refractometer (Shibuya), measuring the refractive index of 10 solutions of Pluronic F68 with concentrations within the 5-50 g/L range.

The 3D-DLS Spectrometer was used to obtain I_{θ} for different concentrations and angles, and then R_{θ}. When the left part of equation 2.3 is plotted against (C - CMC), a linear relation results and the inverse of the $MW_{MICELLE}$ value can be calculated, since it will be given by the intersection of the lineal regression with the Y-axis.

2.7 Rheological measurements

As explained in Section 1.4, the experimental parameters that we will obtain from rheological measurements are based basically on three magnitudes: τ (the stress applied), γ (the strain or deformation produced) and/or $\dot{\gamma}$ (the shear rate). These magnitudes can be obtained in a relatively easy manner if a rheometer with a cone-plate geometry is used to carry out the measurements. In this kind of instruments, the plate instrument the liquid under investigation is present in the gap between a cone with a large top angle (at least 170º) and a circular plate, as depicted in Figure 19. The top of the cone, whose axis is perpendicular to the plate, is in principle positioned in the central point of the plate. In order to prevent friction between cone and plate during rotation of the cone, the top of the cone is truncated with the virtual, fictitious top corresponding to the plate center. The angle between the cone and plate, $\Delta\Theta$, is small (less than 5º). The cone rotates at an angular velocity of Ω_0, and counterclockwise when seen from above.

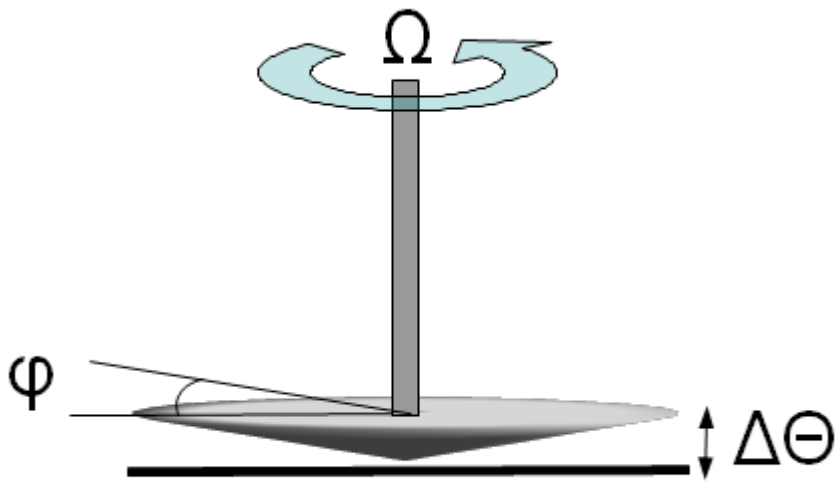

Figure 19. Representation of a cone-plate device and the main magnitudes involved in the measurements.

Measuring torque (M) and the rotated angle (φ) is possible to obtain shear stress, strain and shear rate, since

$$\tau = \frac{3M}{2\pi R^3} \tag{2.6}$$

$$\gamma = \frac{\varphi}{\Delta\Theta} \tag{2.7}$$

and

$$\dot{\gamma} = \frac{\Omega_0}{\tan\Delta\Theta} \approx \frac{\Omega_0}{\Delta\Theta} \tag{2.8}$$

this last assumption being valid due to the fact that ΔΘ is very small, and meaning that the shear rate is constant throughout the gap, which is one of the many advantages of the cone-plate geometry and makes this instrument highly suitable for the determination of the viscosity as function of shear rate (Steffe, 1992).

2.7.1 Viscoelasticity tests

A strain sweep test was used to determine the linear viscoelastic region. Once this region is established, measurements of G´ and G´´ are made as a function of frequency. This frequency sweep is a useful tool when characterizing the microstructure of a viscoelastic material and for this reason is frequently mentioned as the "finger print" of a material. Before this, the sample is pre-sheared at a constant shear rate of 20 s^{-1} for 30 s in torsional mode. Next, the sample is allowed to recover for a period of 60 s. This treatment is called "pre-shear", and is strongly recommended to obtain reproducible results when measuring rheological properties on emulsions, since it eliminates the influence of undesirable alterations of the sample during handling, e.g. the disruption of emulsion structure at rest by the filling process.

2. Experimental details

After pre-shearing, a SAOS amplitude sweep test is performed, by varying the strain amplitude from γ = 0.01 % to γ = 100 %, keeping a constant angular frequency of ω = 10 rad/s. Then, the mechanical spectra of the nanoemulsions are obtained from SAOS frequency sweep tests. In a typical frequency sweep test the applied strain amplitude could be γ = 0.01 % , well in the viscoelastic linear region in all cases, and the excitation frequency ranged from ω = 100 rad/s to ω = 0.1 rad/s. All these measurements were carried out in triplicate.

In order to complete the characterization, the viscoelastic properties were also studied using transient experiments, where the tests are focused on the time domain instead of on the frequency domain (see Figure 20) (Ferry, 1980). Two different experiments were performed. The first one consisted in the application of an instantaneous constant stress τ_0 while measuring the shear strain. In this shear creep flow, the associated rheological material function relates the measured sample deformation (strain γ) to the prescribed (constant) stress τ_0. This material function is called shear creep compliance $J(t) = \gamma(t)/ \tau_0$. At low stress values the measured compliance does not change. However, upon increasing the stress compliance curves do not overlap anymore revealing the onset of the non-linear regime (Dolz, Hernández, & Delegido, 2008)

The second bulk rheological experiment in the time domain involves a stress relaxation. In these tests different initial strains γ_0 were applied while measuring stress relaxation modulus G(t), which is defined as $G(t) = \tau(t)/\gamma_0$. At low deformations, the relaxation modulus remains the same and all G(t) curves overlapped. From this, the linear viscoelastic behaviour was inferred. For large deformations, curves did not overlap and a parameter called damping function was used to compare viscoelasticity in the non-linear region between the nanoemulsions investigated. Damping function is defined as

$$h(\gamma) = \frac{G(t,\gamma)}{G(t)} \tag{2.9}$$

and describes the rheological behavior of nanoemulsions once the microstructure is disturbed (Partal, Guerrero, Berjano, & Gallegos, 1999). The data obtained by transient experiments can be fitted to mechanical models in order to obtain more quantitative

information, which will allow a better comparison of different nanoemulsions (van Vliet & Lyklema, 2005).

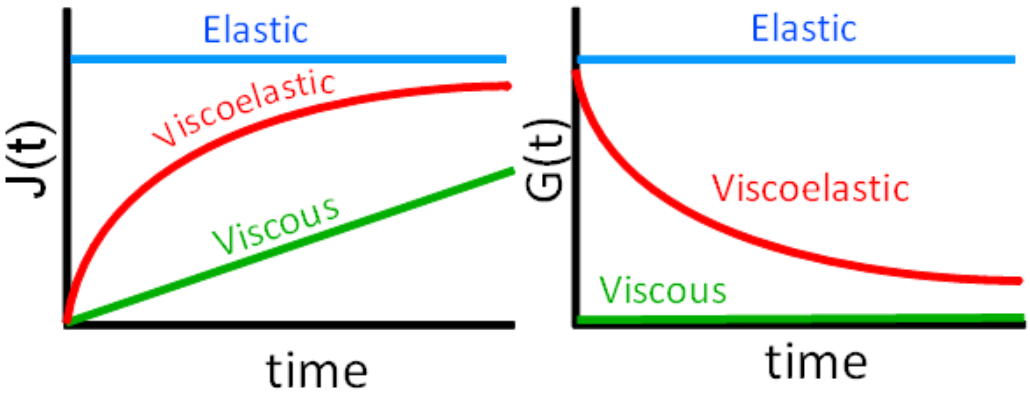

Figure 20. Typical curves obtained from transient experiments for a pure elastic solid, a viscous liquid and a viscoelastic material: a) Creep tests; b) Stress relaxation tests.

2.7.2 Simple Shear tests

The steady shear response of the submicron emulsions was measured by subjecting the sample to increasing shear rates from 0.01 s^{-1} to 1000 s^{-1}. The geometry in these experiments was the same as in the previous section. Again, each test was performed in triplicate.

In addition, a vane tool was used to measure the apparent yield stress of some nanoemulsions. The vane has four blades, a height of 8 mm and a diameter of 5 mm. All the vane and vessel dimensions as well as the depth of the vane immersion were optimized to allow precise measurements according to the standard method of measurement with vane (Steffe, 1992). The torque necessary to overcome the yield stress is measured, and both magnitudes are related by the expression

$$M_0 = \frac{\pi d^3}{2}\left(\frac{h}{d} + \frac{1}{6}\right)\sigma_0 \quad (2.10)$$

where M_0 is the applied torque, σ_0 the yield stress, and h and d the height and diameter of the vane, respectively. The rotational speed was set at 0.006 rpm.

2.8 Evaluation of in vitro lipolysis

2.8.1 Simulation of in vitro duodenal lipolysis

The lipolysis under duodenal conditions was evaluated by mixing the nanoemulsions with simulated duodenal fluids, and then studying their degradation as a consequence of the lipase action. This degradation is frequently evaluated using a pH-stat, a device that titrates automatically the free fatty acids (FFA) released during the lipolysis process. The representation of these FFA titrated against time gives then an estimation of the lipolysis rate (Li, Hu, & McClements, 2011). However, this method presents some limitations, such as requiring a constant pH throughout the process, which does not happen in the real process. In addition, pH-titration assumes that all the pH changes are due to the free fatty acids released. Nevertheless, this method fails when more realistic, chemically complex simulated fluid is used to mimic in vivo conditions, probably due to interference from one or more of the components of the mixture (Hur et al., 2009). For these reasons, alternative methods have been proposed very recently, such as gas chromatography or HPLC to analyze the products of lipolysis at different times (Helbig, Silletti, Timmerman, Hamer, & Gruppen, 2012; Larsen, Sassene, & Müllertz, 2011). In this dissertation, we propose another method based on our previous experience using Turbiscan 2000 (see Section 2.5), and on the generalized decrease in droplet size that takes place during lipolysis. This decrease occurs because of the solubilization of the lipolysis products by endogenous bile salts and phospholipids, as explained in Section "Metabolic degradation of emulsions", and therefore it is related to the lipolysis rate. Thus, our aim was to evaluate this lipolysis rate by monitoring in time the change in the intensity of the light backscattered by the emulsion droplets, since we know that a generalized change in

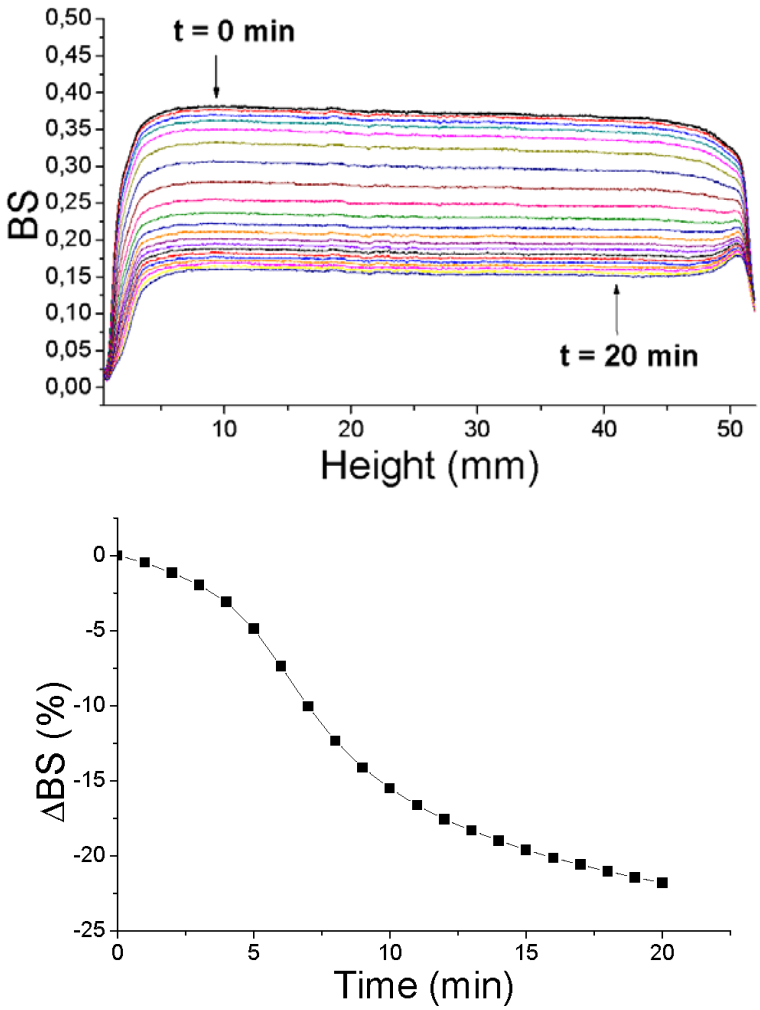

Figure 21. (a) Backscattering profiles obtained during a lipolysis experiment for recording BS every minute. (b) The same experiment, expressed as ΔBS (referred to the first measurement) against time, as an estimation of the lipolysis rate.

BS through the whole height of the cell is related with a change in particle size. For small Rayleigh-Debye scatterers (diameter <0.3 μm), a decrease in particle diameter produces a decrease in BS (Mengual, Meunier, Cayré, et al., 1999). According to their droplet size, our nanoemulsions belong to this type of scatterers. Therefore, the generalized decrease in BS observed can be attributed to a decrease in particle size, which in this system can only be caused by the action of the lipase. Thus, measuring BS changes in the center of the tube

and plotting these changes against time gives us a qualitative estimation of the lipolysis rate (see Figure 21). The lipolysis rate was characterized using the parameter ΔBS, being the difference in mean BS value (recorded for the emulsion sample in the central region that went from 20 to 40 mm of its height) between the first scan and n scan. With this method would be possible also to detect also different destabilization mechanisms that could affect our measurements, such as creaming or sedimentation, which can not be achieved by other methods.

A typical experiment of duodenal lipolysis would consist on mixing our emulsion with a solution simulating duodenal fluids, then inverting this mixture four times and immediately transferring it to a Turbiscan cell, where the time evolution of scattered light is measured. This procedure was repeated three times to test the reproducibility of the method. Also a blank experiment for each nanoemulsion was performed, by adding 1 mL of Milli-Q water instead of the lipase suspension. The composition of the simulated duodenal fluid is based on the in vivo and in vitro components and concentrations reported by other authors (Hur et al., 2009; Versantvoort, Oomen, Van de Kamp, Rompelberg, & Sips, 2005; Zangenberg, Müllertz, Kristensen, & Hovgaard, 2001), in order to compare our results with the previous bibliography. This mixture was composed by NaCl 150 mM, $CaCl_2$ 2 mM, 4.18 g/L bile salt extract, colipase and lipase with a final activity of 136 U/mL, at pH 6.5 and 37 ºC. The lipase and colipase were obtained from pancreatin, a direct extract of porcine pancreatic fluid and therefore very similar to the real secretion.

For some nanoemulsions, the stability under gastric conditions was also tested. To do so, the nanoemulsions were mixed with simulated gastric fluid at 37 ºC, giving a final composition of 3.2 g/L of pepsin, 2 g/L NaCl, pH adjusted to 1.2 with HCl, and a final oil volume fraction of 10%, as described by the United States Pharmacopeia for mimicking in vitro gastric conditions. The stability against coalescence, flocculation and so forth was then measured using the Turbiscan as explained in Section 2.5.

2.8.2 Simulation of in vitro intravenous lipolysis

A buffer containing the main components involved in intravenous lipolysis was prepared, based on the compositions and concentrations used by other authors (Deckelbaum et al., 1990; Rensen & van Berkel, 1996; Ton et al., 2005; Yamamoto et al., 2003). This buffer was composed by NaCl 150 mM, Tris-Base 10 mM, 4% albumin and 66.7 μg/mL heparin at pH 8.6. 10% (v/v) of human plasma, heat-inactivated (30 min at 56 ◦C), was used as a source of apolipoprotein C-II.

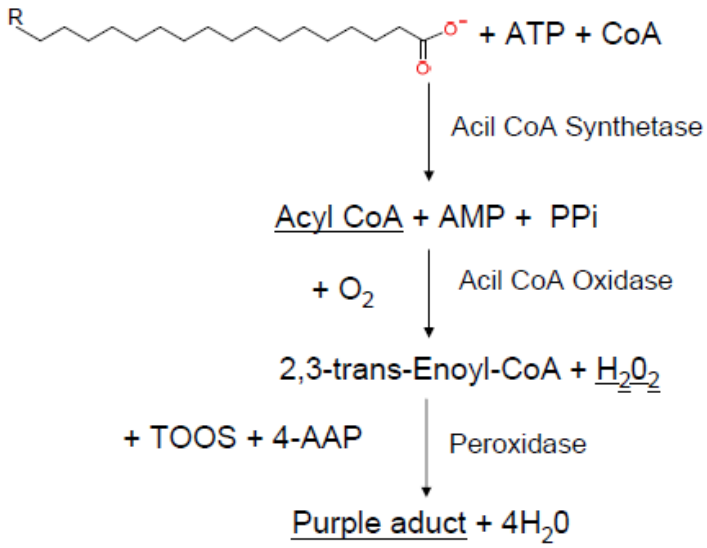

Figure 22. Main reactions involved in the determination of the free fatty acids released in a lipolysis experiment. ATP = Adenosine triphosphate; CoA = Coenzyme A; AMP = Adenosine Monophosphate; PPi = Pyrophosphate; TOOS = N-Ethyl-N-(2-hydroxy-3-sulfopropyl)-3-methylaniline; 4-AAP = 4-aminoantipyrine.

Nanomulsions were diluted with the buffer previously described until a final oil/water volume fraction of 0.1%, being the total volume 400 μL, and incubated at 37 ◦C for 30 min. Then, 4.0 μg/mL LpL were added, starting the lipolysis experiment, and the released free fatty acids from the lipid emulsions were measured at predetermined time

intervals using an enzymatic kit (Non-esterified fatty acid (NEFA) Kit; RANDOX Laboratories Ltd., United Kingdom). This kit analyzes in a very specific manner the free fatty acids released on the lipolysis process, as a series of enzymatic reactions converts these fatty acids into a purple aduct with a strong absorption at λ=550 nm (see Figure 22). Samples were then taken at different times of incubation and mixed with the reagents of the kit. Measuring absorbance of the product formed with a spectrophotometer Spectronic Genesys 5 (Spectronic Instruments, UK) it is possible to quantify the free fatty acids released at different times, i.e., the lipolysis rate.

Studies were performed in triplicates. Blank experiments were also performed in order to correct the possible FFA coming from plasma, impurities, etc., adding Milli-Q water instead of LpL solution.

Chapter 3. Main objectives

The main goal of this dissertation is to study the preparation and characteristics of nanoemulsions, with a special focus on the relationship between these characteristics and the nanoemulsion composition, and the manner in which they could modify the performance of nanoemulsions as drug delivery systems. To achieve this goal, different sets of experiments were planned. The main objectives of these experiments were:

- To design protocols of nanoemulsion preparation, in order to obtain a final product with the desired properties (e.g. droplet size, monodispersity, and so forth). To do so, the influence of the different variables affecting the final nanoemulsion had to be taken into account, such as amount of surfactant or preparation time.

- To carry out an in-depth characterization of nanoemulsions, with a particular emphasis on their mechanisms of stabilization and destabilization. This characterization implies the study of the impact of the surfactant on the nanoemulsion stability combined with the theoretical background concerning colloidal stability.

- To analyze thoroughly the rheological behavior of nanoemulsions stabilized with different surfactants. These studies will provide us with a better understanding on the close relationship between interfacial composition, droplet-droplet interactions and flow properties of nanoemulsions.

3. Main objectives

- To study the biodegradation of nanoemulsions under simulated in vitro conditions mimicking those involved in the fate of nanoemulsions after oral and intravenous administration. Special attention will be paid to the influence of the surfactant on this biodegradation.

- To confirm or discard the possibility of using the surfactant as an active agent in the control of the biodegradation of nanoemulsions. This objective is closely related to the previous one: understanding how the nature of the surfactant affects the lipolysis suffered by nanoemulsions should help us to design nanoemulsions with a tailor-made biodegradation, and therefore to use nanoemulsions as controlled drug delivery systems.

Chapter 4. Brief summary of the presented papers

In this dissertation, the results are presented as five different papers. These papers are not presented chronologically. Instead, they have been ordered to facilitate the understanding: broadly speaking, the first paper deals mainly with the stability of nanoemulsions, the two following papers are focused on the interfacial and rheological studies, whereas the last two ones describe the lipolysis of the nanoemulsions. Obviously, these results are interrelated: the outcomes of one study influence the manner in which another work is carried out, or support its conclusions. A brief summary of the main results of the different papers and their interrelationships will be presented in this chapter.

Paper I. In this work, the first protocols to study the preparation and characterization of nanoemulsions were developed. The nanoemulsions were prepared by ultrasounds and with a single steric surfactant, Pluronic F68, eliminating the presence of traditional ionic surfactants such as phospholipids. These nanoemulsions presented and appropriate size, monodispersity and stability for parenteral administration. In addition, the possible destabilization mechanisms were studied, identifying the instability when an excess of surfactant was present as caused by a depletion-flocculation mechanism. A theoretical DLVO-modified model was applied to explain this phenomenon, obtaining a good agreement between the observed and predicted behavior. The experimental skills obtained during this work, together with the protocols designed to prepare and characterize the

nanoemulsions and the subsequent improvements of these protocols (including the use of high pressure homogenization) led to a collaboration that resulted in the paper written by Jódar-Reyes et al. and published in Food Research International. This last paper is presented in Chapter 7 as aditional material.

Paper II. Nanoemulsions were prepared from this point onwards only by high pressure homogenization. In this work, only one kind of surfactant was used: either the ionic phospholipids mixture Epikuron 145V or the steric copolymer Pluronic F68, in order to study the properties that each type of emulsifier confers to the nanoemulsion. The protocols to prepare and characterize nanoemulsions had to be slightly modified, since notably higher volume fractions were used in these experiments. A comprehensive rheological characterization of the nanoemulsions was then carried out, combining frequency- and time-domain experiments. Strinkingly different behaviors were observed depending only on the surfactant used, presenting the phospholipid-stabilized nanoemulsions higher elastic properties in all the experiments performed. It was also found that the phospholipids form also a more elastic film at the oil/water interface.

Paper III. The background about rheology of nanoemulsions obtained in the previous paper served as a basis to develop this one. Nanoemulsions were prepared only with one surfactant at a time. Five different steric surfactants were used, belonging to two different families: Pluronics and Myrjs, with key differences on their structures. The influence of these differences on the rheological behavior was analyzed, observing quantitative dissimilarities on the viscoelastic response: surfactants with longer hydrophilic tails produced emulsions with higher viscoelasticity. Pluronics, having a central hydrophobic part between two hydrophilic tails, produced emulsions with notably higher viscoelasticity and yield stress than Myrjs with comparable hydrophilic tails. The reason for this seems to be a more efficient steric barrier at the interface, induced by this central hydrophobic part.

Paper IV. A new method to study simulated duodenal lipolysis was developed. This procedure allowed the analysis of the influence of the surfactant on this lipolysis, and in particular the impact of the nature of the surfactant. Phospholipids-stabilized nanoemulsions presented a fast, almost instantaneous lipolysis. In contrast, Pluronic F68 was efective on delaying the digestion of the emulsions. In addition, it was shown that the

enzymatic degradation of nanoemulsions can be speeded up or slowed down by varying the proportion between steric and ionic emulsifiers.

Paper V. The results of the previous paper were used to proceed further with the study of the biodegradation of nanoemulsions. In this paper, the influence of the characteristics of different steric surfactants on the lipolysis was studied, both under duodenal and intravenous conditions. The lipolysis rates observed were strikingly different depending on the structure of the steric surfactant, especially under intravenous conditions, e.g., this lipolysis was completely blocked when Pluronic F127 was used, while it was almost complete within six hours when using Myrj 52. The reason for this seems to be the steric hindrance that the surfactant produces around the droplet and at the interface. As a result, we can modify the lipolysis rate by changing some characteristics of the surfactant, or by varying the proportion between two surfactants in a mixture. The formation of a more effective steric barrier for Pluronics, observed in Paper III, would support and complement these results.

Chapter 5. Results

5. Results

Paper I.

Stability of emulsions for parenteral feeding: Preparation and characterization of o/w nanoemulsions with natural oils and Pluronic-F68 as surfactant.

M. Wulff-Pérez, A. Martín-Rodríguez, M. J. Gálvez-Ruíz, A. Torcello Gómez

Biocolloid and Fluid Physics Group. Department of Applied Physics. Faculty of Sciences, University of Granada, 18071 Spain.

Published in:

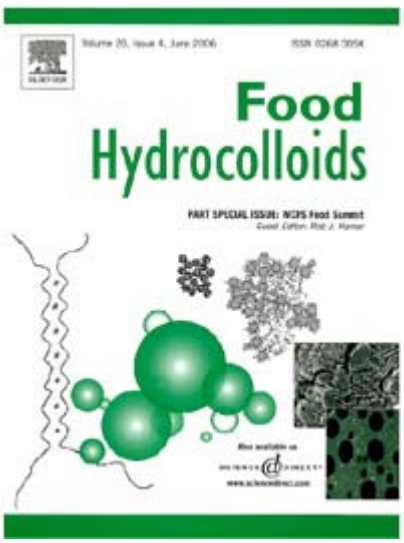

Food Hydrocolloids

Volume 23, Issue 4, June 2009, Pages 1096–1102

Abstract

For hydrophobic bioactive compounds, poor water solubility is a major limiting factor for their use in different applications in the field of food industry or pharmacy. For this reason they are administrated as emulsions, in which the substance is dissolved in an organic compound, which is dispersed in an aqueous phase as droplets stabilized by a surfactant. It has been demonstrated that the colloidal stability of the nanoemulsion formulations can be precisely controlled by the chemical structure of the interface. In this paper, a promising delivery system has been studied. As surfactant, we have used the amphiphilic uncharged tri-block copolymer Pluronic-F68, and natural oils from soybean, sesame and olive as the organic phase. The nanoemulsions were prepared by ultrasonication, and their stability at different synthesis conditions such as ultrasound power and surfactant concentration has been studied by monitoring backscattering using a Turbiscan. The more stable emulsions have been characterized by DLS, and their droplet size was below 500 nm, which has resulted very appropriate for parenteral administration. A destabilization of the system always takes place above certain surfactant concentration. This phenomenon was described as a depletion-flocculation effect caused by non-adsorbed micelles. This destabilization was modelled by adding to the DLVO interaction energy a contribution addressing the force between two spherical particles in the presence of non-adsorbing spherical macromolecules.

1. Introduction

Oil-in-water emulsions are important vehicles for the delivery of hydrophobic bioactive compounds into a range of food products, nutraceuticals, cosmetic compounds, and drugs. Many of their properties are determined by the droplet size and size distribution, e.g., small droplet sizes in general lead to a creamier mouth feel and greater emulsion stability (McClements, 2004). Depending on droplet diameter, emulsions can be divided into mini/nano- (20–500 nm) and macro-emulsions (0.5–100 μm). Nanoemulsions, unlike microemulsions, are not thermodynamically stable but kinetically, and they do not form spontaneously. However, the long-term physical stability of nanoemulsions (with no apparent flocculation or coalescence) makes them unique (Tadros, Izquierdo, Esquena and Solans, 2004). Besides, they do not require a large amount of surfactant as microemulsions do; they can be prepared with reasonable surfactant concentrations: for a 20% O/W nanoemulsion, a surfactant concentration in the region of 5-10% (w/w) will be sufficient (Tadros et al., 2004).

To prepare nanoemulsions a large amount of energy is required. Low-energy emulsification methods involve transitional inversion induced by changing factors that affect the hydrophilic-lipophilic balance (HLB), e. g. temperature and/or electrolyte concentration, in order to transform an o/w emulsion into a w/o emulsion or vice versa (Tadros et al., 2004). However, they have several limitations, such as their requiring a large amount of surfactant, a careful selection of surfactant-cosurfactant combination, and careful control of the temperature. Yet, they are inapplicable to large-scale industrial productions. On the other hand, high-energy emulsification methods such as high-pressure homogenizers and high shear motionless mixers have several advantages that are applicable to industrial operations. Those advantages included the flexible control of droplet size distributions and the ability to produce fine emulsions from a large variety of materials (Seekkuarachchi, Tanaka and Kumazawa, 2006)

Studies comparing ultrasonic emulsification with rotor–stator dispersing have found ultrasound to be competitive or even superior in terms of droplet size and energy efficiency (Canselier, Delmas, Wilhelm, and Abismaïl, 2002). The same studies also have

shown that microfluidization has been found to be more efficient than ultrasound, but less practicable with respect to production cost or equipment contamination. Comparing mechanical agitation to ultrasound at low frequency, Tadros et al. (2004) found that for a given desired diameter, the surfactant amount required was reduced, energy consumption (through heat loss) was lower and the ultrasonic emulsions were less polydisperse and more stable.

In this study we used ultrasound to prepare nanoemulsions from natural oils like soybean, olive and sesame oil, due to their biocompatibility, their similarity with nutraceutical oils and their ability to dissolve hydrophobic compounds. We also intended to test Pluronic F68© as surfactant (also known as Poloxamer 188) which is a triblock ABA-type copolymer. It has the advantage of being non-ionic, and therefore its ability as surfactant does not depend on ionic strength. As a non-toxic surfactant (Kibbe, 2000), it has been used as micellation agent for drug and gene delivery (Kabanov, Batrakova and Alakhov, 2002). Nevertheless, there are very few reports on Pluronic F68© as surfactant (Yalin, Öner, Öner and Hincal, 1997; Jumaa and Müller, 1998), despite its good behaviour in blood systems, which does not rule out its application also in parenteral feeding. On the contrary, polyoxyethylene-polyoxypropylene copolymers inhibit the neutrophil activation by IgG against nanodroplets and therefore allow prolonged circulation times, which are essential for a controlled release of the drug in the blood stream (Jackson, Springate, Hunter and Burt, 2000)

On the other hand, nowadays it is well established that in presence of high concentration of surfactant or polymer, the micelles can play an important role in the stability of the emulsions (Dickinson, Golding and Povey, 1998; Dickinson, 2003). After interface saturation by the adsorbed surfactant, micelles do not adsorb on the surfactant coated surface, and they can cause attraction between drops by a depletion mechanism. Thus, when two droplets approach in a solution of non-adsorbing micelles, the latter are expelled from the gap, generating a local region with almost pure solvent. The osmotic pressure in the liquid surrounding the particle pair exceeds that between the drops and consequently forces the droplets to aggregate. (Napper, 1983). Understanding this phenomenon is relevant to understand when and why phase separation occurs in mixtures

of polymers and colloids, which are often jointly present in biological and industrial dispersions such as food dispersions (Tolstoguzov, 2001). For this reason, the present work aims to show an exhaustive study of the colloidal stability of emulsions in a wide range of the nonionic surfactant concentrations. We analyse flocculation by evaluating the aggregation using light backscattering technique.

Finally, a theoretical approach which models the depletion interaction was used to calculate the stability of the system, comparing it later with the observed stability. To do it, some parameters should be obtained and therefore a thorough characterization of the micelles was necessary. At least, the size and the aggregation number, i.e., the number of surfactant monomers forming one micelle had to be evaluated. These two data were also obtained by light scattering measurements. The depletion potential was included in the total DLVO interaction energy to predict the destabilization of the colloidal system in the presence of micelles.

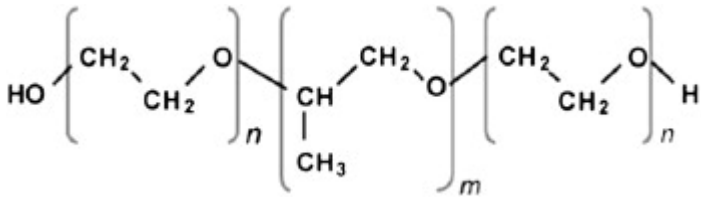

Fig. 1. Chemical structure of a poloxamer. It presents a central hydrophobic fragment of polyoxypropylene (PPO) and identical hydrophilic chains of polyoxyethylene (PEO) at both sides. For Pluronic F68, n = 75 PEO units and m = 30 PPO units.

2. Materials and Methods

2.1 Materials

Pluronic F68 was obtained from Sigma. It is a triblock copolymer based on poly(ethylene oxide)-block-poly(propylene oxide)-block-poly(ethylene oxide) structure which is also typically expressed as PEOa-PPOb-PEOa, being a=75 and b=30 (Fig. 1).

The olive, sesame and soybean oils were also obtained from Sigma, and purified with Activated Magnesium Silicate (Florisil, Fluka) to eliminate free fatty acids. The water was purified in a Milli-Q Academic Millipore system.

2.2 Preparation of emulsions

We have prepared emulsions of 25% (v/v) o/w, being the non-aqueous phase olive, sesame or soybean oil, and the aqueous phase a solution of Pluronic F68 at different concentrations. Those emulsions were prepared as follows: 5.25 ml of Pluronic solution were added to 1.75 ml of oil, and then a Branson Sonifier W450 (f=20 kHz) was employed for dispersing them via ultrasound. Our protocol was designed adapting the available bibliographic data about ultrasound emulsification (Tomoko and Fumiyoshi, 2004; Canselier et al., 2002) to our own system, by modifying the time of sonication and the amount of energy supplied to our emulsion considering the final stability and reproducibility.

2.3 Stability of Emulsions

The destabilization of the emulsions was evaluated using a Turbiscan MA 2000 (Formulaction, Toulouse, France), which allows the optical characterization of any type of dispersion in a faster and more sensitive way than just with the naked eye (Chauvierre, Labarre, Couvreur and Vauthier, 2004). The dispersion is placed in a flat - bottomed cylindrical glass cell and scanned from the bottom to the top with a light source (near infrared, λ_{air}=850nm) and 2 detector devices, in order to monitor light transmitted through the sample (180° from the incident light, transmission sensor), and light backscattered by the sample (45° from the incident radiation, backscattering detector) along the height of the cell. The Turbiscan works in scanning mode: the optical reading head scans the length of the sample acquiring transmission and backscattering data every 40 μm. The corresponding curves provide the transmitted and backscattered light flux as a function of the sample height (in mm). Scans are repeated over time, each one providing a curve, and all curves are overlaid on one graph to show stability over time. We can also use the reference mode, which subtracts the first curve from the subsequent ones, in order to see the variations of profiles related to the initial state, that is, the loss or gain of backscattered

intensity of each measure referred to the first one (t = 0). Transmission is used to analyze clear to turbid dispersions and backscattering is used to analyze opaque dispersions, as in the case we are dealing with. The backscattered light intensity is related with the amount of droplets presents in the dispersion: an increase of backscattered light in time measured in the bottom of the cell means an increase of particles in the bottom, i.e. sedimentation, whereas a decrease means a decreasing amount of particles, i.e. creaming. The same variation of backscattering in the whole cell height means a generalized change in the amount of particles, which is a sign of coalescence. Backscattering remains unchanged in almost the whole height of the cell when the number of particles and interfaces is not changing, i.e. if no coalescence, creaming or sedimentation occurs. Emulsions in which this behaviour was observed were considered stable. The samples were measured every 20 minutes, for 9 hours, which according to Mengual, Meunier, Cayre, Puech and Snabre (1999) should be enough to study destabilization phenomena due to the fact that Turbiscan detects them more than 20 times earlier than the naked eye for concentrated emulsions.

2.4 Measurement of droplet size

The mean droplet size in stable emulsions was measured at 25ºC with an ALV-NIBS/HPPS (ALV-Laser Vertriebsgesellschaft mbH, Langen, Germany). This set-up is specially designed to study very concentrated samples and minimizes multiple scattering by combining high performance particle sizer (HPPS) technology with a non-invasive backscattering (NIBS) method, where the measurement is taken at an angle of 173º. This backscattering technique detects only light scattered from the surface of the sample, which minimizes the optical path and consequently multiple scattering.

The detected light is processed by a digital correlator (ALV 5000/E) that provides the correlation function, from which the diffusion coefficient of the emulsion droplets is calculated using the cumulant method (Koppel, 1972). Finally, the hydrodynamic radius is obtained by means of the Stokes–Einstein relation and its polydispersity is weighted, obtaining the volume-weighted mean diameter ($D_{[4,3]}$)

5. Results

$D_{[4,3]}$ was measured four times for every sample, and three samples were prepared for each kind of oil. To reach optimal measurement conditions, emulsions had to be diluted 1/25 (i.e., 1% oil-in-water).

2.5 Measurement of micelle size

The hydrodynamic radius of the micelle formed by Pluronic F68 molecules was determined using 3D-DLS Spectrometer (LS Instruments) equipped with a 632.8 nm He-Ne laser. The temperature was set at 25 ºC. The basic principle of this spectrometer relies on the technique of cross-correlation. Two experiments are performed simultaneously under the compliance of a particular 3D geometry, having the same scattering volume and identical scattering vectors. The correlation of the measured scattering intensities of both experiments with each other results in a cross-correlation function where only single scattering events contribute to the signal. Thereby multiply scattered light is effectively suppressed.

We have measured 4 solutions, from 10 g/L to 30 g/L, and each solution was measured twice.

2.6 Micelle characterization

The aggregation number (N_{agg}) of the micelle was calculated as follows. The average molecular weight of the micelles (M_W(micelle)) was first determined by SLS. If the molecular weight of the surfactant molecule (M_W) is known, N_{agg} can be calculated from the ratio between the former and the latter. Details concerning the method for measuring the M_W(micelle) through SLS can be found in the literature (Kwon and Kim, 2001; Jódar-Reyes, Martín-Rodríguez and Ortega-Vinuesa, 2006). The equation applied in this work to determine M_W(micelle) was

$$\frac{K(C-CMC)}{R_\theta^{exc}} = \frac{1}{M_w(micelle)} + 2A_2(C-CMC) \qquad (1)$$

where R^{exc}_{θ} is the so-called excess Rayleigh ratio, i.e., the value resulting from the difference between the Rayleigh ratio of the sample and that of the solvent. The Rayleigh ratio of a given sample (R_{θ}) is calculated through that of toluene (R_{Tol}):

$$R_{\theta} = \frac{I_{\theta}}{I_{Tol}} \cdot R_{Tol} \tag{2}$$

where I_{θ} and I_{Tol} are the scattered intensity of the sample and the toluene, respectively. For a laser with λ = 632.8 nm, R_{Tol} = 1.34 x 10-3 m^{-1} at 25 ◦C (Molina-Bolivar, Aguiar, Ruiz and Carnero, 2001). The scattering angle was set at 90◦. In Equation 1, C represents the surfactant concentration and A_2 is the second virial coefficient. K is an optical constant calculated from the following expression

$$K = \frac{4\pi^2 n_0^2}{N_A \lambda_0^4} \left(\frac{dn}{dc} \right)^2 \tag{3}$$

where n_0 is the solvent refraction index (1.33262 ± 0.00003), $\lambda 0$ is the wavelength of the incident light, and (dn/dc) is the refractive index increment of the sample solution due to a change in the surfactant concentration. This increment was calculated at 25◦C using an Abbé refractometer (Shibuya), measuring the refractive index of 10 solutions with concentrations within the 5-50 g/L range. A value of the optical constant K= 1.41 10^{-8} mol L/g^2m was obtained.

The 3D-DLS Spectrometer was used to obtain Iθ for different concentrations and then Rθ. When the left part of Equation 1 is plotted against (C − CMC), a linear relation results and the inverse of the Mw (micelle) value can be calculated, since it will be given by the intersection of the lineal regression with the Y-axis.

3. Results and Discussion

3.1 Emulsion preparation and reproducibility

A set of experiments was performed to obtain stable emulsions with a reproducible method. Several protocols of supplying ultrasound were tested by using power and sonication time as variables. In addition, different concentrations of Pluronic were tested in order to find and use an optimal surfactant concentration for each method. Thus, we analysed via Turbiscan several emulsions prepared with one method and then we repeated this procedure with the other one.

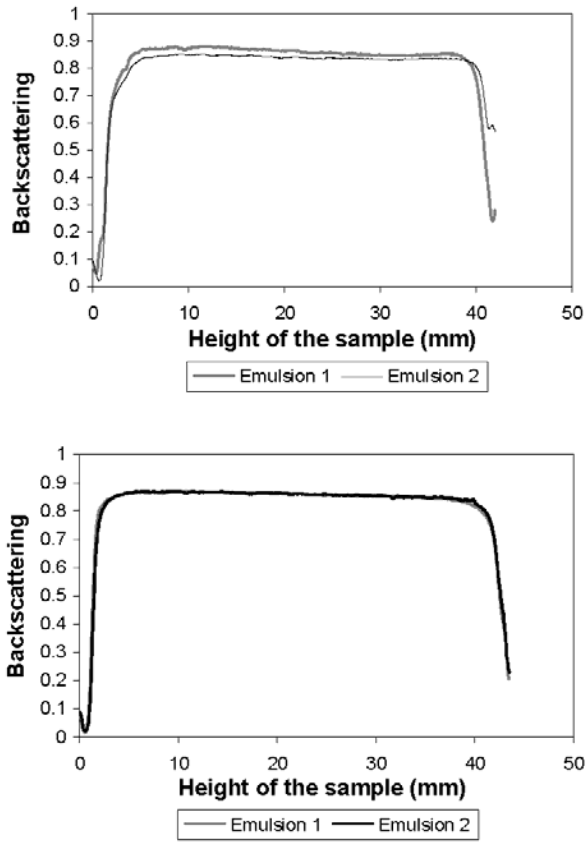

Fig. 2. 2a) Emulsions prepared with the non-reproducible method.2b) Emulsions prepared with the reproducible method, t=0h.

The method with higher power but shorter sonication time applied to the same emulsion produced different curves, i. e., this one was non-reproducible, as we can see in Figure 2a.

The method that resulted in almost identical graphs was considered to be the most reproducible one. This sonication protocol was that with lower power and longer sonication time, and consisted of four 40 W pulses of 15 s each, with a pause of 15 s between pulses in order to avoid overheating of our sample (Figure 2b).

3.2 Stability of emulsion

The stability of emulsions containing a wide range of Pluronic concentrations, and soybean, olive or sesame oil as lipid phase, was analysed by observing the backscattered profiles along the emulsions as a function of time (see Table 1).

Table 1. Stability of the nanoemulsions prepared with 25% oil (v/v), testing different Pluronic F68 concentrations. X symbol means that the nanoemulsion turned out to be unstable, O symbol means that the nanoemulsion turned out to be stable.

	Stability		
[Pluronic] (M)	**Soybean**	**Sesame**	**Olive**
3.9E-04	X	X	X
5.1E-04	X	X	X
7.8E-04	O	O	O
1.2E-03	O	O	O
1.6E-03	O	O	O
1.9E-03	O	O	O
2.2E-03	O	O	O
2.5E-03	O	O	O
2.8E-03	O	O	O
3.1E-03	X	X	X
3.9E-03	X	X	X
6.2E-03	X	X	X

5. Results

In our experiments, two main highlights should be remarked: i) the behaviour of the emulsions was not dependent on the oil used for a given surfactant concentration, ii) three different regions could be distinguished depending on the surfactant concentration added:

I) Below 7.8 10-4 mol/l, emulsions destabilized quickly, and coalescence was observed. In this case, the amount of surfactant is not enough to stabilize the emulsion, and droplets come closer and finally merge, becoming larger droplets.

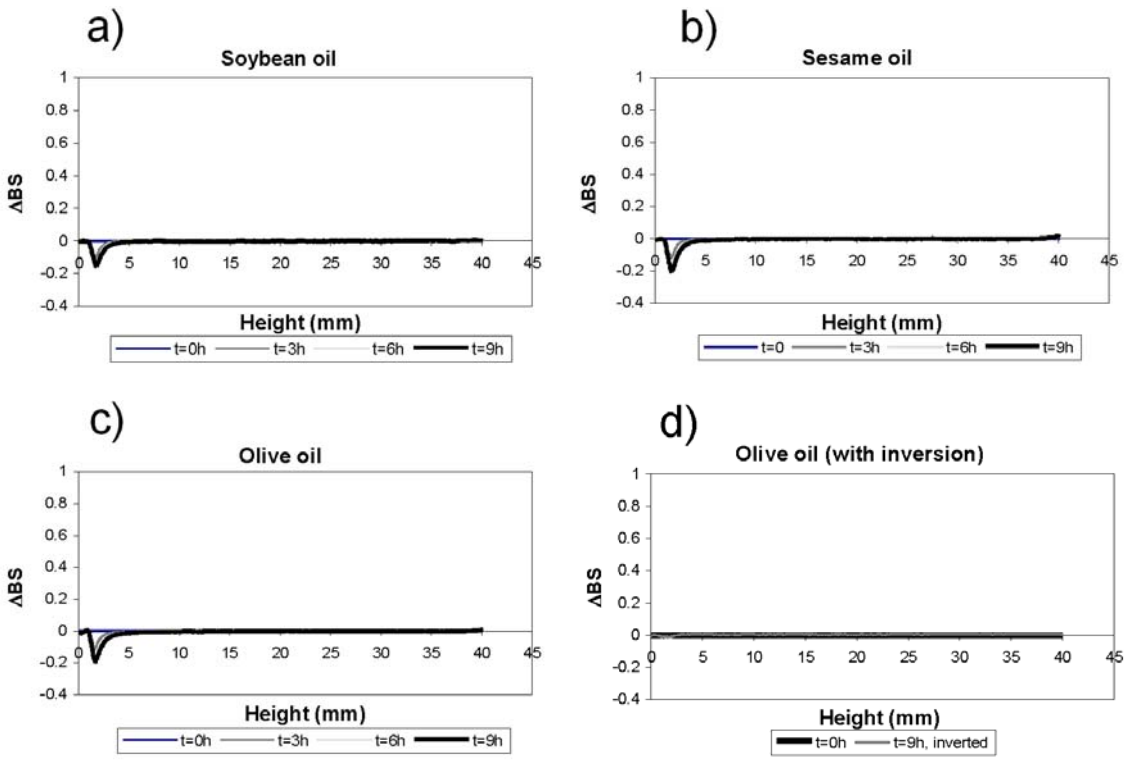

Fig. 3. Backscattered intensity at different times referred to the first measurement (t = 0) vs. height of the cell. 3a) Soybean oil emulsion, 1% Pluronic, t=9h. 3b) Sesame oil emulsion, 1% Pluronic, t=9h. 3c) Olive oil emulsion, 1% Pluronic, t=9h. 3d) Soybean oil emulsion, 1% Pluronic, t=9h, after gentle inversion.

II) Between 7.8 10-4 and 3.1 10-3 mol/l, emulsions were stable, since the backscattered profile did not vary along the middle part of the emulsion, i.e., the number and size of the droplets were not changing, as we can see in Figure 3. A little clarification was observed at the bottom of the cell, while most of the emulsion remained stable, which rules out the possibility of coalescence. Furthermore, this clarification was completely reversible, since it disappears by simply inverting gently the container (see Figure 3d). That is further evidence that coalescence is not taking place. The stabilization is due to the adsorption of surfactant: the central PPO block links to the oil droplet because of its hydrophobicity, while the two lateral hydrophillic chains of PEO remain in the aqueous phase, stabilizing the droplets by steric hindrance.

III) Above 3.1 10-3 mol/l, a quick phase separation is observed as observed in Figure 4a. Nevertheless, no coalescence was observed, since this change turned out to be reversible by gentle inversion (see Figure 4b). This led us to think on a depletion-flocculation mechanism, in which the excess of surfactant results in micelles formation, and those micelles make the droplets come closer via depletion. They do not merge due to their surfactant layers, but they are close enough to flocculate and cream, giving rise to two different phases. This model is theoretically treated in section 3.5.

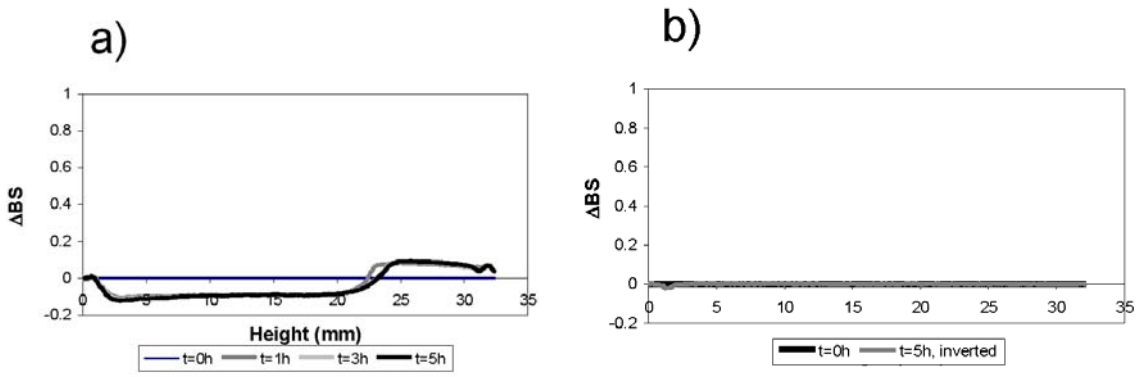

Fig. 4. a) Soybean oil emulsion, 2,5 % Pluronic, t=5h. 4b) Soybean oil emulsion, 2,5 % Pluronic, t=5h, after gentle inversion.

3.3 Measurement of droplet size.

Once we managed to obtain stable emulsions, the hydrodynamic diameter of the droplets was measured. The volume-weighted mean diameters and widths of the distributions for olive, sesame and soybean oil emulsions were 379 ± 54 nm, 368 ± 53 nm and 380 ± 48 nm respectively, which confirms that the emulsions prepared with those oils are not significantly different. In addition, these sizes are consistent with values reported by others (Abismaïl, Canselier, Wilhelm, Delmas, & Gourdon, 1999) for emulsification by ultrasound with similar oil volume fractions.

3.4 Micelle characterization

In order to study the destabilization by the depletion mechanism above mentioned, micelles had to be characterized, in terms of CMC, size and aggregation number. The measurement of the micelle radius by DLS gave a result of 9.4 ± 0.8 nm, which is very close to previous results obtained for similar systems (Mortensen and Pedersen, 1993; Kabanov et al., 2002). The CMC of Pluronic F68© was obtained by tensiometry in our laboratory, i.e., CMC = 10^{-5} mol/l. As explained in section 2.6, we obtained Mw(micelle) = 129870 g/mol, which is of the order of magnitude reported for similar systems by Kwon and Kataoka (1995). Since Pluronic F68 has a Mw=8400g/mol, dividing the former by the latter we obtain the aggregation number, i.e., N_{agg}=15 molecules of Pluronic per micelle.

3.5. Theoretical Treatment

A theoretical treatment related to the attraction, repulsion and depletion potential has been applied using our own experimental parameters. Applying the DLVO theory to this system, the total interaction energy (V_T) as a function of the shortest distance between the droplet surfaces (H), when they are completely covered by Pluronic F68©, is assumed to be the sum of all attractive and repulsive potentials:

$$V_T(H) = V_A(H) + V_R(H) + V_{dep}(H) \tag{4}$$

where V_A is the attraction potential, V_R is the repulsion potential due to osmosis and steric hindrance, and V_{dep} is the depletion potential when a considerable excess of surfactant is added. In the case in question, an electrostatic repulsion potential was neglected, due to fact that neither the oils nor the surfactant are ionic species.

In this paper we have also studied the possible stabilization mechanism based on repulsive hydration forces. The physical origin of this type of force arises from the local order of water layer adjacent to the surface (Israelachvili & Adams, 1978). It is not only correlated to the hydrophilicity of the surface but also depends strongly on the nature and concentration of the hydrated ions (Molina-Bolívar, Galisteo-González & Hidalgo-Álvarez, 1997) that surround the surface, i.e., the presence of calcium (a highly hydrated cation) should stabilize more than sodium, a less hydrated ion. However, we carried out some experiments preparing the emulsions also with $CaCl_2$ until a final concentration of 1M, without observing any changes in stability.

3.5.1 Attraction potential

The attractive potential energy expression used was the Van der Waals interaction for spherical particles of equal size as employed by Einarson and Berg (1992),

$$V_A(H) = -\frac{A}{6}\left(\frac{2a^2}{H(4a+H)} + \frac{2a^2}{(2a+H)^2} + \ln\frac{H(4a+H)}{(2a+H)^2}\right) \tag{5}$$

where A is the Hamaker constant and *a* is the radius of the particle. In this paper, we considered the suggestions of Vincent (1973) regarding the effect of the absorbed layer on the Van der Waals interaction through the Hamaker constant, based on the polymer volume fraction and the individual Hamaker constants of the medium and the polymer,

$$A = \left(\Phi A_p^{\frac{1}{2}} + (1-\Phi)A_m^{\frac{1}{2}}\right)^2 \tag{6}$$

where A_p is the Hamaker constant of the adsorbed polymer, Am the constant of the medium and ϕ the volume fraction of the adsorbate at a separation H. ϕ is given by

$$\Phi = \frac{2\delta\,\Phi_0}{H} \tag{7}$$

where ϕ_0 is the volume fraction in the adsorbed layer on the surface of the particle and δ is the average thickness of the polymer adsorbed layer.

3.5.2 Osmotic and steric repulsion potential

Vincent, Edwards, Emmett, and Jones (1986) made a quantitative study of the steric stabilization effect including two contributions: osmotic and coil compression. If there are polymeric chains covering the external surface of a particle, the average thickness of such coils being δ, then an osmotic effect will appear when the two particles are closer than a distance equal to 2δ. The osmotic pressure of the solvent in the overlap zone will be less than that in the external regions, leading to a driving force for the spontaneous flow of solvent into the overlap zone, which pushes the particles apart. In that case the osmotic potential of repulsion (V_{osm}) can be expressed as

$$V_{osm} = \frac{4\pi a}{\nu_1}(\phi_0)^2\left(\frac{1}{2}-\chi\right)\left(\delta-\frac{H}{2}\right)^2 \tag{8}$$

where ν_1 is the molecular volume of the solvent, ϕ_0 is the effective volume fraction of segments in the adsorbed layer, and χ is the Flory-Huggins solvency parameter.

If, however, the two particles are closer than a distance equal to δ, at least some of the polymer molecules will be forced to undergo elastic compression. Thermodynamically, this compression corresponds to a net loss in configurational entropy. This effect gives rise to a new repulsion potential (V_{VR}) related to the restriction of the movement of the hydrophilic tails extended toward the solvent. This elastic-steric repulsion is given by

$$V_{VR} = \left(\frac{2\pi a}{MW_p}\phi_0\delta^2 d_p\right)\left(\frac{H}{\delta}\ln\left[\frac{H}{\delta}\left(\frac{3}{2}-\frac{H}{2\delta}\right)^2\right]-6\ln\left[\frac{3}{2}-\frac{H}{2\delta}\right]+3\left(1-\frac{H}{\delta}\right)\right) \tag{9}$$

where d_p and MW_p are the density and the molecular weight of the polymer forming the hydrophilic tail. This modifies the osmotic potential, which in this case is given by

$$V_{osm} = \frac{4\pi a}{v_1}(\phi_0)^2\left(\frac{1}{2}-\chi\right)\delta^2\left[\left(\frac{H}{2\delta}\right)-\frac{1}{4}-\ln\left(\frac{H}{\delta}\right)\right] \quad (10)$$

and therefore the total repulsion potential will be given by

$$V_R = V_{osm} + V_{VR} \quad (11)$$

3.5.3 Depletion potential

Walz and Sharma (1994) developed a theoretical model to study the interaction between two spherical particles due to the presence of spherical macromolecules with a penetrable hard sphere approach, which, according to Tuinier, Rieger and de Kruif (2003), adapts better to a system where the sizes of the droplet and the micelle that causes the depletion are not of the same order of magnitude. This model was adapted by Jódar-Reyes et al. (2006) who expressed the pair potential between two identical spherical particles resulting from spherical micelle depletion, in k_BT units, as

$$\frac{V_{dep}(H)}{k_BT} = -\rho_\infty\pi\left[\frac{4}{3}r^3 + 2r^2a - r^2H - 2raH + \frac{aH^2}{2} + \frac{H^3}{12}\right] \quad (12)$$

in the range $0 \le H < 2r$, where H is the shortest distance between the particle surfaces, a is the radius of the particle, r is the radius of the micelle, and ρ_∞ is the number of micelles per unit volume in the system.

3.5.4 Total interaction potential

We have plotted the different potentials and the sum of all of them (equation 4) against the distance between droplet surfaces, using our experimental parameters: i) radius of the particle (see section 3.3) ii) radius of the micelle (section 3.4), iii) thickness of surfactant in the adsorbed layer, δ = 7 nm (inferred from the previous value taking into account the structure of Pluronic F68©, which is close to that reported by Baker and Berg (1988) for

Pluronic-PLGA complexes) iv) the value of ρ_∞, which was estimated as follows: the difference between the surfactant concentration that causes depletion and the first surfactant concentration that causes the most stable emulsions (approximately in the middle of the stability range) was considered the excess of surfactant on the medium, and therefore the concentration of surfactant available to form micelles. The amount of free surfactant together with the average aggregation number (section 3.4) gives us the amount of micelles.

We also used the same fit parameter ϕ_0 reported by Vincent, Luckham & Waite (1980) for a similar system, i.e., $\phi_0 = 0.28$.

When there is enough Pluronic F68 to cover the droplets but not to form a considerable amount of micelles, the depletion potential is negligible, and only the Van der Waals attraction and the osmotic-steric repulsion are considered as can be observed in Figure 5a. In this case, the PEO adsorbed layers feel a weak attraction when the droplets are very close to a distance of 2δ, in any case not strong enough to maintain the layers attached (lower than $10k_BT$).

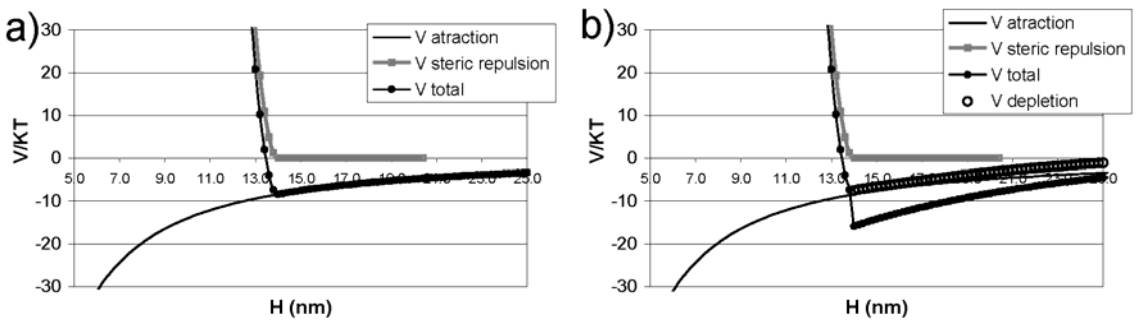

Fig. 5. a)Potential vs. distance between droplets around 2δ (14nm), without depletion 5b)Potential including depletion.

If we add the depletion potential to the total potential (Figure 5b), the minimum diminishes and a larger well potential is created around 2δ. This could explain the experimental results: when a large amount of surfactant is added, the presence of a large number of micelles forces the droplets to come closer enough to merge their adsorbed layers. Nevertheless, the PEO layers prevent the droplets to merge due to their size,

therefore depletion-flocculation occurs but not coalescence. This flocculation causes droplet aggregates, which due to their size lose the stability against creaming that nanoemulsions have, and a two-phase separation takes place.

4. Conclusions

Our first aim has been to prepare nanoemulsions of natural oils with the non-toxic surfactant Pluronic F68 via ultrasound, and to characterize them experimentally in terms of stability and droplet size. Those emulsions proved to be stable against coalescence, even with a relatively small amount of surfactant and with volumes of oil as high as 25% (v/v).

We observed a reversible destabilization when a high amount of surfactant was added. In order to explain this phenomenon we adapted a theoretical model of depletion-flocculation using experimental parameters. We found good agreement between the calculated and observed stability.

Acknowledgments

This research is supported by FEDER funds and "Ministerio de Educación y Ciencia" under project MAT2007-66662-C02-01 and by "Junta de Andalucía – Consejería de Educación, Ciencia y Empresa" under project P07- FQM – 03099. M.W.P. thanks the latter project referred for the scholarship received. We express our gratitude to Fernando Vereda for revising the final English version.

References

Abismaïl, B., Canselier, J.P., Wilhelm, A.M., Delmas, H. & Gourdon, C. (1999) Emulsification by ultrasound: drop size distribution and stability. Ultrasonics Sonochemistry, 6 , 75-83

Baker, J. A. & Berg, J. C. (1988) Investigation of the adsorption configuration of polyethylene oxide and its copolymers with polypropylene oxide on model polystyrene latex dispersions. Langmuir, 4(4), 1055-61

Canselier, J. P., Delmas, H., Wilhelm, A.M. & Abismaïl, B. (2002) Ultrasound emulsification-An overview. Dispersion Science and Technology, 23(1-3), 333-349

Chauvierre, C., Labarre, D., Couvreur P. & Vauthier, C. (2004). A new approach for the characterization of insoluble amphiphilic copolymers based on their emulsifying properties. Colloid Polym Science 282: 1097–1104

Dickinson, E. (2003). Hydrocolloids at interfaces and the influence on the properties of dispersed systems. Food Hydrocolloids 17, 25-39.

Dickinson, E., Golding, M. & Povey M. J. W. (1998) Creaming and flocculation of oil-in-water emulsions containing sodium caseinate. Journal of Colloid and Interface Science 185, 515–529

Einarson, M. B., & Berg, J. C. (1992) Electrosteric stabilization of colloidal latex dispersions. Journal of colloid and interface science. Journal of Colloid and Interface Science, 155, 165-172.

Israelachvili, J. N. & Adams, G. E. (1978) Measurement of forces between two mica surfaces in aqueous electrolyte solutions in the range 0–100 nm J. Chem. Soc., Faraday Trans. 1, 74, 975 – 1001.

Jackson, J. C., Springate, C. M. K., Hunter, W. L. & Burt, H. M. (2000) Neutrophil activation by plasma opsonized polymeric microspheres: inhibitory effect of Pluronic F127. Biomaterials 21, 1483-1491.

Jumaa, M. & W. B. Müller (1998) The stabilization of parenteral fat emulsion using non-ionic ABA copolymer surfactant. International Journal of Pharmaceutics 174, 29–37

Jódar-Reyes, A. B., Martín-Rodríguez, A. & Ortega-Vinuesa, J.L.(2006) Effect of the ionic surfactant concentration on the stabilization/destabilization of polystyrene colloidal particles. Journal of Colloid and Interface Science, 298, 248–257

Kabanov, A. V., Batrakova E.V. & Alakhov, V. A. (2002) Pluronic® block copolymers as novel polymer therapeutics for drug and gene delivery. Journal of Controlled Release 82, 189–212

Kibbe, A.H. (2000) Handbook of Pharmaceutical Excipients. American Pharmaceutical Association, Washington, 386-8.

Koppel, D. E.(1972) Analysis of macromolecular polydispersity in intensity correlation spectroscopy. Method of cumulants. Journal of Chemical Physics, 57(11), 4814-20.

Kwon G.S. & K. Kataoka, K. (1995). Block copolymer micelles as long circulating drug vehicles. Adv. Drug Deliv. Rev. 16:295Y309.

Kwon, S. Y. & Kim, M. W. (2001) Structure and growth control of a nonionic surfactant micelle by adding a phospholipid. Langmuir, 17 (26), 8016 -8023.

McClements, D. J. (2004) Food emulsions: principles, practice, and techniques. CRC Press, USA.

Mengual, O., Meunier, G., Cayre, I., Puech, K., and Snabre, P. (1999). Characterisation of instability of concentrated dispersions by a new optical analyser: the TURBISCAN MA 1000. Colloids and Surfaces A: Physicochemical and Engineering Aspects 152, 111–123

Molina-Bolivar, J. A.; Aguiar, J., Ruiz & Carnero C. (2001) Light scattering and fluorescence probe studies on micellar properties of Triton X-100 in KCl solutions. Molecular Physics, 99(20), 1729-174

Molina-Bolívar, J. A., Galisteo-González, F., & Hidalgo-Álvarez R. (1997) Colloidal stability of protein-polymer systems: A possible explanation by hydration forces Phys. Rev. E 55, 4522 – 4530

5. Results

Mortensen, K. & Pedersen J. S. (1993). Structural study on the micelle formation of Poly(ethy1eneoxide)-Poly(propy1ene oxide)-Poly(ethy1ene oxide) triblock copolymer in aqueous solution . Macromolecules, 26, 805-812.

Napper, D.H. (1983) Polymeric Stabilization of Colloidal Dispersions, Academic Press INC, London.

Seekkuarachchi, I.N, Tanaka K, Kumazawa, H. (2006) Formation and Characterization of Submicrometer Oil-in-Water (O/W) Emulsions, Using High-Energy Emulsification. Industrial & Engineering Chemical Research, 45:372–390

Tadros, T., Izquierdo, P., Esquena, J., & Solans, C. (2004) Formation and stability of nano-emulsions. Advances in Colloid and Interface Science 108 –109, 303–318

Tolstoguzov, V. (2001) Some thermodynamic considerations in food formulation. Food Hydrocolloids, 17(1), 1-23

Tomoko, N. & Fumiyoshi, I. (2004) Properties of various phosphatidylcholines as emulsifiers or dispersing agents in microparticle preparations for drug carriers. Colloids and Surfaces B: Biointerfaces, 39, 57–63

Tuinier, R., Rieger, J., de Kruif, C.G. (2003). Depletion-induced phase separation in colloid-polymer mixtures. Advances in Colloid and Interface Science 103, 1-31.

Vincent, B. (1973) The van der Waals attraction between colloid particles having adsorbed layers. II. Calculation of interaction curves. Journal of Colloid and Interface Science, 42, 270-285.

Vincent, B., Edwards, J., Emmett, S., & Jones, A., (1986) Depletion flocculation in dispersions of sterically-stabilized particles ("soft spheres"). Colloids and Surfaces, 18, 261

Vincent, B., Luckham, P. F. & Waite, F.A. (1980) The Effect of Free Polymer on the Stability of Sterically Stabilized Dispersions. Journal of Colloid and Interface Science, 73, 508-521

Walz, J. Y. & Sharma, A. (1994) Effect of long range interactions on the depletion force between colloidal particles. Journal of Colloid and Interface Science, 168(2), 485-96

Yalin, M., Öner, F., Öner, L., and Hincal, A. A. (1998) Preparation and properties of a stable intravenous lorazepam emulsion. Journal of Clinical Pharmacy and Therapeutics 22, 39–44

Paper II.

Bulk and interfacial viscoelasticity in concentrated emulsions: The role of the surfactant.

Miguel Wulff-Pérez, Amelia Torcello-Gómez, Antonio Martín-Rodríguez, María J. Gálvez-Ruíz and Juan de Vicente

Biocolloid and Fluid Physics Group. Department of Applied Physics. Faculty of Sciences, University of Granada, 18071 Spain.

Published in:

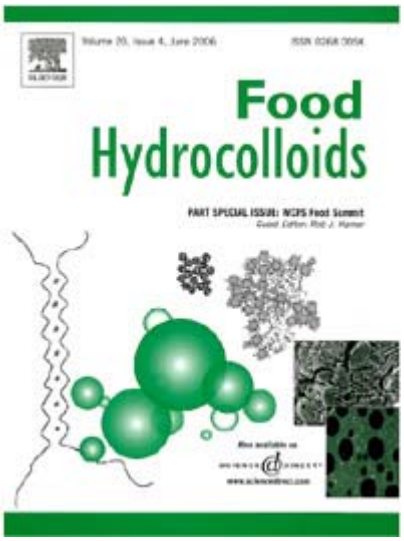

Food Hydrocolloids

Volume 25, Issue 4, June 2011, Pages 677-686

Abstract

The aim of this study was to investigate and compare bulk and interfacial viscoelasticity of emulsions stabilized with two surfactants of a markedly different nature: the ionic phospholipids mixture Epikuron 145V and the steric emulsifier Pluronic F68. Emulsions of olive oil in water were prepared by high-pressure homogenization using only one of these surfactants. The impact of the surfactant used on the final linear viscoelastic properties was investigated by means of small-amplitude dynamic oscillatory shear tests, obtaining the values of the storage and loss moduli as a function of frequency, as well as by retardation and relaxation essays. Our results show that for concentrated emulsions, the viscoelastic properties are considerably different depending on which surfactant is used, i.e., the employed surfactant influences to a major extent the bulk rheological properties. In order to explain these differences, an interfacial study of the adsorbed surfactant layers has been carried out, measuring interfacial tension and dilatational viscoelasticity by means of the pendant drop technique. A correlation between the results obtained in bulk and interface has been found.

1. Introduction

Emulsions are not a thermodynamically stable system. However, the presence of surfactant at the interface between continuous and disperse phases provides them with kinetic stability, i.e., long term stability against destabilizing phenomena such as flocculation, aggregation and coalescence. The surfactant to be used in the formulation of emulsions strongly depends on the application. Most surfactants have an ionic character (anionic, cationic or zwitterionic) that provides the droplets with a certain Zeta-potential, preventing them from merging by means of ionic repulsion. However, in many practical cases where emulsions are applied under high ionic strength conditions, this stabilization mechanism fails. For this reason, much attention has been paid on surfactants that do not provide the droplet surface with a significant charge, but with steric-stabilizing groups protruding from the interface into the dispersion medium and forming a bulky layer with thicknesses of several nanometers, reducing direct contact between droplets and hence coalescence (Grigoriev & Miller, 2009).

In this work two model surfactants are employed to investigate which is their effect on bulk and interfacial viscoelastic properties of concentrated oil-in-water emulsions. As a model of surfactant acting as steric stabilizer, we used Pluronic F68 (also known as Lutrol F68 or poloxamer 188). It is a triblock copolymer able to form a bulky adsorbed layer that prevents the droplets from coalescence. Due to its low toxicity, Pluronic F68 has been used as emulsifier, solubilizer, and suspension stabilizer in liquid oral, topical, ocular and parenteral dosage forms (Kabanov, Batrakova, & Alakhov, 2002; Croy & Kwon, 2004; Tong, Chang, Liu, Kao, Huang & Liaw, 2007). As a model of ionic surfactant, we used a commercial deoiled phosphatidylcholine-enriched fraction of soybean lecithin known as Epikuron 145V. Lecithin is a well-tolerated and non-toxic surfactant approved by the United States Food and Drug Administration for human consumption with "Generally Recognized As Safe" (GRAS) status, and Epikuron 145V has been specifically employed as surfactant in enteral and parenteral emulsions.

Diluted emulsions typically behave as Newtonian fluids, however viscoelastic properties appear for highly concentrated emulsions when droplets are in close contact.

5. Results

Small-amplitude dynamic oscillatory shear (SAOS) tests are a powerful tool to obtain information about the microscopic structure of a viscoelastic material providing us with a storage, G´, and loss moduli, G´´. G´ is proportional to the extent of the elastic component of the system, and G´´ is proportional to the extent of the viscous component of the system (Macosko, 1994).

A strain amplitude sweep test is frequently used to determine the yield and flow points and hence the extent of the linear viscoelastic region. Once this region is established, measurements are made as a function of strain frequency to get the mechanical spectrum of the material (Mackley, Marshall, Smeulders, & Zhao, 1994; Steffe, 1996). Apart from oscillatory testing, other complimentary essays can be performed to characterize the viscoelasticity of concentrated emulsions: retardation (shear creep) and relaxation (step-strain) tests. This last type of experiments has been used in this work to characterize also the non-linear viscoelasticity of the emulsions, since this kind of viscoelasticity is involved in many processes related e.g. with food rheology, from mastication and swallowing to processability, quality and texture of the end product (Steffe, 1996; Bengoechea, Puppo, Romero, Cordobés & Guerrero, 2008).

In the case of colloidal systems having large specific surface, such as sub-micron emulsions, interfacial rheological knowledge may prove indispensable for understanding bulk hydrodynamic behavior. There are two well differentiated scenarios where interfacial and bulk rheology do necessarily interplay. On the one hand, at (very) low interfacial dilatational moduli bulk rheological behavior of emulsions is directly related to the interfacial rheology since the latter determines the coupling between the flow in the emulsion droplets and that of the continuous phase directly outside the emulsion droplets. However, this is not the case at higher surface dilatational moduli. Then the flow of the liquid inside the emulsion droplets is not affected anymore by that of the continuous phase outside the droplets. On the other hand, there can again be a direct relation between the rheology of emulsions and the interfacial rheology when the volume fractions are so high that the emulsion droplets strongly deform each other. For other cases the relation will be indirect for the studied conditions of stress levels. As the bulk-phase macroscale rheology of a concentrated emulsion is related to the interfacial rheology, microscale interfacial

hydrodynamics may influence emulsion flow behavior (Edwards, Brenner, & Wasan, 1991). Surfactant molecules adsorb spontaneously at the oil/water interface, thereby reducing the interfacial tension forming a surfactant molecular layer. The characteristics of the adsorbed layer can be quantitatively accounted for by the interfacial dilatational viscoelasticity which in fact, describes the response of the interfacial tension to dilatational stresses of the interface. It is possible to determine the dynamic compression (or dilatation) interfacial properties at fluid-liquid interfaces using different methods. In particular, oscillating drop techniques are used here. In general, the layers can also resist shearing forces, but for surfactants, the shear viscoelasticity is expected to play a small role (Georgieva, Schmitt, Leal-Calderon, & Langevin, 2009).

Little is yet known about the actual values of oil-water interfacial viscoelasticity of surfactant monolayers (Bonfillon & Langevin, 1994; Santini, Liggieri, Sacca, Clausse, & Ravera, 2007). A huge difficulty is posed by the existence of surfactant exchange between the surface and bulk that lowers the surface viscoelastic parameters to a large extent, especially when the surfactant concentration is high. This is the case of surfactant monolayers formed at the surface of the emulsion droplets. In the present work, we used polymeric surfactant, which possesses larger adsorption energies and is essentially irreversibly adsorbed (Hansen, 2008), and ionic surfactant for which electrostatic repulsion between the molecules and the interface slows down the exchanges (Bonfillon & Langevin, 1994).

In this article, in order to investigate possible correlations between interfacial rheology and bulk-phase rheology, the respective oil-water interfaces have been investigated, by measuring interfacial tension and dilatational viscoelasticity on concentrated solutions of Pluronic F68 and Epikuron 145V.

2. Materials and methods

2.1. Materials

The poloxamer Pluronic F68 was obtained from Sigma-Aldrich. It is a triblock copolymer based on poly(ethylene oxide)-block-poly(propylene oxide)-block- poly(ethylene oxide) structure which is also typically expressed as PEOa-PPOb-PEOa, being a = 75 and b = 30. The central block has an hydrophobic character and is adsorbed at the surface of the droplet, whereas the two chains of poly(ethylene oxide) remain in the aqueous phase, forming the bulky layer. This non ionic polymeric surfactant has a molecular weight of 8400 Da. Epikuron 145V is a highly purified deoiled phosphatidylcholine-enriched fraction of soybean lecithin, with an average molecular weight of 760 Da (de Vleeschauwer & Van der Meeren, 1999). According to the manufacturer, it contains 61% phosphatidylcholine, 22% phosphatidylethanolamine and 16% phytoglycolipids. Epikuron 145V was kindly provided by Cargill Ibérica S. L. Olive oil was obtained from Sigma-Aldrich, and purified with Activated Magnesium Silicate (Florisil, Fluka) to eliminate free fatty acids. The oil was kept under mild agitation with the resins for 3 h and centrifuged at 12,000 rpm for 30 min in a bench centrifuge. It was then filtered and stored away from light.

2.2. Preparation of the emulsions

Oil-in-water emulsions were prepared mixing olive oil and Milli-Q purified water (0.054 μS) with volume fractions ranging from 0.525 to 0.65, on basis of a total volume of 30 mL. Firstly, we defined a protocol for emulsification to achieve the desired droplet size and monodispersity. For Pluronic F68 emulsions, surfactant was added to the water under stirring, whereas for Epikuron 145V emulsions, surfactant was added to the oil under stirring and gentle warming to guarantee complete dissolution. Then, a pre-emulsion was formed mixing both phases using a high speed Heidolph Diax 900 stirrer for 4 minutes at 13,000 rpm, by dropwise addition of oil to the water under stirring. This coarse emulsion was immediately homogenized using the high pressure Emulsiflex-C3 homogenizer (Avestin, CA) at 103 MPa. All emulsions were passed through the homogenizer 8 times.

The surfactant/olive oil ratio (w/w) was kept constant, being 0.07 for Epikuron 145V and 0.044 for Pluronic F68 emulsions i.e., ranging from 3.87 to 4.87 wt% on the total emulsion volume for Epikuron, and from 2.68 to 3.05 wt% for Pluronic. These ratios were chosen after preparing emulsions with the protocol specified above, varying the amount of surfactant and keeping constant the volume fraction, and then measuring droplet size and stability of the emulsion (see section below for further details). When a lower surfactant/oil ratio was used, the droplet sizes obtained were higher (for Pluronic F68 emulsions), or were not constant and coalescence was observed (for Epikuron 145V emulsions). On the other hand, a higher surfactant/oil ratio than 0.044 and 0.07 w/w for Pluronic F68 and Epikuron 145V, respectively, did not produce a reduction in droplet size when the emulsion was homogenized, which means that there is more surfactant than needed to cover the interface when the droplets are produced.

2.3. Characterization of the emulsions

The stability against coalescence or creaming was evaluated using a Turbiscan 2000 (Formulaction, France) as described elsewhere (Wulff-Pérez, Torcello-Gómez, Gálvez-Ruíz & Martin-Rodríguez, 2009). Briefly, the emulsion is placed in a flat-bottomed cylindrical glass cell and scanned from the bottom to the top with a light source and two detector devices, in order to monitor light transmitted through the sample (180º from the incident light, transmission sensor), and light backscattered by the sample (45º from the incident radiation, backscattering detector, more appropriate for concentrated emulsions). The Turbiscan works in scanning mode. This means that the optical reading head scans the length of the sample acquiring transmission and backscattering data every 40 μm. Scans are repeated over time, each one providing a new curve, and all curves are overlaid on one graph to show stability over time. Backscattering remains unchanged in the whole height of the cell when the number of particles and interfaces is not changing, i.e. if no coalescence, creaming or sedimentation occurs.

Mean droplet size and polydispersity index (PDI) were measured by Dynamic Light Scattering at 25 ºC with an ALV-NIBS/HPPS (ALV-Gmbh, Germany), where the measurement of scattered light is taken at an angle of 173º. This backscattering technique detects only light scattered from the surface of the sample, which minimizes the optical

path and consequently multiple scattering. The detected light is then processed by a digital correlator (ALV 5000/E) that provides the correlation function, from which the diffusion coefficient of the emulsion droplets is calculated using the cumulant method. Finally, the hydrodynamic radius is obtained by means of the Stokes–Einstein relation, as well as the polydispersity index (PDI), corresponding to the square of the normalised standard deviation of an underlying Gaussian size distribution. Before measuring, each sample had to be diluted with Milli-Q water to reach optimal measurement conditions (in all cases below 1 % (v/v) oil-in-water emulsion).

2.4. Bulk shear rheology

An MCR Rheometer (Anton Paar Gmbh, Austria) was used to study the bulk rheology of emulsions, using a cone-plate geometry (50 mm diameter, 1º), maintaining temperature at 25 ºC with a peltier. To avoid evaporation a solvent-trap system was used and some low-viscosity silicone oil was poured on the rim of the cone. The same protocol was used to characterize both Pluronic F68-stabilized and Epikuron 145V-stabilized emulsions. Each test was run in triplicate with fresh samples. It is worth to stress here that wall slip was not observed under similar operation conditions using rough surfaces and plate-plate geometries.

The viscoelastic linear region was first determined by means of small-amplitude oscillatory shear (SAOS) rheology. In particular, strain amplitude sweep tests at a constant frequency were run. Initially the sample is pre-sheared at a constant shear rate of 20 s^{-1} for 30 s in torsional mode. Next, the sample is allowed to recover for a period of 60 s. Finally a SAOS amplitude sweep test is performed, by varying the strain amplitude from γ_0 = 0.01 % to γ_0 = 100 %, keeping a constant angular frequency of ω = 10 rad/s. If the strain amplitude γ_0 is small enough, the resulting shear stress signal τ is a sine wave of the same frequency as the input strain wave. The shear stress, however, usually will not be in phase with the strain, but could be built up by the addition of two terms, one in phase with the strain and the other out-of-phase with the strain according to:

$$\tau/\gamma_0 = G'\sin\omega t + G''\cos\omega t \quad (1a)$$

$$G'(\omega) = \frac{\tau_0}{\gamma_0}\cos\delta \tag{1b}$$

$$G''(\omega) = \frac{\tau_0}{\gamma_0}\sin\delta \tag{1c}$$

Here, G' and G" represent the storage and loss modulus respectively, being δ the existing phase difference between the strain and the stress.

Once the linear viscoelastic region was determined, the mechanical spectra of the emulsions were obtained from SAOS frequency sweep tests. Pre-shear and recovery steps were applied prior to each test as described previously in SAOS amplitude sweeps. In the frequency sweep test the applied strain amplitude was γ_0 = 0.1 % well within the viscoelastic linear region in all cases, and the excitation frequency ranged from ω = 100 rad/s to ω = 0.1 rad/s.

For completeness, the viscoelastic properties were also studied using transient experiments (Ferry, 1980). Two experiments were performed. The first one consisted in the application of an instantaneous constant stress τ_0 while measuring the shear strain. In this shear creep flow, the associated rheological material function relates the measured sample deformation (strain γ) to the prescribed (constant) stress τ_0. This material function is called shear creep compliance $J(t) = \gamma(t)/\tau_0$. Several τ_0 were tested for each type of emulsion. At low stress values the measured compliance does not change. However, upon increasing the stress compliance curves do not overlap anymore revealing the onset of the non-linear regime (Dolz, Hernández & Delegido, 2008). Creep experiments were performed with the most concentrated emulsions (ϕ = 0.65 vol%) because the differences between the emulsions are highlighted at this concentration.

The second transient rheological experiment involves a stress relaxation. In these tests also the most concentrated emulsions were only analyzed. Different initial strains γ_0 were applied while measuring stress relaxation modulus G(t), which is defined as $G(t) = \tau(t)/\gamma_0$. At low deformations, the relaxation modulus remains the same and all G(t) curves overlapped. From this, the linear viscoelastic behavior was inferred. For large

deformations, G(t) curves did not overlap and so obtained damping function was used to compare viscoelasticity in the non-linear region between the two emulsions investigated.

2.5. Interfacial tension set-up and adsorption process

Solutions were prepared by successive dilution from a concentrated solution, in Milli-Q purified water (0.054 μS) in the case of Pluronic F68, and in olive oil for Epikuron 145V. Only freshly prepared solutions were used for each experiment. All the glassware was washed with Micro-90 (International Products Corp.) and rinsed with water, followed by ethanol 96º, and then repeatedly rinsed with distilled and ultrapure water. The interfacial tension of the clean oil-water interface (Γ_0) was measured before each experiment to ensure the absence of surface-active contaminants obtaining values of 26.0 ± 0.5 mJ/m2. All the experiments were performed at T = 25 ºC and the reproducibility of the experiments was verified through replicate measurements.

The interfacial tension measurements were performed in a Pendant Drop Film balance based on Axisymmetric Drop Shape Analysis (ADSA), which is described in detail elsewhere (Cabrerizo-Vílchez, Wege, Holgado-Terriza & Neumann, 1999). The setup, including the image capturing, the microinjector, the ADSA algorithm, and the fuzzy pressure control, is managed by a Windows integrated program (DINATEN). The computer program fits experimental drop profiles, extracted from digital drop micrographs, to the Young-Laplace equation of capillarity by using ADSA, and provides as outputs the drop volume V, the interfacial tension Γ, and the interfacial area A. The interfacial pressure values, π, are obtained from the relationship $\pi = \Gamma_0 - \Gamma$, where Γ_0 is the interfacial tension of pure oil-water interface (26.0 ± 0.5 mJ/m^2), and Γ is the interfacial tension of the interface covered with the adsorbed film. Interfacial pressure and area control use a modulated fuzzy logic PID algorithm (proportional, integral, and derivative control) (Wege, Holgado-Terriza & Cabrerizo-Vílchez, 2002). The drop is immersed in a glass cuvette (Hellma), which contains the oil phase and is kept in a thermostatized cell at 25 °C. The droplet is formed at the tip of a coaxial double capillary, connected independently to a double microinjector.

The adsorption process of Pluronic F68 and Epikuron 145V is studied independently by recording the change of interfacial tension at a constant interfacial area of 33 mm2 for 30 minutes, at different bulk concentrations. For Pluronic F68, the bulk concentrations varied between 1.2 μM (0.01 g/L) and 24 mM (200 g/L). In the case of Epikuron 145V, the concentrations ranged from 1.1 μM ($8 \cdot 10^{-4}$ g/L) to 2 mM (1.6 g/L). The largest concentration reached is limited by the maximum concentration associated to the droplet fall due to the fast drop in the interfacial tension.

2.6. Interfacial dilatational rheology

The dilatational rheology of the adsorbed layers has been measured with the pendant drop technique. An oscillatory perturbation was applied to the interface by injecting and extracting volume to the drop. The system records the response of the interfacial tension to the area deformation, and the dilatational modulus (E) of the interfacial layer can be inferred from this response. This technique requires a quasi-equilibrium drop shape for the calculation of the interfacial tension. Hence, the applied interfacial area oscillations were maintained below 1 % of amplitude to avoid excessive perturbation of the interfacial layer and the departure from the viscoelastic linear region. The oscillation frequency (f) was set to 0.1 Hz.

In a general case, the dilatational modulus is a complex quantity that contains a real and an imaginary part:

$$E^* = E' + iE'' = \varepsilon + i2\pi f\eta \qquad (2)$$

where E' is the storage modulus and accounts for the elasticity of the interfacial layer and E" is the loss modulus and accounts for the viscous dissipation of the interfacial layer.

3. Results and discussion

This section is organised as follows. First of all, we present the emulsion characterization. Then, the bulk rheology is described. Next, we show the interfacial

pressure isotherms of Pluronic F68 and Epikuron 145V. Finally, the properties of the interfacial layers are further characterized by the interfacial dilatational modulus.

3.1. Emulsion characterization

The emulsions obtained were stable against creaming or coalescence during the measured period (24 h). Since the rheological tests were performed with freshly prepared emulsions, neither coalescence nor creaming is expected to affect bulk rheological measurements. Phase inversion was not observed upon increasing oil content.

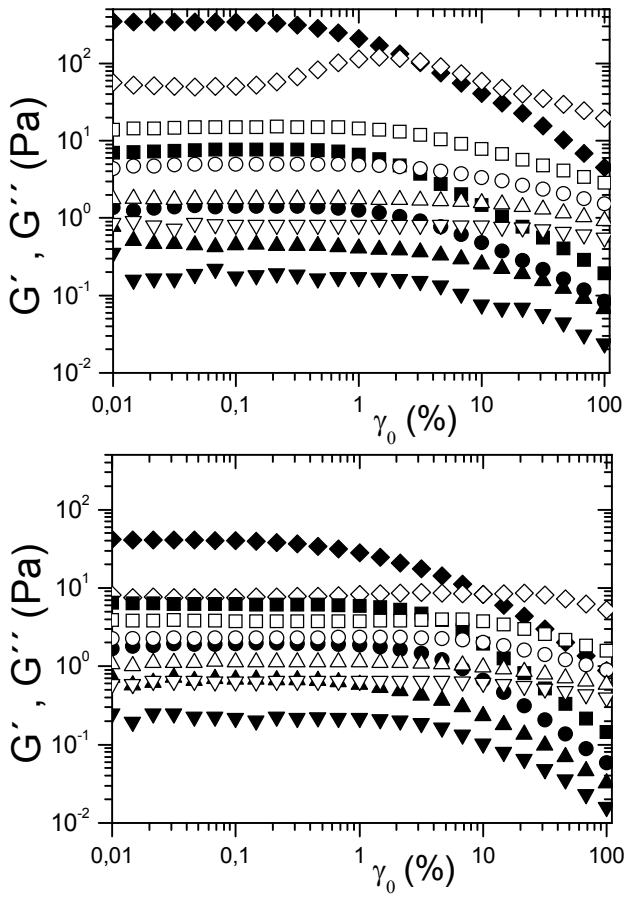

Fig. 1. Strain amplitude sweep tests at a constant frequency of ω= 10 rad/s; closed symbol, G´; open symbol, G´´;-♦-, ϕ = 0.65; -■-, ϕ = 0.60; -●-, ϕ = 0.575; -▲-, ϕ = 0.55; -▼-, ϕ = 0.525. (a) Pluronic F68-stabilized emulsions, (b) Epikuron 145V-stabilized emulsions.

The mean droplet sizes and PDI were between 288-293 nm and 0.056-0.060, for Pluronic F68-stabilized emulsions, and 301-308 nm and 0.031-0.040 for phospholipid-stabilized emulsions.

3.2. Bulk rheology

SAOS strain amplitude sweep results are shown in Figure 1. Here we show storage and loss modulus dependence on strain amplitude. As long as the strain amplitude is small, G' and G" curves present a constant plateau value. Here, the structure of the sample is only slightly perturbed and it behaves in the viscoelastic linear region. Analyzing the behavior in this regime any sample can be classified as a gel- or liquid-like material depending if the ratio G"/G' is smaller or larger than one, respectively. According to this ratio a new definition arises which is called loss tangent tanδ = G"/G'. As observed from Figure 1, in all cases emulsions behave as liquid like materials at low particle concentrations (G' < G"). However, strongly concentrated systems present a larger storage modulus possibly associated to the interparticle contacts (G" < G'). Interestingly, for the same particle content at large concentrations, both kinds of emulsions behave differently, presenting Epikuron 145V based oil-in-water emulsions a larger storage modulus than Pluronic F68 based ones.

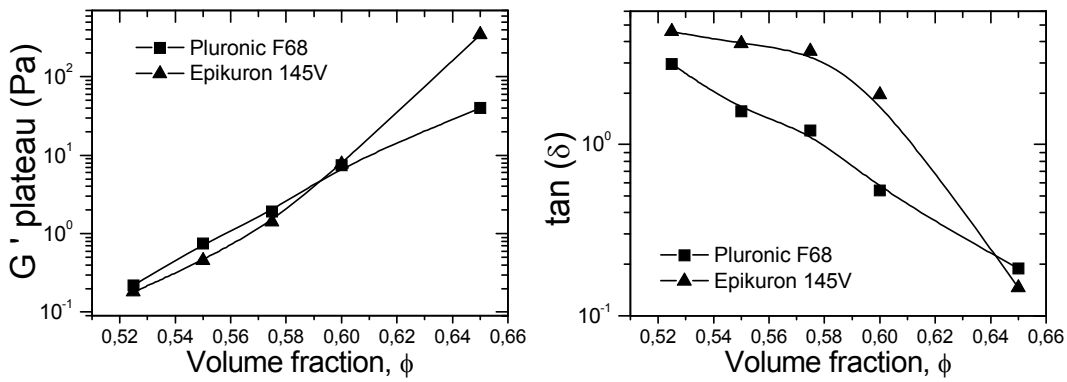

Fig. 2. Low-strain G' (a) and loss tangent (b) as a function of particle volume fraction. Lines are plotted as a guide for the eye.

5. Results

More quantitative information can be obtained from Figure 2. Here, we show results corresponding to low-strain G' and tanδ volume fraction dependences. As observed, the values of G´ differed notably when the volume fraction becomes the highest, being more than an order of magnitude higher for the phospholipid-stabilized emulsion at $\phi = 0.65$. Interestingly, not only G' but also G" increases at the highest concentration. This results in the sudden decrease of tan δ for Epikuron 145V being now lower than tanδ for Pluronic F68 at $\phi = 0.65$. As observed in Figure 2, droplets in Pluronic F68 stabilized emulsions seem to start to interact with each other earlier, since the Pluronic F68 layers are expected to be thicker than Epikuron 145V. However, for the highest volume fraction Epikuron 145V based o/w emulsions have a larger storage modulus than Pluronic F68 based ones.

Table 1. Yield Points corresponding to Pluronic F68 and Epikuron 145V oil-in-water emulsions.

	Pluronic F68		Epikuron 145V	
Volume fraction	**Strain (%)**	**Stress (Pa)**	**Strain (%)**	**Stress (Pa)**
0.65	0.327	0.121	0.294	0.941
0.60	1.24	0.100	0.812	0.132
0.575	1.40	0.041	0.950	0.048
0.55	0.854	0.010	1.06	0.019
0.525	2.38	0.015	2.25	0.018

When the strain amplitude is large enough, non-harmonics appear in the resulting signal as a result of non-linear phenomena. The yield point is usually taken as a quantitative parameter to describe the extent of the linear viscoelastic region. The most common criteria for this being the stress/strain value corresponding to a G_0 which is equal 90% the storage value at the low deformation plateau. In Table 1 we show the corresponding yield points for the two systems investigated. As observed, for a given concentration, the yield strain remains approximately the same in both samples, in contrast to the yield stress which significantly changes at large concentration. For the highest concentration, yield stress for Epikuron-stabilized emulsions is almost eight times that one of Pluronic-

stabilized emulsions. Upon further increasing the strain amplitude, the system does experience a transition from solid-like to liquid-like behavior. This occurs at the flow point when the storage modulus equals the loss modulus ($\tan\delta = 1$). For completeness, flow point data corresponding to our emulsions are presented in Table 2.

Table 2. Flow Points corresponding to Pluronic F68 and Epikuron 145V oil-in-water emulsions.

	Pluronic F68		Epikuron 145V	
Volume fraction	**Strain (%)**	**Stress (Pa)**	**Strain (%)**	**Stress (Pa)**
0.65	10	8.24	2.84	109
0.60	4.64	4.36	-	-

Once the linear viscoelastic region has been determined, it is possible to investigate the frequency dependence of the bulk. Results of SAOS frequency sweep tests performed are shown in Figure 3. In all cases, a strain amplitude of $\gamma_0 = 0.1$ % is chosen well in the viscoelastic regime (according to Figure 1). Frequency curves obtained show a transition from viscoelastic liquid (sol) to viscoelastic semisolid (gel) for both kinds of

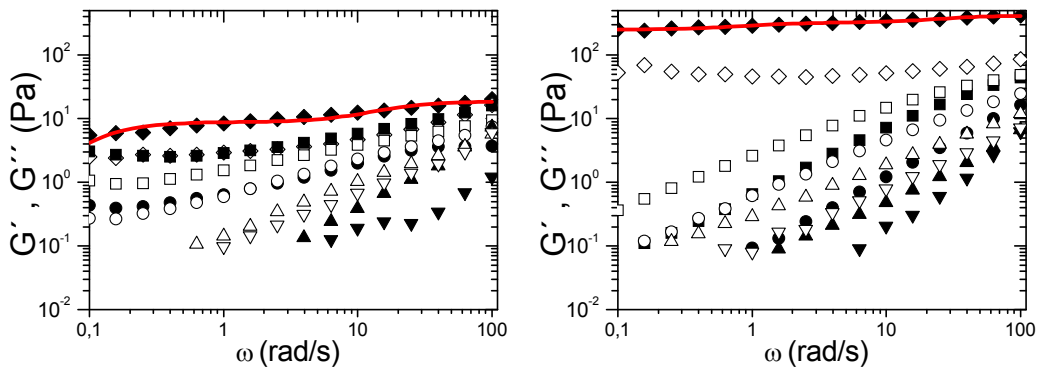

Fig. 3. Frequency sweep tests at a constant strain of $\gamma_0 = 0.1$ %; closed symbol, G´; open symbol, G´´;-♦-, ϕ = 0.65; -■-, ϕ = 0.60; -●-, ϕ = 0.575; -▲-, ϕ = 0.55; -▼-, ϕ = 0.525. (a) Pluronic F68-stabilized emulsions, (b) Epikuron 145V-stabilized emulsions. Lines: fitting to a discrete Maxwell model of two elements (Equation 5).

emulsions when ϕ increases (Macosko, 1994; Steffe, 1996). In agreement with previous results, moduli measured are again an order of magnitude higher for phospholipid-stabilized emulsions at the highest volume fraction.

To further complete the rheological characterization of the bulk, retardation tests were performed by applying a small constant stress during one minute. The shear stress was τ = 0.03 Pa, for Pluronic F68-stabilized emulsions, and τ = 1 Pa for Epikuron 145V-stabilized emulsions. During the application of the stress, the strain was monitored and the compliance calculated. Compliance creep data are shown in Figure 4.

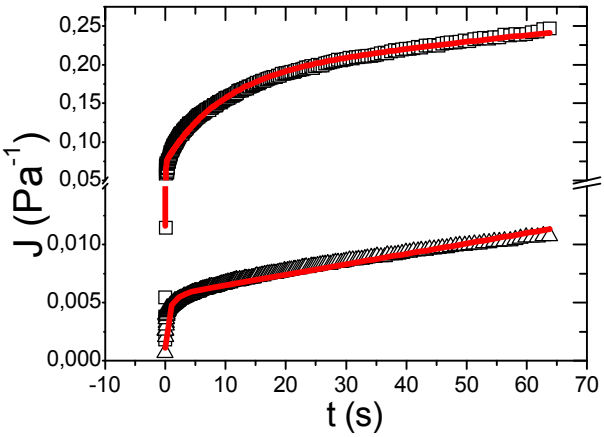

Fig. 4. Creep experiments performed with emulsions (ϕ =0.65) and fitting to Equation (3) (lines); white squares: Pluronic F68-stabilized, τ_0 = 0.03 Pa; white triangles: Epikuron 145V-stabilized, τ_0 =1 Pa.

Compliances obtained for the Epikuron 145V-stabilized emulsions are considerably lower, as expected from a larger storage modulus (cf. Figure 3). More quantitative information can be obtained if a mechanical model is used to fit the data. In Figure 4 we also show (as solid lines) results obtained by fitting a Kelvin-Voigt model which comprises two retardation processes, i.e.,

$$J(t) = J_0 + \frac{t}{\eta_0} + J_1\left(1 - e^{-t/\theta_1}\right) + J_2\left(1 - e^{-t/\theta_2}\right) \quad (3)$$

where J_0 is the instantaneous compliance, representing the instantaneous elastic deformation of the material (van Vliet & Lyklema, 2005), η_0 is the Newtonian viscosity, J_1 and J_2 are the retarded compliances and θ_1 and θ_2 are the retardation times. A similar model was used successfully by Gladwell, Rahalkar and Richmond (1986) to fit creep data from soybean oil emulsions. The addition of a third term retardation process to the model did not improve the fitting, giving rise in fact to an extremely small retarded compliance J_3. The results obtained by fitting to the mechanical model are shown in Table 3. It is worth mentioning the appearance of an instantaneous compliance J_0 for Epikuron 145V-stabilized emulsions which is negligible for Pluronic F68-stabilized emulsions. This fact highlights the larger storage modulus of the emulsions stabilized with phospholipids at this concentration. Regarding to the retarded compliances J_1 and J_2, their values are two and one order of magnitude lower for the Epikuron 145V-stabilized emulsions, respectively, confirming that they have a higher resistance to deformation. Furthermore, the Newtonian viscosity of Epikuron 145V-based emulsions is again the largest.

Table 3. Fit parameters for the creep experiments using Equation 3.

	J_0 (Pa^{-1})	J_1 (Pa^{-1})	J_2 (Pa^{-1})	η_0 (Pa·s)	θ_1 (s)	θ_2 (s)	r^2
Pluronic F68	0 ± 0	0.1154 ± 0.0017	0.07339 ± 0.00062	1212 ± 57	9.43 ± 0.37	0.065 ± 0.005	0.990
Epikuron 145V	0.00200 ± 0.00025	0.00220 ± 0.00007	0.00304 ± 0.00026	11140 ± 130	1.120 ± 0.046	0.040 ± 0.005	0.983

Stress relaxation experiments were also carried out. Results corresponding to the viscoelastic linear region (low deformations, γ_0 = 0.5 %) are shown in Figure 5. From this figure it is clear that emulsions stabilized with phospholipids require a stress almost an

order of magnitude higher to get a given deformation in agreement with SAOS and creep experiments. Here, Maxwell model is used to explain experimental data. Actually, we have fitted the obtained data to a two parameter Maxwell model, represented by

$$G(t) = G_0 + G_1 e^{-t/\theta_1} + G_2 e^{-t/\theta_2} \quad (4)$$

where G_0, G_1 and G_2 are the relaxation strength of the different modes, and θ_1 and θ_2 the relaxation times. Fits are shown as solid lines in Figure 5 and the parameters are tabulated in Table 4. As a first approximation, relaxation times used to fit experimental data to Equation 4 were taken from previous creep tests due to the highly viscoelastic solid-like behaviour observed (Tropea, Yarin, & Foss, 2007). A reasonably good agreement is found using Maxwell model to predict the relaxation modulus. Observed and predicted data agree much better at short times than at long times, as expected from the fact that relaxation times where taken from creep tests, given the different nature of both type of experiments (creep and relaxation) and the times required to perform them. Besides, it has been reported that low torque signal and transducer hysteresis affect data at long time especially in step strain experiments (Kapoor & Bhattacharya, 2001).

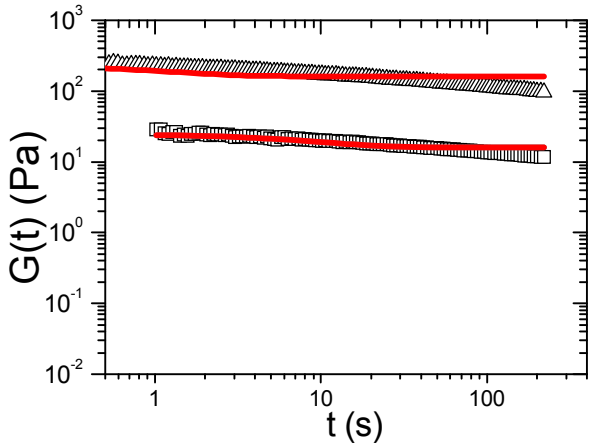

Fig. 5. Relaxation tests performed with emulsions (ϕ = 0.65, γ_0 = 0.5 %) and fitting to Equation 4 (lines): White squares: Pluronic F68-stabilized; white triangles: Epikuron 145V-stabilized.

Table 4. Fit parameters for the step-strain experiments using Equation 4.

	G_0 (Pa)	G_1 (Pa)	G_2 (Pa)
Pluronic F68	15.97 ± 0.17	8.9 ± 0.5	10 ± 1
Epikuron 145V	162 ± 3	71 ± 6	96 ± 7

Finally, using relaxation strength and times obtained from the creep and the step strain experiments we used Maxwell model again to construct the dynamic modulus G´ according to Baumgaertel and Winter (1989)

$$G'(\omega) = G_e + G_1 \frac{\omega^2\theta_1^2}{1+\omega^2\theta_1^2} + G_2 \frac{\omega^2\theta_2^2}{1+\omega^2\theta_2^2} \quad (5)$$

where G_e is the equilibrium modulus. The comparison between the G´(ω) measured and estimated from this equation is shown in Figure 3. Taking into account the simplicity of the model, the different techniques used and the fact that we are comparing time-domain and frequency-domain experiments, the agreement is reasonably good ($r^2 = 0.989$ and $r^2 = 0.950$ for Epikuron 145V- and for Pluronic F68-stabilized emulsions, respectively). It is also worth mentioning that the better fittings were obtained with no G_e for emulsions stabilized with Pluronic F68 and with $G_e = 252 \pm 4$ Pa for emulsions stabilized with phospholipids, which is in agreement with the results obtained in the creep experiments, where the instantaneous compliances were $J_0 = 0$ and $J_0 = 0.002$ Pa^{-1} respectively. This is another evidence that Epikuron 145V-stabilized emulsions have a higher resistance to deformation. In this kind of systems, it is possible to obtain an approximate G_e from this J0, since $G_e \approx 1/J_0$ (Kulicke, Arendt & Berger, 1998; Meechai, Jamieson, Blackwell & Carrino, 2001). In this case, calculating from creep measurements yields $G_e \approx 500$ Pa, which is in the same order of magnitude of that obtained from the fitting. Even though a qualitative agreement also exists for G", fittings were not as good as those for G'.

5. Results

Non-linear viscoelasticity was also explored using stress relaxation tests outside the linear viscoelastic regime. A typical behavior of the emulsions investigated here is as follows. As shear strain is increased, G(γ, t) decreases with strain. Furthermore, the log(G) vs. log(t) curves are nearly parallel, irrespective of the strain applied suggesting that emulsions obey a time-strain factorability, i.e. the non-linear shear relaxation modulus G(γ,t) can be separated into two components: a time dependent function, the linear relaxation modulus, G(t), and a strain-dependent function, the so-called damping function, h(γ). This factorability is therefore expressed by

$$h(\gamma) = \frac{G(t,\gamma)}{G(t)} \tag{6}$$

This time-strain factorability has been previously reported for similar systems such as oil-in-water emulsions stabilized with proteins (Bengoechea, Puppo, Romero, Cordobés & Guerrero, 2008) or sucrose palmitate (Partal, Guerrero, Berjano & Gallegos, 1999) as well as mayonnaises (Bower, Gallegos, Mackley & Madiedo, 1999; Guerrero, Partal & Gallegos, 2000). In order to compare different materials, this damping function is often fitted to

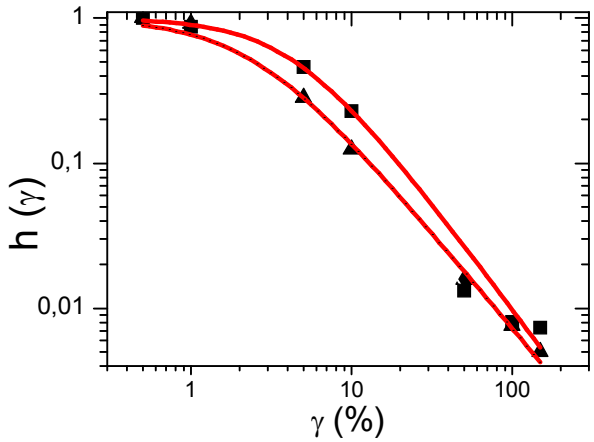

Fig. 6. Damping functions obtained for emulsions stabilized with Pluronic F68 (squares) or with phospholipids (triangles), and fittings to the Soskey-Winters model (Equation 7) (lines).

the Soskey-Winters model (Soskey & Winter, 1984), described by

$$h(\gamma) = \frac{1}{1 + a \cdot \gamma^{b}} \tag{7}$$

where a and b are dimensionless material parameters. It can be seen in Figure 6 that this model fits fairly well the relaxation data.

In both cases a noticeable strain softening behavior is observed, i.e., outside the viscoelastic linear region they are strongly influenced by the strain applied. Also, the material parameters obtained are quite similar for both emulsions (see Table 5), meaning that these emulsions do not behave differently when the imposed strain exceeds the critical strain amplitude. However, it should not be overlooked that damping function is a normalized magnitude, i.e., it is still necessary to apply a higher stress to get a given deformation on emulsions stabilized with phospholipids.

Table 5. Material parameters obtained from the Soskey-Winters fitting of the relaxation data outside the viscoelastic linear region.

	a	b	r^2
Pluronic F68	0.112 ± 0.007	1.48	0.9976
Epikuron 145V	0.23 ± 0.04	1.32	0.9795

3.3. Individual adsorption of Pluronic F68 and Epikuron 145V

The magnitude of interfacial pressure provides us quantitative information about the amount of material adsorbed and the velocity at which it is adsorbed at the interface. In this way, Figure 7 shows the time evolution of the interfacial pressure for different bulk concentrations of Pluronic F68 and Epikuron 145V. As a general trend, both figures show a higher rate of increase of the interfacial pressure as the concentrations grow higher in the

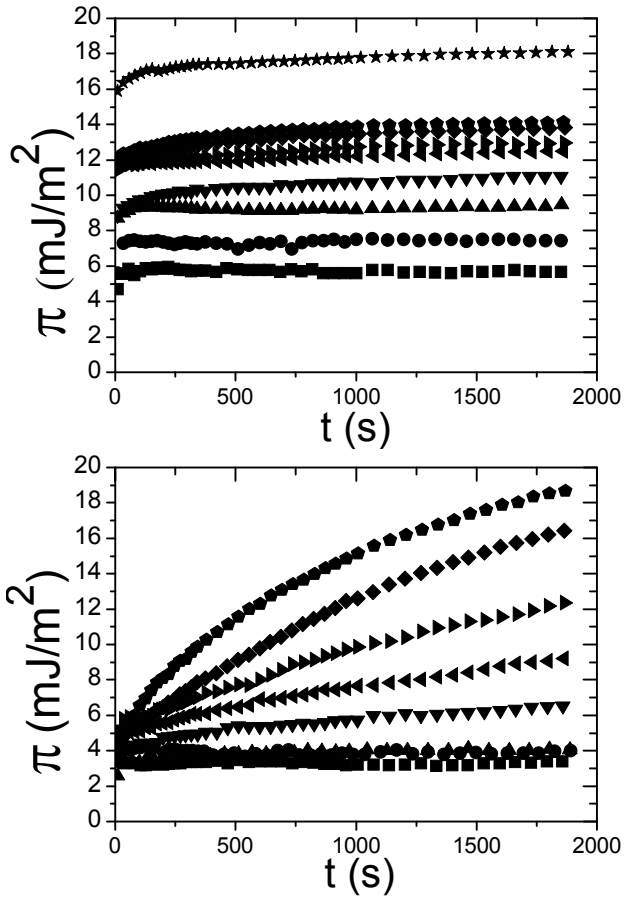

Fig. 7. a) Dynamic adsorption curves of Pluronic F68 at the oil-water interface: (■) 12 μM (0.1 g/L), (●) 0.12 mM (1 g/L), (▲) 1.2 mM (10 g/L), (▼) 2.4 mM (20 g/L), (◄) 4.8 mM (40 g/L), (►) 7.1 mM (60 g/L), (◆) 9.5 mM (80 g/L), (⬟) 12 mM (100 g/L), (★) 24 mM (200 g/L). b) Dynamic adsorption curves of Epikuron 145V at the oil-water interface: (■) 1.1 μM ($8 \cdot 10^{-4}$ g/L), (●) 13.2 μM (0.01 g/L), (▲) 27.6 μM (0.021 g/L), (▼) 79 μM (0.06 g/L), (◄) 0.11 mM (0.08 g/L), (►) 0.22 mM (0.17 g/L), (◆) 0.43 mM (0.33 g/L), (⬟) 2 mM (1.6 g/L).

bulk. Also, the steady interfacial pressure value increases as the bulk concentration increases for both species. However, comparing Figure 7a and 7b, it can be seen that the rate of increase of interfacial pressure is much higher for Pluronic F68 than for Epikuron 145V. This fact is due to the higher concentrations of the poloxamer, but even for the same concentration of the two systems, this rate is also higher for the Pluronic F68. This

indicates that Pluronic F68 adsorbs much faster onto the interface due to a higher diffusion from the aqueous phase as compared to phospholipids diffusing through the oil phase with a larger viscosity. This feature can be noticed in the initial moment of the adsorption process.

Let us now analyse the interfacial pressure isotherms of Pluronic F68 and Epikuron 145V (Figure 8). These curves are obtained from the kinetic adsorption curves shown in Figures 7a and 7b by plotting the interfacial pressure (± 0.2 mJ/m²) values attained at 30 min for each of the bulk concentrations considered. Regarding Epikuron 145V, we can observe from Figure 8 that the process of adsorption proceeds within a range of concentration from 1.1 μM ($8 \cdot 10^{-4}$ g/L) to 2 mM (1.6 g/L). Furthermore, the interfacial pressure isotherm seems to show a plateau at a bulk concentration of 0.43 mM (0.33 g/L) with a saturation surface pressure of 16.5 ± 0.5 mJ/m², and higher concentrated solution leads to the saturation of the interface.

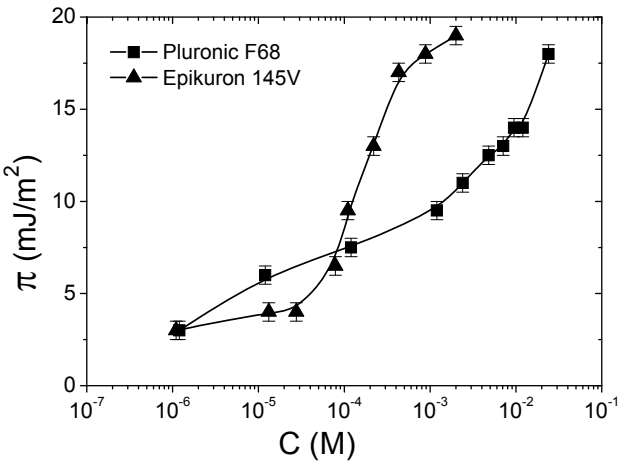

Fig. 8. Adsorption isotherm of Pluronic F68 and Epikuron 145V at the oil-water interface. Adsorption time 30 min. Lines are plotted to guide the eye.

On the other hand, the interfacial pressure isotherm of Pluronic F68 ranges from a concentration of 1.2 μM (0.01 g/L) to 24 mM (200 g/L), which is one order of magnitude

higher than the concentration range of phospholipids, and exhibits a complicated shape (Figure 8). This means that, although Pluronic F68 has a higher diffusion from the bulk, more concentrated solutions are needed in order to saturate the interface as compared to Epikuron 145V. This fact might be related to the surface activity of both systems. Due to the amphiphatic character, phospholipids have a hydrophilic-lipophilic balance (HLB) value much smaller (lecithins have HLB numbers of 8-14 depending on their exact composition) (Malik, Washington & Purewal, 1999) than that for poloxamer (29 in the case of Pluronic F68) (Kabanov, Batrakova & Alakhov, 2002), and hence, Pluronic F68 is less surface-active than Epikuron 145V. Finally, the interfacial pressure of adsorbed Pluronic F68 does not seem to reach a plateau within the range of concentrations considered here. This feature might be related to the formation of a very dense layer of Pluronic that seems to be able to reach very large interfacial concentrations.

3.4. Interfacial dilatational rheology

Unfortunately it was not possible to characterize the shear rheological properties of the interfaces by means of an interfacial rheometer equipped with a biconical bob device, because of the extremely low values measured. These results agree with the recent works of Georgieva et al. (2009), which affirm that the shear elastic modulus is zero for surfactants (the layers are liquid-like), and therefore the shear viscoelasticity plays a small role on these systems. For this reason we have characterized the interfacial structure of pure Pluronic F68 and pure Epikuron 145V in terms of their interfacial dilatational modulus, since it seems to be a general trend for an interfacial layer that the magnitude of the dilatational response is always higher than that obtained for a shear deformation (Erni, Fischer, & Windhab, 2005). Figure 9 shows the dilatational modulus of adsorbed layers of Pluronic F68 and Epikuron 145V at the same concentrations used in the adsorption experiments at the oil-water interface. In order to compare the dilatational moduli of both systems, these have been represented as a function of the interfacial pressure attained for each concentration. In this manner, we obtained a dilatational modulus value at an interfacial coverage considered, which allows us to compare the interfacial behavior of Pluronic F68 and Epikuron 145V at the same interfacial pressure. The dilatational rheology was measured at a fixed frequency of 0.1 Hz after 30 min of adsorption. The frequency of

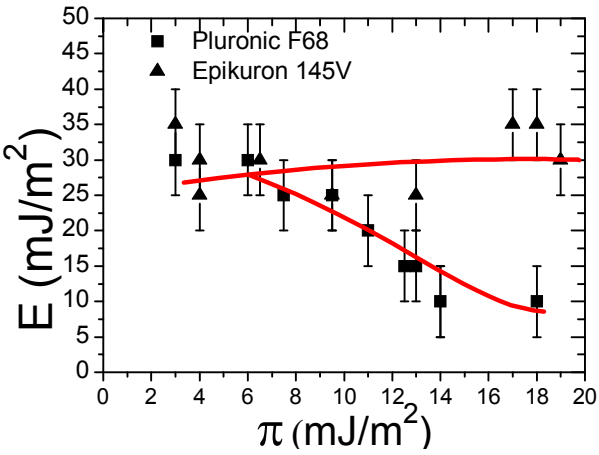

Fig. 9. Dilatational modulus of Pluronic F68 and Epikuron 145V measured at 30 min after adsorption at the oil-water interface. Lines are plotted as a guide for the eye.

0.1 Hz corresponds to the angular frequency of 0.6 rad/s within the range studied in bulk rheology. Although this is a low frequency compared to normal exchange rates of surfactants, it was too fast to allow any relaxation process or exchange with the bulk phase for these systems (Georgieva et al. 2009). Hence, at this frequency the viscous component (loss modulus) of the dilatational modulus is very small (keeping constant with surface concentration) and the adsorbed layer appears predominantly elastic. Accordingly, the values presented in Figure 9 correspond to the dilatational modulus and the viscous component is not reported here. It can be seen in Figure 9 that although the interfacial pressure values attained by Pluronic F68 and phospholipids at these bulk concentrations are very similar, the dilatational modulus of both species is different at high interfacial coverage, i.e., at high interfacial pressure. This feature proves the importance of the dilatational rheology in the characterization of interfacial layers. It is a very powerful tool that provides further structural information of the interfacial film.

With respect to the Epikuron 145V adsorbed layer, it can be observed that the phospholipids have a constant dilatational elastic modulus within the whole range of interfacial pressure, taking into account the margin of error. This fact suggests that

5. Results

Epikuron 145V forms an elastic network of interacting adsorbed phospholipid molecules at the interface, forming a closed-packed layer, due to the double tail anchoring group of the phospholipid, giving rise to a higher degree of accumulation at the oil-water interface, and further changes in the adsorbed phospholipids do not have an effect on the dilatational modulus. This might be related to the intermolecular electrostatic interactions, in which the stabilisation mechanism of phospholipid-stabilised emulsions is based on (de Vleeschauwer & Van der Meeren, 1999).

As regards the interfacial dilatational modulus of Pluronic F68, the values appear lower than those obtained for Epikuron 145V at high interfacial coverage, which correspond to a saturated interface, as mentioned before. A reason for this might be found in the small surface activity of Pluronic F68 compared to that of Epikuron 145V, as we observed in Figure 8. This would counteract the rigidity of the adsorbed layer to a deformation of the interface, diminishing the elasticity of the interfacial layer, and therefore the dilatational modulus. Also the high degree of packing of Pluronic F68 at the interface accounts for this feature, resulting in a lower elasticity, which means a lower level of structure at the interface. At concentrations exceeding the saturation of the adsorption layer, dilatational elasticity decreases. The poloxamer molecules adsorb in a compact form in the range of saturation. This realizes an optimal mechanical stability. When the concentration is increased further, this optimal structure is disturbed by the large amount of molecules which enter the interface at the same time and cannot be optimally arranged. This might be related to the brush organization of Pluronic F68 at this concentrated regime, as described by Svitova and Radke (2005). In addition, the difference in solubility of poloxamer and phospholipids in the water and in the oil phase might be also taken into account in the interpretation of these results.

So, contrary to the phospholipids, Pluronic F68 does not seem to develop a very elastic network at the interface at high interfacial pressure. High elasticity values are associated with a film that has strong cohesive interfacial structure (Maldonado-Valderrama, Wege, Rodríguez-Valverde, Gálvez-Ruiz & Cabrerizo-Vílchez, 2003), and hence Epikuron 145V network offers more resistance to a change in area than that of Pluronic F68 in the case of most saturated interfaces, which can be compared to the

droplet surfaces in emulsions. Therefore, these results correlate with those obtained in bulk rheology, in which a larger storage modulus was observed for phospholipids at the highest volume fraction. However, the complexity of those systems makes difficult to assert categorically that only interfacial rheology determines bulk rheology. Different surfactants also give rise to different droplet sizes, polydispersities, droplet charges and layer thicknesses. Interfacial viscoelastic properties, although important, should be considered as one of these many factors.

4. Conclusions

In this paper we show the strong influence of the nature of the surfactant on the final rheological properties of concentrated emulsions. Both ionic and sterically stabilized emulsions were prepared and their bulk rheological behavior characterized in the frequency and time domains. Kelvin-Voigt and Maxwell models satisfactorily predict the bulk behavior under both descriptions using SAOS, creep and step-strain shear tests. At low volume fractions emulsions typically behave as Newtonian fluids independently of the stabilization mechanism. However, when the volume fraction is large enough, droplets get closer and viscoelasticity dramatically increases. At this stage Epikuron 145V based emulsions show the largest viscoelastic response if compared to Pluronic F68.

In order to explain these findings, we carried out interfacial studies of adsorbed layers of these two surfactants, where the interface covered with phospholipids presented again higher elastic properties, suggesting a correlation between bulk rheology in concentrated emulsions and interfacial rheological properties. However, the influence of other parameters such as the different solubilities of the emulsifiers, their headgroup sizes, and the differences that they produce on charge and size of the droplets, should not be overlooked. These factors will be studied in future investigations.

Regarding the non-linear viscoelasticity, both ionic and sterically stabilized emulsions showed a strong dependence on the strain applied, although Epikuron 145V stabilized emulsions still show notably higher viscoelastic properties.

As a summary, in this manuscript we show that it is possible to influence to a major extent the rheological properties of the bulk by changing the nature of the surfactant used to stabilize the emulsions. This finding may be of interest in the design of model emulsions having controlled bulk rheological properties.

Acknowledgments.

This research is supported by FEDER funds and "Ministerio de Educación y Ciencia" under project MAT2007-66662-C02-01 and by "Junta de Andalucía – Consejería de Educación, Ciencia y Empresa" under project P07-FQM-03099. M.W.P. thanks the latter project referred for the scholarship received. We greatly thank Cargill Iberica for donating the Epikuron-145V used in this study.

References

Baumgaertel, M., & Winter, H. H. (1989), Rheol. Acta, 28, 511-519.

Bengoechea, C., Puppo, M.C., Romero, A., Cordobés, F., & Guerrero, A. (2008), J. Food Eng., 87,124–135.

Bonfillon, A., & Langevin, D. (1994), Langmuir, 10, 2965-2971.

Bower, C., Gallegos, C., Mackley, M. R., & Madiedo, J. M. (1999), Rheol. Acta, 38, 145-159.

Cabrerizo-Vílchez, M. A., Wege, H. A., Holgado-Terriza, J. A., & Neumann, A. W. (1999), Rev. Sci. Instrum., 70, 2438.

Croy, S. R., & Kwon, G. S. (2004), J. Controlled Release, 95, 161-171.

de Vleeschauwer, D., & Van der Meeren, P. (1999), Colloids Surf., A, 152, 59–66.

Dolz, M., Hernández, M. J., & Delegido, J. (2008), Food Hydrocolloids, 22, 421–427.

Edwards, D. A., Brenner, H., & Wasan, D. T. (1991) Interfacial Transport Processes and Rheology, Stonheam: Butterworth-Heinemann.

Erni, P., Fischer, P., & Windhab, E. J. (2005), Langmuir, 21, 10555-10563.

Ferry, J. D. (1980), Viscoelastic Properties of Polymers, John Wiley and Sons. Chapter 1.

Georgieva, D., Schmitt, V., Leal-Calderon, F., & Langevin, D. (2009), Langmuir, 25, 5565–5573.

Gladwell, N., Rahalkar, R. R., & Richmond, P. (1986), Rheol. Acta, 25, 55-61.

Grigoriev, D. O., & Miller, R. (2009), Curr. Opin. Colloid Interface Sci., 14, 48–59.

Guerrero, A., Partal, P., & Gallegos, C. (2000), Food Sci. Technol. Int., 6, 165-172.

Hansen, F. K. (2008), Langmuir, 24, 189-197.

Kabanov, A. V., Batrakova, E. V., & Alakhov, V. A. (2002), J. Controlled Release, 82, 189–212.

Kapoor, B., & Bhattacharya, M. (2001), Carbohydr. Polym., 44, 217-231.

Kulicke, W. M., Arendt, O., & Berger, M. (1998), Colloid Polym. Sci., 276, 1024-1031.

Mackley, M. R., Marshall, R. T. J., Smeulders, J. B. A. F., & Zhao, F. D. (1994), Chem. Eng. Sci., 49, 2551-2565.

Macosko, Ch. W. (1994), Rheology. Principles, Measurements, and Applications, New York: Wiley-VCH. Chapter 3.

Maldonado-Valderrama, J., Wege, H. A., Rodríguez-Valverde, M. A., Gálvez-Ruiz, M. J., & Cabrerizo-Vílchez, M. A. (2003), Langmuir, 19, 8436-8442.

Malik, S., Washington, C., & Purewal, T. S. (1999), Int. J. Pharm., 186, 63-69.

Meechai, N., Jamieson, A. M., Blackwell, J., & Carrino, D. A. (2001), Biomacromolecules, 2, 780–787.

Partal, P., Guerrero, A., Berjano, M., & Gallegos, C. (1999), J. Food Eng., 41, 33-41.

Santini, E., Liggieri, L., Sacca, L., Clausse, D., & Ravera, F. (2007), Colloids Surf., A, 309, 270-279.

Soskey, P.R., & Winter, H. H. (1984), J. Rheol., 28, 625–645.

Steffe, J. F. (1996), Rheological methods in food engineering, 2nd ed., East Lansing, MI: Freeman Press. Chapter 5.

Svitova, T. F., & Radke, C. J. (2005), Ind. Eng. Chem. Res., 44, 1129-1138.

Tong, Y. C., Chang, S. F., Liu, C. Y., Kao, W. W., Huang, & C. H., Liaw, J. (2007), Gene Med., 9, 956-966.

Tropea, C., Yarin, A. L., & Foss, J. F. (2007), Springer handbook of experimental fluid mechanics, Berlin: Springer.

van Vliet, T., & Lyklema, H. (2005) In: Fundamentals of Interface and Colloid Science IV: Particulate Colloids, J. Lyklema, Ed., Morgan Kaufmann.

Wege, H. A., Holgado-Terriza, J. A., & Cabrerizo-Vílchez, M. A. (2002), J. Colloid Interface Sci., 249, 263-273.

Wulff-Pérez, M., Torcello-Gómez, A., Gálvez-Ruíz, M. J., & Martin-Rodríguez, A. (2009), Food Hydrocolloids, 23, 1096-1102.

Paper III.

The effect of polymeric surfactants on the rheological properties of nanoemulsions

Miguel Wulff-Pérez, Antonio Martín-Rodríguez, María J. Gálvez-Ruiz and Juan de Vicente

Biocolloid and Fluid Physics Group. Department of Applied Physics. Faculty of Sciences, University of Granada, 18071 Spain.

Under revision in:

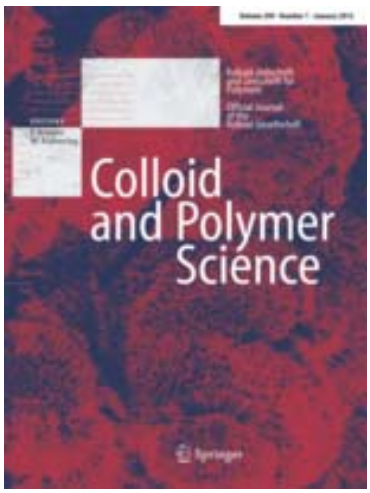

Colloid and Polymer Science

Abstract

We have investigated the rheological properties of submicron emulsions and how they are affected by the structure of polymeric surfactants. We have prepared oil in water emulsions stabilized with five steric surfactants, Pluronics and Myrjs, with key differences on their structures. Droplet size and volume fraction have been kept constant to analyze only the influence of the surfactant. The viscoelasticity has been characterized by dynamic oscillatory shear experiments, while the shear viscosity was measured during steady shear flow tests. The results show a qualitatively similar gel-like behavior for all the emulsions, but with remarkable quantitative differences. Surfactants with longer hydrophilic tails produced emulsions with higher viscoelasticity. Pluronics, having a central hydrophobic part between two hydrophilic tails, produced emulsions with notably higher viscoelasticity and yield stress than Myrjs with comparable hydrophilic tails. The reason for this seems to be a more efficient steric barrier at the interface, induced by this central hydrophobic part.

1. Introduction

Emulsions are a broadly used colloidal system in many industrial fields, such as foods, pharmacy, paintings or cosmetics. Their flow properties determine some essential characteristics directly related with their applications, including shelf stability, sensorial properties, filling/dosing behavior, spreadness and so forth [1]. Therefore, to acquire a better understanding and control over these flow properties is of utmost importance for the abovementioned industries. In these fields there is also a growing interest in emulsions with submicrometer droplet size, typically between 20-500 nm, also known as nanoemulsions [2-4]. Due to this small size some interesting properties arise, such as high stability against gravitational destabilization (creaming or sedimentation), huge surface area and increased surface-area-to-volume ratio [2]. Although there is a considerable number of studies and extensive reviews concerning emulsion rheology [5-8], less attention has been paid to the rheology of emulsions with a droplet size under 500 nm [9,10], even though it is well known that droplet size is a key factor on the final rheological behaviour [11,12]. The flow properties of these emulsions will be even more different from those of conventional emulsions if the volume fraction is high. If we consider the separation between droplets given by the expression

$$H = d \cdot \left(\left(\frac{\phi_{\max}}{\phi} \right)^{1/3} - 1 \right) \tag{1}$$

where H is the interdroplet separation, d is the droplet diameter, ϕ is the volume fraction and ϕ_{max} is the maximum volume fraction [13], then it becomes evident that, for a given volume fraction, the interparticle separation will be considerably shortened if the droplet size is brought within the submicrometer range. As a consequence, the influence of the interfacial composition should be notably enhanced. In spite of the particular rheological behavior distinctive of emulsions having this small size and high volume fractions, to the best of our knowledge only a few reports concerning the rheology of these systems are found in the literature [14-19].

For many of the applications related with emulsions, non-ionic steric surfactants are preferred to stabilize the emulsions instead of classical ionic surfactants (e.g., when a high ionic strength is required). Steric surfactants comprising polymers have the advantage of a huge, almost tailor-made diversity of structures. By changing their composition, it is possible to vary their size, occupation of the interface, disposition, etc. The aim of this work is then to investigate the rheological properties of nanoemulsions and to determine how they are affected by polymeric surfactants. To do so, the emulsions have been prepared with surfactants belonging to two different types, Pluronics and Myrjs, with key differences on their structures. The volume fraction and droplet sizes have been kept constant for all the emulsions, in order to correlate specifically the changes observed in the rheological properties of the emulsions with the different structures of the surfactants.

2. Materials and Methods

2.1 Materials

Surfactants. Pluronics are copolymers based on a polyethylene oxide-block-polypropylene oxide-block- polyethylene oxide ABA structure (see Table 1). The central polypropylene oxide (PPO) block links to the oil because of its hydrophobic character, while the two lateral hydrophilic chains of polyethylene oxide (PEO) remain in the aqueous phase, stabilizing the droplets by steric hindrance [20]. Three Pluronics with key differences in their hydrophobic and hydrophilic chain sizes were used: Pluronic F127 (PF127), Pluronic F68 (PF68) and Pluronic P105 (P105). They were obtained from Sigma-Aldrich. Myrj surfactants consist of stearic acid sterified with a hydrophilic chain of polyethylene oxide, with Myrj 52 (M52) having 40 subunits of PEO and Myrj 59 (M59) having 100 subunits. M52 was obtained from Sigma-Aldrich. M59 was a kind gift from Croda Ibérica S.A.

Oils. Olive oil and coconut oil were obtained from Sigma-Aldrich. Olive oil is liquid at room temperature, while coconut oil melts between 23-27ºC. Both oils were purified to eliminate free fatty acids as described elsewhere [21].

Table 1. Chemical structure of the surfactants used in this study to prepare and stabilize the nanoemulsions.

Pluronic F127 (PF127)	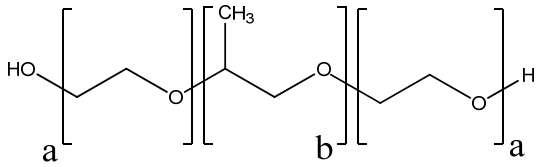	**a = 100 b = 65**
Pluronic F68 (PF68)		**a = 75 b = 29**
Pluronic P105 (P105)		**a = 37 b = 56**
Myrj 59 (M59)	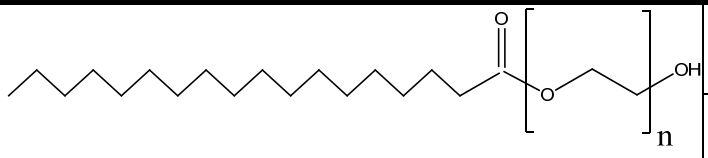	**n = 100**
Myrj 52 (M52)		**n = 40**

2.2 Preparation of nanoemulsions

Oil-in-water emulsions were prepared mixing oil and water to obtain a final volume fraction of 0.65, on basis of a total volume of 30 mL. The oil used was either olive oil or coconut oil. Each emulsion was prepared with only one kind of surfactant. For the sake of simplicity, each emulsion will be given a name according to its composition (see Table 2). The amount of surfactant to be used in each case was selected based upon three criteria: a) to achieve a comparable final droplet size and monodispersity, b) to use the minimal amount of surfactant (in order to avoid an excess of surfactant in the continuous phase), and c) to use an equimolar amount of surfactant between different emulsions, providing that the first two criteria were satisfied. As explained in the introduction, to obtain droplets with similar sizes for the emulsions stabilized with different surfactants is a key factor to study the impact of these surfactants on the final rheological properties. The final surfactant concentrations are also listed in Table 2.

The protocol was as follows: first, surfactant was added to the water phase under stirring until complete dissolution. Then, a pre-emulsion was formed mixing both phases

using a high speed Heidolph Diax 900 stirrer for 4 minutes at 13,000 rpm, by dropwise addition of oil to the water under stirring. This coarse emulsion was immediately homogenized using the high pressure Emulsiflex-C3 homogenizer (Avestin, CA) at 100 MPa. All emulsions were passed through the homogenizer 10 times. This homogenization process was carried out at 50 ºC and at 60 ºC for olive oil and coconut oil emulsions, respectively.

Table 2. Composition of the submicron emulsions and hydrodynamic diameter (± standard deviation) measured by dynamic light scattering.

Emulsion name	Oil	Surfactant	[Surfactant] (mmol/L)	Diameter (± sd) (nm)
O-PF127	Olive	PF127	3.09	300 ± 43
O-PF68	Olive	PF68	3.09	315 ± 45
O-P105	Olive	P105	6.15	280 ± 35
O-M52	Olive	M52	16.1	322 ± 42
O-M59	Olive	M59	7.02	314 ± 47
C-PF127	Coconut	PF127	3.09	310 ± 20
C-PF68	Coconut	PF68	3.09	298 ± 38
C-P105	Coconut	P105	6.15	310 ± 45
C-M52	Coconut	M52	16.1	315 ± 42
C-M59	Coconut	M59	7.02	304 ± 47

2.3 Characterization of submicron emulsions

The mean droplet size of the different emulsions was measured by Dynamic Light Scattering (DLS) using an ALV-NIBS/HPPS particle sizer with an ALV 5000 multiple digital correlator (ALV-Laser Vertriebsgesellschaft GmbH, Langen, Germany) at 37 ºC. The emulsions were diluted to a final volume fraction below 1 %, in order to reach optimal measurement conditions. Measurements were repeated after 24 hours to check that no coalescence was taking place.

2.4 Viscoelasticity measurements

A torsional MCR 501 Rheometer (Anton Paar Gmbh, Austria) was used to study the bulk rheology of emulsions, using a cone-plate geometry (50 mm diameter, 1º), maintaining temperature at 25 ºC with a peltier. To avoid evaporation a solvent-trap system was used and some low-viscosity silicone oil was poured on the rim of the cone. Each test was run in triplicate with fresh samples. It is worth to stress here that wall slip was not observed under similar operation conditions using rough surfaces and plate-plate geometries in a previous study with similar emulsions [21]. In any case, the absence of wall slip in these experiments was confirmed by measurements with a vane tool (see section 2.6).

The linear viscoelastic (LVE) region was first determined by means of oscillatory shear rheometry. In particular, strain amplitude sweep tests at a constant excitation frequency were run. Initially the sample was pre-sheared at a constant shear rate of 20 s^{-1} for 30 s in torsional mode. Next, the sample is allowed to recover for a period of 60 s. Finally an oscillatory amplitude sweep test was performed, by varying the strain amplitude from γ_0 = 0.01 % to γ_0 = 100 %, keeping a constant angular frequency of ω = 10 rad/s.

Once the LVE range was determined, the mechanical spectra of the emulsions were obtained from frequency sweep tests. Pre-shear and equilibration steps were again applied prior to each test as described previously in the amplitude sweeps. In the frequency sweep test the applied strain amplitude was γ_0 = 0.05 %, well within the LVE range in all cases, and the excitation frequency ranged from ω = 100 rad/s to ω = 0.1 rad/s. Each test was performed in triplicate.

2.5 Shear viscosity measurements

The steady shear response of the submicron emulsions was measured by subjecting the sample to increasing shear rates from 0.01 s^{-1} to 1000 s^{-1}. The geometry in these experiments was the same as in the previous section. Again, each test was performed in triplicate.

2.6 Measurements with a vane geometry

A vane tool was used to measure the apparent yield stress of the emulsions. The vane has four blades, a height of 8 mm and a diameter of 5 mm. All the vane and vessel dimensions as well as the depth of the vane immersion were optimized to allow precise measurements according to Steffe [22]. The torque necessary to overcome the yield stress is measured, and both magnitudes are related by the expression

$$M_0 = \frac{\pi d^3}{2}\left(\frac{h}{d} + \frac{1}{6}\right)\sigma_0 \qquad (2)$$

where M_0 is the applied torque, σ_0 the yield stress, and h and d the height and diameter of the vane, respectively. The rotational speed was set at 0.006 rpm.

3. Results and Discussion

3.1 Emulsion characterization

The mean droplet sizes and standard deviations of each emulsion are listed in Table 2. These sizes did not change when the measurements were repeated after 24 hours, i.e., well below the timeframe of the experiments since only freshly prepared emulsions were used in the experiments.

3.2 Viscoelastic properties of olive oil emulsions

A clear LVE range was found for all the emulsions studied in strain amplitude sweep tests. The curves obtained exhibited low-strain plateaux for both storage (G') and loss (G") moduli, until the value of G´ is reduced at higher strains, indicating the disruption

Table 3. Values of the storage and loss moduli in the LVE range obtained from strain amplitude sweep experiments for olive oil emulsions stabilized with different steric surfactants.

	O-PF127	O-PF68	O-P105	O-M59	O-M52
G´ (Pa)	1095	68	41	36	18
G´´ (Pa)	92	15	10	7.2	3.7

of the microstructure of the sample. The values of G´ and G´´ corresponding to these plateaux are given in Table 3.

The behavior of these emulsions is notably more elastic than viscous, since in all cases G´ is dominant over G´´ within the LVE range. As mentioned previously in the introduction, this highly elastic behavior is a consequence of the repulsive forces between droplets, magnified at this high droplet concentration [23]. However, although the qualitative response is similar for all the emulsions, the quantitative response is clearly dependant on the surfactant used to stabilize the emulsion. We will analyze more profoundly the influence of the surfactant with the help of the frequency sweep tests. As a way of example, the frequency dependence of G', in the LVE regime, is shown in Figure 1 (loss moduli will not be shown for the sake of clarity). As observed, G´ remains almost constant through the whole frequency range, showing a typical gel-like behavior, in good agreement with the results obtained in the amplitude sweep tests, being this behavior typical of structural arrested systems. Considering these experiments, some findings should be highlighted:

3.2.1 Effect of the length of the hydrophilic chain

The only difference between M52 and M59 is the number of subunits of the PEO chain (40 vs. 100, respectively), having the same hydrophobic part. Therefore, it is possible to interrogate the effect of the length of the hydrophilic chain on the final viscoelastic properties of O-M52 and O-M59, given that all the other properties of the emulsions such as volume fraction and droplet size are similar. Not surprisingly, the trend observed for G´ is the same at that of the PEO chain length, i.e., G´(O-M59) > G´(O-M52). It is worth to

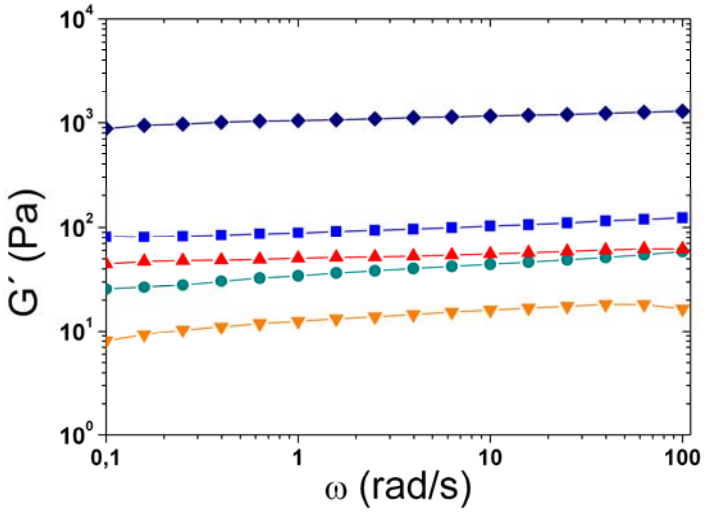

Fig. 1 Frequency sweep tests at a constant strain amplitude of γ_0 = 0.05 % for olive oil emulsions stabilized with different steric surfactants: -♦-, PF127; -■-, PF68; -●-, P105; -▲-, M59; -▼-, M52.

mention here that the PEO chain length is proportional to the thickness of the adsorbed layer of surfactant [24], i.e., the steric barrier around the droplet. Considering the volume fraction and droplet sizes of these emulsions, it becomes evident that this steric barrier is of the order of the separation between droplets (see Eq. 1); if we assume an ordered structure (ϕ_{max} between 0.68 and 0.74), then the interdroplet separation will be 4-13 nm, i.e., in the range of the thickness of the adsorbed layer of similar PEO chains [25]. As a consequence, droplets are expected to be slightly compressed and deformed, taking into account that they start to deform even before their surfaces actually touch [17]. Of course, the compression would be even higher if we assume a random, close packed structure (ϕ_{max} = 0.64). This argumentation presents a scenario where interdroplet repulsion and interfacial forces will have a major impact on the response to external shearing forces applied on the system. Actually, the repulsion between droplets in O-M59 is presumably higher than in O-M52 and this may explain why G´(O-M59) is greater than G´(O-M52).

Table 3. Values of the storage and loss moduli in the LVE range obtained from strain amplitude sweep experiments for olive oil emulsions stabilized with different steric surfactants.

	O-PF127	O-PF68	O-P105	O-M59	O-M52
G´ (Pa)	1095	68	41	36	18
G´´ (Pa)	92	15	10	7.2	3.7

3.2.2 Effect of the length of the hydrophilic chain vs. the size of the hydrophobic central part

In this section, the emulsions stabilized with different Pluronics will be compared. As can be observed in Table 1, these surfactants differ in the length of their hydrophilic chains, as well as in the size of their hydrophobic central part. The former is directly proportional to the thickness of the adsorbed layer (δ) around the droplet [26], similarly as explained in section 3.2.1, whereas the latter will essentially influence the occupied area per molecule at the interface. Approximate values for δ have been extracted from the literature for these surfactants: 8-9 nm for PF127 [27], 6-7 nm for PF68 [26,28] and 3-4 nm for P105 [19,26]. The area per molecule at analogous interfaces has also been extracted from the bibliography: 6.5-7.2 nm^2/molecule for PF127 [29,30], 3-3.4 nm^2/molecule for PF68 [31,32] and 3.9-6.6 nm^2/molecule for P105 [31,33]. Therefore, the tendencies observed are

$\delta(PF127) > \delta(PF68) > \delta(P105)$

whereas the trend of area per molecule is

PF127 > P105 > PF68.

Again, as both droplet size and volume fraction are similar for the emulsions investigated in this work, the only parameter explaining the qualitative differences on the viscoelastic properties is the structure of the surfactant. Inspection of Table 3 reveals that G´(O-PF127) > G´(O-PF68) > G´(O-P105). Importantly, the fact that the storage modulus for O-PF68 is higher than that for O-P105 suggests that on these ABA copolymers the impact

of the hydrophilic tails length prevails over that of the size of the hydrophobic central part. In other words, the elasticity of these emulsions is more influenced by the length of the repulsive barrier than by the occupation and contribution of the hydrophobic part to the interface.

3.2.3 Effect of the architecture of the surfactant

In this section, the emulsions stabilized with Pluronics will be compared to the emulsions stabilized with Myrjs. This will help us to get a better understanding on how the structure of the steric surfactants affects the final viscoelastic properties. For example, looking at the structure of PF127 and M59 we find that both emulsifiers have the same subunits of PEO on their hydrophilic chain. Hence, it could be anticipated a similar thickness of the steric barrier around the droplet, given that the hydrophobic part will be linked at the interface and/or immersed in the droplet [27], and that the hydrophilic tails of both polymers are extended in a brush-like conformation [33,34]. Nevertheless, the elastic response of O-PF127 is notably higher than that of O-M59, being G´(O-PF127) more than 30 times larger than G´(O-M59). Likewise, the steric barrier formed by P105 and M52 should be very similar, having these surfactants 37 and 40 PEO subunits, respectively. However, also in this case the Pluronic surfactant produces a higher elastic response, being G´(O-P105) even closer to G´(O-M59) than to G´(O-M52). This fact confirms that the hydrophobic central part of Pluronics is not a mere passive linker of the two hydrophilic chains, but an active agent in the acquisition of elastic properties by concentrated submicron emulsions. The nature of this influence will be analyzed in more depth on the section corresponding to the results of coconut oil emulsions.

3.3 Flow curves of olive oil emulsions

The steady-state viscosity curves of the five different olive oil emulsions are presented in Figure 2. In all cases the curves obtained reflect a non-newtonian behavior, as viscosity strongly depends on shear rate; it is well known that the increasing shear rate breaks down the colloidal structure and therefore the viscosity is reduced [23]. However,

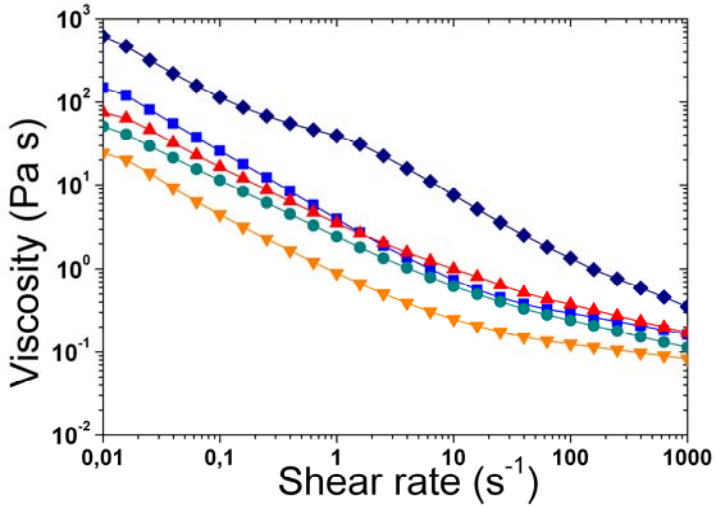

Fig. 2 Flow curves obtained for olive oil emulsions stabilized with different steric surfactants: -♦-, PF127; -■-, PF68; -●-, P105; -▲-, M59; -▼-, M52

. although again the qualitative behavior of the different emulsions is similar, important differences can be observed (please note the logarithmic scales). As expected, these differences are more pronounced at low shear rates in which the interparticle forces are dominant rather than hydrodynamic forces imposed by the shear flow. As the shear rate increases, the hydrodynamic contribution prevails and eventually the shear viscosity curves approach each other as both concentration and particle size are very similar. Therefore, dissimilarities between the interparticle forces of the different emulsions are noticed at low shear, in good agreement with the oscillatory shear experiments. From the inspection of Figure 2 it is clear that Pluronics provide emulsions with a stronger structure.

It is also worth to mention that these emulsions do not have any upper Newtonian region up to the minimum shear rates investigated. Instead, the emulsions exhibit an apparent yield stress, inferred from the slope of -1 in the log-log representation of the viscosity versus shear rate [23]. The presence of a yield stress in emulsions is indicative of the formation of a three-dimensional structure under no-flow conditions. Generally speaking, the magnitude of this yield stress is known to increase with increasing particle

volume fraction, decreasing particle size, and increasing magnitude of interparticle forces [35]. As volume fraction and particle size are almost equal to all emulsions reported in this manuscript, it is then possible to relate the values of yield stress with the magnitude of the repulsion between adjacent droplets. In Table 4 we show apparent yield stresses, σ_B, as obtained by regression fitting the flow curves shown in Figure 2 to the plastic Bingham equation.

As it could be expected, M59 produces more repulsion than M52, due to its longer PEO chain. We observe again also a higher repulsion for Pluronics (PF127 vs. M59 and P105 vs. M52), in spite of having theoretically an equivalent hydrophilic layer thickness around the droplet (because of the similar length of the PEO chain). In other words, triblock copolymers present a more efficient steric barrier for a given hydrophilic chain. However, the measurement of the apparent yield stress by extrapolation from shear stress-shear rate data to zero shear rate strongly relies on highly accurate experimental data in the low shear rate range. This is often difficult to obtain owing to the inherent nature of the yield stress material, mainly due to thixotropy, shear banded flows and wall slip effects [36]. Importantly, this latter is considerably reduced when a vane geometry is used, allowing to a more precise and reliable measurement of the yield stress [37]. The values obtained using a vane for the yield stress of the different emulsions are shown in Table 4, σ_V, together with the values obtained by extrapolation, σ_B. As observed, the measured yield stresses are of the same order of magnitude and agree reasonably well. This precludes the presence of a significant wall slip, and reinforces the tendencies previously described (effect of the length of PEO chain, differences between Pluronics and Myrjs for a given PEO chain length, etc.).

Table 4. Apparent yield stresses measured for the different olive oil emulsions. (1) = calculated from a fit to the Bingham equation; the shear rate range considered for the fit is 63-1000 s^{-1}. (2) = calculated from the measurements with the vane tool.

	O-PF127	O-PF68	O-P105	O-M59	O-M52
σ_B (1) (Pa)	125	5.6	4.6	9.0	1.6
σ_V (2) (Pa)	150	3.0	2.0	2.1	1.5

3.4 Viscoelasticity of coconut oil emulsions.

From the aforementioned results, it is evident that the structure of the surfactants affects critically the rheological properties of the emulsions, despite being all of them steric surfactants. The effect of the length of the PEO chain on viscoelasticity and yield stress has been also shown and explained. However, the reason for the strikingly different behavior observed for the emulsions stabilized by Pluronics against the emulsions stabilized by Myrjs remains unclear. The long hydrophobic central part of Pluronics is forced to be at (or very close to) the interface due to the structure of these surfactants, since the two hydrophilic tails protrude into the water phase [38]. Therefore, it is possible that this block of the polymer influences to a great extent the interfacial properties of the droplets, e.g. providing a high resistance against change of shape and/or surface area. From another standpoint, it is also possible that the presence of this central part forces the hydrophilic chains to create a more efficient steric barrier, e.g. by disposing them in a more extended conformation, or a disposition more perpendicular to the interface.

With the aim of understanding the different behavior of Pluronic- and Myrj-stabilized emulsions, the rheology of coconut oil emulsions was studied. The droplets were formed and stabilized at 60 ºC, turning into semisolid droplets at room temperature (25 ºC) when rheology experiments were carried out. The oil-water interface should be now notably more rigid than in olive oil emulsions, reducing the influence of the emulsifier on the viscoelasticity of that interface. If this influence was the main cause of the observed differences in olive oil emulsions, then these differences should be attenuated when coconut oil emulsions are measured.

The storage and loss moduli obtained in the LVE range are shown in Table 5. These values are higher than those obtained for olive oil emulsions (see Table 3), since, for a given volume fraction, a lower deformability is known to produce a higher viscoelastic response [33]. However, the differences between Pluronics and Myrjs have been increased instead of attenuated. The value of G´(C-PF127) is again about 30 times that of G´(C-M59), in spite of PF127 and M59 having a similar PEO chain length. Likewise, the value of G´(C-P105) is not closer to G´(C-M52), but five times larger.

Table 5. Values of the storage and loss moduli in the viscoelastic linear regime for coconut oil emulsions stabilized with different steric surfactants.

	C-PF127	C-PF68	C-P105	C-M59	C-M52
G´ (Pa)	1547	620	102	55	20
G´´ (Pa)	102	185	45	11	3.8

With these results in mind, it seems that the different behavior observed for Pluronic- and Myrj-stabilized emulsions is not due to a viscoelastic contribution of the hydrophobic central part of Pluronics to the interface, but rather to some effect of that hydrophobic part on the disposition of the two hydrophilic tails. This tails would be in this case more efficient in creating a steric barrier around the droplet, increasing the interdroplet repulsion and therefore providing the emulsions with higher viscoelastic properties. The increasing of the stiffness of the droplets and interfaces would not diminish in this case the differences between Pluronic- and Myrj-stabilized emulsions, since the disposition of the surfactants should not change. Instead, this disposition could be even more fixed, which would explain the observed increase of the differences.

4. Conclusions

In this paper we study the viscoelastic properties of concentrated emulsions stabilized with two different families of steric surfactants, Pluronics and Myrjs, with key differences on their structures. These experiments helped us to analyze the influence of some characteristics of the surfactants on the bulk rheological properties of the emulsions, since the volume fraction and the droplet size were kept constant for all the emulsions investigated. Although these rheological properties were qualitatively alike (elasticity prevailing at low strains, presence of an apparent yield stress, etc), quantitative dissimilarities were observed and analyzed:

- Effect of the length of the hydrophilic tail of the surfactant: for a given hydrophobic part, a higher viscoelastic response is obtained when the PEO chain length is increased. This is most likely due to a longer steric barrier around the droplet that will produce more repulsion between droplets and therefore a higher resistance when the droplets are compressed.

- Effect of the length of the hydrophilic tail vs. the size of the hydrophobic part: when different Pluronics are compared, the length of the PEO chain seems to prevail over that of the PPO central part, i.e., a surfactant with a longer PEO chain (but shorter PPO block) produces a higher viscoelasticity and yield stress than a surfactant with a shorter PEO chain (but longer PPO block).

- Effect of the architecture of the surfactant: the triblock copolymers used in this study present notably higher viscoelastic properties than the Myrjs, even when the hydrophilic chains are comparable. The reason for this seems to be a more efficient steric barrier induced by the presence of the central hydrophobic part, rather than a direct influence of this hydrophobic part on the interfacial rheological properties of the droplets.

These findings should help us to improve our knowledge about how steric surfactants affect the final rheological properties of the emulsions that they stabilize, as well as to use these polymeric surfactants as active agents to control these properties.

Acknowledgments

This research is supported by FEDER funds and "Ministerio de Educación y Ciencia" under Project MAT2010-20370 and by "Junta de Andalucía – Consejería de Educación, Ciencia y Empresa" under Project P07-FQM-03099. M.W.P. thanks the latter project referred for the scholarship received.

References

5. Results

1. Partal P, Guerrero A, Berjano M, Gallegos Cs (1999) Transient flow of o/w sucrose palmitate emulsions. J Food Eng 41 (1):33-41. doi:10.1016/s0260-8774(99)00071-0

2. Forgiarini A, Esquena J, González C, Solans C (2001) Formation of Nano-emulsions by Low-Energy Emulsification Methods at Constant Temperature. Langmuir 17 (7):2076-2083. doi:10.1021/la001362n

3. Izquierdo P, Esquena J, Tadros TF, Dederen C, Garcia MJ, Azemar N, Solans C (2001) Formation and Stability of Nano-Emulsions Prepared Using the Phase Inversion Temperature Method. Langmuir 18 (1):26-30. doi:10.1021/la010808c

4. Gutiérrez JM, González C, Maestro A, Solè I, Pey CM, Nolla J (2008) Nano-emulsions: New applications and optimization of their preparation. Curr Opin Colloid Interface Sci 13 (4):245-251. doi:10.1016/j.cocis.2008.01.005

5. Tadros TF (1994) Fundamental principles of emulsion rheology and their applications. Colloids Surf, A 91 (0):39-55. doi:10.1016/0927-7757(93)02709-n

6. Barnes HA (1994) Rheology of emulsions — a review. Colloids Surf, A 91 (0):89-95. doi:10.1016/0927-7757(93)02719-u

7. Lequeux F (1998) Emulsion rheology. Curr Opin Colloid Interface Sci 3 (4):408-411. doi:10.1016/s1359-0294(98)80057-5

8. Pal R (2011) Rheology of simple and multiple emulsions. Curr Opin Colloid Interface Sci 16 (1):41-60. doi:10.1016/j.cocis.2010.10.001

9. Mason TG, Bibette J, Weitz DA (1996) Yielding and Flow of Monodisperse Emulsions. J Colloid Interface Sci 179 (2):439-448. doi:10.1006/jcis.1996.0235

10. Mason TG (1999) New fundamental concepts in emulsion rheology. Curr Opin Colloid Interface Sci 4 (3):231-238. doi:10.1016/s1359-0294(99)00035-7

11. Tropea C, Yarin AL, Foss JF (2007) Springer Handbook of Experimental Fluid Mechanics. Springer, Berlin

12. Pons R, Taylor P, Tadros T (1997) Investigation of the interactions in emulsions stabilized by a polymeric surfactant and its mixtures with an anionic surfactant. Colloid Polym Sci 275 (8):769-776. doi:10.1007/s003960050146

13. Saiki Y, Prestidge CA, Horn RG (2007) Effects of droplet deformability on emulsion rheology. Colloids Surf, A 299 (1–3):65-72. doi:10.1016/j.colsurfa.2006.11.022

14. Bécu L, Manneville S, Colin A (2006) Yielding and Flow in Adhesive and Nonadhesive Concentrated Emulsions. Phys Rev Lett 96 (13):138302

15. Mason TG, Lacasse M-D, Grest GS, Levine D, Bibette J, Weitz DA (1997) Osmotic pressure and viscoelastic shear moduli of concentrated emulsions. Physical Review E 56 (3):3150-3166

16. Welch CF, Rose GD, Malotky D, Eckersley ST (2006) Rheology of High Internal Phase Emulsions. Langmuir 22 (4):1544-1550. doi:10.1021/la052207h

17. Dimitrova TD, Leal-Calderon F (2001) Bulk Elasticity of Concentrated Protein-Stabilized Emulsions. Langmuir 17 (11):3235-3244. doi:10.1021/la001805n

18. Howe AM, Pitt AR (2008) Rheology and stability of oil-in-water nanoemulsions stabilised by anionic surfactant and gelatin 2) addition of homologous series of sugar-based co-surfactants. Adv Colloid Interface Sci 144 (1–2):30-37. doi:10.1016/j.cis.2008.08.004

19. Datta SS, Gerrard DD, Rhodes TS, Mason TG, Weitz DA (2011) Rheology of attractive emulsions. Physical Review E 84 (4):041404

20. Wulff-Pérez M, Torcello-Gómez A, Gálvez-Ruíz MJ, Martín-Rodríguez A (2009) Stability of emulsions for parenteral feeding: Preparation and characterization of o/w nanoemulsions with natural oils and Pluronic f68 as surfactant. Food Hydrocolloids 23 (4):1096-1102. doi:10.1016/j.foodhyd.2008.09.017

21. Wulff-Pérez M, Torcello-Gómez A, Martín-Rodríguez A, Gálvez-Ruiz MJ, de Vicente J (2011) Bulk and interfacial viscoelasticity in concentrated emulsions: The role of the surfactant. Food Hydrocolloids 25 (4):677-686. doi:10.1016/j.foodhyd.2010.08.012

22. Steffe JF (1992) Rheological Methods in Food Process Engineering. Freeman Press, East Lancing

23. Pal R (1999) Yield stress and viscoelastic properties of high internal phase ratio emulsions. Colloid Polym Sci 277 (6):583-588. doi:10.1007/s003960050429

24. Needham D, Kim DH (2000) PEG-covered lipid surfaces: bilayers and monolayers. Colloids and Surfaces B: Biointerfaces 18 (3–4):183-195. doi:10.1016/s0927-7765(99)00147-2

25. Lasic DD, Needham D (1995) The "Stealth" Liposome: A Prototypical Biomaterial. Chem Rev 95 (8):2601-2628. doi:10.1021/cr00040a001

26. Sedev R, Steitz R, Findenegg GH (2002) The structure of PEO–PPO–PEO triblock copolymers at the water/air interface. Phys B 315 (4):267-272. doi:10.1016/s0921-4526(02)00513-6

27. Elisseeva OV, Besseling NAM, Koopal LK, Cohen Stuart MA (2005) Influence of NaCl on the Behavior of PEO−PPO−PEO Triblock Copolymers in Solution, at Interfaces, and in Asymmetric Liquid Films. Langmuir 21 (11):4954-4963. doi:10.1021/la046933g

28. Baker JA, Berg JC (1988) Investigation of the adsorption configuration of polyethylene oxide and its copolymers with polypropylene oxide on model polystyrene latex dispersions. Langmuir 4 (4):1055-1061. doi:10.1021/la00082a042

29. Phipps JS, Richardson RM, Cosgrove T, Eaglesham A (1993) Neutron reflection studies of copolymers at the hexane/water interface. Langmuir 9 (12):3530-3537. doi:10.1021/la00036a031

30. Blomqvist BR, Wärnheim T, Claesson PM (2005) Surface Rheology of PEO−PPO−PEO Triblock Copolymers at the Air−Water Interface: Comparison of Spread and Adsorbed Layers. Langmuir 21 (14):6373-6384. doi:10.1021/la0467584

31. Chang L-C, Lin C-Y, Kuo M-W, Gau C-S (2005) Interactions of Pluronics with phospholipid monolayers at the air–water interface. J Colloid Interface Sci 285 (2):640-652. doi:10.1016/j.jcis.2004.11.011

32. Noskov BA, Lin SY, Loglio G, Rubio RG, Miller R (2006) Dilational Viscoelasticity of PEO−PPO−PEO Triblock Copolymer Films at the Air−Water Interface in the Range of High Surface Pressures. Langmuir 22 (6):2647-2652. doi:10.1021/la052662d

33. Faers MA, Luckham PF (1994) Rheology of polyethylene oxide—polypropylene oxide block copolymer stabilized latices and emulsions. Colloids Surf, A 86 (0):317-327. doi:10.1016/0927-7757(94)02825-7

34. Garcia-Fuentes M, Torres D, Martín-Pastor M, Alonso MJ (2004) Application of NMR Spectroscopy to the Characterization of PEG-Stabilized Lipid Nanoparticles. Langmuir 20 (20):8839-8845. doi:10.1021/la049505j

35. Genovese DB, Lozano JE, Rao MA (2007) The Rheology of Colloidal and Noncolloidal Food Dispersions. J Food Sci 72 (2):R11-R20. doi:10.1111/j.1750-3841.2006.00253.x

36. Liddel PV, Boger DV (1996) Yield stress measurements with the vane. J Non-Newtonian Fluid Mech 63 (2–3):235-261. doi:10.1016/0377-0257(95)01421-7

37. Fischer P, Windhab EJ (2011) Rheology of food materials. Curr Opin Colloid Interface Sci 16 (1):36-40. doi:10.1016/j.cocis.2010.07.003

38. Wulff-Pérez M, Gálvez-Ruíz MJ, de Vicente J, Martín-Rodríguez A (2010) Delaying lipid digestion through steric surfactant Pluronic F68: A novel in vitro approach. Food Res Int 43 (6):1629-1633. doi:10.1016/j.foodres.2010.05.006

Paper IV.

Delaying lipid digestion through steric surfactant Pluronic F68: A novel in vitro approach

M. Wulff-Pérez, M.J. Gálvez-Ruíz, J. de Vicente, A. Martín-Rodríguez

Biocolloid and Fluid Physics Group. Department of Applied Physics. Faculty of Sciences, University of Granada, 18071 Spain.

Published in:

Food Research International

Volume 43, Issue 6, July 2010, Pages 1629–1633

Abstract

The objective of this study was to investigate and compare the lipolysis rate of emulsions stabilized with two surfactants of a markedly different nature: an ionic mixture of phospholipids and the almost purely steric surfactant Pluronic F68. We have studied emulsions stabilized with only one of them, and also with mixtures with different proportions of these two emulsifiers. The impact on lipolysis of the addition of different amounts of β-casein, which is capable of forming thick interfacial layers, was also investigated. To carry out this study, we propose an alternative method to analyze the digestion of emulsions in complex media, which relies on the changes in backscattered light monitored in time by means of a Turbiscan.

Our results show that the steric emulsifier is considerably more efective on delaying the digestion of the emulsions than the ionic one. Besides, it is possible to speed up or slow down the lipolysis by varying the proportion between steric and ionic emulsifiers, and therefore to influence the absorption of lipids and/or hydrophobic compounds dissolved on them. β-casein is not able to delay lipolysis under duodenal conditions, since it is easily cleaved by proteases and displaced by endogenous bile salts.

Introduction

Lipid digestion has a strong impact on human health, not only because it determines the bioavailability of dietary fat (Carey, Small & Bliss, 1983), but also because it influences critically the release of hydrophobic drugs and nutraceuticals when they are dissolved on lipids (Porter, Pouton, Cuine & Charman, 2008). With this in mind, a better understanding and control of the digestion process could lead to significant improvements in our own health. For example, delaying this digestion would reduce the absorption of lipids and therefore it could hinder the development of obesity and associated diseases (type II diabetes, cardiovascular diseases and so forth). Besides, a delayed absorption can activate the ileal brake, a feedback mechanism to control nutrient digestion in which the presence of undigested lipid and/or lipolysis products in the ileum stimulates the secretion of satiety promoting hormones and peptides that slow gastric emptying and reduce appetite (Schirra & Göke, 2005; Maljaars, Peters, Mela & Masclee, 2008). Regarding the hydrophobic drugs/nutraceuticals, a delayed duodenal lipolysis will release them more gradually over time, which would result in a longer duration of their action, whereas a fast lipolysis would be preferable when a quick release is needed (MacGregor et al., 1997).

Processing of dietary lipids generally begins in the stomach, where triglycerides are hydrolysed to diglycerides and fatty acids by the acid-stable lipases, mainly gastric lipase (Porter et al, 2008). This lipase hydrolyses the medium-chain triglycerides (predominantly those with 8- to 10-carbon chain lengths) better than it hydrolyses the long-chain triglycerides. Gastric lipase plays an important role in the absorption of lipids in newborns, but in healthy adult humans it only hydrolyses 10–30% of ingested triglycerides (Singh,Ye & Horne, 2009), and therefore plays an insignificant role in the overall lipid digestion in healthy human adults (Sarkar, Goh, Singh & Singh, 2009). Lipolysis goes mainly to completion in the upper small intestine under the action of the pancreatic lipase: the presence of lipids in the duodenum stimulates the secretion of endogenous surfactants like bile salts, phospholipids (primarily phosphatidylcholine) and cholesterol, and also of pancreatic lipase with its coenzyme, named colipase.

Pancreatic lipase, as other lipases, acts on the oil-water interface hydrolysing triglycerides to fatty acids and monoglycerides. In addition, an efficient fat digestion by pancreatic lipase requires also bile salts and colipase: the former displace dietary proteins and oligosaccharides from the oil-water interface, removing potential inhibitors of pancreatic lipase, while the latter helps the lipase to anchor to a bile salt-covered interface and activates the lipase through a conformational change (Gargouri, Julien, Bois, Verger & Sarda, 1983; Miled, Beisson, de Caro, de Caro, Arondel, & Verger, 2001; Lowe, 2002). Taking into account the interfacial nature of the lipase activity, a series of in vitro studies have been carried out relating interfacial composition with duodenal lipolysis rate (Gargouri et al., 1983; Wickham, Garrood, Leney, Wilson & Fillery-Travis, 1998; Mun, Decker & McClements, 2007; Hur, Decker & McClements, 2009). We wanted to contribute to this knowledge by comparing the effect of two surfactants of markedly different nature on the lipolysis rate. In addition to this, it has been recently pointed out the need to study lipid digestion in emulsions with different proportions between surfactants, since the information on this subject in the literature is scarce (Chu, Rich, Ridout, Faulks, Wickham & Wilde, 2009). For this reason we have prepared emulsions only with phospholipids acting as ionic emulsifiers, emulsions with the non-ionic block copolymer Pluronic F68, acting as a purely steric emulsifier, and also emulsions with mixtures with different ratios of these two emulsifiers. We have also tested the effect of the addition of different concentrations of β-casein, a widely used emulsifier that provides oil droplets with a thick interfacial layer (Dickinson, 2006; Singh et al., 2009), to a preformed emulsion stabilized with Pluronic F68.

In this work, we have tested a novel method based on backscattered light to analyze lipid digestion. Traditionally, lipolysis studies have been carried out either by interfacial measurements (Gargouri et al., 1983) or by automatic titration with NaOH (Wickham et al., 1998; Zangenberg, Mullertz, Kristensen, & Hovgaard, 2001, Mun et al., 2007). This last method assumes that all the pH changes measured during the titration are due to the free fatty acids released. Nevertheless, this method fails when a very chemically complex simulated digestion media is used to mimic in vivo conditions, probably due to interference from one or more of the components (Hur et al., 2009). Keeping this in mind, we have tested an alternative method based on the generalized decrease in droplet size

taking place during lipolysis. This decrease occurs because of the solubilization of the lipolysis products by endogenous bile salts and phospholipids (Reis, Holmberg, Watzke, Leser & Miller, 2009), and therefore it is related to the lipolysis rate. Thus we propose to evaluate this lipolysis rate by monitoring in time the change in the intensity of the light backscattered by the emulsion droplets. In order to avoid creaming of the droplets, which would interfere with the measurements, we have prepared emulsions with a droplet size in the nanoemulsion range. Moreover, the small droplet size provides nanoemulsions with a large interfacial area (Izquierdo et al., 2004), which in this case will shorten the time consumption of the tests. In our experiments we have focused on lipolysis under duodenal conditions because gastric lipases are considerably less active, especially, as was mentioned earlier, when acting on long chain triglycerides.

2. Materials and Methods

2.1 Materials

The poloxamer Pluronic F68 (also known as Poloxamer 188) was obtained from Sigma-Aldrich. It is based on a poly(ethylene oxide)-block-poly(propylene oxide)-block-poly(ethylene oxide) structure which is also typically expressed as PEOa-PPOb-PEOa, being a = 75 and b = 30. The central PPO block links to the oil because of its hydrophobicity, while the two lateral hydrophilic chains of PEO remain in the aqueous phase, stabilizing the droplets by steric hindrance (Wulff-Pérez, Torcello-Gómez, Gálvez-Ruíz & Martín-Rodríguez, 2009). It has been approved as inactive ingredient for oral intake by U.S. Food and Drug Administration. Epikuron 145V is a highly purified deoiled phosphatidylcholine-enriched fraction of soybean lecithin, which contains 61% phosphatidylcholine, 22% phosphatidylethanolamine and 16% phytoglycolipids (De Vleeschauwer & Van der Meeren, 1999), and was kindly provided by Cargill Ibérica S. L. Olive oil was obtained from Sigma-Aldrich, and purified to eliminate free fatty acids. Concretely, 8g of Activated Magnesium Silicate (Florisil, Fluka) were added to every 50 mL of oil and stirred for 3 h, and then removed by centrifugation at 12,000g for 20 min.

Sodium chloride (99.5%), calcium chloride (96%), β-casein (bovine, >98%), Tris-maleate (>99.5%), pancreatin (from porcine pancreas, Product # P8096, lipase activity 4.9 USP/mg), and bile salt extract (B8631, porcine) were also purchased from Sigma-Aldrich. Pancreatin is assumed to have equivalent moles of lipase and colipase (Patton, Albertsson, Erlanson & Borstrom, 1978), whereas bile salt extract contains 49 wt% of bile salts, with 10–15% glycodeoxycholic acid, 3–9%, taurodeoxycholic acid, 0.5–7% deoxycholic acid and 5 % phosphatidylcholine (Zangenberg et al., 2001). The water was purified in a Milli-Q Academic Millipore system.

2.2 Preparation of emulsions

Olive oil-in-water emulsions of 30 ml were prepared with a volume fraction of 25 %. Four different types of emulsions were obtained, according to the surfactant used to stabilize the droplets: a) only Pluronic F68 as surfactant (0.3g), b) only phospholipids (0.48g), c) a 1:1 mixture of Pluronic and phospholipids (0.2g + 0.2g) and d) a 3:1 mixture of Pluronic and phospholipids (0.3g + 0.1g). In all cases, the surfactant was dissolved in water and then the resulting solution pre-mixed with oil using a high speed Heidolph Diax 900 stirrer for 4 minutes at 13,000 rpm. This coarse emulsion was immediately homogenized using the high-pressure Emulsiflex C-3 (Avestin, CA) homogenizer for 8 passes at 100 MPa.

2.3 Measurement of droplet size

The mean droplet size of the different emulsions was measured by Dynamic Light Scattering (DLS) using an ALV-NIBS/HPPS particle sizer with an ALV 5000 multiple digital correlator (ALV-Laser Vertriebsgesellschaft GmbH, Langen, Germany) at 37ºC. The emulsions had to be diluted to a final volume fraction under 1%, in order to reach optimal measurement conditions.

2.4 In vitro duodenal conditions

Solutions of NaCl, CaCl2, bile salt extract and Tris-maleate were mixed and maintained at 37 ºC in order to mimic the chemical conditions of duodenal digestive fluids. The final compositions are listed in Table 1, and they were chosen in order to produce

final concentrations similar to those used by other authors (Zangenberg et al., 2001; Versantvoort, Oomen, Van de Kamp, Rompelberg & Sips, 2005; Hur et al., 2009).

Table 1: Final composition and concentrations of the samples used on the lipolysis experiments (V = 7.5mL, pH= 6.5

	Concentration	Units
NaCl	150	mM
$CaCl_2$	2	mM
Tris-Maleate	2	mM
Bile Salt Extract	4.18	g / L
Pancreatic lipase activity	136	U / ml
Olive oil	12	g / L

The lipase and colipase were obtained from pancreatin as reported in Zangenberg et al., 2001. Briefly, an accurately weighed amount of pancreatin was suspended in 5 mL of purified water at 37ºC and mixed thoroughly. This suspension was then centrifuged for 7 min at 4000 rpm at 37ºC to remove solid, insoluble impurities. One milliliter of the supernatant was withdrawn and used. In all cases this suspension was freshly prepared (within 15 min) in order to avoid denaturation of the lipase.

a) Emulsions with phospholipids/Pluronic F68

Aliquots of 0.4 mL of the freshly prepared emulsion, 3.6 mL of Milli-Q water and 2.5 mL of duodenal juice were mixed together. Then, 1 mL of fresh pancreatin suspension (prepared as described above) was added. This mixture was inverted four times and immediately transferred to the cell of the measuring system.

b) Addition of β-casein

A weighed amount of β-casein was dissolved in 3.6 mL of Milli-Q water at 37ºC, and then mixed with 0.4 mL of a pre-formed nanoemulsion stabilized with Pluronic F68.

The mixture was incubated for 10 minutes at 37ºC. Then, 2.5 mL of duodenal juice and 1 mL of pancreatin suspension were added, and the mixture was transferred to the measuring cell as described above. Four different concentrations of β-casein were used to give a final concentration of 0, 0.13, 1.3 and 4 g/L or, referred to the amount of Pluronic, concentrations of 0, 0.062, 0.620 and 1.860 g β-casein/g Pluronic F68.

2.5 Evaluation of the in vitro lipolysis

The emulsion-pancreatin mixture was inverted four times and immediately transferred to a flat-bottomed cylindrical cell, where the time evolution of scattered light was measured with a Turbiscan MA 2000 (Formulaction, France). In this device the sample was scanned by using two synchronous optical sensors that detected the intensity of light transmitted through and backscattered by the vertical sample (180º and 45º from the incident laser light, respectively). The reading head acquired backscattering (BS) and transmission data every 40μm while moving along the entire height of the cell (60 mm). The light source was an electro-luminescent diode (λ_{air} = 880 nm). As the emulsions studied were opaque, only the backscattering measurements provided useful data. Changes in BS values correspond to changes in the structure of an analyzed sample, i.e., variations of particle size and/or particle volume fraction (Mengual, Meunier, Cayré, Puech & Snabre, 1999a). For example, in the case of particle migration, the increase in BS levels can be observed at the top or bottom of sample, depending on the type of migration, i.e., creaming or sedimentation, respectively, since the concentration of particles would increase in these regions (Macierzanka, Szeląg, Szumała, Pawłowicz, Mackie & Ridout, 2009b). On the other hand, a generalized change in BS through the whole height of the cell is related with a change in particle size. For small Rayleigh – Debye scatterers (diameter < 0.3 μm), a decrease in particle diameter produces a decrease in BS (Mengual, Meunier, Cayré, Puech & Snabre, 1999b). According to their droplet size, our nanoemulsions belong to this type of scatterers. Therefore, the generalized decrease in BS observed can be attributed to a decrease in particle size, which in this system can only be caused by the action of the lipase. Thus, measuring BS changes in the center of the tube and plotting these changes against time gives us a qualitative estimation of the lipolysis rate (see Figure 1). The lipolysis rate

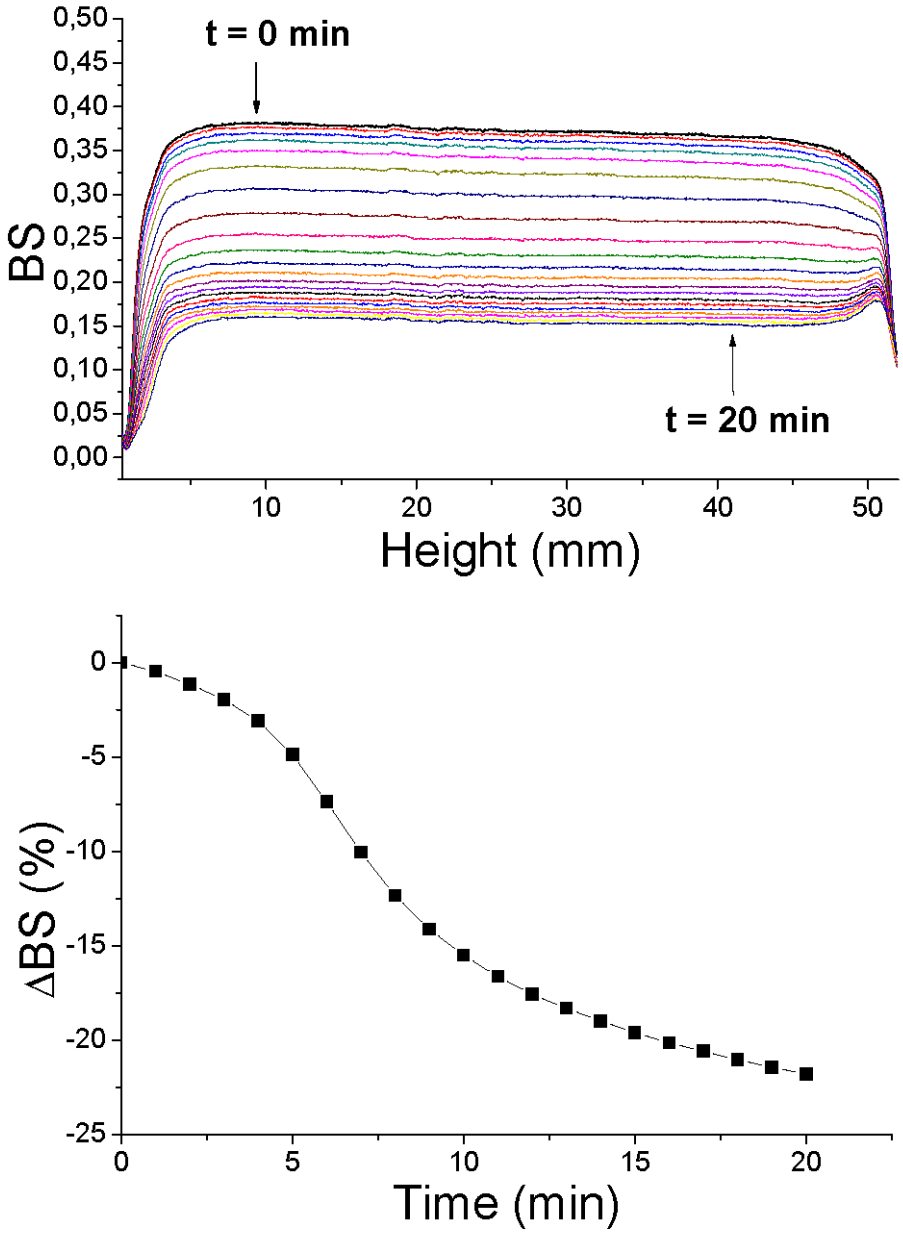

Fig. 1. a) Backscattering profiles obtained during a lipolysis experiment for a 3:1 Pluronic-phospholipids stabilized nanoemulsion, recording BS every minute. b) The same experiment, expressed as ΔBS (referred to the first measurement) as a function of time.

was characterized using the parameter ΔBS. The parameter ΔBS was defined in way a similar to that reported in Macierzanka et al. (2009b), ΔBS being the difference in mean BS value (recorded for the emulsion sample in the central region that went from 20 to 40 mm of its height) between the first scan and n scan.

This procedure was repeated three times for each type of emulsion, to test the reproducibility of the method. Also a blank experiment for each emulsion was performed, by adding 1mL of Milli-Q water instead of the pancreatin suspension

3. Results and discusión

The mean droplet sizes of the different emulsions are shown in Table 2. It can be seen that in all cases their diameter is under 300 nm, therefore remaining both in the nanoemulsion and in the small Rayleigh-Debye scatterers range. Unfortunately, our particle sizer does not allow us to obtain a size distribution, but rather a mean size and an estimate of the width of the distribution, and therefore it fails when the polydispersity of the sample is high. For this reason it was not possible to obtain reliable final droplet sizes.

Regarding the experiments performed without lipase (the blanks), no changes in backscattering were observed for two hours, i.e., the presence of duodenal juice did not affect in any manner the stability of the nanoemulsions under our experimental conditions

Table 2: Initial droplet diameters and standard deviations of the different nanoemulsions

Type of emulsion	Mean droplet size (nm)	Standard deviation (nm)
Pluronic F68	239	± 20
Pluronic-Phospholipids 3:1	274	± 43
Pluronic-Phospholipids 1:1	264	± 27
Phospholipids	274	± 35

(although higher concentrations of calcium, as those reported for the fed state by Zangenberg et al, 2001, may produce droplet flocculation in ionically stabilized emulsions). Therefore all the changes observed in the subsequent lipolysis experiments can be attributed to the action of the lipase.

When pancreatic lipase was added, the measurements showed good reproducibility for every type of emulsion.

a) Effect of the surfactant type and relative amount

Arithmetic averages of the three profiles obtained for each type of nanoemulsion are shown in Figure 2. For the nanoemulsion stabilized only with phospholipids, a very fast initial digestion of the lipids is observed. This noticeably high rate of lipolysis within the first minutes correlates fairly well with the results obtained by Zangenberg et al., 2001,

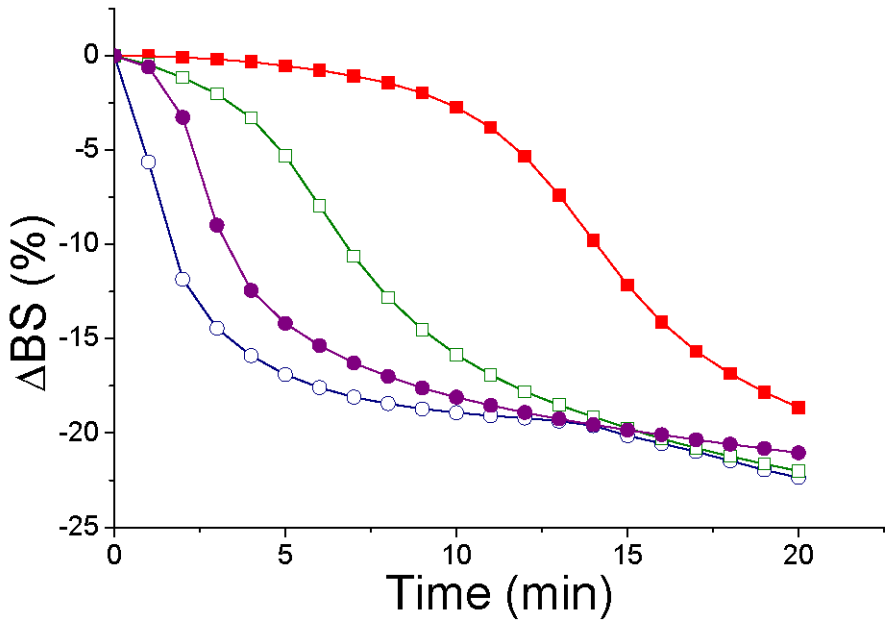

Fig. 2. Changes in backscattering measured during a lipolysis experiment for four nanoemulsions stabilized with different ratios of Pluronic F68 and phospholipids: -■-, only Pluronic F68; -○-, only phospholipids; -□- , Pluronic + phospholipids (3:1); -●-, Pluronic + phospholipids (1:1).

as well as by Mun et al., 2007, using the pH-stat method and similar chemical conditions (pH, phospholipids as surfactant, bile salt concentration, lipase activity, etc). However, for the emulsion with only Pluronic F68 as surfactant, two effects should be highlighted: i) a clear lag phase appears and ii) the lipolysis rate is slowed down. In mixtures, an intermediate behavior is observed: the effects of Pluronic at the interface are still present (lag phase, slowed down lipolysis) but to a lesser extent and clearly depending on the proportion between the two emulsifiers. In other words, it is possible to modify the lipolysis rate varying the proportions between different emulsifiers. These results are consistent with those recently obtained by Chu et al. (2009), who used different proportions of lecithin and galactolipids to stabilize emulsions and estimated their effect on lipolysis rate by titration. They also observed a lag phase with a similar dependence on the amount of steric surfactant, which in their experiments was digalactosyldiacylglycerol.

The mechanism of this lipolysis inhibition seems to be then the steric hindrance caused by the hydrophilic tails of Pluronic F68, which makes more difficult the formation of the bile salt-colipase-lipase complex at the droplet interface. This is in agreement with the results obtained by Mun et al. (2007), who also observed a slowed down lipolysis with the steric emulsifier Tween 20. However, in their experiments this inhibition did not take place in the presence of bile extract, since the surface-active components of the bile extract displaced Tween 20 molecules from the oil-water interface. This displacement by bile salts was also observed by Gargouri et al (1983) for small molecule surfactants. Nevertheless, the appearence of a lag phase in our experiments even in the presence of a high concentration of bile salts shows that this displacement is also partially hindered in Pluronic-stabilized emulsions (although not completely prevented). The reason to this could be the relatively thick surfactant layer adsorbed: whereas Tween 20 has only 20 polyoxyethylene units distributed in four tails, Pluronic F68 has two tails of 75 polyoxyethylene units each, providing the droplets with a thick layer of approx. 7 nm (Baker & Berg, 1988 ;Wulff-Pérez et al., 2009). Therefore, Pluronic F68 would not only partially hinder the action of the bile salt-colipase-lipase complex, but also its own displacement by bile salts.

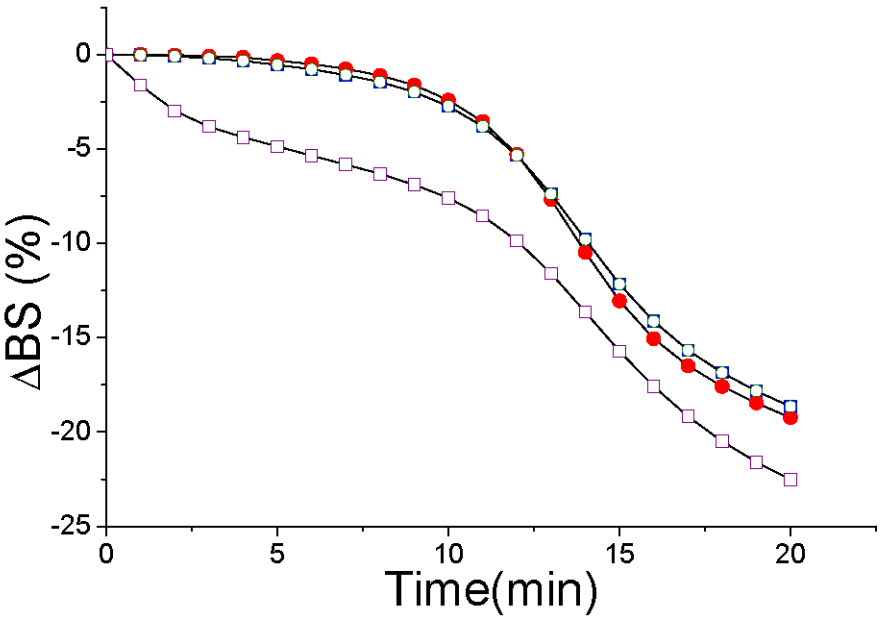

Fig. 3. ΔBS profiles obtained for the lipolysis of a nanoemulsion stabilized only with Pluronic F68, to which different amounts of β-casein were added: -■-, without β-casein; -●- , 0.13 g/L; -○-, 0, 1.33 g/L; -□- , 4.00 g/L.

b) Effect of the addition of β-casein

The lipolysis profiles obtained for the systems in which different amounts of β-casein were added to a preformed Pluronic-stabilized emulsion are shown in Figure 3. When the amount of added β-casein is small, the lipolysis rate observed is almost undistinguishable from that obtained without β-casein. However, when this amount is sufficiently increased (almost doubling the Pluronic F68 concentration), a change in the lipolysis behavior is observed. First, a faster initial lipolysis takes place. After this, a lag phase and a slowed-down lipolysis are observed again, in a similar way as in emulsions stabilized only with Pluronic F68. The initial speeded up lipolysis indicates that the interface has been modified and some displacement has occurred. After this initial speeded up lipolysis, the lag phase appears again. This fact indicates that there is still enough Pluronic at the interface to slow down the lipolysis to some extent, ruling out a total displacement of Pluronic by β-casein. It can be seen that this part of the curve does not differ much from the profiles obtained for the Pluronic-Phospholipids mixtures,

confirming the fact that the amount of Pluronic present at the interface determines the length of the lag phase and the lipolysis rate.

The initial speeded up lipolysis and the delayed appearance of the lag phase lead us to propose the following mechanism: first, when a sufficiently high concentration is present, the β-casein is able to displace Pluronic from some regions of the interface. When bile extract is added to this emulsion, the access of the bile salts to the interface is facilitated, since bile salts remove easily β-casein from oil-water interfaces under duodenal conditions (Macierzanka, Sancho, Mills, Rigby & Mackie, 2009a), in the same way as they remove similar proteins as caseinates and β-lactoglobulin (Mun et al., 2007; Maldonado-Valderrama et al., 2008). The addition of pancreatin suspension, containing lipase and colipase, starts the lipolysis. Moreover, pancreatin contains proteases, which cleave β-casein adsorbed at oil-water interfaces (Macierzanka et al., 2009a), facilitating to a larger degree the access of bile salts to the interface. The lipolysis at interfaces covered by bile salts, which were intially β-casein covered interfaces, would be then the initial speeded up lipolysis observed. However, Pluronic F68 has not been completely displaced, and therefore it is still able to hinder its own displacement by bile salts, as well as to prevent the lipase from coming in close proximity with the lipids. This fact would explain the subsequent delay of the lipolysis.

4. Conclusions

In this study, a novel in vitro method to obtain information on lipolysis rate has been developed. This method is not meant to replace other types of studies (interfacial, titrimetric) but rather to complement them, especially when dealing with chemically complex systems. Furthermore, the required instruments are not uncommon in laboratories that work with emulsions.

It has been shown that it is possible to alter the lipolysis rate by varying the proportions between two surfactants of different nature, one being a small ionic emulsifier and the other being a non-ionic emulsifier capable of forming bulky adsorbed

layers, at least in vitro, under duodenal conditions. The concentration of steric surfactant at the interface is related with the length of the lag phase and the delayed lipolysis. It has been also observed that surface active proteins such as β-casein are not useful to delay lipolysis, despite the fact that they could also form thick interfacial layers. This is probably due to the fact that they are easily removed by bile salts and/or cleaved by proteases.

Acknowledgments

This research is supported by FEDER funds and "Ministerio de Educación y Ciencia" under project MAT2007-66662-C02-01 and by "Junta de Andalucía – Consejería de Educación, Ciencia y Empresa" under project P07-FQM-03099. M.W.P. thanks the latter project referred for the scholarship received. We greatly thank Cargill Iberica for donating the Epikuron-145V used in this study. We also thank F. Vereda for revising the final English version.

References

Baker, J. A., & Berg, J. C. (1988). Investigation of the adsorption configuration of polyethylene oxide and its copolymers with polypropylene oxide on model polystyrene latex dispersions. Langmuir, 4(4), 1055–1061.

Carey, M.C., Small, D. M., & Bliss, C. M. (1983) Lipid Digestion and Absorption. Annual Review of Physiology, 45, 651-677

Chu, B., Rich, G. T., Ridout, M. J., Faulks, M. J., Wickham, M. S. J., & Wilde, P. J. (2009) Modulating Pancreatic Lipase Activity with Galactolipids: Effects of Emulsion Interfacial Composition. Langmuir, 25(16), 9352 9360

De Vleeschauwer, D., & Van der Meeren, P. (1999) Colloid chemical stability and interfacial properties of mixed phospholipid–non-ionic surfactant stabilised oil-in-water emulsions. Colloids and Surfaces A: Physicochemical and Engineering Aspects, 152, 59–66

Dickinson, E. (2006) Structure formation in casein-based gels, foams, and emulsions. Colloids and Surfaces A: Physicochemical and Engineering Aspects, 288(1-3), 3-11

Gargouri, Y., Julien, R., Bois, A. G., Verger, R., & Sarda, L. (1983) Studies on the detergent inhibition of pancreatic lipase activity. Journal of Lipid Research, 24, 1336–1342

Hur, S. J., Decker, E. A., & McClements, D. J. (2009) Influence of initial emulsifier type on microstructural changes occurring in emulsified lipids during in vitro digestion. Food Chemistry, 114, 253–262

Izquierdo, P., Esquena, J., Tadros, T. F., Dederen, J. C., Feng, J., Garcia-Celma, M. J., Azemar, N., & Solans, C. (2004) Phase behavior and nano-emulsion formation by the phase inversion temperature method. Langmuir, 20, 6594-6598

Lowe, M. E. (2002) The triglyceride lipases of the pancreas. Journal of Lipid Research, 43, 2007-2016

MacGregor, K. J., Embleton, J.K., Lacy, J. E., Perry, E. A., Solomon, L. J., Seager, H., & Pouton, C. W. (1997) Influence of lipolysis on drug absorption from the gastro-intestinal tract. Advanced Drug Delivery Reviews, 25, 33-46

Macierzanka, A., Sancho, A. I., Mills, E. N. C., Rigby, N. M., & Mackie, A. R. (2009a) Emulsification alters simulated gastrointestinal proteolysis of β-casein and β-lactoglobulin. Soft Matter, 5, 538–550

Macierzanka, A., Szeląg, H., Szumała, P., Pawłowicz, R., Mackie, A. R., & Ridout, M. J. (2009b) Effect of crystalline emulsifier composition on structural transformations of water-in-oil emulsions: Emulsification and quiescent conditions. Colloids and Surfaces A: Physicochemical and Engineering Aspects, 334, 40–52

Maldonado-Valderrama, J., Woodward, N. C., Gunning, A. P., Ridout, M. J., Husband, F. A., Mackie, A. R., Morris, V. J., & Wilde, P. J.(2008) Interfacial characterization of beta-lactoglobulin networks: Displacement by bile salts. Langmuir, 24(13), 6759–6767

Maljaars, P. W, Peters, H. P, Mela, D. J, & Masclee, A. A. (2008) Ileal brake: a sensible food target for appetite control. A review. Physiology & Behavior, 95(3), 271-81.

Mengual, O., Meunier, G., Cayre, I., Puech, K., & Snabre, P. (1999a) Characterisation of instability of concentrated dispersions by a new optical analyser: the TURBISCAN MA 1000. Colloids and Surfaces A: Physicochemical and Engineering Aspects, 152, 111–123

Mengual, O., Meunier, G., Cayre, I., Puech, K., & Snabre, P. (1999b) TURBISCAN MA 2000: multiple light scattering measurement for concentrated emulsion and suspension instability analysis. Talanta, 50, 445–456

Miled, N., Beisson, F., de Caro, J., de Caro, A., Arondel, V., & Verger, R. (2001) Interfacial catalysis by lipases. Journal of Molecular Catalysis B: Enzymatic, 11,165–171

Mun, S., Decker, E. A., & McClements, D. J. (2007) Influence of emulsifier type on in vitro digestibility of lipid droplets by pancreatic lipase. Food Research International, 40, 770–781

Patton, J.S., Albertsson, P.A., Erlanson, C., & Borstrom, B. (1978) Binding of porcine pancreatic lipase and colipase in the absence of substrate studied by 2-phase partition and affinity chromatography. Journal of Biological Chemistry 253, 4195–4202

Porter, C. J. H., Pouton, C.W., Cuine, J. F., & Charman, W. N. (2008) Enhancing intestinal drug solubilisation using lipid-based delivery systems. Advanced Drug Delivery Reviews, 60, 673–691

Reis, P., Holmberg, K., Watzke, H., Leser, M. E., & Miller, R. (2009) Lipases at interfaces: A review. Advances in Colloid and Interface Science,147-148, 237-250

Sarkar, A., Goh, K. K. T., Singh, R. P., & Singh, H. (2009) Behaviour of an oil-in-water emulsion stabilized by β-lactoglobulin in an in vitro gastric model. Food Hydrocolloids, 23(6), 1563-1569

Schirra, J., & Göke, B. (2005) The physiological role of GLP-1 in human: incretin, ileal brake or more? Regulatory Peptides, 128 (15),109-115

Singh, H., Ye, A., & Horne, D. (2009) Structuring food emulsions in the gastrointestinal tract to modify lipid digestion. Progress in Lipid Research, 48, 92–100

Versantvoort, C. H. M., Oomen, A. G., Van de Kamp, E., Rompelberg, C. J. M., & Sips, A. (2005). Applicability of an in vitro digestion model in assessing the bioaccessibility of mycotoxins from food. Food and Chemical Toxicology, 43(1), 31–40

Wickham, M., Garrood, M., Leney, J., Wilson, P. D. G., & Fillery-Travis, A. (1998) Modification of a phospholipid stabilized emulsion interface by bile salt: effect on pancreatic lipase activity. Journal of Lipid Research, 39, 623-632

Wulff-Pérez, M., Torcello-Gómez, A., Gálvez-Ruíz, M. J., & Martín-Rodríguez, A. (2009) Stability of emulsions for parenteral feeding: Preparation and characterization of o/w nanoemulsions with natural oils and Pluronic f68 as surfactant. Food Hydrocolloids, 23(4), 1096-1102

Zangenberg, N. H., Müllertz, A., Kristensen, H. G., & Hovgaard, L. (2001) A dynamic in vitro lipolysis model I. Controlling the rate of lipolysis by continuous addition of calcium. European Journal of Pharmaceutical Sciences, 14, 115–122

Paper V.

Controlling lipolysis through steric surfactants: new insights on the controlled degradation of submicron emulsions after oral and intravenous administration

Miguel Wulff-Pérez, Juan de Vicente, Antonio Martín-Rodríguez, María J. Gálvez-Ruiz

Biocolloid and Fluid Physics Group. Department of Applied Physics. Faculty of Sciences, University of Granada, 18071 Spain.

Published in:

International Journal of Pharmaceutics

Volume 423, Issue 2, 28 February 2012, Pages 161–166

Abstract

In this work we have investigated how steric surfactants influence the metabolic degradation of emulsions (lipolysis). To do so, we have prepared submicron emulsions stabilized with Pluronic F68, Pluronic F127, Myrj 52 or Myrj 59, four non-ionic surfactants with key differences on their structure. Submicron emulsions have been prepared also with mixtures of these surfactants with different proportions between them. Then, in vitro methods have been applied to analyze the lipolysis of these emulsions, both under duodenal and intravenous conditions, to simulate lipolysis after oral and intravenous administration. Our results show that the properties of the surfactant influence dramatically the lipolysis rates observed both under duodenal and intravenous conditions, e.g., intravenous lipolysis was completely blocked when Pluronic F127 was used, while it was almost complete within six hours when using Myrj 52. The reason for this seems to be the steric hindrance that the surfactant produces around the droplet and at the interface. As a result, we can modify the lipolysis patterns by changing some characteristics of the surfactant, or by varying the proportion between two surfactants in a mixture. These findings may be applied in the development of novel strategies to rationally design submicron emulsions as lipophilic drug carriers.

1. Introduction

It has been estimated that nearly 50% of new potential drugs have low solubility in water, which leads to poor bioavailability and makes the control of their release a challenging issue (S. Tamilvanan, 2009). In order to bypass these difficulties, the use of lipid dispersion carrier systems, such as lipid emulsions or liposomes, has attracted particular interest in recent years, since they have significant and beneficial effects on the absorption and exposure of co-administered lipophilic drugs, leading to higher bioavailability (Porter et al., 2008). Submicron emulsions are one especially interesting drug delivery system, due to their biocompatibility, biodegradability, ease of preparation on a large scale, large surface area, and proven long-term stability against destabilizing phenomena such as creaming or sedimentation (Tamilvanan, 2004).

Traditionally, phospholipids have been used as surfactants to prepare submicron emulsions for drug delivery applications. However, phospholipids are rapidly displaced from interfaces by bile salts in the duodenum when phospholipid-stabilized emulsions are administered orally (Torcello-Gómez et al., 2011). Also, if these emulsions are administered by the intravenous route, they are rapidly eliminated according to their colloidal foreign body character by the mononuclear phagocyte system (MPS) (Lucks et al., 2000). In both cases, the use of phospholipids as the only surfactant does not allow us to control the processes involved in the metabolic degradation of the emulsions in order to use lipid emulsions as controlled-release drug carriers (Lucks et al., 2000; Kurihara et al., 1996). Non-ionic, steric surfactants containing polyethylene oxide (PEO or PEG) have been proposed to overcome those problems, both for oral (Wulff-Pérez et al., 2010) and parenteral applications (Tamilvanan, 2009). However, there is still a lack of understanding of how these surfactants affect the metabolic processing of lipid carrier systems.

The release of hydrophobic drugs from lipid based delivery systems is strongly related with the natural degradation of these emulsions in the body (Larsen et al., 2011), i.e., the lipolysis or enzymatic hydrolysis of the triglycerides composing the drug delivery system. Therefore, a better understanding of how to alter the lipolysis rate should provide us with a finer control of the drug release from submicron o/w emulsions when

administered both orally and parenterally. By oral route, this lipolysis occurs mainly in the upper small intestine. When oil droplets arrive to the duodenum, they are mixed with pancreatic lipase, colipase and bile salts. Bile salts displace molecules adsorbed at the oil–water interface, removing potential inhibitors of pancreatic lipase, while colipase helps the lipase to anchor to a bile salt-covered interface and activates the lipase through a conformational change (Miled et al., 2001; Reis et al., 2008). Then, pancreatic lipase starts the hydrolysis of triglycerides into free fatty acids and monoglycerides, which are small, more soluble molecules. These lipolysis products leave the droplet forming a series of colloidal structures, including multilamellar and unilamellar vesicles, mixed micelles and micelles. Hydrophobic drugs leave the droplets within these species, which significantly increase the solubilization capacity of the small intestine for these drugs (Porter et al., 2007). Therefore, the lipolysis rates influence directly the release and absorption of the hydrophobic drugs delivered in lipidic systems.

Regarding the intravenous (IV) route, emulsions can be recognized as foreign bodies by the MPS and retired from circulation, or they can behave as chylomicrons and enter the fat metabolism pathway (Buszello and Müller, 2000). Chylomicrons are the oil droplets responsible for the transport of dietary lipids from the intestines to other locations in the body. In the blood they acquire apolipoproteins, and with the help of apolipoprotein C-II (apoC-II), the hydrolysis of lipids begins via the action of the endothelial cell bound Lipoprotein Lipase (LpL). Some LpL dissociates from endothelial cells during lipolysis and continues its enzymatic action in the bloodstream (Yamamoto et al., 2003; Rensen and Van Berkel, 1996; Goldberg, 1996) while the free fatty acids leave the droplets, being these fatty acids now available for the body cells or for binding to the serum albumins (Lucks et al., 2000). Again, the release of highly lipophilic drugs will be directly related with the lipolysis rate. Surprisingly, there is a vast literature on the relation between stability against MPS and control of the drug release, but very little regarding lipolysis under IV conditions and lipidic drug delivery systems, even for emulsions that have already proven to be stable against MPS uptake.

In this work, we have focused on the first stage of the enzymatic degradation of the drug delivery system, i.e., the lipolysis. Four different steric surfactants were used to

prepare submicron emulsions, in order to study how the structure and properties of these surfactants affect the lipolysis, both under in vitro duodenal and intravenous conditions. These surfactants were Pluronic F68, Pluronic F127, Myrj 52 or Myrj 59, as well as mixtures with different proportions between them. A better understanding on the relation between the structure of the surfactant and the lipolysis rate should help us to control the time when the hydrophobic drug is released. This knowledge may be applied in the development of novel strategies to rationally design submicron emulsions as lipophilic drug carriers.

2. Materials and methods

2.1. Materials

Surfactants: The poloxamer Pluronic F68 (PF68) and Pluronic F127 (PF127), also known as Poloxamer 188 and 407 respectively, were obtained from Sigma-Aldrich and used without further purification. They are based on a poly(ethylene oxide)-block-poly(propylene oxide)-block- poly(ethylene oxide) structure (see Table 1). The central polypropylene oxide (PPO) block links to the oil because of its hydrophobic character, while the two lateral hydrophilic chains of polyethylene oxide (PEO) remain in the aqueous phase, stabilizing the droplets by steric hindrance. PF127 has been approved as inactive ingredient for oral intake by U.S. Food and Drug Administration (FDA), whereas PF68 has been approved for both oral and intravenous administration. Myrj surfactants consist of stearic acid esterified with polyethylene oxide, with Myrj 52 (M52) having 40 subunits of PEO and Myrj 59 (M59) having 100 subunits. M52 is approved by both FDA and European Food Safety Authority as a food ingredient (number E431) and was obtained from Sigma-Aldrich. M59 was a kind gift from Croda Ibérica S.A. Epikuron 145V is a deoiled phosphatidylcholine enriched fraction of soybean lecithin. This phospholipids mixture was used for a comparative analysis and was kindly provided by Cargill Ibérica S. L.

Table 1. Chemical structure of the surfactants used in this study to prepare and stabilize the submicron emulsions

Pluronic F68 (PF68)	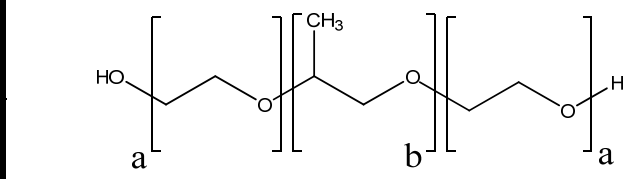	**a = 75 b = 29**
Pluronic F127 (PF127)		**a = 100 b = 65**
Myrj 52 (M52)	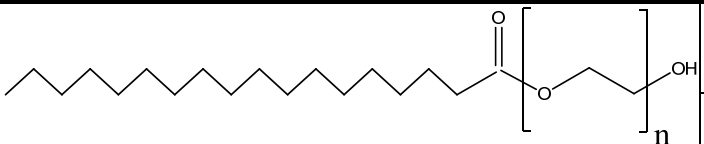	**n = 40**
Myrj 59 (M59)		**n = 100**

Oils: Sunflower oil was obtained from Sigma-Aldrich. This oil was purified to eliminate free fatty acids as described elsewhere (Wulff-Pérez et al., 2011).

Gastric conditions: Pepsin (924 U/mg), sodium chloride and hydrochloric acid (38%) were obtained from Sigma-Aldrich to prepare the simulated gastric fluid.

Duodenal conditions: Sodium chloride (99.5%), calcium chloride (96%), Tris-Maleate (>99.5%), pancreatin (from porcine pancreas, lipase activity 4.9 USP/mg), and bile salt extract (B8631, porcine) were also purchased from Sigma. Pancreatin is assumed to have equivalent moles of lipase and colipase whereas bile salt extract contains 49 wt % of bile salts. The water was purified in a Milli-Q Academic Millipore system.

IV conditions: Purified bovine milk LpL (4510 units/mg, 0.37 mg/mL), suspended in 3.8 M ammonium sulfate, 0.02 M Tris-HCl at pH 8.0, was obtained from Sigma. Human serum plasma, heparin ammonium salt (196 U/mg), albumin from bovine serum (lyophilized powder, ≥98, essentially fatty acid free, essentially globulin free) and Tris-Base were also obtained from Sigma.

2.2. Preparation of submicron emulsions

Sunflower oil-in-water emulsions of 30 mL were prepared with a volume fraction of 25%. Different types of emulsions were obtained, according to the surfactant used to stabilize the droplets: (a) only Pluronic F68 as surfactant, (b) Pluronic 127 (c) Myrj 52 and (d) Myrj 59. Emulsions were also prepared with mixtures PF68/PF127 and M52/M59 with different proportions between them (3:1, 1:1 and 1:3 in weight), as well as with phospholipids for comparison purposes. The final surfactant concentration was 1% (w/v) for polymeric surfactants and 1.5% (w/v) for phospholipids. In all cases, the surfactant was dissolved in water and then the resulting solution pre-mixed with oil using a high speed Heidolph Diax 900 stirrer for 4 min at 13,000 rpm. This coarse emulsion was immediately homogenized using the high pressure Emulsiflex C-3 (Avestin, CA) homogenizer for 10 passes at 100 MPa.

2.3. Measurement of droplet size

The mean droplet size of the different emulsions was measured by Dynamic Light Scattering (DLS) using an ALV-NIBS/HPPS particle sizer with an ALV 5000 multiple digital correlator (ALV-Laser Vertriebsgesellschaft GmbH, Langen, Germany) at 37 ºC. The emulsions were diluted to a final volume fraction below 1%, in order to reach optimal measurement conditions.

2.4. Stability of submicron emulsions under gastric conditions

Emulsions were mixed with simulated gastric fluid in order to achieve a final oil volume fraction of 10%, with 3.2 g/L of pepsin, 2 g/L NaCl and pH adjusted to 1.2 with HCl, according to the compositions given by the U. S. Pharmacopeia for simulated gastric fluid. This mixture was immediately transferred to the measuring cell, where the stability of the emulsions was measured for 2 hours. Gastric lipase is not commercially available for research and was not used. In any case, gastric lipases play a small role in comparison to duodenal lipase in the overall lipid digestion in healthy human adults (Sarkar et al., 2009) and hydrolyze the medium-chain triglycerides (predominantly those with 8- to 10-carbon chain lengths) much better than they hydrolyze the long-chain triglycerides of vegetable oils (Porter et al., 2007), as the sunflower oil used in this study.

The stability of the emulsions under simulated gastric fluid was evaluated using a Turbiscan MA 2000 (Formulaction, Toulouse, France). The emulsion is placed in a flat-bottomed cylindrical glass cell and scanned from the bottom to the top with a light source (near infrared, λair= 850 nm) and the light backscattered by the sample (45º from the incident radiation) is detected. The Turbiscan works in scanning mode: the optical reading head scans the length of the sample acquiring transmission and backscattering data every 40 μm. The corresponding curves provide the backscattered (BS) light flux as a function of the sample height, and scans are repeated over time. The BS light intensity is related with the amount and size of droplets present in the dispersion. BS remains unchanged in the whole height of the cell when the number of particles and interfaces is not changing, i.e. if no coalescence, flocculation, creaming or sedimentation occurs (Wulff-Pérez et al., 2009). Emulsions in which this behavior was observed were considered stable. This stability was later confirmed by DLS measurements.

2.5. In vitro duodenal lipolysis

Solutions of NaCl, CaCl2, bile salt extract and Tris-maleate were mixed and maintained at 37 ºC in order to mimic the chemical conditions of duodenal digestive fluids. The final compositions were chosen in order to produce final concentrations similar to those used by other authors and in previous works (Hur et al., 2009; Versantvoort et al., 2005; Zangenberg et al., 2001): pH 6.5, NaCl 150mM, CaCl2 2mM, 12 g/L of sunflower oil and 4.18 g/L bile salt extract. The final volume was 7.5 mL. The lipase and colipase were obtained from pancreatin as previously reported (Wulff-Pérez et al., 2010) obtaining a final lipase activity of 136 U/mL.

The in vitro duodenal lipolysis was evaluated by measuring the time evolution of BS light with the Turbiscan MA 2000 as described in detail elsewhere (Wulff-Pérez et al., 2010). Aliquots of 0.4 mL of the freshly prepared emulsion, 3.6 mL of Milli-Q water and 2.5 mL of duodenal juice were mixed together. Then, 1 mL of fresh pancreatin suspension was added. This mixture was inverted four times and immediately transferred to the measuring cell of the Turbiscan. For small Rayleigh–Debye scatterers (diameter <0.3 μm), a decrease in particle diameter produces a decrease in BS (Mengual, 1999). According to their droplet size, our emulsions belong to this type of scatterers, and therefore the

generalized decrease in BS observed through the whole height of the cell can be attributed to a decrease in particle size, which in this system can only be caused by the action of the lipase, as the oil from the droplets is digested and solubilized in mixed micelles, vesicles, etc (Hur et al., 2009). Thus, measuring BS changes in the center of the tube and plotting these changes against time gives us a quick qualitative estimation of the lipolysis rate: the faster the lipolysis, the sharper the decrease in BS observed. The lipolysis rate was characterized using the parameter ΔBS, defined as the difference in mean BS value (recorded for the emulsion sample in the central region that went from 20 to 40 mm of its height) between the first scan and n scan.

This experiment was repeated three times for each type of emulsion. Also a blank experiment for each emulsion was performed, by adding 1 mL of Milli-Q water instead of the pancreatin suspension.

2.6. In vitro intravenous lipolysis

A buffer containing the main components involved in intravenous lipolysis was prepared, based on the compositions and concentrations used by other authors (Yamamoto et al., 2003; Rensen and Van Berkel, 1996; Ton et al., 2005; Deckelbaum et al., 1990) in order to obtain a final composition for the experiments with pH 8.6, NaCl 150mM, Tris-Base 10mM, 4% Albumin and 66.7 μg/mL Heparin. 10 % v/v of human plasma, heat-inactivated (30 min at 56 °C), was used as a source of apolipoprotein C-II.

Emulsions were diluted with the buffer previously described until a final oil/water volume fraction of 0.1%, being the total volume 400 μL, and incubated at 37 ºC for 30 min. Then, 4.0 μg/mL LpL were added, starting the lipolysis experiment, and the released free fatty acids from the lipid emulsions were measured at predetermined time intervals using an enzymatic kit (Non-Esterified Fatty Acid (NEFA) Kit; RANDOX Laboratories Ltd., United Kingdom). Studies were performed in triplicates. A blank experiment was performed in order to correct the possible FFA coming from plasma, impurities, etc, adding Milli-Q water instead of LpL solution.

3. Results and Discussion

3.1. Characterization of the emulsions

The droplet sizes were between 200-230 nm for the emulsions stabilized with polymeric surfactants and between 275-290 nm for the phospholipid-stabilized emulsions. The standard deviations were ±20nm and ±35 nm, respectively. All the emulsions remained stable for 24 hours, i.e., under the time frame of the experiments.

3.2. Stability under gastric conditions

No changes (ΔBS<0.3%) in backscattering were observed under gastric conditions for two hours for any of the polymer-stabilized emulsions, i.e., the droplets remained unaffected under these conditions, with no destabilizing phenomena such as coalescence or flocculation. This was confirmed by DLS measurements, where no change in particle size was observed. Therefore, these emulsions are expected to protect effectively any drugs dissolved in them against the harsh gastric conditions, allowing these hydrophobic drugs to arrive mostly unaffected to the intestine, where most of these drugs are absorbed when administered orally (Porter et al., 2007).

3.3. In vitro duodenal lipolysis

3.3.1. Pure PF68, PF127, M52 and M59

The results of the experiments are shown in Figure 1. Regarding the experiments performed without lipase (the blanks), no changes in backscattering are observed for two hours, i.e., the presence of duodenal juice does not affect in any manner the stability of the emulsions (ΔBS<0.3%, data not shown). When lipase is added, lipolysis takes place in all cases, with the typical lag-phase previously reported for emulsions stabilized with steric surfactants, in contrast to the fast, almost instantaneous lipolysis observed when phospholipids are used as the only surfactant (Wulff-Pérez et al., 2010; Chu et al., 2009). It is also worth to note here that the decrease of backscattering was equal both at the bottom

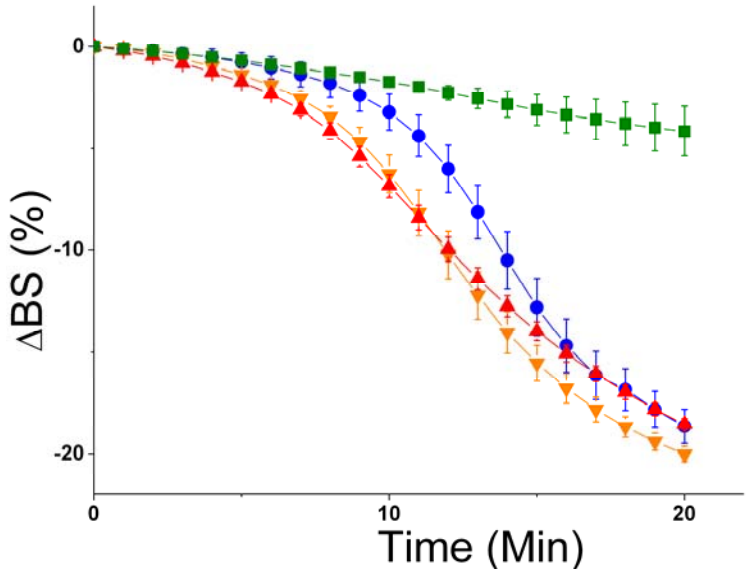

Fig. 1. Changes in backscattering measured during a lipolysis experiment under duodenal conditions for four submicron emulsions stabilized with different steric surfactants: -■-, Pluronic F127; -●-, Pluronic F68; -▼-, Myrj 52; -▲-, Myrj 59. n=3.

and at the top part of the measuring cell, meaning that no phase separation was happening within the time frame of the experiment. This indicates that no coalescence is taking place, i.e., the observed changes can be attributed to the lipolysis of the oil droplet and not to the hydrolysis of the surfactants stabilizing the droplet.

However, the lipolysis observed is not equal for all the surfactants, being this lipolysis notably slower for the biggest surfactant of all of them, PF127. If we check the curves for M52, PF68 and PF127, we may think on a relation between the length of the PEO chain (i.e., the length of the steric barrier around the droplet) and the lipolysis observed: M52, having a PEO chain of 40 subunits, presents the fastest lipolysis, while PF127, having a 100 PEO chain, presents the slowest lipolysis. The lipolysis rate for an emulsion stabilized with PF68, having a PEO chain of 75 subunits, is intermediate between the other two. However, the lipolysis observed for emulsions stabilized with M59 suggests a more complex explanation. This lipolysis is slower than that of PF68 and PF127, in spite of the fact that M59 has a PEO chain of 100 subunits, i.e., longer than that of PF68 and equal to PF127. This leads us to think that the mechanism by which steric surfactants delay

the lipolysis rate under duodenal conditions is not only influenced by the length of the steric barrier around the droplet, but also by the architecture of the surfactant at the interface, i.e., how the surfactant occupies that interface. The reported area per molecule at a water/air interface for M52 is between 0.4 and 1.2 nm^2/molecule (Lee et al., 2001; Shen et al., 2008). Unfortunately, to our knowledge, this value has not been reported for M59. However, we may think on a similar value to that of M52, due to the fact that the hydrophobic part that links to the droplet is exactly the same for the two surfactants (see Table 1). Regarding the Pluronics, the area per molecule reported for PF68 lies between 3-3.4 nm^2/molecule (Chang et al. 2005; Noskov et al. 2006), while this value increases to 6.5-7.21 nm^2/molecule for PF127 due to its longer hydrophobic PPO block (Phipps et al., 1993; Blomqvist et al., 2005). Therefore, PF127 occupies double area at the interface than PF68, and approximately five times that area occupied by M52 and M59, which is consistent with the structure and size of the hydrophobic part of the surfactants (see Table 1). Lipolysis is an interfacial process, where bile salts have to displace adsorbed molecules from the lipid-water interface before colipase and lipase are adsorbed Wickham et al., 2002). As bile salts tend to lie flat on that interface (Maldonado-Valderrama et al., 2008), it should be more difficult for them to remove molecules that adsorb strongly to that interface and that occupy a high amount of its area. This combination between steric hindrance and high occupation of the interface could explain the strong inhibition of the duodenal lipolysis by PF127 observed in our experiments. The same inhibition has been previously observed in the in vivo experiments performed by Johnston and Goldberg following an oral administration of PF127 solution to mice (Johnston and Goldberg, 2006).

3.3.2. Mixtures of PF68-PF127

The results of the experiments performed with mixtures of PF68 and PF127 are depicted in Figure 2. It can be noted that the behavior observed for all the mixtures is almost undistinguishable from that of PF127 alone, even for that mixture with less PF127 (3:1 mixture). This remarks the great influence of PF127 on the interfacial processes related to duodenal lipolysis, as it still dominates the interfacial behavior when its concentration is just a quarter of the total surfactant concentration.

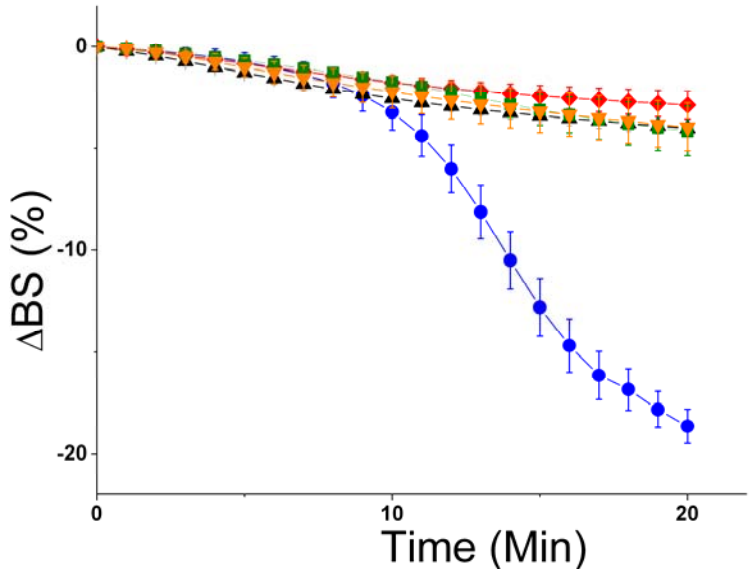

Fig. 2. Changes in backscattering measured during a lipolysis experiment under duodenal conditions for five submicron emulsions stabilized with different mixtures of Pluronics: -■-, only Pluronic F127; -●-, only Pluronic F68; -▲-, PF68-PF127 3:1; -♦-, PF68-PF127 1:1; -▼-, PF68-PF127 1:3. n=3.

3.3. In vitro intravenous lipolysis

3.3.1. Pure PF68, PF127, M52 and M59

In vitro experiments about IV lipolysis without using phospholipids as surfactant are very scarce in the literature (Arimoto et al., 1998; Kurihara et al., 1996). In order to check our experimental conditions (lipase concentration and activity, amount of plasma added, etc) and to compare our results with other authors, we have prepared emulsions stabilized only with phospholipids, obtaining similar lipolysis rates to that observed by other authors under similar conditions (Ton et al., 2005; Arimoto et al., 1998), i.e., the lipolysis was complete within the first 30-60 min. For the emulsions stabilized with steric surfactants, a slower lipolysis is observed, as depicted in Figure 3.

It can be observed that the surfactant employed to prepare the emulsions influences critically the lipolysis rate under IV conditions: lipolysis is almost complete

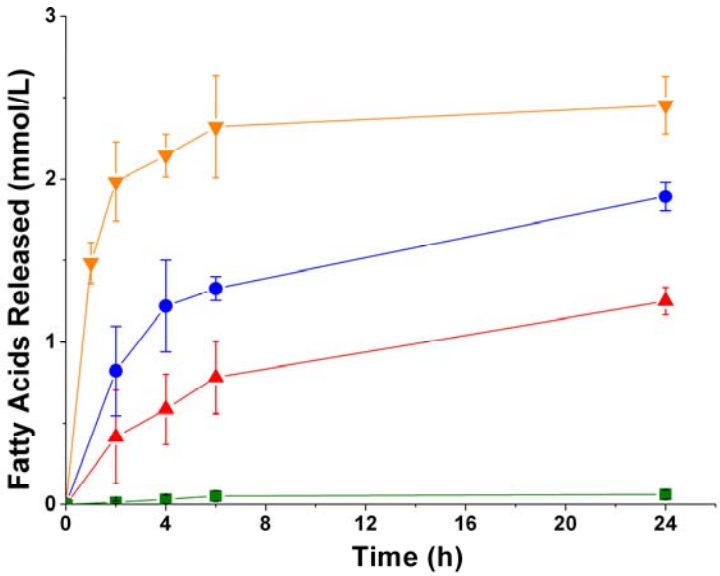

Fig. 3. Free fatty acids released during a lipolysis experiment under intravenous conditions for four submicron emulsions stabilized with different steric surfactants: -■-, Pluronic F127; -●-, Pluronic F68; -▼-, Myrj 52; -▲-, Myrj 59. n=3.

within the first 4-6 hours for the emulsions stabilized with M52, the smallest surfactant, while this lipolysis is almost completely blocked when PF127 is used as surfactant. For the other two surfactants, an intermediate behavior is observed, and no plateau indicating the end of lipolysis is observed within 24 hours. It is also worth to mention that under IV conditions the inhibition by steric hindrance seems to prevail over that caused by occupation of the interface, since M59 in this case reduces more efficiently the lipolysis rate than PF68. However, the coverage of the interface by the surfactant still plays an important role, since M59 does not block completely the lipolysis, as PF127 does, although both surfactants have the same PEO chain and therefore should present a similar steric barrier. These results show some similarities with the trends observed for the different surfactants under duodenal conditions. This is not surprising, as in both cases structurally similar lipases are being used, as well as indispensable co-factors (colipase under duodenal conditions, and apolipoprotein-CII under IV conditions). However, the intravenous lipolysis is considerably slower, and the influence of each surfactant is clearly more pronounced under IV conditions. This could be explained by the differences in concentrations and compositions between duodenal fluids and IV fluids: the

concentrations of lipase and co-factor are notably higher under duodenal conditions, and the presence of a high concentration of bile salts will undoubtedly lead to a faster lipolysis, taking into account their ability to displace other surfactants from surfaces and to bind co-lipase to that interface

The mechanism for this inhibition seems to be then the steric hindrance that these polymeric surfactants produce both around the droplet and at the interface. The access to the triglycerides of the interface is difficult to a greater degree for apolipoprotein-CII and lipoprotein lipase, and therefore the lipolysis is slowed-down or even completely blocked when the surfactant used has a proper size. This mechanism would explain the very low adsorption of apoliproteins to emulsions partially covered by PF127 (Harnisch and Müller, 2000) in the same way that Pluronics prevent the adsorption of major plasma proteins (Tamilvanan et al., 2005; Jackson et al., 2000). These results and the mechanism suggested are in good agreement with the in vivo works of Johnston and Palmer, where the in vivo LpL activity was reduced more than 90% as long as 24 hours after a single injection of a PF127 solution (Johnston and Palmer, 1993).

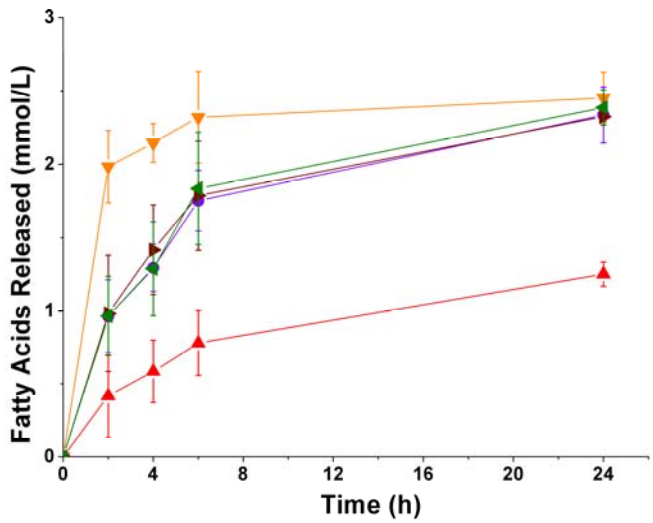

Fig. 4. Free fatty acids released during a lipolysis experiment under intravenous conditions for five submicron emulsions stabilized with different mixtures of Myrj surfactants: -▼-, only M52; -▲-, only M59; -►-, M52-M59 3:1; -●-, M52-M59 1:1; -◄-, M52-M59 1:3. n=3.

3.3.2. Mixtures of M52 and M59

The lipolysis rates observed for emulsions stabilized with different mixtures of M52 and M59 are shown in Figure 4. For the three different mixtures used, 3:1, 1:1 and 1:3, the behavior observed was quite similar, and different from that of pure M52 or pure M59. In other words, by combining two surfactants we are able to obtain a new lipolysis pattern, intermediate between that of the original surfactants: within the first 2 hours is slower than with M52 alone, but it leads also to completeness within 24 hours.

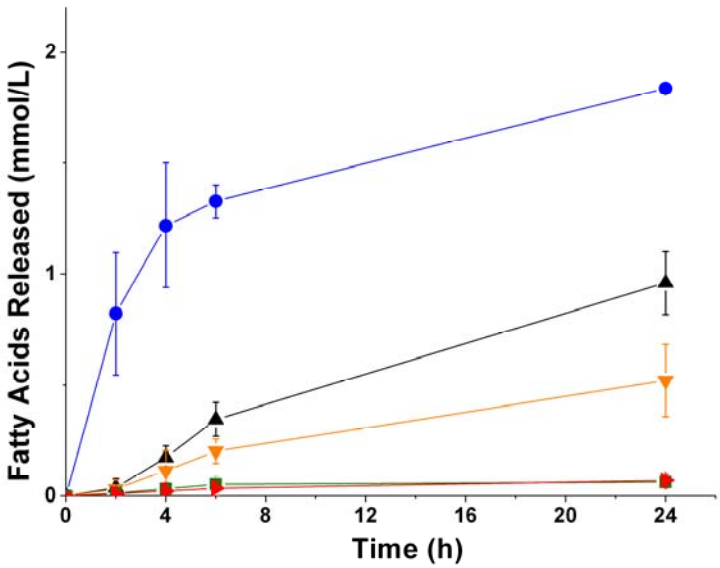

Fig. 5. Free fatty acids released during a lipolysis experiment under intravenous conditions for five submicron emulsions stabilized with different proportions of Pluronics: -■-, only Pluronic F127; -●-, only Pluronic F68; -▲-, PF68-PF127 3:1; -▼-, PF68-PF127 1:1; -►-, PF68-PF127 1:3. n=3.

3.3.3. Mixtures of PF68 and PF127

The results of the lipolysis experiments performed using mixtures of PF68 and PF127 as surfactant under IV conditions are depicted in Figure 5. Depending on the proportion between the two surfactants, different lipolysis rates are observed. For a 3:1 mixture, the lipolysis is slower than that with PF68 alone. When the content of PF127 is

increased up to a 1:1 mixture, the lipolysis is slowed-down, but still takes place. If a mixture 1:3 is used as surfactant, i.e., the amount of PF127 triplicates that of PF68, the lipolysis observed is almost undistinguishable from that obtained when PF127 was the only surfactant. Again, we are able to obtain different lipolysis rates under IV conditions just by changing the proportions between the two surfactants used to prepare the emulsions. This could be a relatively easy manner to modify the lipolysis of lipid carrier systems, and therefore to achieve a better control of the release of the hydrophobic drugs dissolved in them.

4. Conclusions

In this paper, we have studied how polymeric non-ionic surfactants modify the enzymatic degradation (i.e., lipolysis) of submicron emulsions both under duodenal and intravenous conditions. It has been depicted that the chosen surfactant influences critically the lipolysis rates, being able even to completely block this lipolysis, as occurs with Pluronic F127 under IV conditions. Thus, the election of the surfactant used to prepare such lipid carrier systems is not a trivial issue, since it will modify the hydrolysis of the carrier and therefore the release of the hydrophobic drugs dissolved in it. The mechanism of this inhibition seems to be the steric hindrance produced by these surfactants both around the droplet and at the interface. As a consequence, it is possible to modify the lipolysis pattern by selecting a surfactant with the desired properties (size, disposition at the interface, etc), e.g., we could slow-down the lipolysis by using a surfactant that produces a longer steric barrier or that occupies a higher amount of lipid/water interface.

In addition, we have shown that under intravenous conditions it is possible to alter the lipolysis rate only by changing the proportions between the two surfactants used, obtaining intermediate lipolysis patterns than those of pure surfactants.

These findings give us new insights on the rational design of controlled-release submicron emulsions, for both oral and intravenous administration, and emphasize the influence of the characteristics of the surfactant on this control as an active agent.

Acknowledgements

This research is supported by FEDER funds and "Ministerio de Educación y Ciencia" under Project MAT2010-20370 and by "Junta de Andalucía – Consejería de Educación, Ciencia y Empresa" under Project P07-FQM-03099. M.W.P. thanks the latter project referred for the scholarship received.

Bibliography

Arimoto, I.; Matsumoto, C.; Tanaka, M.; Okuhira, K.; Saito, H.; Handa, T., 1998. Surface composition regulates clearance from plasma and triolein lipolysis of lipid emulsions. Lipids 33, 773-779.

Arimoto, I.; Saito, H.; Kawashima, Y.; Miyajima, K.; Handa, T., 1998 Effects of sphingomyelin and cholesterol on lipoprotein lipase-mediated lipolysis in lipid emulsions. J. Lipid Res. 39, 143-151.

Blomqvist, B.R., Wärnheim, T., Claesson, P.M., 2005. Surface rheology of PEO-PPO-PEO triblock copolymers at the air-water interface: comparison of spread and adsorbed layers. Langmuir 21, 6373-6384.

Buszello, K., Müller, B. W., 2000. Emulsions as drug delivery systems, in: Nielloud, F., Marti-Mestres, G. (Eds.), Pharmaceutical Emulsions and Suspensions, Marcel Dekker Inc., New York, pp. 191-228.

Chang, L.-C, Lin, C.-Y., Kuo, M.-W., Gau, C.-S., 2005. Interactions of Pluronics with phospholipid monolayers at the air-water interface. J. Colloid Interface Sci. 285, 640-652.

Chu, B.-S., Rich, G.T., Ridout, M.J., Faulks, R.M., Wickham, M.S.J.,Wilde, P.J., 2009. Modulating pancreatic lipase activity with galactolipids: effects of emulsion interfacial composition. Langmuir 25, 9352-9360.

Deckelbaum, R. J., Hamilton, J. A., Moser, A., Bengtsson-Olivecrona, G., Butbul, E., Carpentier, Y. A., Gutman, A., Olivecrona, T., 1990. Medium-chain versus long-chain triacylglycerol emulsion hydrolysis by lipoprotein lipase and hepatic lipase: implications for the mechanisms of lipase action. Biochemistry 29, 1136-1142.

Goldberg, I.J., 1996. Lipoprotein lipase and lipolysis: central roles in lipoprotein metabolism and atherogenesis. J. Lipid Res. 37, 693-707.

Harnisch, S., Müller, R.H., 2000. Adsorption kinetics of plasma proteins on oil-in-water emulsions for parenteral nutrition. Eur. J. Pharm. Biopharm. 49, 41-46.

Hur, S. J., Decker, E.A., McClements, D.J., 2009. Influence of initial emulsifier type on microstructural changes occurring in emulsified lipids during in vitro digestion. Food Chem. 114, 253-262.

Jackson, J.K., Springate, C.M.K., Hunter, W.L., Burt, H.M., 2000. Neutrophil activation by plasma opsonized polymeric microspheres: inhibitory effect of Pluronic F127. Biomaterials 21, 1483-1491.

Johnston, T.P., Palmer, W.K., 1993. Mechanism of poloxamer 407-induced hypertriglyceridemia in the rat. Biochem. Pharmacol. 46, 1037-1042.

Johnston, T.P., Goldberg, I.J., 2006. Inhibition of pancreatic lipase by poloxamer 407 may provide an adjunct treatment strategy for weight loss. J. Pharm. Pharmacol. 58, 1099-1105.

Kurihara, A., Shibayama, Y., Mizota, A., Yasuno, A., Ikeda, M., Sasagawa, K., Kobayashi, T., Hisaoka, M., 1996. Lipid emulsions of palmitoylrhizoxin: effects of composition on lipolysis and biodistribution. Biopharm. Drug Dispos. 17, 331-342.

Larsen, A. T., Sassene, P., Müllertz, A., 2011. In vitro lipolysis models as a tool for the characterization of oral lipid and surfactant based drug delivery systems. Int. J. Pharm. 417, 245– 255

Lee, S., Kim, D.H., Needham, D., 2001. Equilibrium and dynamic interfacial tension measurements at microscopic interfaces using a micropipet technique. 1. A new method for determination of interfacial tension. Langmuir 17, 5537-5543.

Lucks, J.-S., Müller, B.W., Klutsch, K., 2000. Parenteral Fat Emulsions: Structure, Stability and Applications, in: Nielloud, F., Marti-Mestres, G. (Eds.), Pharmaceutical Emulsions and Suspensions, Marcel Dekker Inc., New York, pp. 229-259.

Maldonado-Valderrama, J., Woodward, N.C., Gunning, A.P., Ridout, M.J., Husband, F.A., Mackie, A.R., Morris, V. J., Wilde, P. J., 2008. Interfacial characterization of beta-lactoglobulin networks: displacement by bile salts. Langmuir 24, 6759-6767.

Mengual, O., 1999. Characterisation of instability of concentrated dispersions by a new optical analyser: the TURBISCAN MA 1000. Colloids Surf., A 152, 111-123.

Miled, N., Beisson, F., de Caro, J., de Caro, A., Arondel, V., Verger, R., 2001. Interfacial catalysis by lipases. J. Mol. Catal. B: Enzym.11, 165-171.

Noskov, B. A., Lin, S.-Y., Loglio, G., Rubio, R.G., Miller, R., 2006. Dilational viscoelasticity of PEO-PPO-PEO triblock copolymer films at the air-water interface in the range of high surface pressures. Langmuir 22, 2647-2652

Phipps, J.S., Richardson, R.M., Cosgrove, T., Eaglesham, A., 1993. Neutron reflection studies of copolymers at the hexane/water interface. Langmuir 9, 3530-3537.

Porter, C.J.H., Pouton, C.W., Cuine, J.F., Charman, W.N., 2008. Enhancing intestinal drug solubilisation using lipid-based delivery systems. Adv. Drug Delivery Rev. 60, 673-691.

Porter, C.J.H., Trevaskis, N.L., Charman, W.N., 2007. Lipids and lipid-based formulations: optimizing the oral delivery of lipophilic drugs. Nat. Rev. Drug Discovery 6, 231-248.

Reis, P., Holmberg, K., Watzke, H., Leser, M.E., Miller, R., 2008. Lipases at interfaces: a review. Adv. Colloid Interface Sci. 147-148, 237-250.

Rensen, P.C., Van Berkel, T.J., 1996. Apolipoprotein E effectively inhibits lipoprotein lipase-mediated lipolysis of chylomicron-like triglyceride-rich lipid emulsions in vitro and in vivo. J. Biol. Chem. 271, 14791-14799.

Sarkar, A., Goh, K.K.T., Singh, R.P., Singh, H., 2009. Behaviour of an oil-in-water emulsion stabilized by β-lactoglobulin in an in vitro gastric model. Food Hydrocolloids 23, 1563-1569.

Shen, Y., Powell, R.L., Longo, M.L., 2008. Interfacial and stability study of microbubbles coated with a monostearin/monopalmitin-rich food emulsifier and PEG40 stearate. J. Colloid Interface Sci. 321, 186-194.

Tamilvanan, S., 2004. Oil-in-water lipid emulsions: implications for parenteral and ocular delivering systems. Prog. Lipid Res. 43, 489-533.

Tamilvanan, S., 2009. Formulation of multifunctional oil-in-water nanosized emulsions for active and passive targeting of drugs to otherwise inaccessible internal organs of the human body. Int. J. Pharm. 381, 62-76

Tamilvanan, S., Schmidt, S., Müller, R.H., Benita, S., 2005. In vitro adsorption of plasma proteins onto the surface (charges) modified-submicron emulsions for intravenous administration. Eur. J. Pharm. Biopharm. 59, 1-7.

Ton, M.N., Chang, C., Carpentier, Y.A, Deckelbaum, R.J., 2005. In vivo and in vitro properties of an intravenous lipid emulsion containing only medium chain and fish oil triglycerides. Clin. Nutr. 24, 492-501.

Torcello-Gómez, A., Maldonado-Valderrama, J., de Vicente, J., Cabrerizo-Vílchez, M.A., Gálvez-Ruiz, M.J., Martín-Rodríguez, A., 2011. Investigating the effect of surfactants on lipase interfacial behaviour in the presence of bile salts. Food Hydrocolloids 25, 809-816.

Versantvoort, C.H.M., Oomen, A.G., Van de Kamp, E., Rompelberg, C.J.M., Sips, A.J.A.M., 2005. Applicability of an in vitro digestion model in assessing the bioaccessibility of mycotoxins from food. Food Chem. Toxicol. 43, 31-40.

Wickham, M., Wilde, P., Fillery-Travis, A., 2002. A physicochemical investigation of two phosphatidylcholine/bile salt interfaces: implications for lipase activation. Biochim. Biophys. Acta, Mol. Cell Biol. Lipids 1580, 110-122.

Wulff-Pérez, M., Gálvez-Ruíz, M.J., de Vicente, J., Martín-Rodríguez, A., 2010. Delaying lipid digestion through steric surfactant Pluronic F68: A novel in vitro approach. Food Res. Int. 43, 1629-1633.

Wulff-Pérez, M., Torcello-Gomez, A., Gálvez-Ruiz, M.J., Martín-Rodríguez, A., 2009. Stability of emulsions for parenteral feeding: Preparation and characterization of o/w nanoemulsions with natural oils and Pluronic f68 as surfactant. Food Hydrocolloids 23, 1096-1102.

Wulff-Pérez, M., Torcello-Gómez, A., Martín-Rodríguez, A., Gálvez-Ruiz, M.J., de Vicente, J., 2011. Bulk and interfacial viscoelasticity in concentrated emulsions: The role of the surfactant. Food Hydrocolloids 25, 677-686.

Yamamoto, M., Morita, S., Kumon, M., Kawabe, M., Nishitsuji, K., Saito, H., Vertut-Doï, A., Nakano, M., Handa, T., 2003. Effects of plasma apolipoproteins on lipoprotein lipase-mediated lipolysis of small and large lipid emulsions. Biochim. Biophys. Acta, Mol. Cell Biol. Lipids 1632, 31-39.

Zangenberg, N.H., Müllertz, A., Kristensen, H.G., Hovgaard, L., 2001. A dynamic in vitro lipolysis model. II: Evaluation of the model. Eur. J. Pharm. Sci. 14, 237-244.

Chapter 6. Conclusions

- It was possible to prepare nanoemulsions with the required droplet size, monodispersity, and stability, by using natural oils and a single steric surfactant. Traditional phospholipids could be then entirely replaced for surfactants like Pluronic F68 without affecting negatively these nanoemulsion properties.

- The mechanisms of destabilization of these nanoemulsions were studied and identified. The destabilization observed in the presence of an excess of surfactant was explained by a depletion-flocculation mechanism. The observed results were compared with the theoretical prediction given by a relatively simple DLVO-modified model that included measured experimental parameters of the system. A good agreement was found between the observed and predicted stability. This finding provided valuable information about the optimal concentrations of Pluronic F68 to be used, and also represented another evidence of the undesirable effects of an excess of surfactant.

- High pressure homogenization was found superior than ultrasounds to prepare nanoemulsions, in terms of droplet size, monodispersity and scalability. Therefore, protocols based on high pressure homogenization were used in the subsequent works.

- A strongly different rheological behavior was found depending on the surfactant used to stabilize the nanoemulsions, especially at high volume fractions. Phospholipids

provided nanoemulsions with higher elasticity, which was confirmed both by frequency-domain (SAOS) and time-domain (relaxation/creep) tests. These experiments provided a better understanding on the differences between the interfacial films formed by ionic and steric surfactants, and should help to design nanoemulsions with the desired rheological properties. They also laid the foundations for the following rheological studies carried out in Paper III.

- The structure of steric surfactants has an impact as well on the rheological behavior of nanoemulsions. Surfactants with longer hydrophilic chains produce nanoemulsions with higher elastic properties. This influence prevails over that of the length of the hydrophobic central part for triblock surfactants, as shown for Pluronic F68 and Pluronic P105. The cause of this increment of the elastic behavior seems to be then the higher steric repulsion that takes place when a surfactant with longer POE chain is used.

- The architecture of the surfactant also influences greatly the final rheological properties of the nanoemulsions that they stabilize, as seen in the experiments comparing Pluronics (triblock copolymers) and Myrjs (diblock copolymers). The presence of a hydrophobic central part in Pluronics provides the nanoemulsions stabilized by them with higher elastic properties, even when their POE chains are shorter than those of Myrjs. This hydrophobic central part apparently forces the molecule to a conformation that provides the droplet with a more efficient steric barrier.

- A new fast and reproducible in vitro method to obtain information about lipolysis rate of nanoemulsions has been developed. This method is based on the generalized decrease in droplet size that takes place during lipolysis, and could complement the other current methods, especially when dealing with chemically complex systems. Furthermore, the required instruments are not uncommon in laboratories devoted to the study of emulsions.

- Steric surfactants delay effectively duodenal lipolysis, with the exception of proteins, which are easily cleaved by proteases and/or displaced by endogenous bile salts. Steric

surfactants hinder the access of lipases and bile salts to the oil/water interface, therefore making difficult both the access to the interface and their own displacement by bile salts.

- In addition, it was shown that by varying the proportion between steric and ionic emulsifiers is possible to speed up or slow down this lipolysis. This opens the possibility of controlling this lipolysis through the composition of the surfactants, with direct applications in the fields of nutrition or drug delivery.

- This delaying of the duodenal lipolysis by steric surfactants takes place in an analogous way under in vitro intravenous conditions of lipolysis. In both cases, lipolysis can be controlled by changing some specific properties of the surfactant, such as the length of the hydrophilic tail or the disposition at the interface, even leading to a complete blockade of the lipolysis.

- It is possible also to obtain different patterns of lipolysis only by changing the proportions between the two steric surfactants used under simulated intravenous conditions, obtaining intermediate behaviors between those obtained when using pure surfactants.

- The possibility of using the surfactant to control the biodegradation of nanoemulsions is then confirmed, under in vitro duodenal and intravenous lipolysis conditions.

- As a summary, these findings give us new insights on the rational design of controlled-release nanoemulsions for oral and intravenous administration of highly lipophilic drugs, and emphasize the influence of the characteristics of the surfactant on this control as an active agent.

Chapter 7. Aditional material

Collaboration in:

Different stability regimes of oil-in-water emulsions in the presence of bile salts.

A.B. Jódar-Reyes , A. Torcello-Gómez, M. Wulff-Pérez, M.J. Gálvez-Ruiz, A. Martín-Rodríguez

Biocolloid and Fluid Physics Group. Department of Applied Physics. Faculty of Sciences, University of Granada, 18071 Spain.

Published in:

Food Research International

Volume 43, Issue 6, July 2010, Pages 1634–1641

Abstract

In this work, we study the stability of emulsified olive oil-in-water emulsions at different bile salt (BS) concentrations. The effect of the interfacial properties of the emulsion is analyzed by using different emulsifiers (Epikuron 145V and Pluronic F68). Emulsion characteristics (electrophoretic mobility, average droplet size) are measured under the different conditions, and the stability of these systems is characterize by monitoring backscattering, using a Turbiscan. Adsorption of BSs at the emulsion interface would explain the higher stability at low bile salt concentrations as well as the more negative electrophoretic mobility when comparing with the emulsion in the absence of BS. The stability of the emulsion decreases above a critical BS concentration, which is higher when the emulsifier is Pluronic, and is much higher than the critical micelle concentration of the BS. Depletion flocculation induced by BS micelles is the destabilizing mechanism proposed at high BS concentrations.

1. Introduction

The knowledge of the mechanisms of lipid digestion and absorption is of great interest due to the importance of these nutrients in the human diet (Singh, Ye, & Horne, 2009). During the digestion process, most lipids are present as oil-in-water (O/W) emulsions due to the mechanical stresses they experience and the role of different stabilizing agents. Lipid digestion takes place in the stomach and in the small intestine. When the partially digested food moves from the stomach into the small intestine it is mixed with bile and pancreatic secretions in the duodenum, which contain a variety of surface-active substances e.g., bile salts (BSs), enzymes, proteins and phospholipids (Mun, Decker, & McClements, 2007). It is well known that bile salts play an important role in the hydrolysis of lipids by lipases and lipid absorption in the small intestine (Wickham, Garrood, Leney, Wilson, & Filley-Travis, 1998). Different effects of BSs on such processes have been described (Mun et al. 2007): on the one hand, they inhibit the activity of lipases at O/W interfaces as the salts displace lipase molecules in the absence of colipase; On the other hand, high levels of BS promote desorption of any other surface active material from the surface of emulsified lipids and lipase/colipase can adsorb onto the interfacial layer of BS and promote digestion. In addition, the adsorption of negatively charged BS enhances the repulsion between the lipase and the interface, and the penetration of the lipase is reduced (Wickham et al. 1998).

The concentration of BS involved in the processes mentioned above is far above the critical micelle concentration (cmc), then, a huge amount of micelles is expected in the system. Those micelles play an important role in the solubility of hydrolysis products. Several experimental studies on model O/W emulsions in the presence of different surfactants have shown that depletion flocculation of the emulsion can be induced by non-adsorbed surfactant micelles that are excluded from the interstitial space (Aronson,1991; Bibette, 1991; McClements, 1994; Dimitrova & Leal-Calderón 1999; Shields, Ellis, & Saunders, 2001; Dickinson and Ritzoulis, 2000; Radford & Dickinson 2004; Wulff-Pérez, Torcello-Gómez, Gálvez-Ruiz, & Martín-Rodríguez, 2009). For instance, certain dietary fiber is found to promote droplet flocculation through a depletion mechanism (Beysseriat, Decker, & McClements, 2006), which may decrease the access of digestive enzymes to the

lipids, and therefore, decrease lipid digestion. This depletion phenomenon has been found at very high surfactant concentrations in the case of colloidal systems (Jódar-Reyes, Martín-Rodríguez, & Ortega-Vinuesa, 2006).

In this work, we show that depletion flocculation of olive O/W emulsions can be induced by bile salt micelles, when high concentrations of BSs are involved, as is the case under the physiological conditions of the duodenum. For this, we have studied the colloidal stability of the emulsions at different bile salt concentrations. As we need to control the cmc of the bile salt, we have used sodium taurodeoxycholate (NaTDC), one of the main components in human bile salt (Arleth et al., 2003; Friesen et al., 2008) and its cmc has been well determined in the literature under different conditions.

Also, we have studied the way in which the addition of BS affects the electrokinetic behavior and droplet size of the olive O/W emulsions and the way in which the type of emulsifier (anionic and non-ionic) alters such an effect. The ionic emulsifier (Epikuron 145V) is a natural phospholipid-based emulsifier, and the non-ionic emulsifier (Pluronic F68) is a synthetic block copolymer. These, instead of proteins, have been chosen as emulsifiers because they provide greater protection against lipase-induced destabilization in the presence of bile salts (Mun et al., 2007).

Results from the different techniques point to adsorption of the bile salt at the emulsion interface, making it difficult to control the amount of BS micelles in the system. In addition, there are reports on the formation of BS and emulsifier mixed micelles (Arleth et al., 2003). Therefore, it is not appropriate to make a theoretical analysis of the depletion phenomenon (Wulff-Pérez et al., 2009) for this system.

2. Materials and Methods

2.1. Materials

All chemicals used were of analytical grade. The water was purified by a Milli-Q Academic Millipore system. The pH was controlled using buffered solutions (phosphate, pH 7), maintaining the ionic strength constant at a value of 1.13 mM. The olive oil (Sigma)

was purified with activated magnesium silicate (Florisil, Fluka). The ionic emulsifier, which presents negative charge at pH 7, was Epikuron 145V (around 800 g/mol), a deoiled, wax-like phosphatidylcholine (PC) enriched Soybean lecithin (min. 45 % PC) from Cargill. As non-ionic emulsifier we used Pluronic F68 (PEO75PPO30PEO75, 8350 g/mol) from Sigma. The bile salt was Sodium taurodeoxycholate (NaTDC, 521.69 g/mol) from Sigma with 97% purity. It is negatively charged and presents a cmc of 0.05 %wt in water, 25 ºC, 150 mM NaCl , from Tensiometry (Tejera-García, 2008), and from spectrophotometry (Carey & Small, 1969). In pure water, the cmc is 0.08 %wt at 20 ºC and 0.09 %wt at 30 ºC (Carey et al., 1969). With the aim of getting data at bile salt concentrations below and above the cmc, we chose the following BS concentrations: 0, 0.025, 0.1, 1, 3.35 and 5 % wt.

2.2. Preparation of emulsions

We needed O/W emulsions that kept stable before adding the bile salt solution. When Epikuron was used, this anionic emulsifier was previously dissolved in the buffered solution with 150 mM NaCl, at 50 ºC and 700 rpm during 2 hours. The corresponding Epikuron concentration was 2.07 % wt. A pre-emulsion was prepared with 1.648 ml of purified olive oil and the buffered solution of emulsifier up to a final volume of 50 ml, and mixed with a Diax 900 homogenizer during five minutes at 18800 rpm. Then, it was homogenized in an EmulsiFlex-C3 (11 cycles, 15000psi). The final composition of the emulsion was 3 % wt oil, 2 %wt Epikuron. The average droplet diameter (D=250 nm) and the polydispersity index (PDI=0.10) did not significantly change after four hours. The destabilization of the system took place versus the time, but it was reversible (flocculation) by shaking. Negligible differences were found when NaCl was absent in the preparation, and only a slightly higher droplet size was obtained when the Epikuron concentration was half reduced. The preparation strategy we finally chose was the previously described (2 % wt Epikuron) as it guaranteed that the interface was completely covered by emulsifier. In the case of using Pluronic F68, this emulsifier was previously dissolved in the buffered solution without heating, at a concentration of 0.65 % wt. NaCl was not used. The rest of the procedure was similar to that followed for Epikuron and the final composition of the emulsion was 3 % wt oil, 0.63 %wt Pluronic. Again, the average droplet diameter (D=160

nm) and the polydispersity index (0.06) did not significantly change, even after 24 hours, as the system remained stable. The reproducibility of these results for the two types of emulsions was tested.

2.3. Colloidal stability

The colloidal stability of the emulsion was evaluated from the diffuse reflectance, R(θ=135º), as a function of the height , h, of a vertical sample tube by using a Turbiscan MA 2000 (Formulaction, l'Union, France, incident wavelength λ = 850 nm). This device allows the detection of two kinds of destabilization phenomena: particle migration (creaming, sedimentation) which are often reversible by mechanical agitation, and particle size variations (coalescence, aggregation) (Mengual, Meunier, Cayre', Puech, & Snabre, 1999). Both transmitted and backscattered light from the emulsion depend on the size and concentration of droplets. However, such a dependence is different when the system is below or above certain critical value of size and particle concentration.

Backscattering increases with the volume fraction (ϕ) for $\phi c < \phi < \phi s$ where ϕc is the critical volume fraction and ϕs the saturation volume fraction. The critical volume fraction corresponds to the concentration at which photons begin to be transmitted. For $\phi < \phi c$, only the signal in transmission of the Turbiscan should be used. The transmission flux (T) exponentially decreases with the particle volume fraction until it reaches the value T=0. In our experiments, the transmitted signal was zero, then the volume fraction of droplets was above the critical volume fraction and only the reflectance diffuse (backscattering) was analyzed.

The backscattering flux (diffusive reflectance) increases with the particle mean diameter when the particles are smaller than the incident wavelength and it decreases with the mean diameter for particles larger than λ. Therefore, one has to look at the three parts of the graph: bottom, middle, and top. Changes at the ends of the graph are associated to particle migration whereas changes at the center correspond to particle size variation and/or changes in particle concentration.

To better visualize the change in the colloidal stability of the emulsion, we will present the graphs in the reference mode, this is, the residual diffuse reflectance at time t, $R_t - R_{t=0}$, as a function of the height, h, of the vertical sample tube.

The kinetics of phase separation was also analyzed from the residual diffuse reflectance at the center of the sample tube versus the time.

To determine how the colloidal stability of the emulsion changes by increasing the concentration of bile salt added to the system, the samples were prepared by mixing 5 ml of emulsion with 5 ml of a buffered solution with NaTDC and 150 mM NaCl. A blank was also made without adding NaTDC. A volume of 7 ml of each sample was introduced in the Turbiscan tube.

2.4. Emulsion droplet size

The mean hydrodynamic diameter (D) of the droplets, and the polydispersity index (PDI) of the emulsion were obtained at 25 ºC from dynamic light scattering measurements using ALV®-NIBS/HPPS (ALV-Laser Vertriebsgesellschaft GmbH, Langen, Germany). This device has been designed to analyze very concentrated samples. By combining high performance particle sizer technology and a non-invasive backscattering method, multiple scattering is minimized. The samples were prepared by taking 0.5 ml of the samples used in the stability analysis and by diluting them in a buffered solution up to a final volume of 2.5 ml.

2.5. Electrokinetic characterization

The electrophoretic mobility and the solution conductivity were measured by using Nanozeta dynamic light scattering analyzer (Malvern Instruments, UK).

In order to know how the presence of bile salt in the system affected the interfacial properties of the emulsion, the electrophoretic mobility (μ_e) of the samples was measured at the different NaTDC concentrations, since one of the reasons for the destabilization of the system at high bile salt concentrations could be related to a loss of

charge of the emulsion at these extreme conditions. We chose a particle concentration of 0.02 %wt as it gave rise to good quality measurements in the Nanozeta device.

3. Results and Discussion

In the following, results on the colloidal stability of O/W emulsions in the presence of different concentrations of the bile salt NaTDC will be presented and discussed. The explanations for the different behaviors of the systems will be supported by data from droplet size and electrokinetic analysis.

3.1. Colloidal Stability

In this section we present how the colloidal stability of the emulsion changes by increasing the concentration of bile salt added to the system. In addition, the effect of the electrolyte (NaCl) concentration and the type of emulsifier (ionic, non-ionic) on these results are analyzed. We firstly show the results by fixing time and by observing the change in backscattering along the vertical tube (stability curves). In this way, we can identify the

Fig. 1. Oil-in-water emulsion (emulsified with Epikuron) mixed with bile salt NaTDC. NaCl 150 mM. From left to right: [NaTDC]= 0, 0.025, 0.1, 1, 5 % wt. The volume of the sample in the tube is 7 ml.

destabilization phenomena (creaming, sedimentation, aggregation). Secondly, we fix a position along the tube and study the change in the backscattering versus the time. We obtain then information on the kinetics of the phase separation.

3.1.1. Stability curves

3.1.1.1 Epikuron-emulsified emulsions. Starting with the Epikuron-emulsified O/W emulsion, just after mixing the emulsion and the buffered solutions at the different NaTDC concentrations, we could observe to the naked eye that the sample at a final concentration of 5 % wt NaTDC phase-separated (creamed), as it can be seen in Figure 1.

We shook the samples to get the reference curve at time t = 0 s in Turbiscan (R_t=0) for each NaTDC concentration as shown in Figure 2. It can be seen that the curves overlaid at low bile salt concentrations, but clearly differ when a high amount of NaTDC is present in the system (5 %wt). The slight decrease in the middle part of the graph found at 0.1 and 1 %wt could only be due to small differences in the particle concentration when

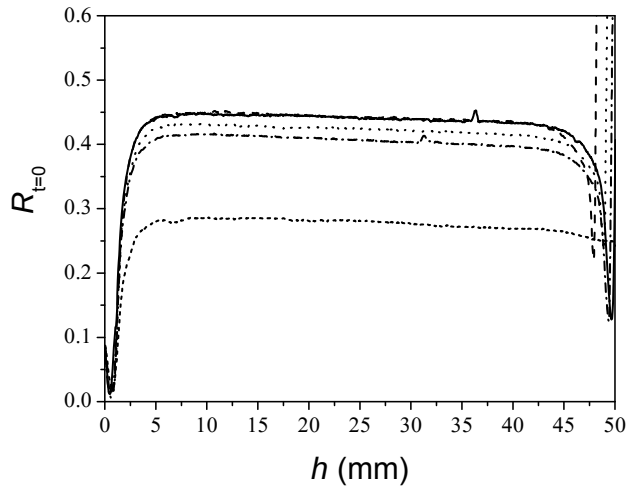

Fig. 2. Reference stability curves (at t = 0 s) for the O/W emulsion (emulsified with Epikuron) at the different NaTDC concentrations (in %wt): 0 (solid), 0.025 (dash), 0.1 (dot), 1 (dash dot), 5 (short dash). NaCl 150 mM

the samples were prepared, as, on the one hand, we will see that the droplet mean size is below the wavelength, and, therefore, backscattering increases with the particle mean diameter. On the other hand, there is no increase in other parts of the graph indicating particle migration (creaming or sedimentation). On the contrary, there is a decrease in the diffuse reflectance at the bottom (left part of the graph) and the top (right part of the graph) that correspond to the lower and upper limits of the sample. An increase at the top is observed, however, when the highest BS concentration is considered (5 %wt), even though the sample was shaken. Then, a quick phase separation takes place at this NaTDC concentration.

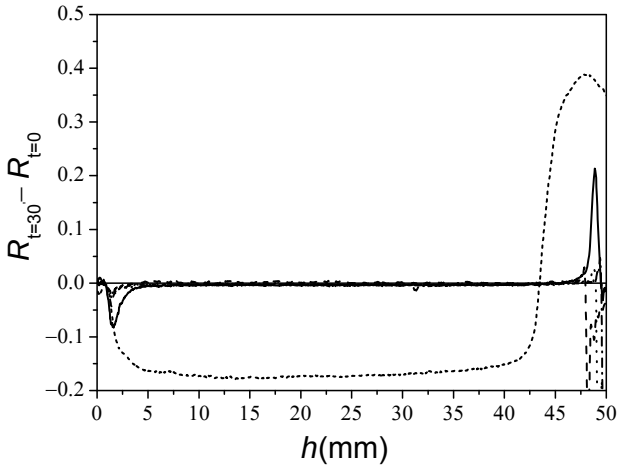

Fig. 3. Stability curves in reference mode for the O/W emulsion (emulsified with Epikuron) 30 minutes after mixing at the different NaTDC concentrations (in %wt): 0 (solid), 0.025 (dash), 0.1 (dot), 1 (dash dot), 5 (short dash). NaCl 150 mM.

Half an hour after mixing, all samples showed a creaming phenomenon. The curves are presented in the reference mode (Figure 3). For NaTDC concentrations up to 1 %wt, there is an increase of the backscattering with respect to the reference curve at the top (increase of the dispersed phase) and a decrease at the bottom (the concentration of particles diminishes), remaining constant at the middle part, which corresponds to a creaming process. It is interesting to note that the curve for the blank (solid) presents

higher values at the top than those ones in the presence of NaTDC up to 1 %wt. Then, we could say that the system is more stable in the presence of these NaTDC concentrations. This result could indicate that bile salt is present at the O/W interface providing an electrosteric effect, which would increase the colloidal stability of the emulsion with respect to the blank. As the emulsifier is thought to totally cover the interface, a displacement of such an emulsifier by the bile salt (as reported for other surfactants (Beysseriat et al., 2006) and phospholipids (Mun et al., 2007; Wickham et al., 1998) or a co-adsorption are the two mechanisms proposed. We will come back to this discussion further in the text, once electrokinetic data have been presented. When the BS concentration is 5 %wt, there is a strong increase of the backscattering with respect to the reference curve at the top of the sample due to a higher particle concentration, and a decrease in the rest of the curve, which corresponds to a lower particle concentration. At this NaTDC concentration, the system presents a lower colloidal stability than in the absence of bile salt. The high amount of BS micelles involved could provoke the flocculation of the emulsion by micelle depletion. This phenomenon should be reversible by micelle dilution (Jódar-Reyes et al., 2006).

Creaming can be coupled with coalescence or flocculation. Both phenomena lead to an increase in the size of the droplets, and therefore, an increase in the backscattering (if droplet size is lower than 850 nm). However, coalescence is irreversible and leads to a fusion of the interfaces, whereas flocculation is a reversible aggregation of the particles. In order to know if our samples had experienced coalescence, we shook them gently after four hours from the mixing and obtained their stability curves. For all bile salt concentrations, except for 5 %wt, the curves overlaid the reference curve, which proves the reversibility of the destabilizing mechanism. At 5 %wt NaTDC, an increase of the backscattering at the top and a decrease in the rest with respect to the reference curve could indicate, in principle, an irreversible destabilization. However, this reasoning could not be true, as the high amount of micelles is kept under shaking, and the destabilization of the system could again quickly take place.

We designed the following set of experiments in order to support the hypothesis of flocculation of the system by depletion of bile salt micelles at 5 %wt NaTDC. It

consisted in checking the reversibility of the system by micelle dilution. We prepared three samples. For sample 1, we shook the emulsion in the presence of 5 %wt NaTDC, took 0.2 ml and mixed them with buffer 150 mM NaCl up to 10 ml. The final bile salt concentration was 0.1 % wt. For sample 2, we shook also the emulsion in the presence of 5 %wt NaTDC, took 0.2 ml and mixed them with a buffered solution 150 mM NaCl containing NaTDC up to 10 ml and a final bile salt concentration of 5 % wt. Sample 3 was prepared by taking 0.2 ml of the blank and mixing them with buffer 150 mM NaCl up to 10 ml, then, the final NaTDC concentration was 0. Reference curves (t=0 s) in the three cases approximately overlaid. Therefore, aggregates formed at 5 %wt broke, even by maintaining the concentration of micelles in the system. As the particle concentration is much lower than in previous experiments, destabilization of the system should take place more slowly. The stability curves four hours after dilution in the reference mode for the three samples are presented in Figure 4. Reversibility by micelle dilution is then demonstrated, as unlike the sample at 5 % wt NaTDC, the sample at a final bile salt concentration of 0.1 %wt remains stable after four hours.

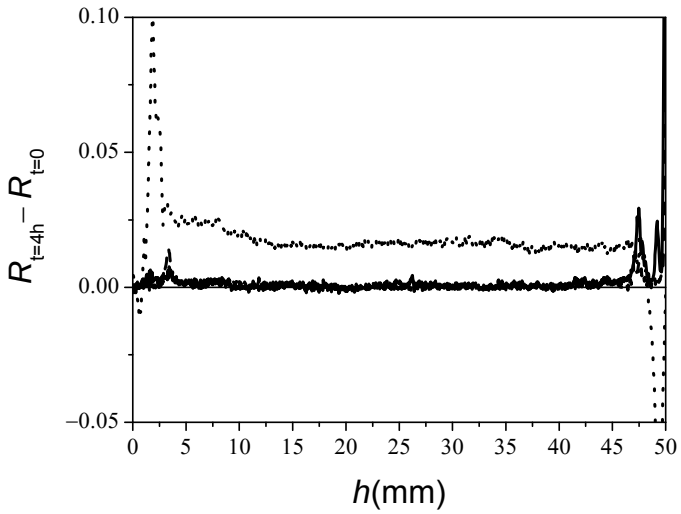

Fig. 4. Stability curves in reference mode for the O/W emulsion (emulsified with Epikuron) 4 hours after dilution at the different NaTDC concentrations (in %wt): 0 (solid), 0.1 (dash), 5 (dot). NaCl 150 mM.

It would be interesting to analyze how the previous results (made at 150 mM NaCl) change at low electrolyte concentration: on the one hand, the emulsion should present a more negative interfacial charge, and, then, a higher colloidal stability; On the other hand, the cmc of the bile salt will increase (Carey et al., 1969). Therefore, it is expected that the system becomes more resistant to the destabilization by micelle depletion.

There will be always certain amount of NaCl coming from the original emulsion. In order to minimize such an amount in our experiments, the samples were prepared by mixing 3.3 ml of emulsion with 6.7 ml of a buffered solution with NaTDC, then, the final NaCl concentration was 49.5 mM. A blank was also made without adding NaTDC. As the emulsion particle concentration was reduced, we repeated the experiments done at 150 mM NaCl by using such a particle concentration. A new bile salt concentration of 3.35 %wt was also tested. At this NaTDC concentration, the destabilization of the emulsion was also observed at 150 mM NaCl. However, at any time, the system was less unstable than at 5 %wt NaTDC. Dilution experiments showed that the sample was reversible by

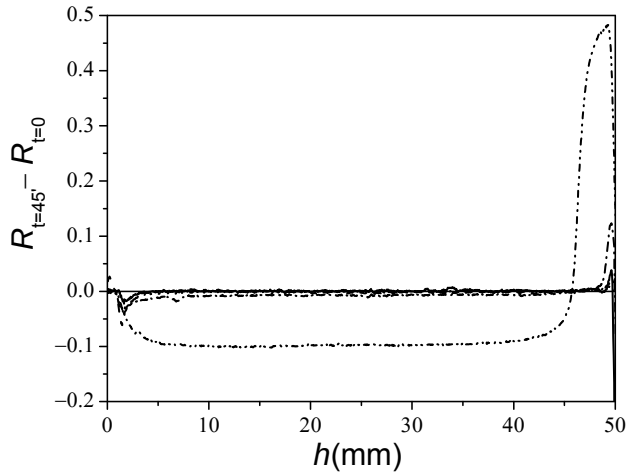

Fig. 5. Stability curves in reference mode for the O/W emulsion (emulsified with Epikuron) 45 minutes after mixing at the different NaTDC concentrations (in %wt): 0 (solid), 0.025 (dash), 0.1 (dot), 1 (dash dot), 3.35 (dash dot dot). NaCl 49.5 mM.

micelle dilution, therefore, flocculation by bile salt micelle depletion was also the destabilizing mechanism proposed at 3.35 %wt NaTDC.

At low electrolyte concentrations, we saw that the reference curves at low bile salt concentrations overlaid, but differed when the NaTDC concentration was equal or higher than 3.35 %wt. In agreement with the results for 150 mM NaCl, at 3.35 %wt NaTDC the emulsion quickly becomes unstable. The stability curves 45 minutes after mixing in the reference mode for the blank and the samples at the different NaTDC concentrations are presented in Figure 5. For NaTDC concentrations up to 0.1 %wt, there is a small increase of the backscattering with respect to the reference curve at the top and a decrease at the bottom, remaining constant at the middle part, which corresponds to a creaming process. The curve for the blank (solid) presents a slightly higher value at the top than those ones in the presence NaTDC. Then, we could say that the system is slightly more stable in the presence of NaTDC concentrations up to 0.1 %wt. At 1 %wt NaTDC there is also a slight decrease in the middle part of the curve, and the top part shows higher values than for the blank. Therefore, the emulsion is less stable in the presence of this bile salt concentration.

When the NaTDC concentration is 3.35 %wt, there is a strong increase of the backscattering with respect to the reference curve at the top of the sample, and a decrease in the rest of the curve. The system presents a lower colloidal stability than in the absence of bile salt, and it is also lower than the corresponding to 1 %wt, which is consistent with the hypothesis of flocculation of the emulsion by micelle depletion as this effect is enhanced when the number of micelles increases. We can see such a dependence in the pair potential between two identical spherical particles resulting from spherical micelle depletion, which can be expressed as in equation 1 (Jódar-Reyes et al., 2006):

$$\frac{V_{dep}(H)}{k_B T} = \begin{cases} +\infty & H < 0 \\ -\rho_\infty \pi \left[\frac{4}{3} r^3 + 2r^2 a - r^2 H - 2raH + \frac{aH^2}{2} + \frac{H^3}{12} \right], & 0 \le H \le 2r \\ 0 & H \ge 2r \end{cases} \quad (1)$$

where H is the shortest distance between the particle surfaces, a is the radius of the particle and r is the radius of the micelle; ρ_∞ is the number of micelles per volume unit in the system, k_B the Boltzmann's constant ,and T the temperature.

This sample was again reversible by micelle dilution.

To analyze the effect of the electrolyte concentration on the stability behavior of the emulsion we compare the stability curves 45 minutes after mixing in the reference mode for the blank, and the sample at 3.35 %wt NaTDC, at low and high electrolyte concentration (Figure 6). Significant differences are not observed. In the absence of bile salt, the emulsion at the lower electrolyte concentration is just slightly more stable. We will discuss on the differences in electrokinetic charge further in the text. At 3.35 %wt, the emulsion is less stable at low NaCl concentration, as discussed above for 1 %wt.

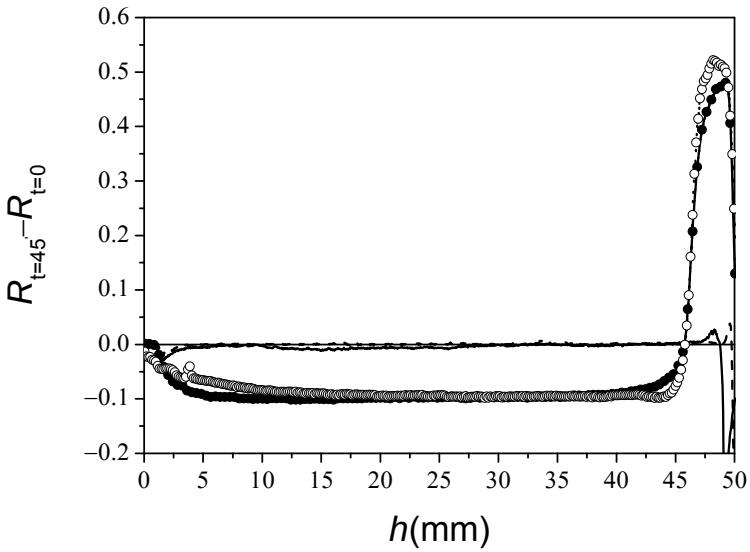

Fig. 6. Effect of the electrolyte concentration on the stability curves in reference mode for the O/W emulsion (emulsified with Epikuron) 45 minutes after mixing at the different NaTDC concentrations (in %wt): 0 (solid line), 3.35(solid circles) at 150 mM NaCl; 0 (dashed line), 3.35 (open circles) at 49.5 mM NaCl.

Therefore, and contrary to what might be expected, the emulsion becomes less resistant to the destabilization by micelle depletion at low electrolyte concentration. This can be explained if we take into account that by decreasing the electrolyte concentration in the system, the "effective size" of charged micelles, which would be equal to the physical size plus the electrostatic screening length or Debye length (this is, $r + K^{-1}$), increases. In equation 2, we show the Debye length for a monovalent salt, where ε_0 is the vacuum permittivity, ε the dielectric constant of the medium, c the salt concentration in mol/L, and e the charge of an electron

$$\kappa^{-1} = \sqrt{\frac{\varepsilon\varepsilon_o k_B T}{2ce^2}} \qquad (2)$$

The insertion of the "effective size" of the micelle in equation 1 would enhance the depletion effect at low electrolyte concentrations (Jódar-Reyes et al., 2006).

3.1.1.2 Pluronic-emulsified emulsions. Up to now, we have seen that the O/W emulsions synthesized with the ionic emulsifier Epikuron 145V show a dependence of the colloidal stability with the concentration of an anionic bile salt (NaTDC). Such stability increases at low NaTDC concentrations, but diminishes at bile salt concentrations well above its cmc due to flocculation by depletion of BS micelles. To see if these results are affected by the type of emulsifier used in the preparation, we repeated the experiments with the non-ionic emulsifier Pluronic F68. The particle concentration was that used for Epikuron-emulsified emulsions at 150 mM NaCl. The stability curves 45 minutes after mixing in the reference mode for the blank and the samples at the different NaTDC concentrations are shown in Figure 7. For NaTDC concentrations up to 1 %wt, there is an increase of the backscattering at the top and a decrease at the bottom, remaining constant at the middle part, as it corresponds to a creaming process. Again, the system is more stable in the presence of NaTDC concentrations up to 1 %wt, which could indicate that bile salt is present at the O/W interface. At a BS concentration of 3.35 %wt the emulsion is just slightly less stable than in the absence of bile salt. There is an increase of the backscattering with respect to the reference curve at the top, and a decrease in the rest of the curve. At 5 %wt NaTDC such a destabilization is more important. Once more, the high amount of BS

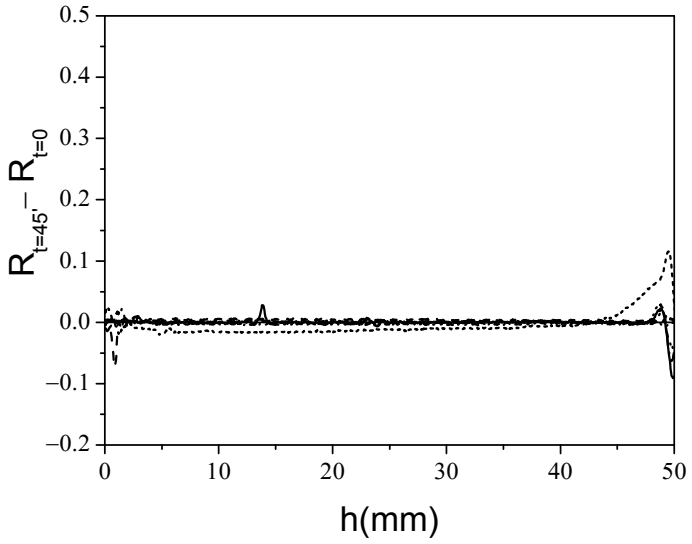

Fig. 7. Stability curves in reference mode for the O/W emulsion (emulsified with Pluronic) 45 minutes after mixing at the different NaTDC concentrations (in %wt): 0 (solid), 0.025 (dash), 0.1 (dot), 1 (dash dot), 3.35 (dash dot dot), 5 (short dash).

micelles involved in the two last situations could provoke the flocculation of the emulsion by micelle depletion. This phenomenon was reversible by micelle dilution.

If we compare with results of Epikuron-emulsified emulsions (Figures 3 and 5), we see that the emulsions made by using Pluronic are more resistant to the destabilization by micelle depletion, as it is evident at 3.35 and 5 %wt NaTDC.

3.1.2. Kinetics of phase separation

Changes at the middle part of the vertical tube can be due to particle migration and to particle size variations. We have already seen in the stability curves (by fixing time) that these changes take place at bile salt concentrations for which the system is less stable than in the absence of NaTDC. By analyzing this change versus time, it is possible to

obtain information on the kinetics of destabilization, i.e. how fast the emulsion loses its colloidal stability, at the different bile salt concentrations.

3.1.2.1 Epikuron-emulsified emulsions Results for the Epikuron-emulsified emulsion at low ionic strength are shown in Figure 8. There is no significant change in backscattering up to 0.1 %wt NaTDC. At 1%wt bile salt, diffuse reflectance decreases at the beginning due to particle migration to the top of the sample, and then remains constant, which could be due to competition between the decrease in particle concentration (R decreases), and the increase of the particle size (R increases). At 3.35 %wt NaTDC, the decrease of R at the beginning is stronger as the destabilization of the system is more important and takes place quickly than at lower bile salt concentrations.

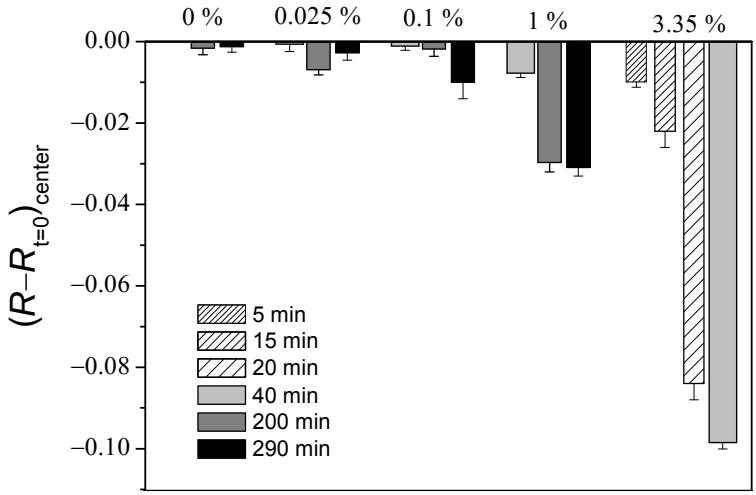

Fig. 8. Residual diffuse reflectance at the center of the sample tube for the O/W emulsion (emulsified with Epikuron) at the different NaTDC concentrations (in %wt), at different times

3.1.2.2 Pluronic-emulsified emulsions. In Figure 9 we show the kinetics of phase separation for the Pluronic-emulsified emulsion. In this case there is no significant change in backscattering up to 1 %wt NaTDC for more than 20 hours. At 3.35 %wt bile salt,

diffuse reflectance decreases slowly due to particle migration to the top of the sample tube. At 5 %wt NaTDC, R decreases at the beginning and increases after more than 2 hours as the increase of the particle size becomes more important. It is clear that the destabilization of the system in the presence of bile salt is more important and takes place more quickly for the Epikuron-emulsified emulsion.

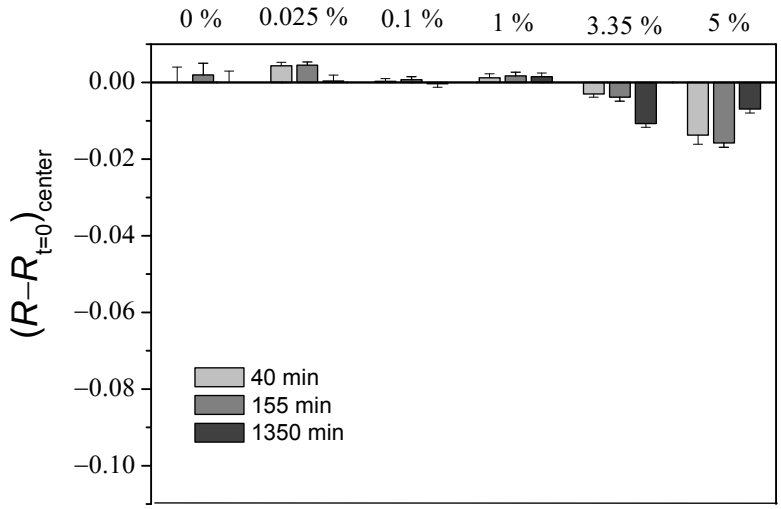

Fig. 9. Residual diffuse reflectance at the center of the sample tube for the O/W emulsion (emulsified with Pluronic) at the different NaTDC concentrations (in %wt), at different times.

3.2. Emulsion droplet size and polydispersity

Dilutions of the samples used in the stability analysis in the buffered solution were made, on one hand, without bile salt, and, on the other hand, by maintaining the corresponding NaTDC concentration. With these two sets of experiments we can observe if there is an effect of the NaTDC concentration on the size distribution of the emulsion droplets, and also if the dilution of the amount of micelles in the system affects to such a distribution.

3.2.1 Epikuron-emulsified emulsions. When Epikuron was used as emulsifier (D=250 nm, PDI=0.10), data obtained around 190 minutes after the samples for Turbiscan

measurements were mixed, showed that only for the samples at or above 3.35 %wt NaTDC and only by maintaining the original bile salt concentration there was a significant change in the mean diameter of the droplet and the polydispersity index (D=570 nm and PDI=0.15). If dilution was done with a buffered solution in the absence of bile salt, the sample at 5 %wt NaTDC in the Turbiscan experiments presented a final BS concentration of 1 %wt, and the corresponding mean diameter and PDI were 220 nm and 0.07, respectively. These results support the hypothesis of a destabilization of the system at 5 % wt NaTDC due to a flocculation mechanism that is reversible by dilution of micelles. The same was checked for 3.35 %wt NaTDC.

Four hours after mixing, we shook the samples and measured again size and polydispersity. For the samples diluted in buffer without bile salt, results were similar to those ones obtained previously. Then, reversibility by shaking was proven. However, by keeping the NaTDC concentration, big aggregates were detected in the system at 5 % wt (D=8000 nm, PDI=0.25). This is consistent with the results obtained with Turbiscan.

There were not significant differences when these experiments were repeated at low electrolyte concentrations.

3.2.2 Pluronic-emulsified emulsions. To analyze the effect, on the previous results, of using another type of emulsifier in the preparation of the emulsion, we repeated the experiments with Pluronic F68 (D=160 nm, PDI=0.06). One hour after mixing, there were no differences in the mean size by taking into account the device error (D=(180□40) nm at 3.35 %wt NaTDC and D=(190□40) nm at 5 %wt NaTDC).

Once more, these results show that Pluronic-emulsified emulsions are more resistant to flocculation by micelle depletion than the Epikuron-emulsified emulsions.

3.3. Electrokinetic behaviour

3.3.1 Epikuron-emulsified emulsions. For the emulsions prepared with Epikuron, important differences were found when dilution was made in buffer (μe = 5.37±0.06) μm cm/Vs, conductivity=0.229 mS/cm) or in a buffered solution 150 mM NaCl (μe = 0.906±0.016)

μm cm/Vs, conductivity=16.7 mS/cm). The droplets are negatively charged due to the presence of Epikuron at the interface.

We also measured the electrophoretic mobility of the three samples used in the experiments described above to check the reversibility by dilution with Turbiscan, at 150 mM and 49.5 mM NaCl. Results are shown in Table 1. It is interesting to note that for the sample with the lowest stability (5 %wt), the system presents a highly negative mobility. Then, the destabilization of the emulsion is not due to the loss of charge of the system. On the other hand, in the presence of bile salt, the emulsion becomes more negative, which indicates changes at the interface by displacement of emulsifier by NaTDC or by co-adsorption. There exist reports on the displacement of Tween80 adsorbed onto O/W emulsions by bile extract by using zeta potential data (Beysseriat et al., 2006). When comparing data at the two electrolyte concentrations, emulsion presents a significantly higher charge (in absolute value) at the lower electrolyte concentration. However, these differences are not evident in the Stability results.

Table 1. Electrokinetic behavior of emulsions made with Epikuron. μe: electrophoretic mobility.

[NaCl] (mM)	[NaTDC] (%wt)	μ_e **(μm cm/Vs)**	**Conductivity** (mS/cm)
49.5	0	−5.86±0.07	0.229
	0.1	−8.55±0.03	0.330
	5	−7.9±0.3	4.5
150	0	−0.89±0.08	17.1
	0.1	−3.83±0.14	16.9
	5	−4.80±0.15	19.4

3.3.2 Pluronic-emulsified emulsions. We have found that O/W emulsions emulsified with Epikuron present a highly negative electrokinetic charge in the presence of the bile salt NaTDC, which is higher (in absolute value) than the corresponding to the original emulsion. The results when using a non-ionic emulsifier in the preparation of the emulsion, particularly Pluronic F68, are shown in Table 2. In the absence of bile salt, the emulsion shows a slightly negative charge. By adding bile salt to the system, the interface becomes more negative. Again, displacement and/or co-adsorption of the emulsifier by the bile salt could explain such results. There is an important increase of the mobility at 1 %wt NaTDC as the displacement is favored at high bile salt concentrations (Beysseriat et al., 2006). At 5 %wt the mobility is similar to that found at lower NaTDC concentrations, which could indicate that saturation of bile salt at the interface is reached. The fact that the emulsions made by using Pluronic are more resistant to destabilization at high NaTDC concentrations than those made with Epikuron cannot be explained by using these electrokinetic results.

Table 2. Electrokinetic behavior of emulsions made with Pluronic. μe: electrophoretic mobility.

[NaTDC] (%wt)	μ_e (μm cm/Vs)	Conductivity (mS/cm)
0	−0.36±0.03	0.105
0.025	−3.03±0.04	0.142
0.1	−2.631±0.015	0.426
1	−6.34±0.24	1.61
3.35	−7.76±0.19	4.86
5	−6.464±0.017	6.3

4. Conclusions

Different stability regimes have been found for olive oil-in-water emulsions as a function of the concentration of bile salt (NaTDC) added to the system. The colloidal stability of these emulsions increases in the presence of bile salt up to a critical BS concentration. Above such a concentration, which is higher than the cmc of the bile salt, the system becomes less stable. Depletion flocculation induced by bile salt micelles is the destabilizing mechanism proposed at high BS concentrations: unstable emulsions re-stabilize by decreasing the micelle concentration in the system.

The emulsion becomes less resistant to the destabilization by micelle depletion at low electrolyte concentrations, as the effective size of charged micelles increases and, as a consequence, there is an enhancement of the depletion effect. For Epikuron-emulsified emulsions, the system is more stable in the presence of NaTDC up to (at least) 20 x cmc at 150 mM NaCl. However, at 49.5 mM NaCl, the system is already less stable at a bile salt concentration of 12.5 x cmc than in the absence of NaTDC.

The critical bile salt concentration at which the stability regime of the emulsion changes from more stable to less stable than in the absence of BS, depends on the type of emulsifier used in the preparation. Such a BS concentration is higher when the non-ionic emulsifier Pluronic F68 is used instead of the ionic emulsifier Epikuron 145V. At 49.5 mM NaCl, the system is more stable in the presence of NaTDC up to 12.5 x cmc, and even at 42 x cmc, the emulsion is just slightly less stable than in the absence of bile salt. The kinetics of phase separation of the emulsion is slower in the first case.

Displacement of the emulsifier by the bile salt and/or co-adsorption at the emulsion interface would explain the increase of the colloidal stability at low bile salt concentrations as well as the electrokinetic behaviour of these emulsions.

As a final conclusion, this work presents novel results on the effects of bile salts on the colloidal stability of O/W emulsions which should be considered for the understanding of the mechanisms involved in lipid digestion.

Acknowledgements

Authors thank the financial support given by the proyects MAT2007-66662-C02-01 (MICINN) and P07-FQM03099 (Junta de Andalucía)

References

Arleth, L., Bauer, R., Gendal, L.H., Egelhaaf, S.U., Schurtenberger, P., & Pedersen J.S. (2003). Growth Behavior of Mixed Wormlike Micelles: a Small-Angle Scattering Study of the Lecithin-Bile Salt System. Langmuir, 19, 4096-4104.

Aronson, M.P. (1991). Flocculation of emulsions by free surfactant in purified systems. Colloids and Surfaces, 58, 195-202.

Beysseriat, M., Decker, E.A., & McClements, D. J. (2006). Preliminary study of the influence of dietary fiber on the properties of oil-in-water emulsions passing through an in vitro human digestion model. Food Hydrocolloids, 20, 800-809.

Bibette, J. (1991). Depletion Interactions and Fractionated Crystallization for Polydisperse Emulsion Purification. Journal of Colloid and Interface Science, 147, 474-478.

Carey, M.C., Small, D.M. (1969). Micellar Properties of Dihydroxy and Trihydroxy Bile Salts: Effects of Counterion and Temperature. Journal of Colloid and Interface Science, 31, 382-396.

Dickinson, E., & Ritzoulis C. (2000). Creaming and Rheology of Oil-in-Water Emulsions Containing Sodium Dodecyl Sulfate and Sodium Caseinate. Journal of Colloid and Interface Science, 224, 148-154.

Dimitrova, T.D., & Leal-Calderón, F. (1999). Forces between Emulsion Droplets Stabilized with Tween 20 and Proteins. Langmuir 15, 8813-8821.

Friesen, D.T., Shanker, R., Crew, M., Smithey, D. T., Curatolo, W.J., & Nightingale, J. A. S. (2008). Hydroxypropyl Methylcellulose Acetate Succinate-Based Spray-Dried Dispersions: An Overview. Mol. Pharmaceutica 5, 1003-1019.

Jódar-Reyes, A.B., Martín-Rodríguez, A. & Ortega-Vinuesa, J.L. (2006). Effect of the ionic surfactant concentration on the stabilization/destabilization of polystyrene colloidal particles. Journal of Colloid and Interface Science, 298, 248-257.

McClements, D.J. (1994). Ultrasonic determination of depletion flocculation in oil-in-water emulsions containing a non-ionic surfactant. Colloids and Surfaces A: Physicochem. Eng. Aspects, 90, 25-35.

Mengual, O., Meunier, G., Cayre´, I., Puech, K., Snabre, P. (1999). TURBISCAN MA 2000: multiple light scattering measurement for concentrated emulsion and suspension instability analysis. Talanta, 50, 445–456.

Mun, S., Decker, E.A., & McClements, D.J. (2007). Influence of emulsifier type on in vitro digestibility of lipid droplets by pancreatic lipase. Food Research International, 40, 770-781.

Radford, S.J., & Dickinson, E. (2004). Depletion flocculation of caseinate-stabilised emulsions: what is the optimum size of the non-adsorbed protein nano-particles. Colloids and Surfaces A: Physicochem. Eng. Aspects, 238, 71-81.

Shields, M., Ellis, R., & Saunders, B.R. (2001). A creaming study of weakly flocculated and depletion flocculated oil-in-water emulsions. Colloids and Surfaces A: Physicochem. Eng. Aspects, 178, 265-276.

Singh, H., Ye, A., & Horne, D. (2009). Structuring food emulsions in the gastrointestinal tract to modify lipid digestion. Progress in Lipid Research, 48, 92-100.

Tejera-García, R. (2008). Estabilidad y actividad interfacial de emulsiones modelo con interés en alimentación funcional. PhD. Thesis, University of Granada. ISBN: 978-84-338-4960-1.

Wickham, M., Garrood, M., Leney, J., Wilson, P. D. G., & Fillery-Travis, A. (1998). Modification of a phospholipid stabilized emulsion interface by bile salt: Effect on pancreatic lipase activity.Journal of Lipid Research, 39, 623-632.

Wulff-Pérez, M., Torcello-Gómez, A., Gálvez-Ruiz, M.J., & Martín-Rodríguez, A. (2009). Stability of emulsions for parenteral feeding: Preparation and characterization of o/w nanoemulsions with natural oils and Pluronic f68 as surfactant. Food Hydrocolloids, 23, 1096-1102.

Chapter 8. References.

Barnes, H. A. (1994). Rheology of emulsions — a review. *Colloids and Surfaces, A: Physicochemical and Engineering Aspects, 91* (0), 89-95.

Benita, S. (1998). Introduction and overview. In S. Benita (Ed.), *Submicron Emulsion in Drug Targeting & Delivery*: Harwood Academic.

Briceño, M. I. (2006). Rheology of Suspensions and Emulsions. In F. Nielloud & G. Marti-Mestres (Eds.), (2nd ed.). London: Taylor and Francis.

Bunjes, H. (2010). Lipid nanoparticles for the delivery of poorly water-soluble drugs. *Journal of Pharmacy and Pharmacology, 62* (11), 1637-1645.

Buszello, K., & Muller, B. W. (2000). Emulsions as Drug Delivery Systems. In F. Nielloud & G. Marti-Mestres (Eds.), *Pharmaceutical Emulsions and Suspensions*. New York: Marcel Dekker Inc.

Canselier, J. P., Delmas, H., Wilhelm, A. M., & Abismaïl, B. (2002). Ultrasound Emulsification—An Overview. *Journal of Dispersion Science and Technology, 23* (1-3), 333-349.

Carreau, P. J., Lavoie, P. A., & Yziquel, F. (1999). Rheological properties of concentrated suspensions. In D. D. K. D.A. Siginer & R. P. Chhabra (Eds.), *Rheology Series* (Vol. Volume 8, pp. 1299-1345): Elsevier.

Chauvierre, C., Labarre, D., Couvreur, P., & Vauthier, C. (2004). A new approach for the characterization of insoluble amphiphilic copolymers based on their emulsifying properties. *Colloid and Polymer Science, 282* (10), 1097-1104.
de Gennes, P. G. (1987). Polymers at an interface; a simplified view. *Advances in Colloid and Interface Science, 27* (3–4), 189-209.

De Vleeschauwer, D., & Van der Meeren, P. (1999). Colloid chemical stability and interfacial properties of mixed phospholipid–non-ionic surfactant stabilised oil-in-water emulsions. *Colloids and Surfaces A: Physicochemical and Engineering Aspects, 152* (1–2), 59-66.

Deckelbaum, R. J., Hamilton, J. A., Moser, A., Bengtsson-Olivecrona, G., Butbul, E., Carpentier, Y. A., Gutman, A., & Olivecrona, T. (1990). Medium-chain versus long-chain triacylglycerol emulsion hydrolysis by lipoprotein lipase and hepatic lipase: implications for the mechanisms of lipase action. *Biochemistry, 29* (5), 1136-1142.

Di Maio, S., & Carrier, R. L. (2011). Gastrointestinal contents in fasted state and post-lipid ingestion: In vivo measurements and in vitro models for studying oral drug delivery. *Journal of Controlled Release, 151* (2), 110-122.

Doenicke, A. W., Roizen, M. F., Rau, J., Kellermann, W., & Babl, J. (1996). Reducing pain during propofol injection: the role of the solvent. *Anesthesia and Analgesia, 82* (3), 472-474.

Dolz, M., Hernández, M. J., & Delegido, J. (2008). Creep and recovery experimental investigation of low oil content food emulsions. *Food Hydrocolloids, 22* (3), 421-427.

Dressman, J. B., Amidon, G. L., Reppas, C., & Shah, V. P. (1998). Dissolution Testing as a Prognostic Tool for Oral Drug Absorption: Immediate Release Dosage Forms. *Pharmaceutical Research, 15* (1), 11-22.

Driscoll, D. F., Ling, P.-R., & Bistrian, B. R. (2009). Pharmacopeial compliance of fish oil-containing parenteral lipid emulsion mixtures: Globule size distribution (GSD) and fatty acid analyses. *International Journal of Pharmaceutics, 379* (1), 125-130.

Du, Y.-Z., Wang, L., Dong, Y., Yuan, H., & Hu, F.-Q. (2010). Characteristics of paclitaxel-loaded chitosan oligosaccharide nanoparticles and their preparation by interfacial polyaddition in O/W miniemulsion system. *Carbohydrate Polymers, 79* (4), 1034-1039.

Einarson, M. B., & Berg, J. C. (1993). Electrosteric Stabilization of Colloidal Latex Dispersions. *Journal of Colloid and Interface Science, 155* (1), 165-172.
Fast, J. P., & Mecozzi, S. (2009). Nanoemulsions for Intravenous Drug Delivery. In M. M. de Villiers, P. Aramwit & G. S. Kwon (Eds.), *Nanotechnology in Drug Delivery*. New York: American Association of Pharmaceutical Scientists.

FDA. (2012). Inactive Ingredients in FDA Approved Drugs. In.

Ferry, J. D. (1980). *Viscoelastic properties of polymers*. New York: John Wiley & Sons.

Finsy, R. (1994). Particle sizing by quasi-elastic light scattering. *Advances in Colloid and Interface Science, 52* (0), 79-143.

Fischer, P., & Windhab, E. J. (2011). Rheology of food materials. *Current Opinion in Colloid and Interface Science, 16* (1), 36-40.

Floyd, A. G. (1999). Top ten considerations in the development of parenteral emulsions. *Pharmaceutical Science & Technology Today, 2* (4), 134-143.

Forgiarini, A., Esquena, J., González, C., & Solans, C. (2001). Formation of Nano-emulsions by Low-Energy Emulsification Methods at Constant Temperature. *Langmuir, 17* (7), 2076-2083.

Freitas, C., & Müller, R. H. (1998). Effect of light and temperature on zeta potential and physical stability in solid lipid nanoparticle (SLN™) dispersions. *International Journal of Pharmaceutics, 168* (2), 221-229.

Genovese, D. B., Lozano, J. E., & Rao, M. A. (2007). The Rheology of Colloidal and Noncolloidal Food Dispersions. *Journal of Food Science, 72* (2), R11-R20.

Georgieva, D., Schmitt, V. r., Leal-Calderon, F., & Langevin, D. (2009). On the Possible Role of Surface Elasticity in Emulsion Stability. *Langmuir, 25* (10), 5565-5573.

Goodwin, J. W. (2009). *Colloids and Interfaces with Surfactants and Polymers* (2nd ed.): John Wiley and Sons.
Goodwin, J. W., Hughes, R. W., Partridge, S. J., & Zukoski, C. F. (1986). The elasticity of weakly flocculated suspensions. *The Journal of Chemical Physics, 85* (1), 559-566.

Gutiérrez, J. M., González, C., Maestro, A., Solè, I., Pey, C. M., & Nolla, J. (2008). Nano-emulsions: New applications and optimization of their preparation. *Current Opinion in Colloid and Interface Science, 13* (4), 245-251.

Harris, J. M., Martin, N. E., & Modi, M. (2001). Pegylation: a novel process for modifying pharmacokinetics. *Clinical Pharmacokinetics, 40* (7), 539-551.

Helbig, A., Silletti, E., Timmerman, E., Hamer, R. J., & Gruppen, H. (2012). In vitro study of intestinal lipolysis using pH-stat and gas chromatography. *Food Hydrocolloids, 28* (1), 10-19.

Hidalgo-Álvarez, R., Martín, A., Fernández, A., Bastos, D., Martínez, F., & de las Nieves, F. J. (1996). Electrokinetic properties, colloidal stability and aggregation kinetics of polymer colloids. *Advances in Colloid and Interface Science, 67* (0), 1-118.

Hippalgaonkar, K., Majumdar, S., & Kansara, V. (2010). Injectable lipid emulsions-advancements, opportunities and challenges. *AAPS PharmSciTech, 11* (4), 1526-1540.

Hur, S. J., Decker, E. A., & McClements, D. J. (2009). Influence of initial emulsifier type on microstructural changes occurring in emulsified lipids during in vitro digestion. *Food Chemistry, 114* (1), 253-262.

Illum, L., West, P., Washington, C., & Davis, S. S. (1989). The effect of stabilising agents on the organ distribution of lipid emulsions. *International Journal of Pharmaceutics, 54* (1), 41-49.

Immordino, M. L., Dosio, F., & Cattel, L. (2006). Stealth liposomes: review of the basic science, rationale, and clinical applications, existing and potential. *International Journal of Nanomedicine, 1* (3), 297-315.

Izquierdo, P., Esquena, J., Tadros, T. F., Dederen, C., Garcia, M. J., Azemar, N., & Solans, C. (2001). Formation and Stability of Nano-Emulsions Prepared Using the Phase Inversion Temperature Method. *Langmuir, 18* (1), 26-30.

Izquierdo, P., Esquena, J., Tadros, T. F., Dederen, J. C., Feng, J., Garcia-Celma, M. J., Azemar, N., & Solans, C. (2004). Phase Behavior and Nano-emulsion Formation by the Phase Inversion Temperature Method. *Langmuir, 20* (16), 6594-6598.

Jafari, S. M., Assadpoor, E., He, Y., & Bhandari, B. (2008). Re-coalescence of emulsion droplets during high-energy emulsification. *Food Hydrocolloids, 22* (7), 1191-1202.

Jódar-Reyes, A. B., Martín-Rodríguez, A., & Ortega-Vinuesa, J. L. (2006). Effect of the ionic surfactant concentration on the stabilization/destabilization of polystyrene colloidal particles. *Journal of Colloid and Interface Science, 298* (1), 248-257.

Kabanov, A. V., Batrakova, E. V., & Alakhov, V. Y. (2002). Pluronic® block copolymers as novel polymer therapeutics for drug and gene delivery. *Journal of Controlled Release, 82* (2–3), 189-212.

Kaparissides, C., Alexandridou, S., Kotti, K., & Chaitidou, S. (2006). Recent advances in novel drug delivery systems. In *Journal of nanotechnology online*.

Kaukonen, A. M., Boyd, B., Charman, W., & Porter, C. (2004). Drug Solubilization Behavior During in Vitro Digestion of Suspension Formulations of Poorly Water-Soluble Drugs in Triglyceride Lipids. *Pharmaceutical Research, 21* (2), 254-260.

Koppel, D. E. (1972). Analysis of Macromolecular Polydispersity in Intensity Correlation Spectroscopy: The Method of Cumulants. *The Journal of Chemical Physics, 57* (11), 4814-4820.

Kozlowska, D., Foran, P., MacMahon, P., Shelly, M. J., Eustace, S., & O'Kennedy, R. (2009). Molecular and magnetic resonance imaging: The value of immunoliposomes. *Advanced Drug Delivery Reviews, 61* (15), 1402-1411.

Kurihara, A., Shibayama, Y., Mizota, A., Yasuno, A., Ikeda, M., Sasagawa, K., Kobayashi, T., & Hisaoka, M. (1996). Lipid emulsions of palmitoylrhizoxin: effects of composition on lipolysis and biodistribution. *Biopharmaceutics & Drug Disposition, 17* (4), 331-342.

Larsen, A. T., Sassene, P., & Müllertz, A. (2011). In vitro lipolysis models as a tool for the characterization of oral lipid and surfactant based drug delivery systems. *International Journal of Pharmaceutics, 417* (1–2), 245-255.

Li, Y., Hu, M., & McClements, D. J. (2011). Factors affecting lipase digestibility of emulsified lipids using an in vitro digestion model: Proposal for a standardised pH-stat method. *Food Chemistry, 126* (2), 498-505.

Liu, F., & Liu, D. (1995). Long-circulating emulsions (oil-in-water) as carriers for lipophilic drugs. *Pharmaceutical Research, 12* (7), 1060-1064.

Lowe, M. E. (2002). The triglyceride lipases of the pancreas. *Journal of Lipid Research, 43* (12), 2007-2016.

Lucks, J.-S., Müller, B. W., & Klütsch, K. (2000). Parenteral Fat Emulsions: Structure, Stability and Applications. In F. Nielloud & G. Marti-Mestres (Eds.), *Pharmaceutical Emulsions and Suspensions*. New York: Marcel Dekker Inc.

Ma, C. (1987). The effect of triton X-100 on the stability of polystyrene latices. *Colloids and Surfaces, 28* (0), 1-7.

Mäder, K. (2006). Solid Lipid Nanoparticles as Drug Carriers. In V. P. Torchilin (Ed.), *Nanoparticulates as Drug Carriers*. London, UK: Imperial College Press.

Maksimochkin, G., Pasechnik, S., Slavinec, M., Svetec, M., & Kralj, S. (2007). Colloidal Emulsions. In E. E. Gdoutos (Ed.), *Experimental Analysis of Nano and Engineering Materials and Structures* (pp. 649-650): Springer Netherlands.

Maldonado-Valderrama, J., Gunning, A. P., Wilde, P. J., & Morris, V. J. (2010). In vitro gastric digestion of interfacial protein structures: visualisation by AFM. *Soft Matter, 6* (19), 4908-4915.

Marti-Mestres, G., & Nielloud, F. (2002). Emulsions in Health Care Applications—An Overview. *Journal of Dispersion Science and Technology, 23* (1-3), 419-439.

Mason, T. G. (1999). New fundamental concepts in emulsion rheology. *Current Opinion in Colloid and Interface Science, 4* (3), 231-238.

Mason, T. G., Wilking, J. N., Meleson, K., Chang, C. B., & Graves, S. M. (2007). Nanoemulsions: formation, structure, and physical properties. *Journal of Physics: Condensed Matter, 19* (7), 079001.

Meleson, K., Graves, S., & Mason, T. G. (2004). Formation of concentrated nanoemulsions by extreme shear. *Soft Materials, 2* (2-3), 109-123.

Mengual, O., Meunier, G., Cayre, I., Puech, K., & Snabre, P. (1999). Characterisation of instability of concentrated dispersions by a new optical analyser: the TURBISCAN MA 1000. *Colloids and Surfaces A: Physicochemical and Engineering Aspects, 152* (1), 111-123.

Mengual, O., Meunier, G., Cayré, I., Puech, K., & Snabre, P. (1999). TURBISCAN MA 2000: multiple light scattering measurement for concentrated emulsion and suspension instability analysis. *Talanta, 50* (2), 445-456.

Miled, N., Beisson, F., de Caro, J., de Caro, A., Arondel, V., & Verger, R. (2001). Interfacial catalysis by lipases. *Journal of Molecular Catalysis B: Enzymatic, 11* (4–6), 165-171.

Moghimi, S. M., & Hamad, I. (2009). Factors Controlling Pharmacokinetics of Intravenously Injected Nanoparticulate Systems. In M. M. de Villiers, P. Aramwit & G. S. Kwon (Eds.), *Nanotechnology in Drug Delivery*. New York: American Association of Pharmaceutical Scientists.

Molina-Bolívar, J. A., Aguiar, J., & Ruiz, C. C. (2001). Light scattering and fluorescence probe studies on micellar properties of Triton X-100 in KCl solutions. *Molecular Physics, 99* (20), 1729-1741.

Mollet, H., Grubenmann, A., & Payne, H. (2008). *Formulation Technology: Emulsions, Suspensions, Solid Forms*. Weinheim: John Wiley & Sons.

Nakajima, H. (1997). Microemulsions in cosmetics. In C. Solans & H. Kunieda (Eds.), *Industrial Applications of Microemulsions*. New York: Marcel Dekker.

Narang, A. S., Delmarre, D., & Gao, D. (2007). Stable drug encapsulation in micelles and microemulsions. *International Journal of Pharmaceutics, 345* (1–2), 9-25.

Ortega-Vinuesa, J. L., Martín-Rodríguez, A., & Hidalgo-Álvarez, R. (1996). Colloidal Stability of Polymer Colloids with Different Interfacial Properties: Mechanisms. *Journal of Colloid and Interface Science, 184* (1), 259-267.

Pal, R. (1999). Yield stress and viscoelastic properties of high internal phase ratio emulsions. *Colloid and Polymer Science, 277* (6), 583-588.

Pal, R. (2011). Rheology of simple and multiple emulsions. *Current Opinion in Colloid and Interface Science, 16* (1), 41-60.

Partal, P., Guerrero, A., Berjano, M., & Gallegos, C. s. (1999). Transient flow of o/w sucrose palmitate emulsions. *Journal of Food Engineering, 41* (1), 33-41.

Pasquali, R. C., Chiappetta, D. A., & Bregni, C. (2005). Los copolímeros en bloques anfifílicos y sus aplicaciones farmacéuticas. *Acta Farmacéutica Bonaerense, 24* (4), 610-618.

Porter, C. J. H., Pouton, C. W., Cuine, J. F., & Charman, W. N. (2008). Enhancing intestinal drug solubilisation using lipid-based delivery systems. *Advanced Drug Delivery Reviews, 60* (6), 673-691.

Porter, C. J. H., Trevaskis, N. L., & Charman, W. N. (2007). Lipids and lipid-based formulations: optimizing the oral delivery of lipophilic drugs. *Nature Reviews. Drug Discovery, 6* (3), 231-248.

Quemada, D., & Berli, C. (2002). Energy of interaction in colloids and its implications in rheological modeling. *Advances in Colloid and Interface Science, 98* (1), 51-85.

Rensen, P. C., & van Berkel, T. J. (1996). Apolipoprotein E effectively inhibits lipoprotein lipase-mediated lipolysis of chylomicron-like triglyceride-rich lipid emulsions in vitro and in vivo. *Journal of Biological Chemistry, 271* (25), 14791-14799.

Rosen, M. J. (2004). *Surfactants and Interfacial Phenomena*. Hoboken: John Wiley & Sons.

Rossi, J., & Leroux, J.-C. (2007). Principles in the development of intravenous lipid emulsions. In K. M. Wasan (Ed.), *Role of lipid excipients in modifying oral and parenteral drug delivery*. Hoboken: John Wiley & Sons.

Rowe, R. C., Sheskey, P. J., & Weller, P. J. (2006). *Handbook of Pharmaceutical Excipients* (5th ed.). London: Pharmaceutical Press.

Rübe, A., Klein, S., & Mäder, K. (2006). Monitoring of In Vitro Fat Digestion by Electron Paramagnetic Resonance Spectroscopy. *Pharmaceutical Research, 23* (9), 2024-2029.

Saiki, Y., Prestidge, C. A., & Horn, R. G. (2007). Effects of droplet deformability on emulsion rheology. *Colloids and Surfaces, A: Physicochemical and Engineering Aspects, 299* (1–3), 65-72.

Salager, J.-L. (2000). Emulsion Properties and Related Know-how. In G. Marti-Mestres & F. Nielloud (Eds.), *Pharmaceutical Emulsions and Suspensions* New York: Marcel Dekker Inc.

Santander-Ortega, M., Lozano-López, M., Bastos-González, D., Peula-García, J., & Ortega-Vinuesa, J. (2010). Novel core-shell lipid-chitosan and lipid-poloxamer nanocapsules: stability by hydration forces. *Colloid and Polymer Science, 288* (2), 159-172.

Sarkar, A., Goh, K. K. T., Singh, R. P., & Singh, H. (2009). Behaviour of an oil-in-water emulsion stabilized by β-lactoglobulin in an in vitro gastric model. *Food Hydrocolloids, 23* (6), 1563-1569.

Saulnier, P., & Benoit, J.-P. (2006). Lipidic Core Nanocapsules as New Drug Delivery Systems. In V. P. Torchilin (Ed.), *Nanoparticulates as Drug Delivery Systems*. London, UK: Imperial College Press.

Sim, J.-Y., Lee, S.-H., Park, D.-Y., Jung, J.-A., Ki, K.-H., Lee, D.-H., & Noh, G.-J. (2009). Pain on injection with microemulsion propofol. *British Journal of Clinical Pharmacology, 67* (3), 316-325.

Singh, H., Ye, A., & Horne, D. (2009). Structuring food emulsions in the gastrointestinal tract to modify lipid digestion. *Progress in Lipid Research, 48* (2), 92-100.

Solè, I., Maestro, A., Pey, C. M., González, C., Solans, C., & Gutiérrez, J. M. (2006). Nano-emulsions preparation by low energy methods in an ionic surfactant system. *Colloids and Surfaces, A: Physicochemical and Engineering Aspects, 288* (1–3), 138-143.

Spernath, A., & Aserin, A. (2006). Microemulsions as carriers for drugs and nutraceuticals. *Advances in Colloid and Interface Science, 128–130* (0), 47-64.

Steffe, J. F. (1992). *Rheological Methods in Food Process Engineering*. East Lancing: Freeman Press.

Svitova, T. F., & Radke, C. J. (2004). AOT and Pluronic F68 Coadsorption at Fluid/Fluid Interfaces: A Continuous-Flow Tensiometry Study. *Industrial & Engineering Chemistry Research, 44* (5), 1129-1138.

Tadros, T., Izquierdo, P., Esquena, J., & Solans, C. (2004). Formation and stability of nano-emulsions. *Advances in Colloid and Interface Science, 108–109* (0), 303-318.

Tadros, T. F. (1986). Control of the properties of suspensions. *Colloids and Surfaces, 18* (2–4), 137-173.

Tadros, T. F. (1994). Fundamental principles of emulsion rheology and their applications. *Colloids and Surfaces, A: Physicochemical and Engineering Aspects, 91* (0), 39-55.

Tamilvanan, S. (2004). Oil-in-water lipid emulsions: implications for parenteral and ocular delivering systems. *Progress in Lipid Research, 43* (6), 489-533.

Tamilvanan, S. (2009). Formulation of multifunctional oil-in-water nanosized emulsions for active and passive targeting of drugs to otherwise inaccessible internal organs of the human body. *International Journal of Pharmaceutics, 381* (1), 62-76.

Ton, M. N., Chang, C., Carpentier, Y. A., & Deckelbaum, R. J. (2005). In vivo and in vitro properties of an intravenous lipid emulsion containing only medium chain and fish oil triglycerides. *Clinical Nutrition, 24* (4), 492-501.

Torcello-Gómez, A., Maldonado-Valderrama, J., de Vicente, J., Cabrerizo-Vílchez, M. A., Gálvez-Ruiz, M. J., & Martín-Rodríguez, A. (2011). Investigating the effect of surfactants on lipase interfacial behaviour in the presence of bile salts. *Food Hydrocolloids, 25* (4), 809-816.

Torcello-Gomez, A., Santander-Ortega, M. J., Peula-Garcia, J. M., Maldonado-Valderrama, J., Galvez-Ruiz, M. J., Ortega-Vinuesa, J. L., & Martin-Rodriguez, A. (2011). Adsorption of antibody onto Pluronic F68-covered nanoparticles: link with surface properties. *Soft Matter, 7* (18), 8450-8461.

Tropea, C., Yarin, A. L., & Foss, J. F. (2007). *Springer Handbook of Experimental Fluid Mechanics*. Berlin: Springer.

Tuinier, R., Rieger, J., & de Kruif, C. G. (2003). Depletion-induced phase separation in colloid–polymer mixtures. *Advances in Colloid and Interface Science, 103* (1), 1-31.

Ueda, K., Kawaguchi, Y., & Iwakawa, S. (2008). Effect of oxyethylene numbers on the pharmacokinetics of menatetrenone incorporated in oil-in-water lipid

emulsions prepared with polyoxyethylene-polyoxypropylene block copolymers and soybean oil in rats. *Biological & Pharmaceutical Bulletin, 31* (12), 2283-2287.

Urban, C., & Schurtenberger, P. (1998). Characterization of Turbid Colloidal Suspensions Using Light Scattering Techniques Combined with Cross-Correlation Methods. *Journal of Colloid and Interface Science, 207* (1), 150-158.

van Vliet, T., & Lyklema, H. (2005). 6 Rheology. In J. Lyklema (Ed.), *Fundamentals of Interface and Colloid Science* (Vol. Volume 4, pp. 6.1-6.88): Academic Press.

Versantvoort, C. H. M., Oomen, A. G., Van de Kamp, E., Rompelberg, C. J. M., & Sips, A. J. A. M. (2005). Applicability of an in vitro digestion model in assessing the bioaccessibility of mycotoxins from food. *Food and Chemical Toxicology, 43* (1), 31-40.

Vincent, B. (1973). The van der Waals attraction between colloid particles having adsorbed layers. II. Calculation of interaction curves. *Journal of Colloid and Interface Science, 42* (2), 270-285.

Vincent, B., Luckham, P. F., & Waite, F. A. (1980). The effect of free polymer on the stability of sterically stabilized dispersions. *Journal of Colloid and Interface Science, 73* (2), 508-521.

Walz, J. Y., & Sharma, A. (1994). Effect of Long Range Interactions on the Depletion Force between Colloidal Particles. *Journal of Colloid and Interface Science, 168* (2), 485-496.

Wilde, P. J., & Chu, B. S. (2011). Interfacial and colloidal aspects of lipid digestion. *Advances in Colloid and Interface Science, 165* (1), 14-22.

Williams, R. O., Watts, A. B., & Miller, D. A. (2012). *Formulating Poorly Water Soluble Drugs*. New York: Springer.

Wooster, T. J., Golding, M., & Sanguansri, P. (2008). Impact of Oil Type on Nanoemulsion Formation and Ostwald Ripening Stability. *Langmuir, 24* (22), 12758-12765.

Yamamoto, M., Morita, S.-y., Kumon, M., Kawabe, M., Nishitsuji, K., Saito, H., Vertut-Doï¨, A., Nakano, M., & Handa, T. (2003). Effects of plasma

apolipoproteins on lipoprotein lipase-mediated lipolysis of small and large lipid emulsions. *Biochimica et Biophysica Acta (BBA) - Molecular and Cell Biology of Lipids, 1632* (1–3), 31-39.

Yechiel, E., & Coste, R. L. (2005). From Ancient Potions to Modern Lotions: A Technology Overview and Introduction to Nano-Vehicles in Topical Delivery Systems. In M. R. Rosen (Ed.), *Delivery System Handbook for Personal Care and Cosmetic Products*. Norwich, NY: William Andrew, Inc.

Zangenberg, N. H., Müllertz, A., Kristensen, H. G., & Hovgaard, L. (2001). A dynamic in vitro lipolysis model: I. Controlling the rate of lipolysis by continuous addition of calcium. *European Journal of Pharmaceutical Sciences, 14* (2), 115-122.